Optimal sizing and control of energy storage systems for the electricity markets participation of intelligent photovoltaic power plants

Andoni Saez de Ibarra Martinez de Contrasta

Communauté
UNIVERSITÉ Grenoble Alpes

THÈSE

Pour obtenir le grade de

DOCTEUR DE LA COMMUNAUTE UNIVERSITE GRENOBLE ALPES

Spécialité : **Génie Electrique**

Arrêté ministériel : 7 août 2006

Présentée par

Andoni SAEZ DE IBARRA MARTINEZ DE CONTRASTA

Thèse dirigée par **Seddik BACHA** et
codirigée par **Vincent DEBUSSCHERE** et **Aitor MILO**

préparée au sein du **Laboratoire de Génie Electrique de Grenoble (G2Elab)** et **IK4-IKERLAN Technology Research Centre**
dans **l'École Doctorale Électronique, Électrotechnique, Automatique & Traitement du Signal (EEATS)**

Dimensionnement et contrôle-commande optimisé des systèmes de stockage énergétique pour la participation au marché de l'électricité des parcs photovoltaïques intelligents

Thèse soutenue publiquement le **7 octobre 2016**,
devant le jury composé de :

M. Cristian NICHITA
Professeur à l'Université Le Havre, Président
M. Bruno BURGER
Fraunhofer ISE, Rapporteur
M. Luis MARTINEZ SALAMERO
Professeur à l'Universitat Rovira i Virgili, Rapporteur
M. Ionel VECHIU
Professeur à l'ESTIA, Rapporteur
M. Seddik BACHA
Professeur à l'Université Grenoble Alpes, Directeur de thèse
M. Vincent DEBUSSCHERE
Maître de Conférences Grenoble INP, Co-encadrant de thèse
M. Aitor MILO
IK4-IKERLAN Technology Research Centre, Co-encadrant de thèse
Mme. Haizea GAZTAÑAGA
IK4-IKERLAN Technology Research Centre, Examinatrice
M. Tuan TRAN QUOC
CEA-INES, Invité

Titre : Dimensionnement et contrôle-commande optimisé des systèmes de stockage énergétique pour la participation au marché de l'électricité des parcs photovoltaïques intelligents

Résumé

L'objet de cette thèse est l'intégration des parcs photovoltaïques intelligents au marché de l'électricité dans un environnement de libre concurrence. Les centrales photovoltaïques intelligentes sont celles qu'incluent systèmes de stockage pour réduire sa variabilité et en plus fournir à l'ensemble une plus grande contrôlabilité. Ces objectives techniques sont obtenues grâce à la capacité bidirectionnelle d'échange et stockage d'énergie qu'apportent les systèmes de stockage, dans ce cas, les batteries. Pour obtenir la rentabilité maximale des systèmes de stockage, le dimensionnement doit être optimisé en même temps que la stratégie de gestion avec laquelle le système de stockage est commandé. Dans cette thèse, une fois la technologie de stockage plus adapté à l'application photovoltaïque est sélectionnée, à savoir la technologie de lithium-ion, une participation innovatrice de part des parcs photovoltaïques intelligents dans le marché de l'électricité est proposée qui optimise à la fois le dimensionnement et la stratégie de gestion d'une manière simultanée. Ce processus d'optimisation ainsi que la participation au marché de l'électricité a été appliquée dans un cas d'étude réel, ce qui confirme que cette procédure permet de maximiser la rentabilité économique de ce type de production.

Mots clés : centrale photovoltaïque, system de stockage d'énergie, réseau, optimisation, marché de l'électricité, dimensionnement, stratégie de contrôle-commande.

Title: Optimal sizing and control of energy storage systems for the electricity markets participation of intelligent photovoltaic power plants

Abstract

The present PhD deals with the integration of intelligent photovoltaic (IPV) power plants in the electricity markets in an environment subject to free competition. The IPV power plants are those that include energy storage systems to reduce the variability and to provide the entire group a controllability increase. These technical objectives are obtained thanks to the bidirectional exchanging and storing capability that the storage system contributes to, in this case, battery energy storage system (BESS). In order to obtain the maximum profitability of the BESS, the sizing must be optimized together with the control strategy that the BESS will be operated with. In the present PhD, once the most performing battery energy storage technology has been selected, the lithium-ion technology, an innovative IPV power plant electricity market participation process is proposed which optimizes both the sizing and the energy management strategy in the same optimization step. This optimization process together with the electricity market participation has been applied in a real case study, confirming that this procedure permits to maximize the economic profitability of this type of generation.

Keywords: photovoltaic power plant, energy storage system, grid, optimization, electricity markets, sizing, energy management strategy.

Título: Dimensionamiento y control óptimos de sistemas de almacenamiento para la participación en los mercados eléctricos de plantas fotovoltaicas inteligentes

Resumen

Esta tesis se centra en la integración de las plantas fotovoltaicas inteligentes en los mercados eléctricos en un entorno de libre competencia. Las plantas fotovoltaicas inteligentes son las que incluyen sistemas de almacenamiento para reducir su variabilidad y dotar al conjunto de una mayor controlabilidad. Estos objetivos técnicos se obtienen gracias a la capacidad bidireccional de intercambio y al almacenamiento de energía que aporta el sistema de almacenamiento, en este caso, baterías. Para obtener la máxima rentabilidad de los sistemas de almacenamiento se tiene que optimizar el dimensionamiento junto con la estrategia de gestión con la que se opere dicha batería. En esta tesis, tras determinar la tecnología de almacenamiento más adecuada para esta aplicación, la tecnología de litio-ion, se ha propuesto una innovadora participación en los mercados eléctricos por parte de las plantas fotovoltaicas inteligentes, la cual optimiza tanto su gestión como su dimensionamiento de manera conjunta. Este proceso de optimización junto con la participación en los mercados eléctricos ha sido aplicado en un caso de estudio real, confirmando que este procedimiento permite maximizar la rentabilidad económica de este tipo de generadores.

Palabras clave: parque fotovoltaico, sistema de almacenamiento, red, optimización, mercado eléctrico, dimensionamiento, estrategia de gestión energética.

Izenburua: Biltegiratze sistemen dimentsionamendu eta kontrol optimoak parke fotoboltaiko adimenduek elektrizitate-merkatuetan parte-hartzeko.

Laburpena

Tesi hau parke fotoboltaiko adimenduen integrazioan oinarritzen da, merkatu elektrikoetan parte hartu ahal izateko konpetentzia libreko inguru batean. Parke fotoboltaiko adimenduak biltegiratze sistemak barneratzen dituztenak dira, euren aldagarritasuna murrizteko eta talde osoari kontrolagarritasun handiagoa emateko. Helburu tekniko hauek potentzi aldaketa bidirekzionalari esker lortzen dira eta baita biltegiratze sistemetan gordeta dagoen energiari esker, kasu honetan, baterietan dagoen energiari esker. Biltegiratze sistemen errentagarritasun handiena lortzeko, bateriaren dimentsionamendua optimizatu behar da bere kudeaketa estrategiarekin batera. Tesi honetan, behin biltegiratze teknologia hoberena aukeratu ondoren, litio ioizko teknologia, parke fotoboltaiko adimenduaren aldetik elektrizitate merkatuan parte hartzeko estrategia berritzaile bat proposatu da, bai bere kudeaketa eta baita bere dimentsionamendua aldi berean optimizatuz. Optimizazio prozesu hau, merkatu parte-hartzearekin batera azterketa kasu erreal batean aplikatu izan da, prozesu hau sorgailu mota hauen errentagarritasun ekonomikoa maximizatzeko aukera ematen duela baieztatuz.

Hitz gakoak: parke fotoboltaikoa, biltegiratze sistema, sare elektrikoa, optimizazioa, merkatu elektrikoa, dimentsionamendua, kudeaketa energetikoko estrategia.

When you talk, you are only repeating what you know; but when you listen, you learn something new.

-Dalai Lama-

Acknowledgements

I want to tell a story that started eight years ago, when I was in the third course of the electrical engineering in Mondragon University when the professor Cecilio Ugarte offered to me the possibility to complete my engineering studies both in ENSEEIHT of Toulouse and in ENSE3 of Grenoble. After having correctly chosen to come to the university where I have already completed 6 years of different studies (engineering and PhD thesis), I prepared my bag plenty of wishes for knowing another culture and for learning different things as technical skills from very distinguished professors, as well as to live beautiful experiences in the place where I met my near future wife.

During a lesson of the strict Prof. Bacha, I proposed a question whose answer was another question from the Prof. Bacha asking to me about my nationality. After a nervous moment and a complicity feeling, the strict and feared Prof. Bacha was transformed into Seddik, my adorable master thesis supervisor and charming PhD Director.

This was possible thanks to him because he introduced me another very important person in which I see myself identified, Ion Etxeberria. This pleasant and close person accepted me and offered me the possibility to work where I am nowadays, one of the best research centre of the Basque Country, IK4-Ikerlan Technology Research Centre, following the human chain of multiple Basque people that after having completed our studies in Grenoble, we came back to Ikerlan, as Ion, Haizea, Amaia, Aitor and Karlos.

There, in Ikerlan, I started a lovely relation with my boss, Haizea, and after the master thesis, with Aitor, the person that has helped (endured) me the most during these long four years. Sorry for my annoying behavior and my extensive null explanations. This powerful trio, we are nowadays part of the electrical energy management team.

Also during the last year of the engineering studies, another young teacher, very concerned about his job fighting to obtain the best of his students was crossed in this lovely story, Vincent. I would like to express my most sincere gratitude for all the emails, calls, visits and questions that I have asked to you, because you always has tried to help or answer me as soon as possible.

Those 5 people, Seddik, Ion, Vincent, Haizea and Aitor, you have helped me to complete this period of my life, to continue being what I have always wanted to be, a researcher concerned about renewable energies and storage systems included in several applications, in a technical aspect, and a more adult, responsible and polite person in other more social skills. Thank you all very much. Merci beaucoup à tous. Eskerrik asko danoi!

I would also like to express my sincere gratitude to the reviewers and jury members for their contributions that have improved the complete manuscript and for their acceptance to come to this PhD dissertation, Prof. Cristian Nichita (Université Le Havre), Prof. Bruno Burger

(Fraunhofer ISE), Prof. Ionel Vechiu (ESTIA), Prof. Martinez Salamero (Universitat Rovira i Virgili) and Dr. Tuan Tran Quoc (CEA-INES).

Regarding the SYREL team and the whole Grenoble Electrical Engineering Laboratory, G2Elab, I am grateful to all the staff and colleagues that helped me so much accepting me in their atmosphere, as the PhD students that I met there: Julian, Ekaitz, Guilherme, Andrés, Rubén, José, Nils, Xavier, Timothé, Olivier, Audrey, Gatien, Kaustav, Gaspard, Aurélien, Victor, Archie and Mounir.

I would also like to thank all the Control Engineering and Power Electronics and Alternative Generation Systems people I have been working with: Luis, Irma, Alex, Sanse, Joseba, Aron, Mamel, Igor, Amaia, Crego, Atzur, Rafa, Valentín, Gabri, Iñigo, Mikel, Jon and Lide.

I also carried out a little stage in Terrassa with the SEER group of the UPC, and I want to express my gratitude to Pedro, Alvaro, Iñaki, Joan, Raul and Catalin.

After this visit, I also carried out another longer internship in Abengoa Research working for Pedro Rodriguez in the Power Systems group. I wanted to thank to him the opportunity to join them during 2014 in Seville, working with Antoni, Daniel, Cosmin, Elyas, Mohamed, Jacobo, Jonas, Zulema, Alvaro, Paquito, Nicolas, Eva and Dulce. During this internship I collaborated with the Batteries 2020 project, where I have also worked with the people of Aalborg University as Maciej and Daniel. Also thank you for your constructive discussions and support.

Of course that I want to thank to my PhD mates of Ikerlan as Endika, Asier, Karlos, Asier, Maitane, Eli, Nerea, Damian, Gustavo, Alejandro, Victor, Ugaitz, Egoitz, Maitane, Leire, Aitor, Ander, Joannes and Iñigo. Sorry for the spam and thank you for your support and comprehension.

I have spent a lot of time going to the work sharing the car with Josu, Karlos, Jean François, Alejandro, Alex and Victor, so thank you for supporting me asleep, half-asleep and awake.

For the commodity of my travels to Grenoble, I cannot forget my near future uncle and aunt, David and Angie Riley. Thank you very much for your help offering me your home and also your time to correct this document, David. Once arrived to Grenoble, my colleagues Xabel, Nuria and Alex have always offered me their home, but more specifically their sofa. Sorry for appropriating your living room. Moreover, Alex, thank you very much for helping me in the yearly registration. You still have my last student card.

Coming back to the technical supports, this PhD started from a previous project called ILIS where Ikerlan worked for Acciona Energia. I would like to thank Asun Padrós and Eugenio Guelbenzu for the possibility of considering the Tudela PV power plant as the case study.

I also wanted to thank all my bosses in Ikerlan, offering me the best technical and social resources. Milesker Ion, Unai, Igor eta Haizea!

Once again I wanted to emphasize my gratitude to Victor Isaac Herrera, my PhD brother for his help, support, discussions, and corrections.

I want to apologize to my *kuadrila* because in the last months I have not had any minute for pleasing them with my modest presence. Sorry but this work has been really hard to me.

And last but not least, I would like to thank to my complete family who is always present. I am thinking in my complete family, not only my Basque family, but also my new Sigüenza's, Swiss and Valencian family.

I have to finish this acknowledgements coming back to the end of the first paragraph expressing my most sincere gratitude to you, Laura. You know that more than the half of this work is thanks to you, for accepting my cries, my long faces and my bad humor in the bad days, but also my smile, my jokes and my caresses in sunny days. Thank you for staying always by my side providing me the necessary support to be able to finish this work.

Eskerrik asko

Muchas gracias

Moltes gràcies

Merci beaucoup

Thank you

Contents

General introduction

General introduction

Renewable energy sources (RES) are today a rising solution to face climate change, environmental pollution and increasing global demand. Renewable energies cover around 20 % of worldwide electricity generation. On this percentage, energy directly coming from the sun, wind, geothermal and non-traditional biomass barely reach 2 % of total installed electricity generation. However, over the last few years these technologies and especially wind and solar ones, are experiencing important worldwide development. According to experts, these sources will provide the biggest proportion of electricity energy generation in the World by the end of the century.

There are multiple reasons that cause interest in these technologies: the advances in the cost reduction, the energetic efficiency improvements, governments' promotion and funds, the easiness of installation and the possibility to get them running in reduced periods of time. From the energetic and environmental point of view the advantages of the wind and solar energies are perfectly well known: they are inexhaustible resources available all over the world and free of greenhouse gas emissions. From the grid integration perspective, the connection between the RES (especially wind and photovoltaic, PV) and the grid is usually made by means of power electronics systems providing a high level of controllability and rapidness. These devices allow a fast reaction of RES in front of any undesired event or situation that occurs or that may occur in the grid.

Nevertheless, the integration of RES in the grid also involves some challenges related to stability and reliability which are caused by the unpredictable and variable nature of RES. The stochastic nature of the wind and the clouds affects the production of renewable energy unbalancing the electric grid in both directions, overloading and discharging the grid. This drawback reduces the controllability and rapidness explained before, necessary in the electric grid and complicates the operation from the energetic and economic point of view compared to other traditional electricity generators.

For that reason there is a need to regulate the RES connection conditions and the many new grid codes will demand more controllable behavior to deal with this drawback (oriented to wind power). Until now PV power plants, due to their relatively smaller size, have not been considered under the scope of these codes. Nevertheless, as the installed PV capacity increases as well as the rating of PV plants, the interest for improvement of their grid integration is also increasing. Some controllable PV power plants could be adapted to those grid codes, working below the MPPT (maximum power point tracking) to create spinning reserves, but this operation mode is not optimal from the PV plant production point of view.

One of the most promising solutions to solve this problem is the use of energy storage systems (ESS). Among the different ESS, battery energy storage systems (BESS) are now considered as a main enabling technology to face the previously explained issues, providing control flexibility to the PV power plants. Due to this control flexibility and energy reserve that the storage system provides to the PV power plant this combination is named in this PhD as Intelligent PV (IPV) power plant.

This flexibility and energy reserve of the BESS contributes to: 1) the fulfillment of the **grid codes** by optimizing the **PV plant production**; 2) the generation of **controllable power**. This **reduces the generation variability** inherent to these plants and offers the possibility to participate in **electricity markets**, allowing a proper and viable integration of IPV plants in the grid.

The **grid codes** require some specific ancillary services for the regulation of active and reactive power separately (for frequency and voltage control participation) and IPV power plants could respond to these requirements demanded by the system operator much faster than other generators do (due to the power electronics systems for reactive power and the BESS for active power). Moreover, the **PV plant production** is optimized due to the fact that the BESS provides the required services, instead of being provided by PV inverters, working below the MPPT.

Related to the **controllable power**, the energy reserves of the BESS are able to provide this controllable power, **reducing the variability** of this type of generation and also enabling the possibility to participate in electricity markets. This **market participation** is based on the constant power production of the power plant during the market period, typically one hour. Thus, with the energy reserves, the IPV power plant could participate in electricity markets as other traditional generators would, offering an important improvement to be taken into account in future electric grids.

Nevertheless, the main issue that these IPV power plants are facing is the high acquisition cost of the BESS and its operational costs due to degradation. Depending on how it is managed, BESS degradation is increased or decreased, and will conclude with replacement of the BESS. Thus, considering each IPV application, the local grid codes, the desired ancillary services and the market participation, the power and energy needs of the BESS are different. In this context, the sizing and optimal operation of the BESS are two crucial factors to assure a viable and efficient operation of these plants. Thus, it is necessary to look for a balance between the size and optimal operation of the BESS. Therefore, the studies and tool developments for a correct sizing and optimal control of the joint operation are presented as an innovative research field essential to ensure the integration and viable operation of these systems in the grid.

Due to the fact that PV power plants have not participated in electricity markets as traditional generators until today the size of the required storage system has not been extensively calculated by taking into account these factors together with the electricity markets operations for this application.

In this framework, **the objective** of this PhD is:

"To develop an innovative IPV power plant electricity market participation process based on BESS optimal sizing and advanced control operation strategies"

In addition to this main objective, other subsidiary objectives proposed in the present study are:

- To review **electrochemical storage technologies lifetime, cost and use**, and **electricity markets operation**.
- To **develop advanced control operation strategies** for the participation of IPV power plants in electricity markets.
- To **test and validate the developed advanced control operation strategies** in a **real time simulator** with real controllers.

The solutions to these objectives will be developed in this thesis. First, together with the photovoltaic power plants' introduction, different electrochemical storage technologies are analyzed, as well as the electricity markets. From this analysis, different energy management strategies are developed and are included in a model predictive control simulation where the market integration of an IPV power plant is simulated. Finally, this simulation is tested and validated in a real-time simulator.

The present thesis has been organized into six chapters:

The first chapter contains the state-of-the-art of the different parts or aspects that compose this PhD work, such as the PV power plants, the energy storage systems and the electricity markets. Aspects of power and control architecture of existing PV power plants, identification of storage systems characteristic parameters, battery energy storage system sizing methods or daily electricity market operation are some of the topics analyzed in this chapter. Moreover, the IPV power plant scenario is introduced together with the services that this type of power plant could provide to the grid. To complete this analysis, some existing plants currently providing services are described and classified, determining that the most beneficial service is the pool market participation.

In the second chapter, the IPV power plant scenario is presented in depth and modeled. From the aforementioned existing plants review, the fact that the storage technology is a very important selection is observed. Therefore, in this chapter a storage technology selection methodology is suggested and applied. Furthermore, the IPV power plant is presented, with its internal architecture and control modes. Moreover, the modeling of different existing IPV agents is described: PV, energy storage, electricity markets and complete IPV power plant models are developed.

In the third chapter, several Rules Based (RB) control strategies are proposed and developed. A comparison of the different RB control strategies is presented. Finally, a Model Predictive Control based on the most suitable RB control strategy is developed for presenting the proposed electricity market participation of the IPV power plant. This new market participation is one of the main contributions of this PhD.

In the fourth chapter, optimization for sizing and control is carried out, where the optimization objective function is oriented to achieve the optimal economic exploitation of the IPV power plant. As a result, the optimal sizing of the storage system is obtained together with the best operation of the IPV power plant. Based on the resultant BESS's sizing, an online model predictive control is proposed which will take into account forecast errors of PV generation. The solver of the MPC is the same optimization that calculates the optimal sizing of the storage system. This online MPC application for market participation of IPV power plants is the major contribution of this PhD work. Finally, the IPV power plant market participation results are presented based on the developed online MPC. To complete this chapter, the comparison of the control strategy developed in the third chapter and the one detailed in this forth chapter is carried out.

In the fifth chapter, real time validation is carried out. The proposed online MPC is validated in a real time simulator where control is executed in a Hardware in the Loop platform. This platform is controlled by a real controller (PLC), the same as the one which controls the IPV power plant before mentioned located in Tudela (Navarre, Spain).

Lastly, the sixth chapter describes the conclusions and contributions of the present PhD work, offering some future lines and possible propositions about the developed topics. A diagram to present the chapters and their organization is presented in Figure 1.

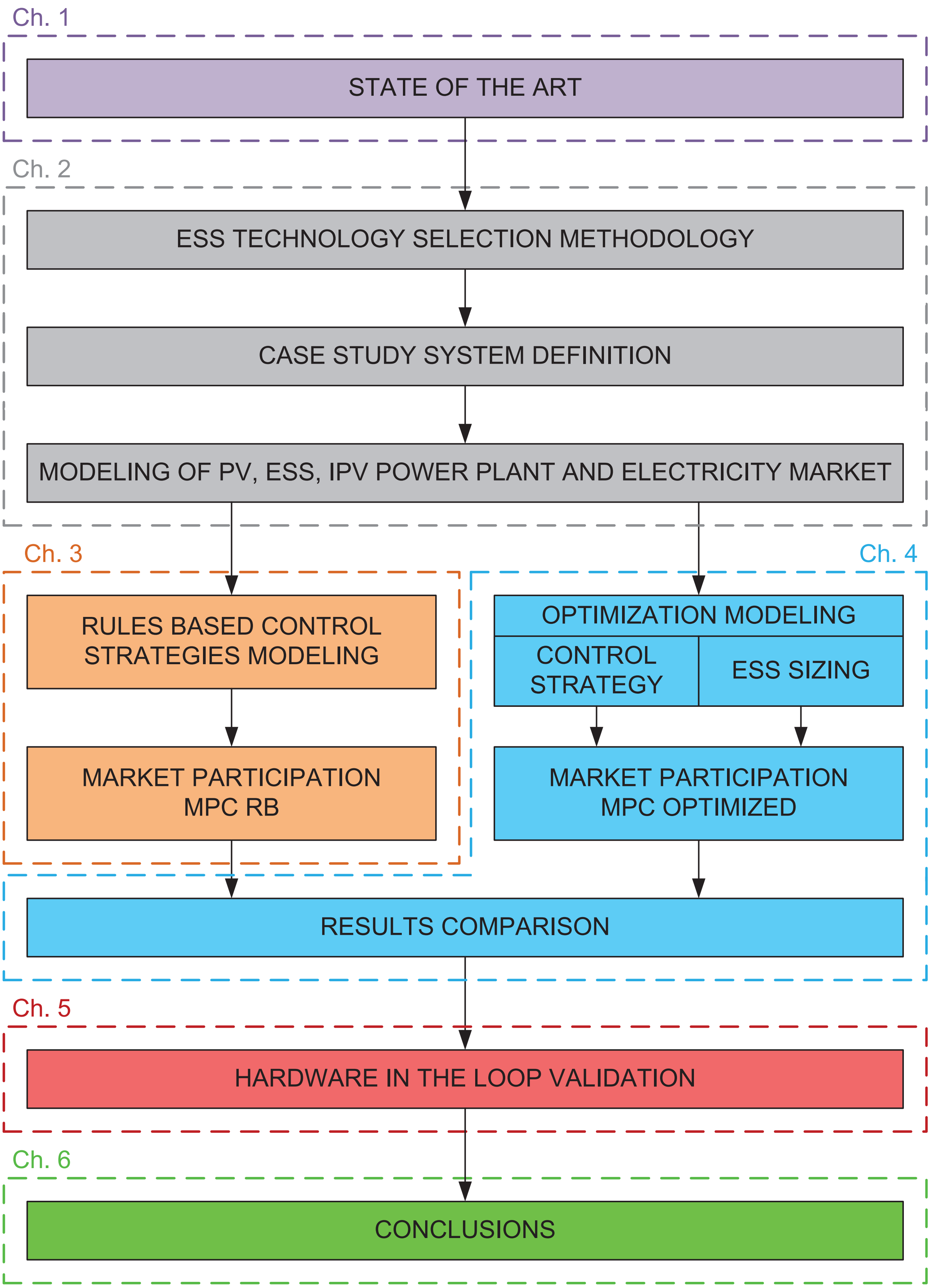

Figure 1: Chapters organization diagram.

1

State of the art of IPV plants, storage systems and electricity markets

1. State of the art of IPV plants, storage systems and electricity markets

Today, the annual installation of solar power capacity is increasing to unbelievable levels, exceeding the installation of 30 GW every year since 2011 [1], and having exceeded 40 GW in 2014 [2]. With the experienced growth in 2014 the global solar photovoltaic sector reaches a cumulative capacity of 178 GW [3]. As it can be verified in Figure 1.1, while the installation rate in Europe is decreasing (still 7 GW in 2014), other regions present a huge growth like Americas (7 GW), China (10.6 GW) and APAC (Asia Pacific 13 GW) as the most growing areas [3-5].

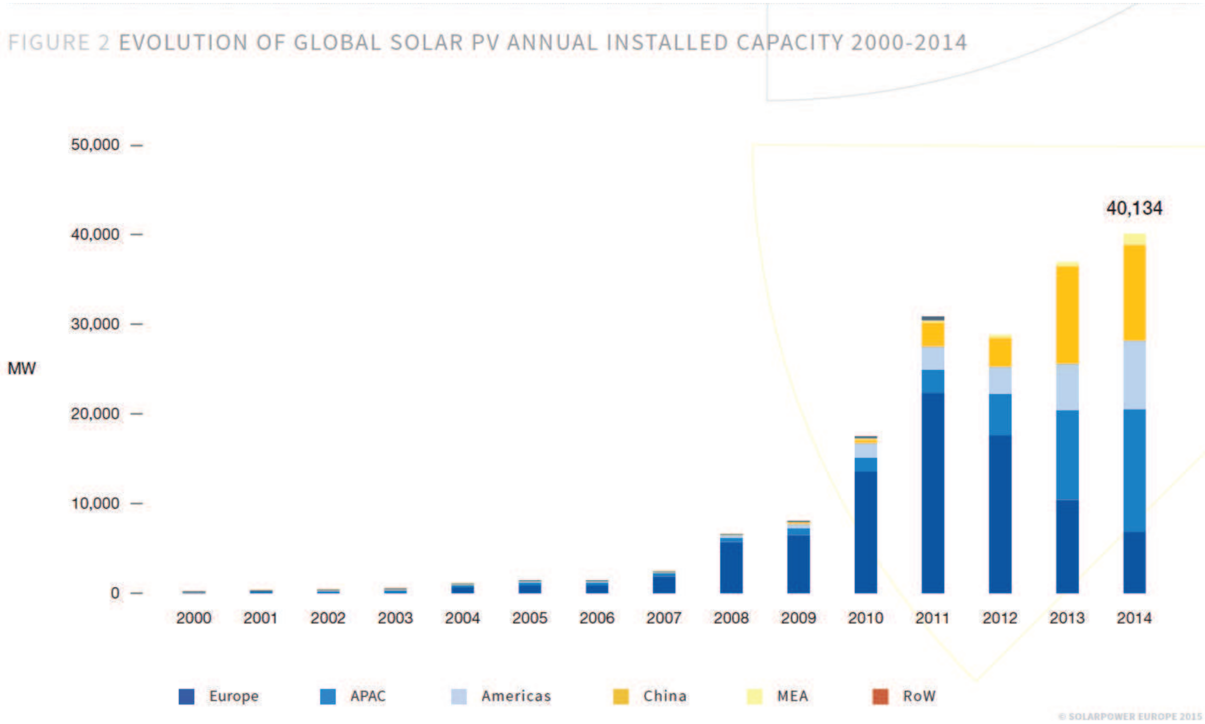

Figure 1.1: Evolution of global solar PV annual installed capacity 2000-2014. Source: Solar Power Europe 2015 [3].

The expectations for 2015 and over the next three years are very positive, where almost 200 GW of cumulative PV power could be reached [3].

Analyzing the segmentation of the installed capacity, last year's worldwide solar PV market showed a correct balance between utility scale installations and distributed or residential ones. In the Iberian Peninsula, the utility scale PV has more relevance due to the important incentives granted from 2007 to 2010.

Together with the PV power plants' development, over the last few years the storage systems grid integration (and more specifically the battery based storage systems, BESS) is also another increasing innovative field which is experiencing an exponential interest from producers and consumers' point of view [1, 3, 4, 6-11]. Both residential scale (contributed by

Tesla Gigafactory and the PowerWall [12]) and utility scale thank to several government support, are emerging as complementary solutions for improving energy efficiency and for increasing renewable integration at grid and end-user levels [7-10, 13-18].

Related to grid-scale demonstrators, the joint operation between PV power plants and battery based storage systems is oriented to validate their technical capacity in order to reach different objectives: to fulfill the recent grid codes [19-22], to provide several ancillary services [14, 23-25], and based on the energy reserves of the BESS, to validate their capacity of participation in electricity markets [23, 26-31]. To reach these objectives, it is necessary to apply advanced control methods which take into account input data as the PV predictions, the BESS state of charge (SOC) or electricity markets' price perspectives [14, 28-31]. Recently, the research and development around these controls, both at energy and at power level, are attracting increasing attention [23-31].

In this chapter, an analysis of the state of the art of the aforementioned grid-scale demonstrators will be done. Starting with the grid-scale intelligent photovoltaic power plants architectures and control structures, the storage systems' technologies and their sizing methods are summarized. The electricity markets' operation is also analyzed (specifically the Spanish electricity market), looking for the most appropriate market or markets to introduce the IPV power plant production. Finally, a conclusion is done, highlighting the opportunities of development about the described topics.

1.1. IPV power plant architecture

The power architecture refers to the electrical connection mode between converters and inverters and the thousands of installed PV panels. The connection modes between PV modules (considering a PV module as parallel and series connection of several hundreds of PV panels) create different power distribution architectures. Without considering the BESS, the existing PV plants' connection modes could be classified into two different ones [32-34], which are direct current (DC) connection and alternative current (AC) connection. Below, a summary description of these two mentioned architectures will be presented. After that, the integration modes of a BESS to the PV plant will be discussed, introducing the IPV power plants.

1.1.1. PV power plant with DC connection

The PV power plant with modules connected in DC is shown in the Figure 1.2 [32, 34]. In this connection model the different PV panel modules have to be controlled by a DC/DC converter. This converter controls the output power of each PV module. It could manage this output power by controlling the output active power (P) reference or with the reference for MPPT (maximum power point tracking) control. The output DC bus voltage of these converters is controlled by the grid-connected inverter, which also controls the reactive power exchanged with the grid. So, each module (PV + DC/DC) injects to the DC bus all the power that could get (MPPT), or the demanded power (active power reference), and the inverter pulls out this active power by means of controlling the bus voltage. Thus, this inverter has to be designed considering the sum of powers that the other converters could provide.

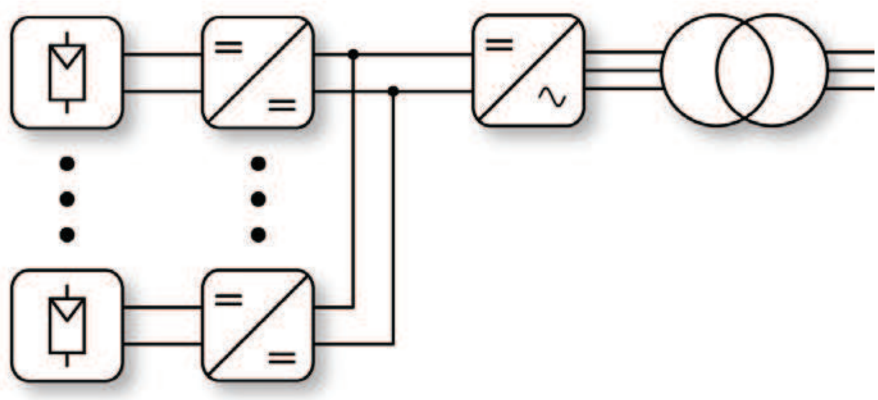

Figure 1.2: PV power plant with the modules connected in DC [32].

The advantage of this power distribution is that it only uses one inverter where reactive power control must be implemented, as well as fault ride through capability. Nevertheless, this inverter has to be designed for injecting all the power generated by the whole PV plant, so it can be a MW scale inverter.

1.1.2. PV power plant with AC connection

Another way to connect the PV modules between them is with an alternative current connection [14, 35]. In this case, the modules are composed by the PV panels, the DC/DC converter and the DC/AC inverter. The Figure 1.3 shows the explained power distribution.

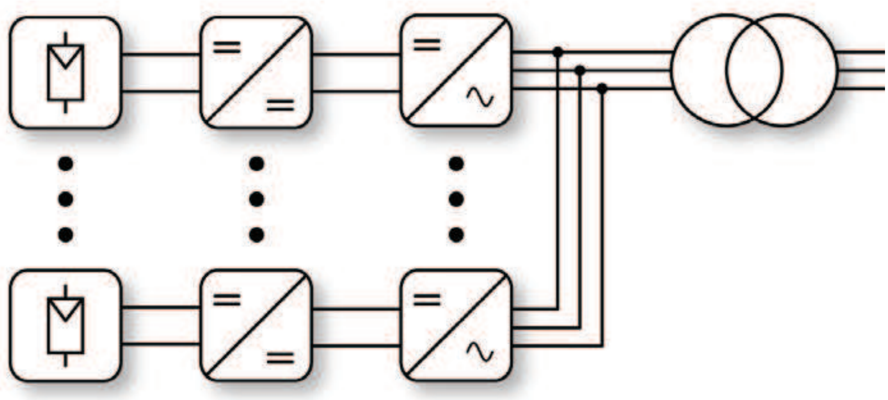

Figure 1.3: PV power plant with the modules connected in AC [14].

The inverter of each module controls the DC bus voltage as well as the reactive power (Q). The DC/DC converter works with the active power reference or with the MPPT control command. This architecture is composed by more inverters, one for each module, and these inverters are designed for the same power of the DC/DC converters, which is much lower regarding the previous explained architecture.

The advantage of this distribution is that each module works with its own control, which increases the resilience of the system, because only one module stops its production during a fault. Furthermore, as the inverters are designed for the rated power of each module, they have to transform less power than in the previous connection, so are designed for this lower power range.

1.1.3. IPV power plant with centralized storage system connected in AC

The previously described PV power plants' connection modes are important due to the fact that the integration of storage systems is different depending on these explained architectures. The energy storage system can be integrated into different parts of the IPV power systems and moreover it can be connected in a centralized mode, or in a distributed connection mode, as it will be described. So, depending on the previous summarized connection modes, the centralized storage system will be differently connected, in an AC connection or in a DC connection.

In the previous AC connection mode, the storage system could also be connected in AC, as it is shown in [14, 23, 36]. In this way, the storage system is centralized and is connected in one point (AC point) to the PV power plant. This architecture is illustrated in the Figure 1.4.

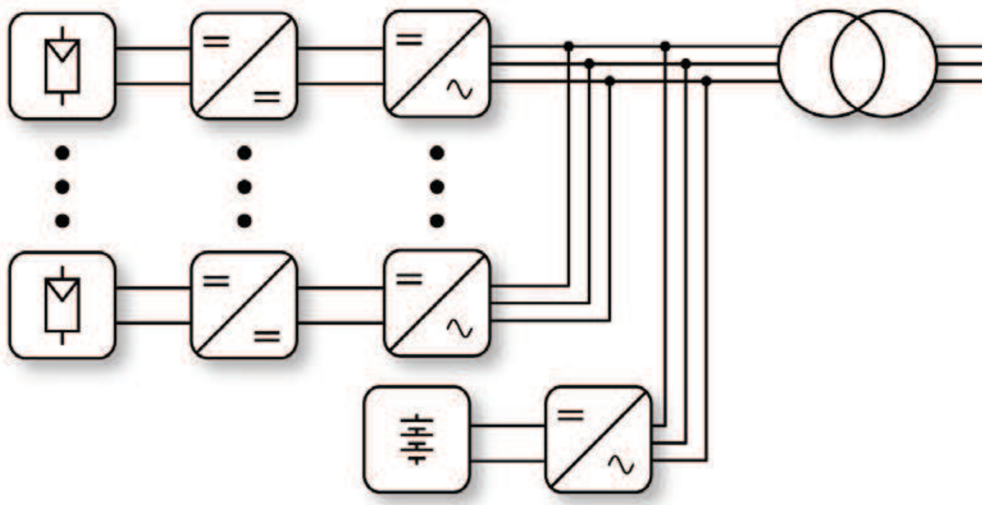

Figure 1.4: Power architecture of IPV power plant with the centralized storage connected in AC [14].

For connecting the storage system in the AC point, it is necessary to use a DC/AC converter. In this case, it could be formed by a DC/DC converter and a DC/AC inverter, or only by a regular inverter. In the first mode, DC/DC + DC/AC, the DC/DC converter controls the charge and discharge of the storage system, then its SOC. The DC/AC controls the bus voltage and the reactive power exchanged. Without using the DC/DC converter, the DC/AC inverter indirectly controls the storage system SOC by regulating the active and reactive power exchanged at its connection point.

The advantage of this connection mode is that the inverter associated to the storage has the capacity to control the reactive power, as to propose a fault ride through service. So, if any PV module inverter fails to follow its reactive power reference, the storage inverter could provide this extra power. Additionally, it could be considered as another module just for being more flexible due to its adaptability to inject and absorb power in the IPV power plant connection point, the Point of Common Coupling (PCC).

1.1.4. IPV power plant with centralized storage system connected in DC

The architecture for the centralized storage system is built with an internal DC grid. As for the previous case, the storage system is connected to a single point, but in this case, it is a DC connecting point. This architecture (Figure 1.5) is proposed and developed in [7, 24, 37, 38].

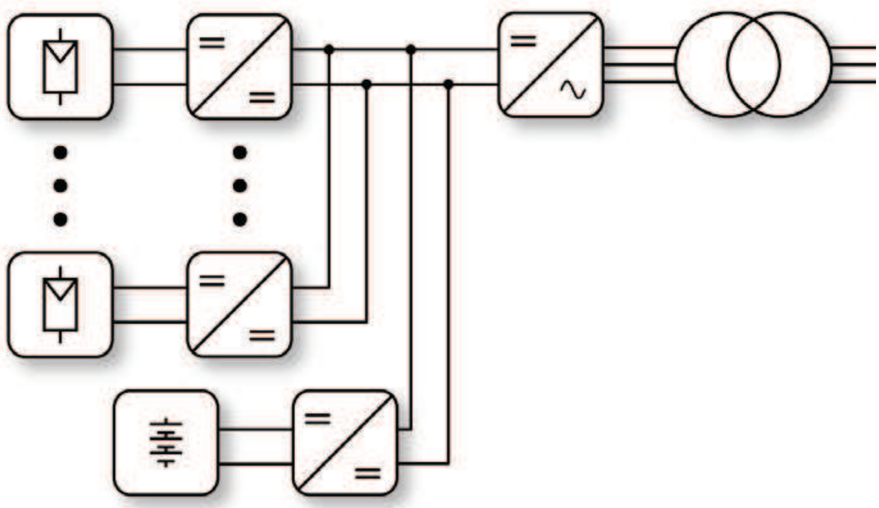

Figure 1.5: Power architecture of IPV power plant with the centralized storage connected in DC.

As it has been mentioned before, this architecture has an internal DC grid and a unique inverter extracts the power of the entire IPV power plant. This inverter has to be designed for the maximum power of the whole system and it must control the reactive power exchange.

For controlling the active power of the installation there are several converters to manage. The DC/DC of PV panels controls the output power of them. It could be controlled by a power reference or by a MPPT mode. If the storage system is connected without any converter to the internal DC bus, it imposes the DC voltage bus and the inverter will manage the active power, indirectly controlling the SOC. Despite the fact that this architecture is widely used on residential PV storage system, this connection is not usually installed in PV plants because the storage system is not properly controlled.

In the configuration presented in Figure 1.5, there are two control modes. In one case, similarly to the previous case, the DC/DC converter of the storage system controls the DC bus voltage, and the inverter controls the active power, indirectly controlling the SOC. In the second case, the most commonly used, [24, 38], the DC/DC converter controls the SOC while the inverter controls the DC bus voltage.

The advantage of this architecture is that the integration of the storage system only includes one DC/DC converter and moreover the storage system helps in the stability of the internal DC bus. This advantage is counteracted with the disadvantage that in case the whole system works at its nominal power and the control-command needs more power for the storage system, the centralized inverter is not able to provide it. Therefore, this architecture is an appropriate distribution if the whole PV power plant is a newly designed IPV plant, but if the project is the integration of the storage system in an existent PV plant, the over-cost caused by the change of the inverter will be a significant setback.

1.1.5. IPV power plant with distributed storage

In this architecture, the storage is divided in PV modules, giving to each module an individual controllable nature. This architecture is illustrated in Figure 1.6.

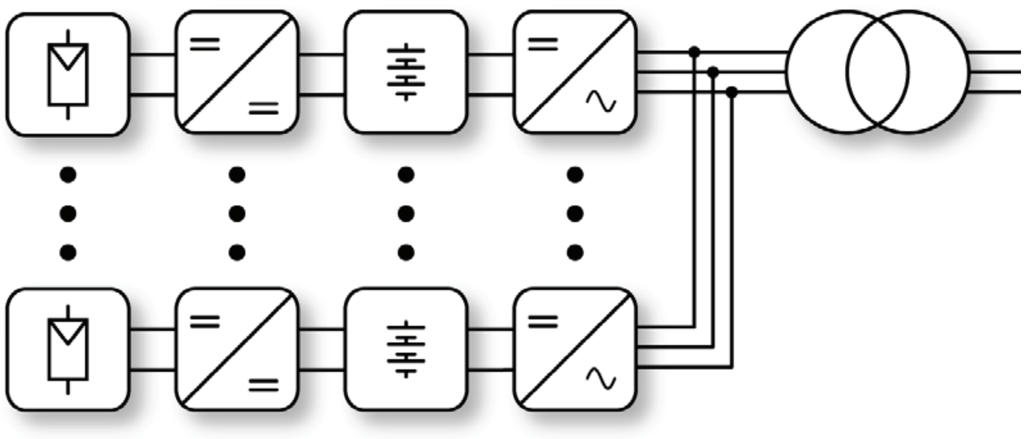

Figure 1.6: Power architecture of IPV power plant with distributed storage.

As it is shown in Figure 1.6, the storage is distributed. In this way, the output power of each module (considering module as PV + DC/DC + storage devices + DC/AC) is more stable and controllable [39-41].

In this configuration, the inverter has to be designed for the maximum power that is desired to be extracted from the PV + storage devices. This inverter must control the active and reactive power exchanges. If the storage system is connected as in Figure 1.6, the DC link bus voltage structure imposes to the grid connected inverter to indirectly regulate the storage system SOC. There is a variation if the storage system is connected to the DC link using another DC/DC converter, and the control modes for this variation are similar to those described in the previous architecture (Section 1.1.4), considering a distributed storage system used in this architecture as the centralized one was considered in the previous architecture.

1.2. IPV plant control structure and management layers

After the power architecture description, in this section the control structure of the IPV plant is presented. The control structure is another key factor for obtaining the wanted reliability, stability and profitability of the IPV power plant.

This control structure is composed of several controllers, from the whole IPV power plant centralized controller (plant controller) to the lower level converters and inverters controllers. A visual example of the control structure is shown in Figure 1.7.

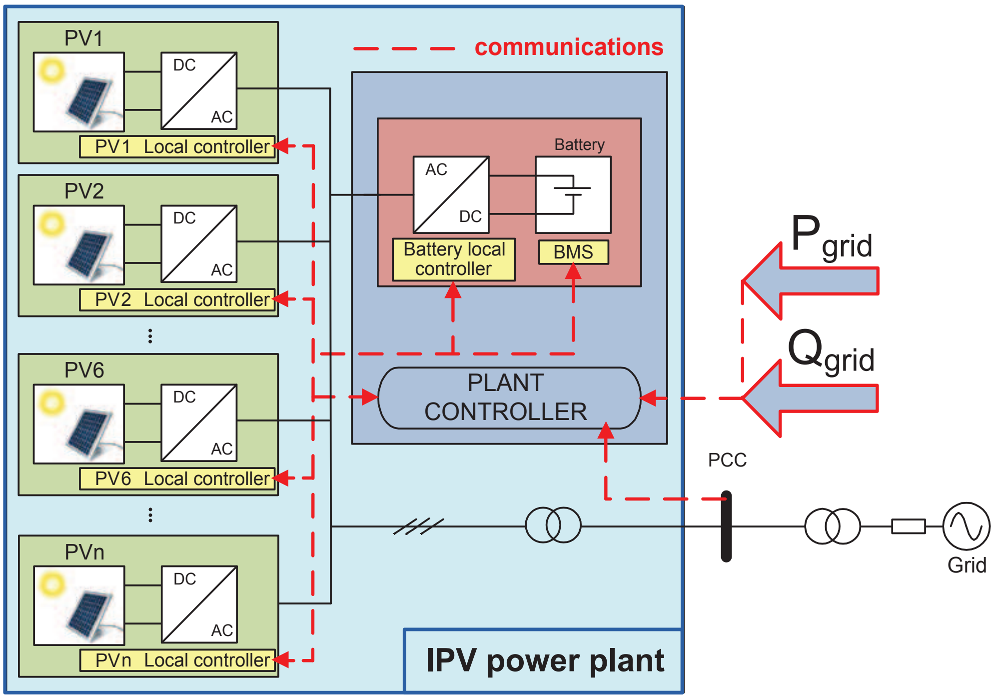

Figure 1.7: IPV power plant overview with the controllers and their communications.

Several controllers are in charge of numerous parameters. Some of them are directly linked to the converters, but there are also some for the BMS (Battery Management System), or for the complete plant. All these controllers can be separated in different management levels, from the local controls to the plant level control.

The classification in different levels of this structure allows addressing the development of each layer in a simpler manner. The analysis of the state of the art of this modular management representation permits to identify a classification which is adapted to the peculiarity of the present scenario [42, 43].

In [42] a hierarchical structure of this control architecture represented in levels is defined, which is called Modular Power and Energy Management Structure (MPEMS). This management structure could be applied to any manageable power device. In [42] the authors apply the structure for managing Electric Vehicles. On the contrary, in [43] the author applies this same structure for managing an elevator system. In Figure 1.8, the representation of the modular power and energy management structure is shown.

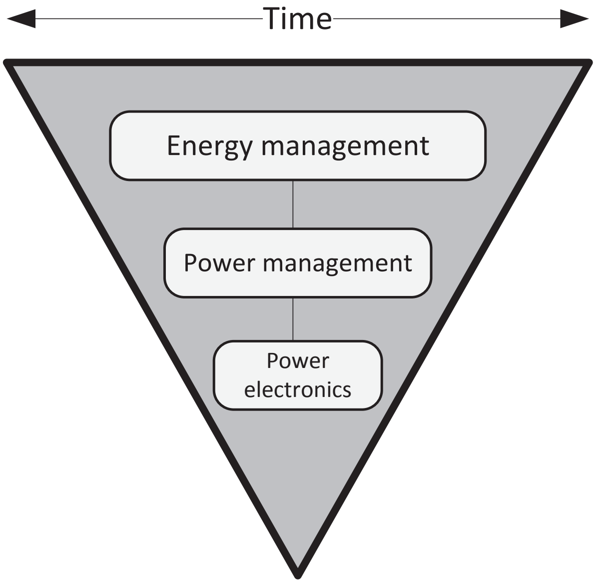

Figure 1.8: Representation of Modular Power and Energy Management Structure [42].

The **energy management** layer is located at the top of this structure. The objective of this layer is to define the strategy or the long term decisions (in IPV plant applications the long term is referring to durations from minutes to days). The dynamics of the energy management level is the lowest one, due to its long term previsions. In the IPV plant application, the long term services or functions of this layer are developed for energy arbitrage, power firming, demand side management, etc.

The second layer, the **power management** layer, is used to transfer the upper level strategy's guidelines to the lower level. So, based on the energy management requirements, the power references for the power electronics devices are calculated. In the IPV plant application, the medium term services are carried out in this layer, like voltage regulation, frequency control, and other ancillary services. The time response is faster than the upper layer one, from milliseconds to seconds. Note that the power dispatching step is also developed in this layer.

The different converters are controlled at the lowest level, the **power electronics** layer. This layer is then dedicated to currents and voltages controls of the various components composing the system. At this layer the dynamics are the fastest ones (few microseconds) due to the fact that control references are the converters' modulation indexes. In the IPV application, all the DC/DC converters and the inverters have to be managed, considering all control modes (MPPT, active power, etc.).

Taking into account the control structure defined in [42] the modular power and energy management structure (MPEMS) applied to IPV power plants is presented in Figure 1.9.

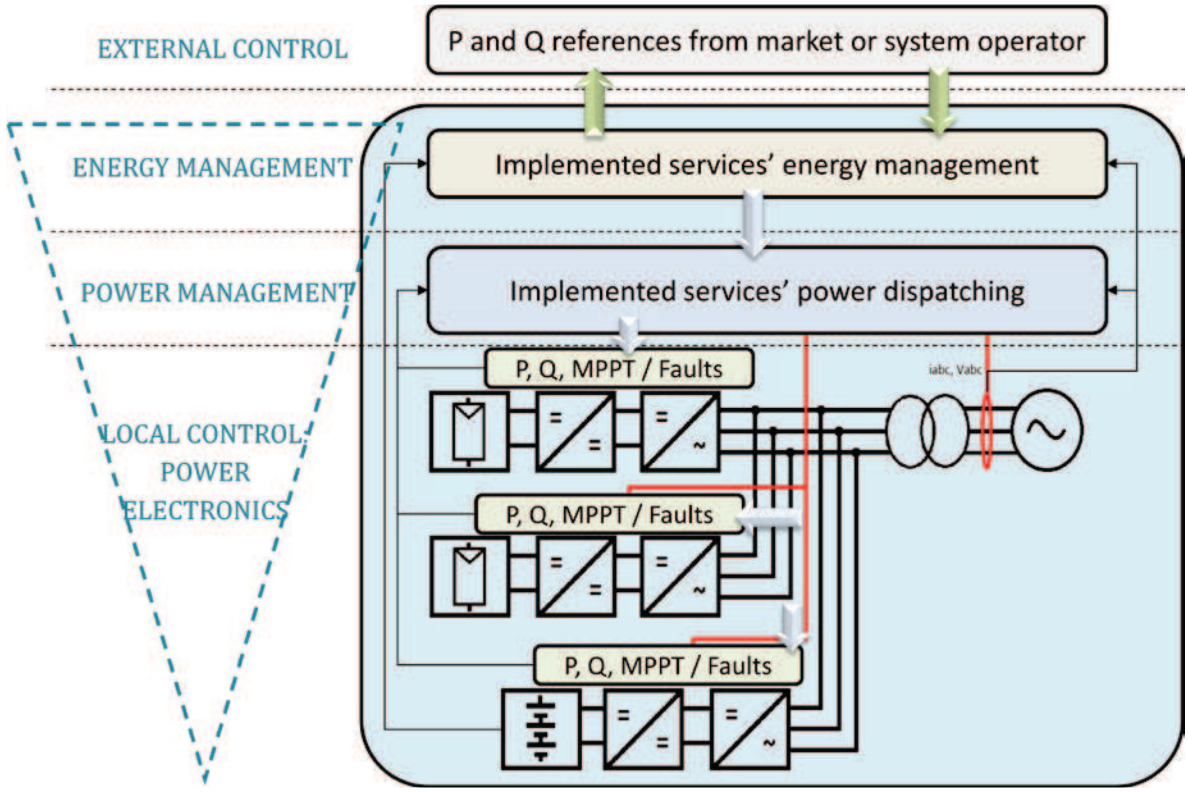

Figure 1.9: Representation of the hierarchical control structure on the IPV application.

In Figure 1.9, a higher level control, which is not defined in [42], has been added. The IPV power plant has an external link which is the market participation. The energy management layer defines some market participation offers and the system operator (SO) determines the amount of energy that has to be provided in each period of time. Therefore, although the IPV power plant presents its market offers, it must accomplish the SO requirements. This requirements are considered as the **external control**, which is managed by the System Operator (SO) [44]. The SO dispatches the reference for the IPV power plant, which are the inputs of the **energy management** control layer. By this communication line between the SO and the IPV power plant, other grid services calls are made, as the secondary regulation [45, 46], other ancillary services, etc. As the energy management control receives the measures of the grid voltages and injected currents from its PCC, it controls the active and reactive power exchanges depending on those measurements [47].

Focusing on the IPV's scenarios, which are the core of the present work, the power management can be a centralized control (as proposed in Figure 1.9) or a distributed one (at the converters level).

The two highest control layers of the modular power and energy management structure, which are the **energy management** layer and the **power management** layer, are considered in the scope of the present work.

1.2.1. IPV plant energy management layer

The IPV power plant energy management layer is an important management layer where long term decisions (minutes to hours) have to be taken into account. There are different strategies to manage this control layer. Some of them are based on deterministic approaches, optimization processes and stochastic approaches. Other ones are directly oriented to a given service. Nevertheless, in some research works different approaches are combined making difficult their classification. The strategies reviewed in this thesis consider multiple applications. The review is carried out from residential scale up to grid scale applications.

In [48], a deterministic approach for the energy management is carried out for an IPV system at residential scale. The authors consider a system composed by PV panels, a storage system based on batteries, loads and a connection to the distribution grid. The connection mode is defined as a centralized system with AC connection. Through the formulation of an economical objective function, the deterministic approach solves the system taking into account the lifetime of the storage system and the replacement cost of it minimizing the objective function. In [24], a Dynamic Programming (DP) algorithm is proposed improving the deterministic approach explained before. In this case, the authors use a predictive optimization stage for the state of the battery, closing the loop with the measures of the SOC and the State of Health (SOH) of the storage system. The energy management algorithm is simulated in real time microcontroller and using real data. Although an important electricity bill gain is obtained, the drawback of this analysis comes from the fact that the authors do not provide any services to the grid and they did not analyze the market participation.

In [49], another IPV residential application is analyzed, but also considering a microgrid composed by some households and other different loads (critical loads and controllable loads). In this case, the authors have considered PV generators as well as storage units (batteries and supercapacitors) on the households and also a gas microturbine for the microgrid. They have analyzed the household level control and the microgrid level control. All the control structure is separated into two stages, the long term (from a day to an hour range) energy management stage and the short term (from seconds to milliseconds) power balancing stage. The used energy management stage is a deterministic operational power planning strategy, which includes from day to hour PV power production program and production adjustment supported by the storage systems. The batteries are used as an energy reserve for this energy management layer, while the supercapacitors are used for power variations and primary control on the power management layer. In this study the market participation of the PV + storage systems is not developed due to the fact that they try to balance the microgrid power consumption, without taking into account the electric grid.

Another residential IPV system is the Zero Energy Building (ZEB) developed by [18]. In this work, the authors work with a grid-friendly hydrogen based ZEB, taking into account the PV panels, a wind generator, house loads, the grid connection, an electric storage system and a hydrogen storage tank with its electrolyzer and its fuel cell. The authors develop optimized energy and power management strategies. The energy management layer is composed by an adaptive optimization-based strategy called Adaptative Optimized Five-step Charge Controller, which optimizes the overall operation cost and reduces the energy exchange with the grid, turning on and off the electrolyzer and the fuel cell depending on the battery SOC. The authors propose an optimization process applying the Genetic Algorithm (GA) to determine the most well suited fuel cell and electrolyzer turning on and off thresholds, but it is not considered to provide any direct services to the grid. The limitation of the study comes from the fact that the market participation is not evaluated, while the grid connected and the stand-alone modes are analyzed.

At grid scale, in wind power application, there are also installations of energy storage systems and in this case they could be named Intelligent Wind Power or IWP. Several research works are also focusing on this type of systems, related to the energy management subject. In [50], the authors consider a wind/hydrogen/supercapacitor hybrid power system. The objective of the control system is to make controllable the generated wind power to provide some ancillary services to the grid (voltage and frequency regulation). The authors also separate three control layers as the above mentioned MPEMS, but with different layers' names. In MPEMS' energy management layer, the authors develop two control strategies, which are called "grid-following" and "source-following". The control strategies, as their names mention, regulate the power related to the grid and to the source. The authors conclude that the one that regulates the power related to the source, the "source-following" control strategy, is better because counteracting the source fluctuations by the energy storage systems, the complete system output power has better performances on the grid regulation. The limitation of the present study is mainly the lack of grid services, despite the development of control strategies.

The papers [51, 52] are also dealing with the IWP application, but in this case, they use a sodium sulphur battery as energy storage system (ESS) connected to a wind power farm. For decreasing the day-ahead forecast errors of the stochastic behavior of the wind power production, the authors use an autoregressive model. For analyzing the behavior and the performance of the ESS, they use a Monte Carlo simulation tool. The authors use the ESS to mitigate the forecast errors in order to fulfill the day-ahead power production commitment and they assess the storage performance using a Mean Absolute Deviation criterion. It is a relevant study which considers the day-ahead commitment (which could be developed by electricity markets), but did not take into account the SOC and ageing level for determining this day-ahead commitment.

Finally, considering the grid scale IPV power plants, in [53], the integration of an energy storage system into a PV power plant is analyzed. In this work, the energy management layer is considered one important fact, and thus it is widely developed. Two main energy management strategies are described which are the constant power steps control strategy and the fluctuations reduction control strategy. Within those energy management strategies, the author has developed multiple complementary control options that are introduced into the power management layer. In the energy management constant power steps control strategy, the author has differentiated between one single constant step, multiple constant steps, and hourly-adapted constant steps per day. This energy management strategy is perfectly adapted to the electricity market pool participation. In this strategy, the ESS has to inject or absorb the difference between the committed step values and the PV production. The other energy management strategy is the fluctuations' reduction control strategy, also called smoothing control strategy. This one uses the ESS capacity as a real energy buffer or as energy filter, filtering the fluctuations of the power variation caused by the instantaneous solar irradiation variations, also called clouds effect. Depending on the filter's time constant the variations will be more flattened or not, and in conclusion, with a greater filter's time constant, the ESS energy capacity has to be higher. This energy management is better adapted for cloudy days, in order to not introduce disturbances into the electric network, but it cannot be used to introduce the IPV power plant in the electricity market.

The constant power steps control strategy, as it is perfectly adapted to electricity market participation, is the base study for the development of the present PhD study, where the hourly steps will be optimized, maximizing the economic exploitation of the IPV power plant based on an innovative market participation. This development is discussed in detail in chapter 2.

1.2.2. IPV plant power management layer

Getting back to the MPEMS and having explained the upper layer, i.e. the energy management layer, in this section, the focus is made on the power management layer. All power management layer strategies are oriented to given services as balance control, ramp rate control, frequency control, peak shaving, inertia response, back up service, islanding mode, fluctuation reduction control, voltage control, etcetera. The applications that are going to be analyzed are the wind energy and the PV systems because the wind energy has similar disadvantages from the grid point of view compared to the application of the present work, the IPV power plants.

As mentioned before, for the energy management layer, the use of an ESS is almost necessary, but for the power management layer, it is not totally required. For that reason, the first application here described includes a power management layer without ESS, but providing some ancillary services to the grid by a wind farm. In [54] the power design of the wind farm controller is explained, providing better grid integration characteristics. The implemented control functions are: balance control, delta control, power ramp rate limitation, automatic frequency control, reactive power control and automatic voltage control. As it will be shown afterwards, these functions can be provided by the ESS, but in this case, they are provided by the wind farm, by means of reducing its power production. For that reason, the use of an ESS may be a better solution for providing those functions (through its charge and discharge) instead of decreasing the power production point, thus reducing the wind farm generation from the optimal production point.

In [55], a wind farm is also assessed but in this case the application is an IWP system: a wind farm with storage capacity. The relevance of this work lies in the fact that the proposed controls are tested in a real facility composed by 12 MW of wind power and 1.6 MW of lithium-ion battery energy storage system. Tested controls are the primary reserve, or the frequency support, the inertia response and the power oscillation damping. On this power management layer, once the mentioned controls are operated, the power dispatch is carried out, for distributing the power references between the wind generators and the energy storage system.

Another IWP application analysis is carried out in [50]. As explained in the previous part, the authors consider a wind/hydrogen/supercapacitor hybrid power system and separate the energy management layer and the power management layer. The power management layer is called Automatic Control Unit (ACU). In this unit, they have separated the power management control for each power device, which are the wind generators, the supercapacitor, the electrolyzer, the fuel cell and the grid connection unit. The control strategy is applied using PI controllers in order to regulate the desired variable of each unit and without causing controlling conflicts between controllers.

The power management layer is also analyzed in [49]. The IPV residential application that has been worked with considers PV generators, batteries and supercapacitors. The authors consider an IPV residential application but they also consider a microgrid composed by some households and other different loads (critical loads and controllable loads). In the power management layer of the IPV household, the authors have presented a strategy to manage solar energy resources and grid requirements, having a primary frequency control mode as well as a PV limitation mode, a storage mode but no real time power dispatching mode. Depending on the working mode, the PV, the batteries and the supercapacitors are controlled on a different control method.

Hydrogen based grid-friendly Zero Energy Building (ZEB) developed by [18] proposes another residential IPV system. Authors develop optimized energy and power management strategies. The power management layer includes some auxiliary services (peak-shaving and Reactive Power Control (RPC)) and a back-up service. In the ZEB facility the auxiliary services together with the back-up service are implemented in the electric energy storage control and fuel cell and electrolyzer operation is commanded taking into account the energy management references. This power management layer is simulated in a RT-Lab real-time simulation platform, where the interaction between the energy management layer and power management layer are tested.

In [56], another IPV system is presented composed by a PV - lithium-ion battery - supercapacitor system. In this case, the IPV system supplies the needed energy of a microgrid. Nevertheless, this microgrid is also connected to the main grid. The power management presented in this work explains a state machine control strategy, taking into account the following states: black-start, islanding and grid-connected. The power management strategy describes a control structure enabling, through the supercapacitor system, fast variations (low energy and high power value) and enabling also, through the lithium-ion battery system, the possibility to balance the PV production and the consumption of the loads (high energy and lower power value).

For the above mentioned energy management strategies, the author in [53] has developed multiple power management complementary controls which are: 1) preferred state-of-charge, 2) power change rate limitation, 3) meteorologically-based adjustments, 4) steps optimization, and 5) predictive control for constant steps value. In the scope of this work, the most important control is the predictive control for constant steps value. This control is also developed in [27]. In this control, the future prices of the electricity and the SOC of the ESS are considered in order to decide whether the commitments are going to be accomplished or not, accepting the corresponding penalties.

The Wakkanai Mega Solar Park, in Japan, is composed of 5MW of PV panels and 1.5 MW - 11.8 MWh of Sodium Sulphur (NaS) battery system [15, 16, 57]. In the power management layer, the NaS battery system is used to reduce the short term fluctuations of the PV production through different strategies: a Moving Average (MA) method and a HYbrid (HY) method. The HY method selectively uses the MA and the Fluctuation Center Following (FCF) methods according to the fluctuation magnitude. In [57], a comparison of these two methods is carried out.

The last project analyzed in this state of the art is the European Union supported ILIS project, Innovative Lithium-Ion System management design for MW solar plants [13]. This project integrates a 1 MW - 560 kWh lithium-ion battery energy storage system to a 1.2 MW PV power plant in Navarre, Spain (Figure 1.10). In [14], the developed power management layer proposes some ancillary services (constant power production, active power ramp rate limitation, frequency control function and voltage control function). The imperative need of a centralized plant controller is demonstrated for the improvement of the PV systems integration into the grid. This power management layer calculates the ancillary services responds (power references) and dispatches them around the lower level, which is the power electronics layer. The advantage of the use of the ESS is clearly concluded with the different control modes, showing the results obtained with and without the use of the ESS.

Figure 1.10: Aerial picture of the ILIS project PV power plant demonstrator.

1.3. Energy storage systems

Energy storage systems are one of the key elements to solve the biggest electric grid challenge: the imperative constant balance between production and consumption. Moreover, it is also important for a lot of different applications which are not always connected to the electric grid. In these applications the storage system provides the energy needed to autonomously work during a specific period of time. And, in the present issue, it is also a key element for a well-suited integration of the RESs to the electric network, due to the fact that it allows the flexibility, reliability, availability and efficiency of these variable and unpredictable energy sources [13-18, 53, 58, 59].

1.3.1. Energy storage systems' technologies

The energy storage system could be classified depending on their technology or their work principle, as mechanical, electromagnetic, electrochemical and thermal [60]. As summarized in [53, 61, 62], a detailed classification of energy storage technologies is shown in Figure 1.11.

Depicted electromagnetic storage technologies are ultracapacitors or supercapacitors and Superconducting Magnetic Energy Storage (SMES). Mechanical storage technologies are Pumped Hydroelectric Storage (PHS), Compressed Air Energy Storage (CAES) and Flywheel Energy Storage (FES). Electrochemical technologies are separated into Battery Energy Storage (BES), Flow Battery Energy Storage (FBES), air batteries and hydrogen based storage. BES can be differentiated into lead acid batteries, nickel cadmium (NiCd) or nickel metal hydride (NiMH) batteries, sodium sulphur (NaS) batteries, zebra batteries and lithium-ion (Li-ion) batteries. FBES, could also be divided into vanadium redox batteries and zinc bromine batteries. Finally, thermal operation principle energy storage is formed by the High Temperature Thermoelectric Energy Storage (HT-TES) and Low Temperature Thermoelectric Energy Storage (LT-TES).

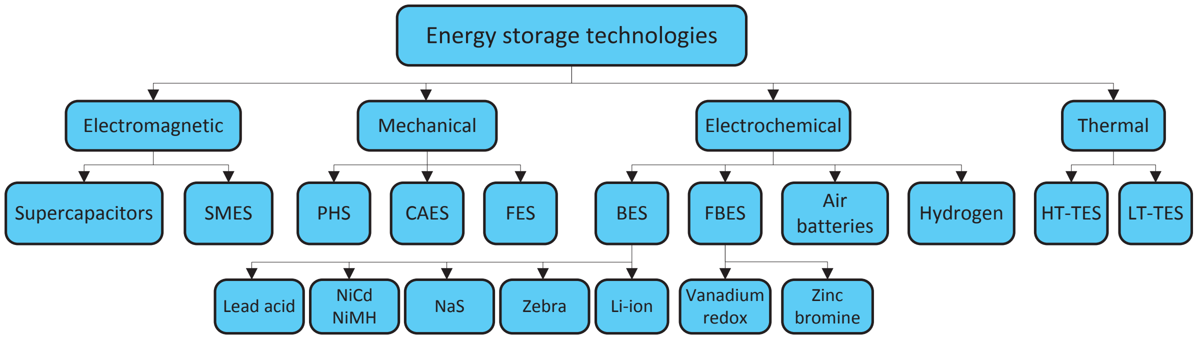

Figure 1.11: Classification of energy storage technologies [53, 61].

Some of these technologies are more suited for the integration of RESs [50, 56, 63-65] due to their characteristics. Note that some of them, like PHS or CAES, require some natural conditions to operate. Nowadays the most emerging technologies are the electrochemical ones and mainly the battery based energy storage systems. Among them, even if lead-acid and nickel based technologies have solid market share due to their maturity and low cost, sodium sulphur and lithium ion are the most installed technologies. Lithium based technologies are expected to dominate the market in a mid-term perspective. An example of this fact is shown in [59], where it is stated that actually one third of all ESS projects are based on lithium-ion technology.

The characteristic parameters to determine the appropriate technology for each application are explained in the following sub-section.

1.3.2. Energy storage systems characteristic parameters

As it has been explained before, there are several technologies of storage system and each one of them has its main characteristics. For each application, some characteristics are much more important than others. In this case, for the integration of RESs, the identified most representative technical parameters of an energy storage system are the next ones [53, 66-68]:

- **Power capacity [W]:** It is the maximum power that the ESS could provide. Its charge power capacity and its discharge power capacity can be different.
- **Energy capacity [Wh]:** It is the amount of energy that the ESS could store. It is also named as capacity (C) and measured in Ampere-hours [Ah].
- **Power to energy ratio [W/Wh]:** It describes the ratio between power and energy.
- **C-rate:** It specifies the speed of charge or discharge rate of the storage system. It determines the storage system's charge or discharge current in relation to its nominal capacity which is expressed by the letter C and measured in Ampere-hours

[Ah]. A charge or discharge of nC rate means that the capacity of the storage system will be charged or discharged in 1/n hours. For example, a 50 Ah storage system which is being discharged at 2C rate implies a 100 A current and a 0.5 h discharge time.

- **Energy density [kWh/m3]:** It represents the available energy per volume unit.
- **Specific energy [kWh/kg]:** It quantifies the ratio of the energy delivered to its weight.
- **Power density [kW/m3]:** It defines the available power per volume unit.
- **Specific power [kW/kg]:** It depicts the ratio of the power delivered to its weight.
- **Energetic efficiency [%]:** It shows the relation between the discharged energy and the amount of energy needed to restore the initial charge state, under specific conditions. It is measured in percentage.
- **Life cycles [cycles]:** It determines the quantity of consecutive charge and discharge processes that a battery can undergo while maintaining some minimum performances.
- **Calendar life [time]:** It determines the period of time in which the battery maintains some minimum performances without being used.

The Electricity Storage Association [60] shows some figures of several storage technologies which include two parameters' relation. In Figure 1.12, the relation between the discharge time and the rated power is depicted, where it can be concluded that for large scale energy storage systems the PHS is the most appropriated technology. In this figure, knowing the discharge time and the rated power, the energy capacity parameter can be obtained, and for that reason, this figure is one of the most illustrative ones to evaluate the power and energy rates of each technology.

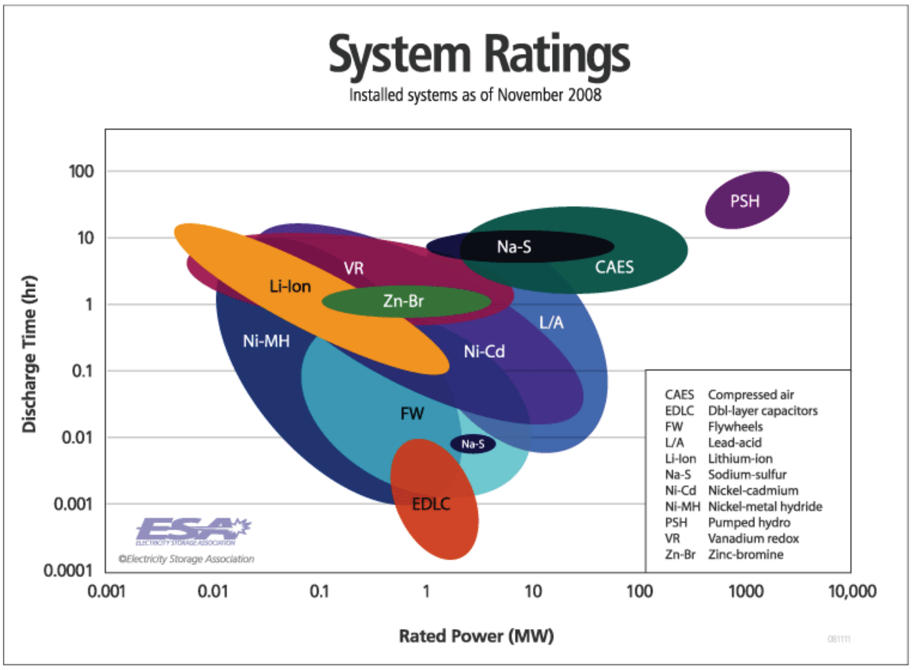

Figure 1.12: Energy storage technologies discharge time versus their rated power [60].

From Figure 1.12 it can be observed that the characteristics of the lithium-ion technology are wide and cover a large region, from large discharge time (over 10 hours) to rated power that overpasses the MW range. Other technologies as lead acid or sodium sulphur have a larger rated power characteristic compared to the lithium-ion technology.

In Figure 1.13, two other important parameters are shown, which are the technology efficiency and the lifetime. These two parameters are proportionally related to the energy storage system cost. On the one hand, the efficiency means losses of energy while charging and discharging the storage system. On the other hand, if the purpose is to cycle the ESS thousand times, the replacement cost has to be evaluated. Thus, this figure is also very illustrative to evaluate the technologies' performances.

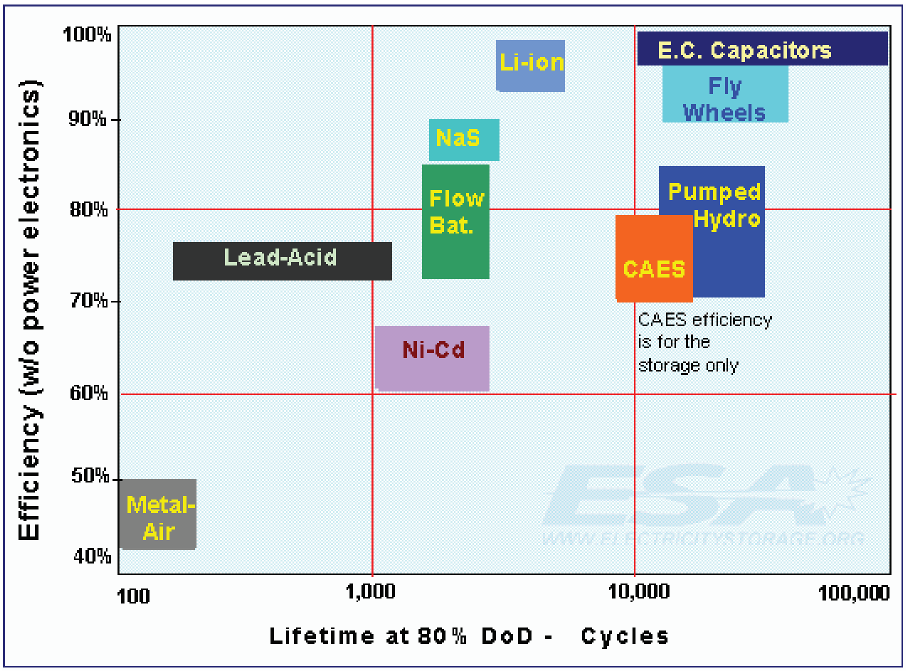

Figure 1.13: Energy storage technologies' efficiency versus their lifetime [60].

The most beneficial area of this Figure 1.13 is the upper right side of the figure, for being very efficient and for having a long lifetime. As it can be extracted, the lithium-ion technology has very high efficiency with a lifetime of several thousands of cycles, so it is demonstrated that currently it is a relevant technology. The characteristics of the other electrochemical technologies are not so good as the ones of the lithium-ion technology.

1.3.3. Energy storage system sizing methods

As stated in the introduction of this document, the sizing process of an energy storage system is one of the key factors of the present work. The sizing process which includes the definition of power and energy requirements is totally correlated with the management of the storage system, and for that reason, the sizing process has to be co-performed with the energy management strategy.

An example of this significant correlation is explained in [23] and shown in Figure 1.14. The power requirement for an energy storage system is the instantaneous value between the PV power production curve (the black one) and the other curves (the power commitment with different energy management strategies, EMSs). As it is shown, the hourly constant power step curve (the orange one, named HCPS) represents the configuration requesting a lower power, because it is continuously close to the PV power production curve. The energy requirements' value is the area drawn between the PV power production and the commitment curves. In this case, the single constant power step curve (the red one, named 1SCPS), which was established by a simpler EMS, needs the highest energy value.

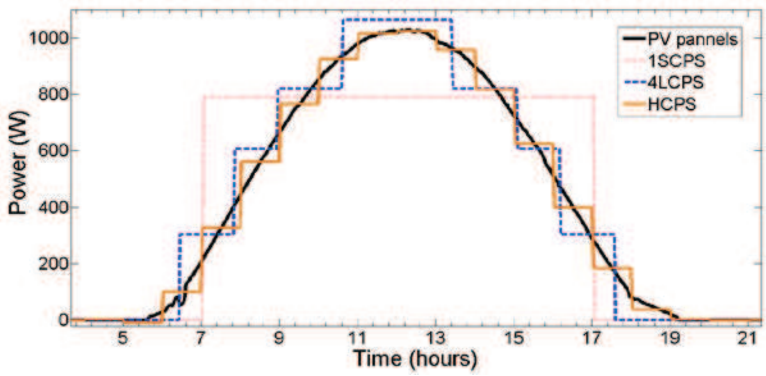

Figure 1.14: Real PV power production pattern and different power commitment according to different EMS configurations [23].

Together with this figure, in the same study, the energy storage sizing is conducted taking into consideration also a simulation of a whole year and still applying each of these three EMS. The results of these simulations are shown in Table 1.1, where the percentage of time that the IPV power plant cannot track the EMS calculated grid power is presented as a function of the storage system capacity. This percentage of time that the IPV power plant cannot track the EMS calculated grid power is due to the fact that the storage system is saturated, upward (fully charged) or downward (fully discharged). As it can be seen, with a simpler EMS configuration as the SCPS, the storage system is saturated much quicker than with more complex strategies. The HCPS, which is the most complicated one, has then the best results with regards to the other storage systems sizing.

Table 1.1: Percentage of time that the IPV power plant cannot track the EMS calculated grid power as a function of the storage system capacity. Source: [23].

EMS configuration	Capacity 0.2 pu	Capacity 0.25 pu	Capacity 0.3 pu	Capacity 0.35 pu	Capacity 0.4 pu	Capacity 0.45 pu	Capacity 0.5 pu
SCPS	9.32	5.40	2.94	1.79	1.08	0.61	0.29
4LCPS	2.68	1.48	0.88	0.50	0.29	0.18	0.11
HCPS	1.63	0.94	0.64	0.37	0.26	0.16	0.09

As a conclusion, with a more complex energy management strategy, lower power and energy requirements are needed and vice versa. For matching these two criteria several sizing methodologies have been described in the literature.

In [69] and in [43] one sizing methodology is presented, which will be the base for other methods explanation. This methodology is separated into three steps, which are the definition of system requirements, the sizing of the energy storage system and the verification of possible solutions. In Figure 1.15, graphical illustration of this methodology is proposed.

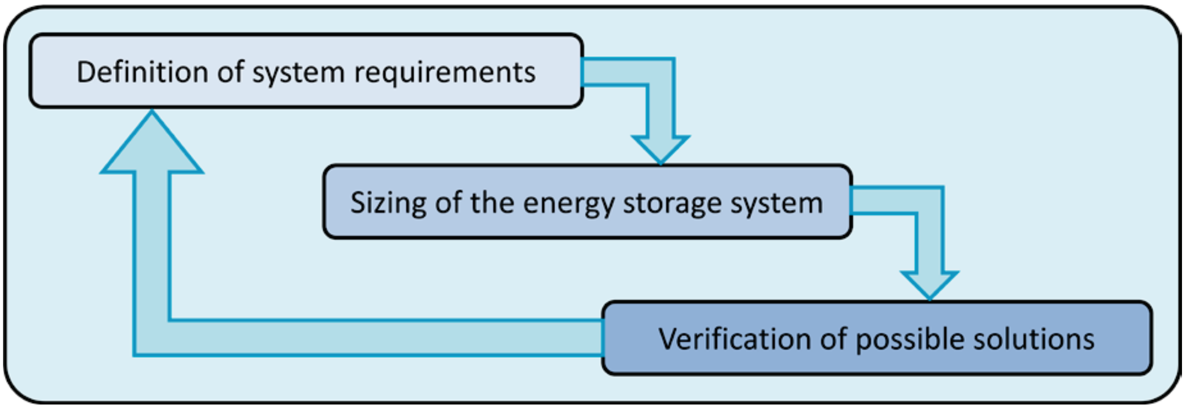

Figure 1.15: Energy storage system sizing methodology [43].

In this first step, the definition of the system requirements is done as well as the system constraints' definition. The storage system's requirements are the power and energy needs. Other important requirements are the energy and power management strategies. In order to determine the optimal sizing of the energy storage system, the energy management strategy definition is necessary. The energy storage system constraints are related to the characteristics of the application. In this case, these are: the connection voltage to the grid, the volume and the weight of the storage system, the operation temperature and the efficiency. But there are some other constraints that are not related to the application, like lifecycles, calendar life, capital and BMS cost and maintenance cost of the storage system.

In the second step, the energy storage sizing is calculated, taking into account the system requirements and constraints. In order to achieve the system's requirements, several solutions can be considered. The third step consists thus in verifying the possibilities and evaluating the options before going back to the first step for changing some requirements or constraints in order to improve the final sizing result. In this feedback, the energy and power management strategy could be changed to calculate the optimal sizing for that new strategy. With several strategies/sizing relation results, the optimal storage sizing could be selected considering its optimal strategy.

The energy management strategy is introduced in the first step, as one of the definitions of the system requirements for the following sizing process. It has been decided to select first the energy management strategy in order to size the storage system based on this strategy. Nevertheless, the energy storage sizing methods can be separated by their nature and they can also be grouped in different categories. As a first work, a classification based on the nature of each sizing method is proposed and shown in Figure 1.16.

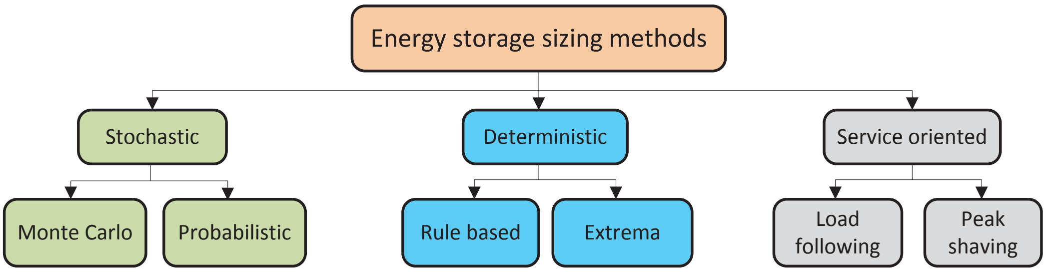

Figure 1.16: Proposed energy storage sizing methods classification by their nature.

1.3.3.1. Stochastic energy storage sizing methods

Stochastic methods for energy storage sizing are, as their name indicates, methods that are dependent to predicted values and also dependent to some random elements. The probability methods are, thus, included in this group.

Monte Carlo method

Monte Carlo sizing method is a stochastic method. It randomly generates some inputs (in this case sizing parameters) and verifies if those inputs accomplish the required performances. The more iteration, the better result is.

For energy storage sizing, this method is used in [70], where an IPV application at the residential scale is considered. Taking into account load profiles, weather forecasts and the local historical outage distribution of a household, the Monte Carlo method calculates energy storage sizing parameters for the demand shift at peak electricity cost and outage protection objectives.

Another energy storage system for wind power application is analyzed in [51]. The authors use an autoregressive model to obtain the correlation of the day-ahead forecast errors. Afterwards, they quantify the impact of this correlation with the storage sizing by means of a Monte Carlo approach, using the autoregressive model as input. Taking into account the time when the storage system is saturated (totally charged or discharged), the authors are able to compute an optimized size of the storage system.

Probabilistic approach

A probabilistic approach is another stochastic method based on probability. Its first step or its input is the predicted value(s). From this data, the probability of having an error is calculated and error probability areas are obtained as shown in Figure 1.17.

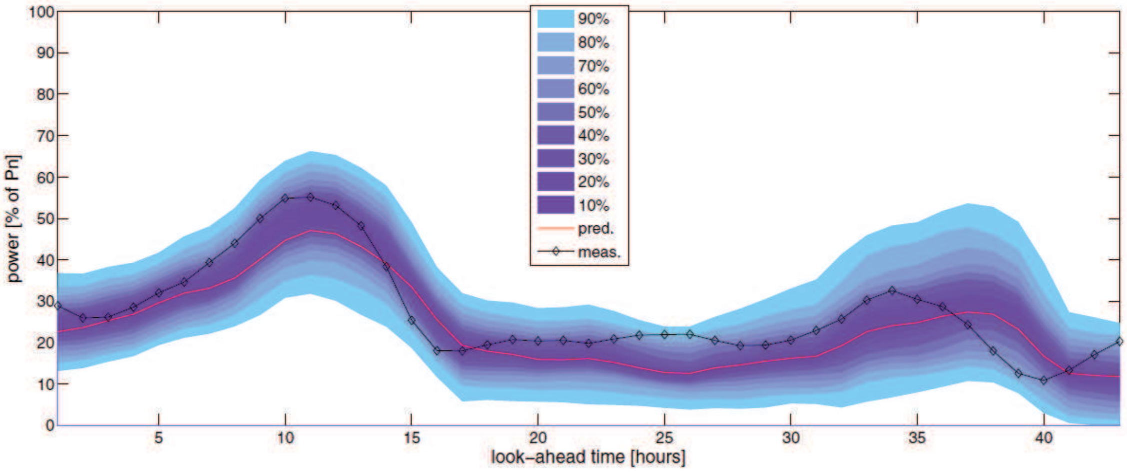

(a) Point and probabilistic forecasts

Figure 1.17: Probability of wind power generation forecast error [71].

The sizing problem also appears for wind energy applications with an energy storage system. In [71] the sizing problem tries to minimize the power production forecasts errors, assuming the market conditions where penalties are considered. Based on a probabilistic forecast, the sizing requirements could be minimized.

In [72], another IWP application where the storage sizing is carried out through a probabilistic approach is developed. The objective of the proposed method is the reduction of the uncertainty on wind power forecasts (up to 48 hours), analyzing the statistical behavior of the forecast error as well as the SOC. Empirical probability density functions are developed reducing the size of the ESS and the uncertainty of the IWP system.

1.3.3.2. Deterministic energy storage sizing methods

Deterministic methods for energy storage sizing are, as their name suggests, methods that are not dependent to randomness to calculate inputs/outputs' relationship.

Rule based method

Rule based method is a simple method that contains some rules. It applies the desired control output to the given inputs of the system. It is an applied method that can be used as a benchmark to assess other more advanced techniques.

For an IPV grid scale application, in [23], the sizing process relation with the energy management system is analyzed and discussed. The authors have developed three EMSs that are 1) one single constant power step; 2) four-level constant power step; and 3) hourly constant power step (HCPS). These energy management strategies are based on rules, so they could be considered as rule based methods. For each of these EMSs and for a different capacity sizes, the authors have calculated the percentage of the time the IPV power plant cannot track the reference grid power. These different sizing capacities are selected depending on the PV plant capacity factor, which is the equivalent value of energy that each kW installed could produce per day. Thus, the sizing is not calculated but analyzed related with the EMS configurations. Nevertheless, they have showed that with the HCPS strategy, the energy requirements are much lower than in the other energy management strategies.

Extrema method

Extrema method is a deterministic strategy which makes a grid search of a set of input values and obtains their feasibility range to keep the optimal solution.

In [73], the application of an industrial customer with a battery energy storage system is considered. The objective service is the peak load shaving, but the methodology used for the calculus of the sizing is optimized maximizing the customer's economic benefits. For doing so, the sizing and the operating steps are developed using the "extrema" method for optimizing the sizing problem and using dynamic programming strategy for the operation optimization. Dynamic programming is an optimization method for large decision problems which breaks the problem into smaller sub-problems, separately solving each one of them and obtaining an optimal decision policy [74].

1.3.3.3. Service oriented energy storage sizing strategies

The strategies included in this section are completely oriented to provide a given service. Multiple applications could be taken into account but only the ones related to grid services are considered in this section.

Load following strategy

The objective of this strategy is to adjust the output power to the demand of electricity. When the demand is important, this strategy leads to produce more, and when the demand is low, the strategy decreases the generation. In the case of an energy storage system, it could refer to absorb energy.

In [75], the analyzed application is a residential distribution feeder where a battery energy storage system is installed. The objective (the service to be provided) is the shaving of the peak where a percentage of the peak power is selected setting a lower peak value. From this value the power requirement is calculated, and with an analysis of the time when this value is exceeded, the energy requirement is also obtained. This method is referred as load following method. In this paper, the impact of the distributed PV generation in a BESS sizing is briefly analyzed, concluding that the power sizing is maintained and the needed amount of energy (for the storage) is reduced.

Peak shaving strategy

The objective of this strategy is to reduce the peak power providing an amount of energy from the storage system, reducing the given peak. This service is used to avoid a higher power contract in end user applications (residential and commercial) and also to avoid having to repower a substation, from the grid operator point of view.

A residential application equipped by a BES/PV system is analyzed in [36, 76, 77]. The authors have studied the sizing problem, proposing upper and lower bounds for the storage size and two algorithms to calculate the exact storage size taking into account a fixed load curve and time-of-use electricity purchase rate. The provided services are power arbitrage and peak shaving and the objective is to minimize the purchase cost from the grid with the optimal battery size while satisfying the fixed loads. It has been verified that for certain scenarios, the characterization of the exact storage size is achievable, but without considering the loads variation possibility as well as real hourly changes in electricity purchase.

1.4. Electricity market analysis

In this section, an electricity market analysis is proposed. This state of the art review concludes with an analysis of the market where the IPV power plants could seek for an economical viability through their participation. The electricity market selected is the Spanish one, due to the fact that Spain is one of the European countries with higher renewable energy integration level.

Similarly to the other European electricity markets, the liberalization of the Spanish sector was established in the 90s [78]. Since that moment, the sector regulation laws have been gradually signed as well as renewable sources referred laws [79-82]. In the first laws, important incentives, financial support and feed-in-tariff were signed [81, 82], which heavily increased the Spanish photovoltaic share. Nevertheless, by means of other laws, these incentives decreased after that [80], until recently (2013) [83, 84]. These last laws have dramatically stopped the renewable energies' incentives.

In this context, the situation for the renewable generation systems over the coming years is that they could participate on the electricity markets in the same conditions, with the same rights, the same obligations and without any incentives as other traditional generation units. So the next section describes the organization of the electricity markets and the markets where the IPV power plants could potentially participate.

1.4.1. Organization of electricity markets

Throughout all Europe, most electricity markets are similar and have the same markets: futures markets, daily market (day-ahead market), intraday markets and operation markets (system adjustment markets). The organization of the electricity markets is distributed in the previously mentioned markets where requirements for offering and bidding are different among all of them. Each market is organized in a different way and the Iberian Peninsula case is summarized in the Figure 1.18.

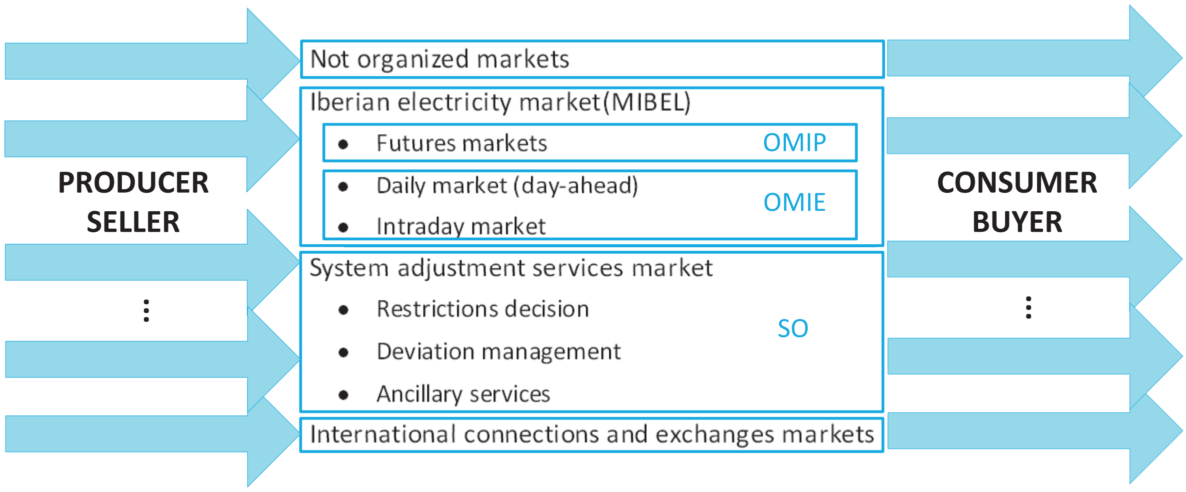

Figure 1.18: Iberian organization of the electricity markets.

"Not organized" markets are energy contracts between some producers and some big consumers like an industrial factory.

The Iberian electricity market (MIBEL, *Mercado Ibérico de la Electricidad*) [85] is the market where almost all of the energy needs are negotiated, using different markets. In the future markets, which are managed by the Portuguese section of the Iberian Market Operator (OMIP, *Operador del Mercado Ibérico – Polo Portugués*), long term contracts (week, month, quarter and annual) are auctioned [86]. The other MIBEL's markets, the daily and the intraday markets, are managed by the Spanish section of the Iberian Market Operator (OMIE, *Operador del Mercado Ibérico – Polo Español*) [87].

Daily market, also known as pool market, is important because its objective is to match the whole energy that will be consumed on the following day [88, 89]. The Market Operator (MO) receives the producer and consumer's offers for each programming period (an hour period in that case). With those offers the matching process is carried out starting from the lowest offers until the crossing point between the offer and the demand with the lowest price in each programming period. That price is known as marginal price. Generators and consumers that have presented a lower generation offer (and greater consumption offer) than the marginal price are scheduled for generation/consumption (power commitment) and are paid at the marginal price.

Besides the daily market, which has been resolved on the previous day, another market exists which is the intraday market and it is resolved closer to operation time. It is not always possible to match the forecasted consumption profile with the daily market scheduled power, and these differences are solved by the intraday markets. In the Iberian markets' case, six intraday markets exist, where the same process as in the daily market is carried out despite the fact that each intraday market has a different duration [89], from 27 hours to 9 hours.

An example for the daily market matching process for the hour 12 of the 7th August 2015 is presented in Figure 1.19.

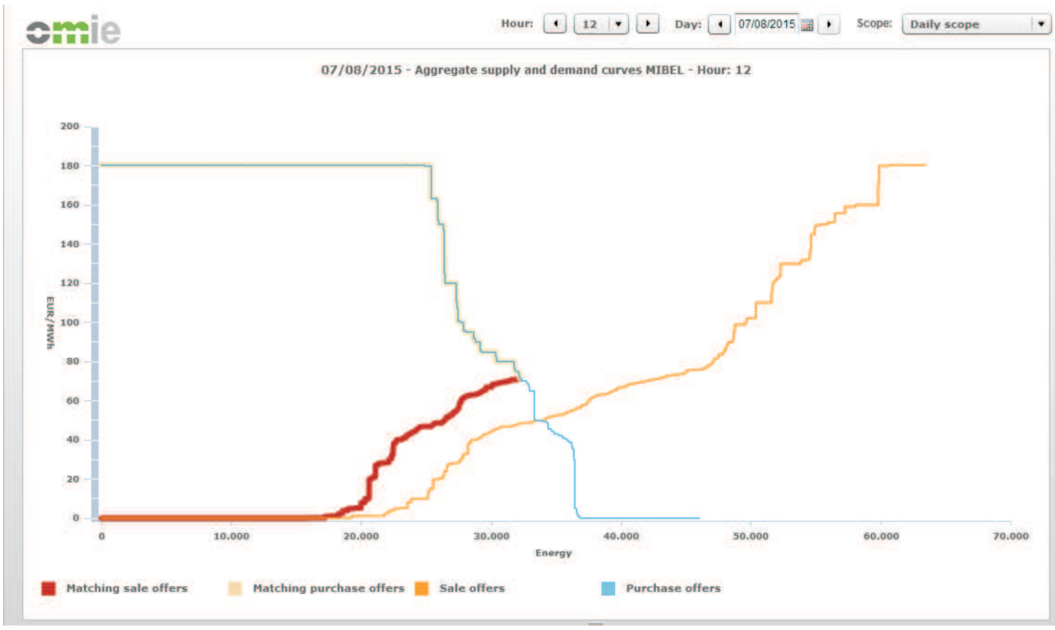

Figure 1.19: Daily market matching process curves of generation and consumption of the hour 12 (from 11:00 to 12:00) of the date 2015/07/08 [87].

Once the daily market has been closed by the OMIE, the information is transferred to the System Operator (SO), REE (*Red Eléctrica de España*) (P.O. 9.0) [90], which makes the necessary technical adjustment and restrictions (P.O. 3.2 and P.O. 3.10) [91, 92]. After this adjustment, the final matching curves are generated, also visible in Figure 1.19, where the final marginal price for each hour is defined. The System Operator also organizes the deviation market, (P.O. 3.3) [93], if necessary, and the ancillary services market. As ancillary services, the Iberian System Operator, REE, considers the voltage control (P.O. 7.4) [94], an additional reserve power to be raised (P.O. 3.9) [95] and frequency regulation. Regarding the frequency regulation service, the primary (P.O. 7.1) [96], secondary (P.O. 7.2) [97] and tertiary (P.O. 7.3) [98] reserves are taken into account. In the Iberian electricity system the primary regulation is a compulsory service that all generators must provide and it is not remunerated.

The last market or power exchange identified in Figure 1.18 is carried out at an international level (P.O. 4.0) [99], including daily markets as well as two intraday markets with France (P.O. 4.1) [100], and daily markets with Morocco and Andorra. These markets are bidirectional, but the power exchange is not always transferred from both countries.

1.4.2. Operation of traditional generators on electricity markets

In this section, the operation of traditional generators on electricity markets is detailed, explaining the process of the most important markets and the timing when offers must be sent to the market operator. A general overview of the mentioned markets is shown in Figure 1.20.

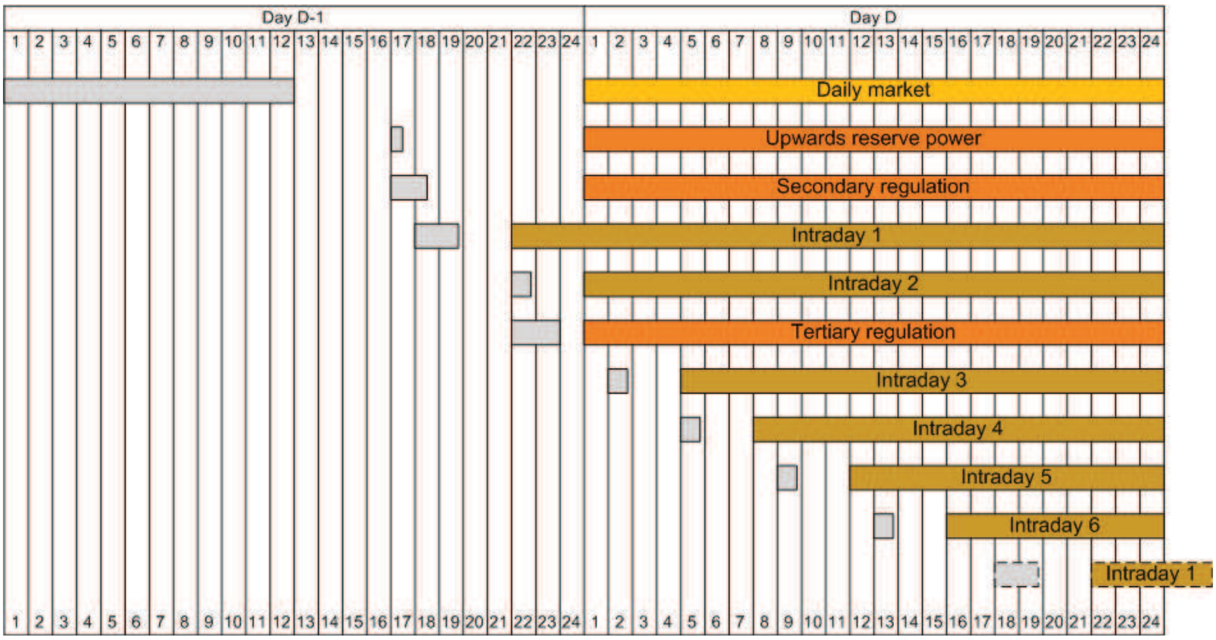

Figure 1.20: Iberian Peninsula electricity markets operation schedule and offers sending period of time.

1.4.2.1. Daily market

The daily market is the most important market of electricity because the whole part of daily energy transactions are bidden and cleared in this market. It is also known as electricity pool market. The horizon of this market is composed by the 24 hours of each day. Generators prepare their generation planning and try to clear themselves in this market.

The planning offers (for the daily market) to the day D must be sent to the market operator before midday of day D-1, as shown in Figure 1.20 [10-12]. These offers (or bids) are composed by an amount of energy at a given price for each market period, normally an hour.

The market operator clears each market period and sends the results to the system operator. The system operator includes the technical constraints concluding with the viable daily schedule [11]. This schedule is sent to all generators, including the cleared amount of energy to produce and the associated marginal price for time step (each hour).

From this moment on, if the offers sent by a generator are accepted, they must be provided as cleared energy, during the cleared market periods of the day D. If the offers are not accepted, the concerned generators do not have to produce energy in this period of time. This means that all generators willing to participate in the daily market need to have very reliable production predictions on a day-ahead basis, to be able to make feasible offers.

As the generation plan is based on the day ahead predictions of generation and consumption, errors are to be expected on these predictions. Moreover, as the daily market cleared energy is resolved by means of offer and demand laws, not all the electricity needs are solved. For that reason, the market participation is not only based on the daily market, and the differences in consumption needs are solved taking advantage of the intraday markets, which are closer to the real time operation. The closer the market period is to real time, the better the system operator consumption predictions are.

1.4.2.2. Intraday market

Intraday markets exist to clear the consumption needs that have not been resolved through the daily market. It can be considered as some kind of adjustment markets. All generators that have participated in the daily market can participate in the different sessions of the intraday market [11]. In the Iberian Peninsula the six intraday sessions are operating on different time horizons, which are depicted on Figure 1.20 and detailed in Table 1.2 [11].

Table 1.2: Intraday sessions detailed information.

	Intraday sessions					
	S1	***S2***	***S3***	***S4***	***S5***	***S6***
Session opening	17:00	21:00	01:00	04:00	08:00	12:00
Session closing	18:45	21:45	01:45	04:45	08:45	12:45
Program publication	20:45	23:45	03:45	06:45	10:45	14:45
Schedule horizon	27h	24h	20h	17h	13h	9h
Operation starting	21:00	00:00	04:00	07:00	11:00	15:00

Market participators (also named market agents) can offer a purchase or sale bids. So, the generators can sell and buy energy, adjusting their operation program. The market operator clears each market period and sends to the system operator the cleared powers and prices. The system operator publishes then the final program, including the technical constraints. This program is named the hourly final program (PHF, in Spanish) [11].

As it could be verified in Table 1.2, the period between the session closing and the operation starting time is closer than in the daily market, which offers the availability to present more performing bids from all generators, and especially from renewable generators, based on closer and better predictions. Another important remark that can be done about the intraday market is that there is a market session every 3-4 hours (except between session 6 and session 1 of the next day, where there are 6 hours). This fact provides the opportunity to adjust all generation programs each 3-4 hours.

1.4.2.3. Ancillary services

The Iberian System Operator, REE, considers as ancillary services voltage control, additional reserve power to raise and frequency and power regulation (with primary, secondary and tertiary reserves). The primary regulation or frequency regulation (P.O. 7.1) [96] is a compulsory service that all generators must provide and it is not remunerated.

The voltage control is remunerated but it is not resolved through market offers due to the local voltage control needs which make impossible its market regulation. For that reason, there is a minimum compulsory service that all generators must furnish. It is also composed by a not compulsory service due to the extra reactive power generation capabilities of some generators. These generators offer their capabilities every year and the system operator take advantage of them only if it is necessary, remunerating them as detailed in (P.O. 7.4) [94].

The additional reserve power to raise service (P.O. 3.9) [95], also known as upwards reserve power, is a service oriented to thermal generation units. As these units are fully controllable and have different operation modes, they can provide a significant amount of power during the periods that the SO needs. It is an optional daily process to guarantee the security of the power system that the SO can call if needed. As it is not a service that renewable power plants could participate on, it is not analyzed more in detail.

The secondary regulation (P.O. 7.2) [97] is a system adjustment service in which frequency deviations are automatically controlled by the Automatic Generation Control (AGC) units. Each AGC unit sends a power variation reference (upward or downward) to the secondary regulation generation units to react to frequency variations. Time horizon of this service is comprised between 30 seconds and 15 minutes. It starts in 30 seconds due to the fact that the primary regulation regulates the frequency until this time. The generation units, selected to provide this service, are paid for two different factors: the power reserve to be provided (cleared in the market) and the actual energy provided (only paid if the service is finally provided). This market is resolved between 16:00 and 17:30 and the generation units that clear this market are the ones that offer the lower price until satisfying the SO requirements. As the frequency could be regulated upward and downward, the generators that want to participate in the secondary reserve market must offer the possibility to raise and to drop the power [95].

If an important frequency deviation is not resolved within 15 minutes, the tertiary regulation (P.O. 7.3) [98] will start. The main objective of the tertiary reserve is the constitution of the secondary reserve. This service is defined as the maximum power variation that a production unit could provide during 15 minutes within a minimum duration of two hours. The SO calls for this service manually, only when it is needed. The market offers to this service are composed by pairs of reserves to upward or downward with the prices for each service. This market is managed between 21:00 and 23:00, once several other markets are resolved for each hour (daily market, other system adjustment markets, intraday session 1, and intraday session2).

Apart from these explained closed services, if the SO detects imbalances predictions greater than 300MWh for long duration periods, it could call for another service named imbalances management, which is very occasional. When this service is called, the deviation requirements and the time duration to cover are published. The offers reception period is 30 minutes from the call presentation and the clearing prize is obtained from the lowest offers that satisfy the SO requirements.

1.4.3. PV plants and electricity markets

In this section the participation of the renewable generation, and more specifically the PV plants market integration in the Iberian Peninsula case study, is considered. The PV generation and renewable generation installed before 2010 have received important incentives and special treatment in terms of injected power. These generators have a fixed price (higher than the market price) for the produced energy and they can inject to the grid all their production, without taking into account markets' requirements of constant power production during each hour nor the bidding system of different markets (daily, intraday, etc.).

These advantageous conditions were developed during the first decade of the XXIst century to promote the renewable generation installations. Nevertheless, due to the overproduction of renewable installations (superior to what was expected), the payment conditions were reduced [80] until 2013, when the government completely cut the incentives [83, 84]. From this moment on, it is not allowed to construct a PV power plant without participating to the market requirements. As the market participation is difficult and needs an important controllability level that not all the PV power plants have, the market participation of PV power plants is happening nowadays by means of the aggregators. An aggregator is an intermediate entity between generators and the market that aggregates the producers' generation curves for participating into the market with a grouped offer. This compensates generators' errors and allows reaching the minimum power offer to participate in electricity markets, which is 100 kW.

If a PV power plant is controllable in power and wants to participate in electricity markets as any other traditional generators, a strategy could be to propose market offers below the maximum power point available, providing the firming service on the lower value of generation predictions of each programming period, as shown in Figure 1.21. In this case, knowing this lower value for each programming period and controlling the converters to provide a constant power production during this hour (which is the firming control), the PV plant can participate in electricity markets. The drawback of this strategy is that not all the available PV generation is being obtained from the PV panels, working out from the optimal point and not optimizing the PV production. Moreover, if predictions are not correct and generation has one or more points below the predicted lower value for each hour, some penalties are applied, which have an influence on the economic viability of the PV power plant.

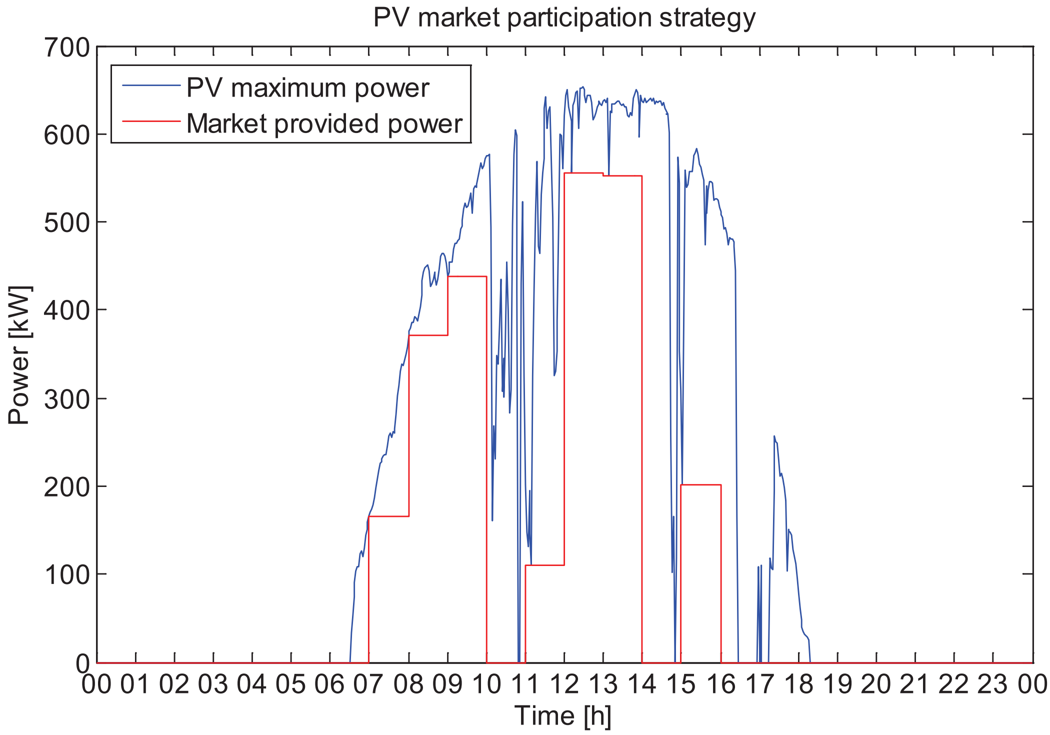

Figure 1.21. First strategy to participate in electricity markets from a PV power plant.

To overpass these drawbacks and to optimize the whole PV generation, another strategy is to directly participate on electricity markets with an associated energy storage system (ESS), forming the intelligent photovoltaic (IPV) power plant. It is the core of this PhD work. The ESS contributes increasing the controllability, flexibility and delivering an energy reserve that provides the capability of optimizing the PV generation while firming control is carried out, balancing the generation fluctuation based on the storage availability. Moreover, depending on the energy storage size, it could store PV generation in cheaper hours to sell them in more expensive hours also taking into account markets' prices for optimizing the economic exploitation of the whole system.

In addition to firming service being able to participate in electricity markets as it has been already explained, there are other services or functions that an IPV power plant could provide to the grid. These services are summarized in Table 1.3, and some of them are nowadays paid in some countries [101].

Table 1.3: Possible functions that an IPV power plant could provide to the grid [101].

Possible functions that an IPV power plant could provide to the grid		
Arbitrage	Frequency control or primary control	Black-start
Power shifting	Inertia emulation	Power quality improvement
Filtering or firming	Power oscillation damping	Load leveling/peak shaving
Voltage control or var regulation	Islanded mode operation	Demand side management

The most representative or usual ones are: the frequency control or primary control service which is referred to primary frequency regulation; the voltage control or var regulation which operates similarly but injecting or absorbing reactive power for controlling the voltage value; the power shifting service which is used to shift the production profile and to match the demand curve; the power quality improvement service which reduces the production fluctuations as well as unbalances and distortions, filtering the output profile of the generator or producer; and the firming or filtering service, which makes the output profile constant for participating in the electricity market.

Some of these functions or services demand a low power and energy requirements, and some other ones demand greater power and energy requirements. For that reason, depending on the objectives (functions or services) for the desired application, it is necessary to consider the benefits obtained due to increasing the size of the storage (providing more services) counteracted with the extra costs assumed by that system. Once weighted up these mentioned issues, the sizing of the ESS has to be carried out, also taking into account the most appropriate storage technology. Nevertheless, it is known that the storage system capacity cost is the most expensive part of the whole IPV power plant, and for that reason it will not be viable to construct an IPV power plant with a huge storage system to provide services of big amounts of energy as secondary or tertiary regulation. The same reason cancels the purely arbitrage service: buying cheap energy for storage and selling expensive energy from the ESS.

Considering the above explained possible services operation, several projects of IPV power plants are being developed as demonstrators all over the world. These demonstrators are developed for showing the usefulness of participating in different markets and services as represented in the Table 1.4. In this review, not only the PV power plants are analyzed, but also a possible combination of wind power with storage systems (named IWP) due to the drawbacks of the PV fluctuations and predictions difficulties also happening with the wind power. Location, battery energy storage system technology, application and provided services are included in this review presented in the Table 1.4, where all included systems are experimental installations.

Table 1.4: Relevant experimental RES + BESS installations summary.

Relevant experimental RES + BESS installations				
Project	**Location**	**BESS Technology**	**Application**	**Provided services**
PNM Prosperity Energy Storage Project [102]	New Mexico, USA	Adv. lead acid and ultrabatteries	**IPV** BESS (750 kW / 2.8 MWh) PV (500 kW)	Voltage control, power shifting and peak shaving
ILIS Project [13, 14]	Navarre, Spain	Lithium-ion	**IPV** BESS (1 MW / 560 kWh) PV (1.2 MW)	Firming, voltage control, frequency control and ramp rate control
Kaua'I Island Utility Cooperative (KIUC) Project [17]	Hawaii, USA	Adv. lead acid	**IPV** BESS (1.5 MW / 1 MWh) PV (3 MW)	Firming and frequency control
Wakkanai Mega Solar Project [16]	Wakkanai, Japan	Sodium sulphur (NaS)	**IPV** BESS (1.5 MW / 11.8 MWh) PV (5 MW)	Firming and short term fluctuation reduction (filtering or firming)
National Wind and Solar Energy Storage and Transmission Demonstration Project (I) [103]	Zhangbei, China	Lithium-ion	**PV + WP + BESS** BESS (6MW / 36MWh) WP (100 MW) PV (40 MW)	Power shifting and firming
Tehachapi Wind Energy Storage project [104, 105]	California, USA	Lithium-ion	**IWP** BESS (8MW / 32MWh) WP (660 MW)	Power shifting, firming and frequency and voltage regulation
Kaheawa Wind Power Project II [106]	Hawaii, USA	Adv. Pb acid	**IWP** BESS (10MW / 7.5 MWh) WP (21 MW)	Power shifting, firming, reserve capacity and frequency and voltage regulation
Rokkasho-Futamata Wind Farm [107]	Rokkasho, Japan	Sodium sulphur (NaS)	**IWP** BESS (34MW / 238MWh) WP (51 MW)	Power shifting, firming, load leveling and spinning reserve
AES Laurel Mountain Wind Farm [108]	West Virginia, USA	Lithium-ion	**IWP** BESS (32 MW / 8MWh) WP (98 MW)	Power shifting and firming

As it can be confirmed from the Table 1.4, most of the installations have the firming capacity, which is the most important function for participating in the electricity markets. Moreover, several demonstrators have also the frequency and voltage regulation control which is a payment service in some countries as USA [109], and is a necessary service in islanded regions as Japan, Hawaii or Puerto Rico [110-113]. In this last one, a new energy storage mandate was signed that requires a 30 % of minimum storage capacity for any new grid-connected solar and wind power projects to help with the control of the frequency [113]. In Chile, the government is introducing a requirement of 7 % of power reserve, which is only feasible by introducing ESS to renewable power plants [114, 115]. In French islands also a mandatory regulation requires at any time of the day that the uncontrollable electricity generation (wind and PV) never exceeds 30 % of the overall electricity consumption [116]. For that reason, in 2012 the French Electricity Regulation Commission (CRE) selected some projects to install more reliable wind generation systems to provide some ancillary services based on storage systems [51].

Another possible control that the renewable generators with storage can provide is the ramp rate control. The regulation of some countries imposes nowadays ramp rate limits [111, 112, 117, 118]. It is the case of islands or weak grids regions. This fact forces to include storage systems in those regions to enable the connection of renewable generation plants. For that reason, the ramp rate control is a very common research topic of the renewable power plants with storage systems [14, 25, 119-122].

Thus, the perspectives about renewable generators are that these types of sources must also operate as other traditional generators, participating in current electricity markets with current laws. To do so, it is necessary to develop operation strategies to maximize the economic exploitation of these systems. In that perspective, most interesting markets are the daily market and the intraday market. The daily market operation is the most beneficial one because the overall PV generation could be cleared in this market requiring a relatively low amount of energy capacity to provide the firming service. The intraday market is as beneficial as daily market when palliating erroneous predictions for example. Services that require a huge amount of energy (secondary or tertiary regulation) are not viable due to the heavy cost of the storage system. Other services, such as inertia emulation or primary control of frequency could be provided but are negligible in terms of energy for the storage system because they need a low amount of energy [25].

1.5. Conclusions

The conclusions of the analysis of the state of the art are focused on summarizing the main lacks found in the topics that are part of the present application. Therefore, the possible improvements detected within this analysis will serve as basis to the developments proposed in this PhD work.

Analyzing the first section about power architectures, one of the conclusions is that, depending whether the IPV power plant is constructed from a given PV power plant or not, the optimal power architecture can differ. Moreover, the possible introduction of supplementary converters has an influence on the cost of the whole system, while also providing some complementary controllability level. Consequently, the configuration of the storage system in the power architecture is considered as another parameter to take into account in the present study and there is not an optimal architecture for all cases. Thus, the optimal power architecture depends on the original PV power plant and the desired level of controllability. As the considered IPV power plant as case study is a real IPV power plant located in Navarre (Spain), the configuration selected for the present PhD is the one of this IPV power plant where the storage system is a centralized system connected to an AC connection mode.

Regarding the control structure, the first and easiest conclusion is that the management layers must be separated to have an easier view of different control layers and the objective of each of them. Thus, different conclusions must be drawn about the energy management layer and the power control layer. The number of works related to researches in the energy management layer is limited for the IPV application at grid scale due to the innovation to participate in electricity markets, accepting that a long-term horizon must be taken into account in that case, and that the storage system plays an important role in the capacities of the management. Nevertheless, there are several works about the energy management layer for wind power applications, which offer an idea of the services that could be integrated in this management layer [49-52, 54, 55]. To counteract this lack of works about energy management of IPV power plants, advanced energy management strategies are developed and are presented in later chapters as main contribution of the scientific community through this PhD.

Analyzing the power control layer, several works have been carried out, changing the maximum power point of the PV converters, but from the scope of this PhD work, the power control layer focuses more on the rapid ancillary services. On this aspect, the main conclusion of the power control layer is that the IPV power plant is able to participate in some services as frequency and voltage regulation, inertia emulation, power oscillation damping, power fluctuation reduction and ramp rate control. Therefore, the combination of the centralized power plant controller explained in [14], with the predictive control constant steps value of [27, 53], could achieve a well performing power management layer, also considering the higher level of the energy management. In this predictive control, some other criteria and constraints could be included in order to improve the general management structure.

As a conclusion of the energy storage system and its sizing, the technology selection is defined as one important milestone which determines the possibility to provide some services or another ones, as well as balances the economic exploitation of the whole IPV system. For that reason, a technology selection methodology is developed in this PhD work and will be presented in the next chapter.

Related to the sizing methods review, it must be underlined that most of the cited authors have shared that the economic viability of the integration of an energy storage system is not clear in most renewable applications. Nevertheless, in the present work and taking into account energy policies that allow the participation of the IPV power plants in the electricity markets and providing ancillary services, the storage system could help or collaborate in the augmentation of the massive integration of the renewable energy sources. For obtaining the desired economic viability of the IPV power plant system, the balance between the sizing of the storage system and the operation strategies to correctly use this storage system is essential. Thus, a combined optimization that calculates the best storage system together with the most interesting operation strategy to obtain the optimal economic exploitation is carried out in the present PhD.

This operation strategy is based on the electricity markets' analysis, showing that nowadays the most interesting markets to participate in are the daily and the intraday markets. With the developed combined optimization mentioned before, some innovative market participations are proposed, which maximize the economic exploitation, reducing the PV uncertainties through a participation in the intraday markets. This market participation follows the perspectives about renewable generators, which states that these types of sources must also work as other traditional generators, participating in the current electricity markets with current laws.

2

IPV power plant description and modeling

2. IPV power plant description and modeling

The objective of this second chapter is to detail the IPV power plant features in order to be able to carry out their modeling issues. As it has been previously verified in the section where the experimental RES + BESS installations have been presented, the storage system size and its technology have to be selected, depending on the services or functions to be provided. For that reason, there are two questions that must be answered which are: “What is wanted to do?” which refers to the functions or services that are required to the given power plant; and the second question is “How is it going to be done?” referring to the technology and the size of the storage system.

As it has been introduced before, the main objective of the present PhD is to develop an electricity market participation process, and therefore, the first question has already been answered. In this chapter, the second question related to which technology is going to be selected will be answered. To do so, a technology selection methodology is developed. This methodology analyzes the services that have to be provided to different grid levels, to finish selecting the correct technology for its following integration.

Once the technology has been chosen, the case study IPV power plant is presented and described. Finally, the modeling of the different IPV power plant agents is carried out considering the electric and economic models of the PV field; the energetic, degradation and economic models of the storage system; the electricity market model; and the IPV power plant model.

2.1. Storage technology selection methodology

Taking into account the several parameters of the storage systems, a technology selection methodology is developed and proposed. This methodology is presented in [66]. First of all, a storage system can be installed in different locations of the whole electricity network: at the generation systems, at the T&D (transport and distribution), at the end-user and at the RES connection point. At each location, the functionalities that the storage system can provide are different and can be summarized in [66]. In the present work, the most relevant grid level is the RES integration. For that reason, once the relevant experimental RES + BESS installations have been summarized (Table 1.4 of Chapter 1.4.3), it can be stated that the most installed BESS technologies are lithium-ion batteries (Li-ion), sodium sulphur batteries (NaS) and advanced lead acid batteries (adv. Pb acid).

Not only technical criteria must be taken into account to determine which of these three technologies is the most adequate one for RES integration. Therefore, other criteria are included to select the most suitable technology.

2.1.1. Considered technical and economic criteria

The considered technical and economic criteria for the following comparison are described below. These criteria are considered to be the most representative ones for the present application. Nevertheless, if the application requires it, other criteria could be included. Some of them are the technical ones explained in the previous chapter (Section 1.3.2), but are also included here to list both technical and economic criteria.

1) ***Power to energy ratio [kW/kWh]:*** It describes the ratio between power and energy.
2) ***Energy density [Wh/m3]:*** It represents the available energy per volume unit.
3) ***Energetic efficiency [%]:*** It shows the relation between the discharged energy and the amount of energy needed to restore the initial charge state, under specific conditions. It is measured in percentage.
4) ***Life cycles [cycles]:*** It determines the quantity of consecutive charge and discharge processes that a battery can undergo while maintaining some minimum performances.
5) ***Calendar life [time]:*** It determines the period of time in which the battery maintains some minimum performances without being used.
6) ***Capital cost & BMS cost [€/kWh]:*** It represents the cost of the BESS with its BMS (Battery Management System) incorporated.
7) ***Maintenance cost [€/kWh]:*** It represents the cost of maintenance of the BESS in order to assure some specific performances.
8) ***Commercial maturity:*** It indicates the period of time in which the technology has been in use and the development experienced in that period.
9) ***Security:*** It represents the safe operation range of the BESS.

2.1.2. Value assignment for each criterion and comparison of technologies

Based on the described criteria, Li-ion, NaS and adv. Pb acid technologies are compared in detail. The results of the comparison in terms of value assignment of criteria are depicted in the spider chart of Figure 2.1.

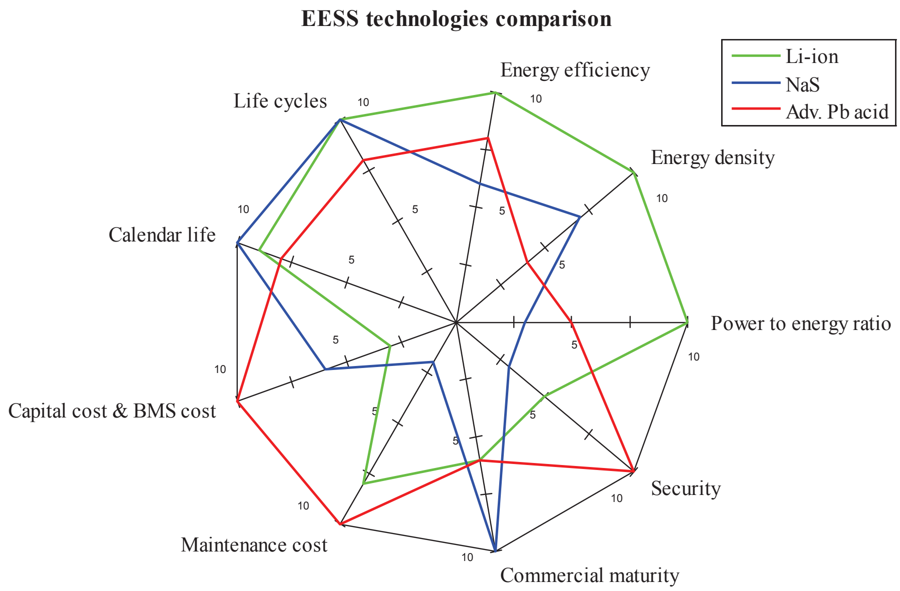

Figure 2.1: Spider chart of relevant BESS technologies comparison.

1) ***Power to energy ratio [kW/kWh]:*** Li-ion technology (~15 kW/kWh) has the highest power to energy ratio, much higher than the one of the adv. Pb acid (~5 kW/kWh) and NaS technologies (~2 kW/kWh) [68, 123].

2) ***Energy density [Wh/m^3]:*** The Li-ion has the greatest energy density (200-350 Wh/m^3) followed by NaS technology (150-250 Wh/m^3). Adv. Pb acid technology has the lowest energy density value (50-100 Wh/m^3) [61].

3) ***Energetic efficiency [%]:*** The Li-ion has the greatest efficiency with 90-94%, followed by the adv. Pb acid (75-90%) and the NaS (75%) [124].

4) ***Life cycles [cycles]:*** Li-ion and NaS technologies have similar life cycles around 5000 cycles and adv. Pb acid technology has approximately a durability of 1000 cycles [124, 125].

5) ***Calendar life [time]:*** The NaS has the best calendar life (15-20 years) followed by Li-ion (5-20 years depending on temperature and SOC) and by adv. Pb acid (5-15 years depending on temperature and SOC) [68].

6) ***Capital cost & BMS cost [€/kWh]:*** Li-ion batteries are the most expensive ones. So they have the lowest value in this criterion followed by NaS technology. Adv. Pb acid technology is much cheaper than other technologies having the best score [61, 126].

7) ***Maintenance cost [€/kWh]:*** NaS batteries have the most expensive maintenance cost, due to their high operation temperature. This technology is followed by Li-ion and adv. Pb acid technologies, which require little maintenance. Thus, the lowest score is for NaS, followed by Li-ion and adv. Pb acid [127].

8) ***Commercial maturity:*** The NaS is the most mature technology and Li-ion and adv. Pb acid technologies are still in demonstration stage [128].

9) ***Security:*** The adv. Pb acid is the most secure technology followed by Li-ion and NaS technologies [68].

In conclusion, as it can be observed in Figure 2.1, there is not a technology that prevails over the others at all criteria. The comparison between the arithmetic additions of criteria's values shows that Li-ion is the best positioned technology. However, for a specific functionality, some characteristics are considered to be much more important than others, i.e. the security characteristic in transport applications (trains, electric vehicles, planes). As a result, this arithmetic addition could not be enough to select a battery energy storage technology. In order to rate the importance of some BES characteristics for a specific application a new selection methodology is proposed in this PhD work and is presented as follows.

2.1.3. Description of the proposed methodology

The objective of the proposed methodology is to offer the possibility to rate the importance of some BES characteristics for the specific application where the methodology is applied. The methodology is based on the flowchart depicted in Figure 2.2.

The first step of the methodology consists in defining the main aspects of the application where the BESS will be installed. These aspects include, among others, the energetic and location requirements, specific legal regulations, functionality to be provided, etc. The second step includes the numerical identification of the above described criteria for each considered BES technology. The third step contains the weigh up value assignment for each criterion. This assignment process will be done based on the analysis of the application of the step 1. The following step calculates each technology qualification applying Eq. 2.1.

$$Qualif = a_1(f)\cdot K_{PERatio} + a_2(f)\cdot K_{Energy\ density} + a_3(f)\cdot K_{Energetic\ efficiency} + a_4(f)\cdot K_{Life\ cycles} + a_5(f)\cdot K_{Calendar\ life} + a_6(f)\cdot K_{Capital\ \&\ BMS\ cost} + a_7(f)\cdot K_{Maint\ cost} + a_8(f)\cdot K_{Commercial\ Maturity} + a_9(f)\cdot K_{Security} \quad \text{Eq. 2.1}$$

Where:

$a_i(f)$ is the weigh up value of the f functionality for the i criterion. The sum of all a_i values for each functionality must be 100, so each criterion has a weigh up value between 0 and 100. It must be noticed that if a given $a_i(f)$ value increases over 11.11 (which represents the equitable weighting value as it can be verified in Table 1.1), another value must decrease.

$K_{Criterion}$ is the value of each criterion for each technology, with a value between 0 and 10. These values can be obtained from the spider chart of Figure 2.1.

The result of this equation will be a value up to 900 because there are 9 criteria multiplied each one by the functionality weigh up value. The higher the value, the better is the technology. The different qualifications obtained for the different BES technologies are then compared to select the best technology for the considered application. By replacing the coefficients K_x of each criterion by cost values, equation (Eq. 2.1) could also represent a cost equation. In that case, the lower the value, the better is the corresponding technology.

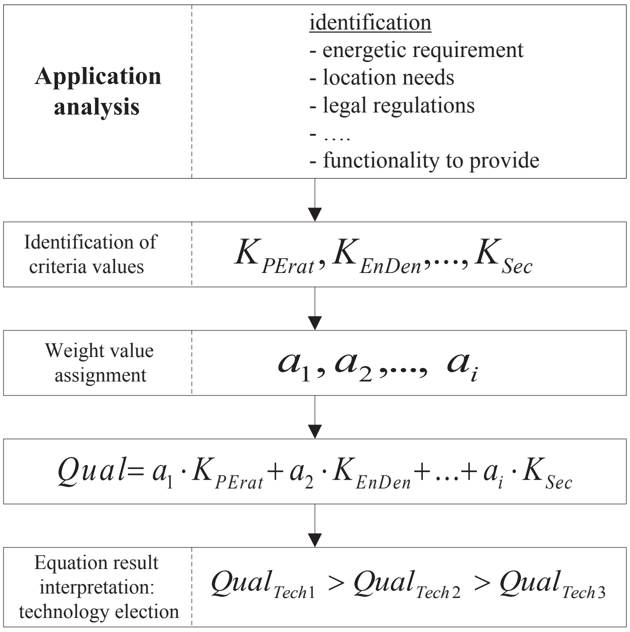

Figure 2.2: BES technologies selection methodology flowchart.

2.1.4. Application of the proposed methodology

For demonstrating the usefulness of the methodology, its application is presented in this section. The considered case study is a 500 kWh/1MW BESS for RES integration functionality. The following requirements are defined for the application:

- Country legal regulations demand a high security installation.
- In order to follow green politics an efficient installation is required.
- The cost factor is considered to be very important.
- It is considered that the RES integration functionality requires a high power to energy ratio for high peak power response.

Based on those requirements, among the technical and economical characteristics identified in section 2.4.1.1, the most important criteria for this application are the security, the energetic efficiency, the capital cost and the BMS cost, the power to energy ratio and the life cycles (since it affects on the replacement cost). These criteria are weighed up with a 15% value. In terms of importance, the next family criteria are considered to be the commercial maturity with a weigh up value of 10%. The other characteristics that are the calendar life, the maintenance cost and the energy density, which are less relevant in this application, are weighed up with a 5% value. These values for different criteria are depicted in Table 2.1. The defined values are compared with the values obtained by applying the equitable weighting.

Table 2.1: Weigh up value table with equitable weighting and for RES integration functionality.

Weigh up value	Technical and economic criteria	Equitable weighting	RES integration functionality
$a_1(f)$	Power to energy ratio	11.11	15
$a_2(f)$	Energy density	11.11	5
$a_3(f)$	Energetic efficiency	11.11	15
$a_4(f)$	Life cycles	11.11	15
$a_5(f)$	Calendar life	11.11	5
$a_6(f)$	Capital and BMS cost	11.11	15
$a_7(f)$	Maintenance cost	11.11	5
$a_8(f)$	Commercial maturity	11.11	10
$a_9(f)$	Security	11.11	15
$\sum a_i(f)$	Total	99.99	100

Considering the weigh value assignment in Table 2.1 (corresponding to the equitable weighting for one and a customization for RES integration for the other one) the proposed methodology is applied and the results obtained are shown in Table 2.2.

Table 2.2: Methodology application results for equitable weighting and for RES integration functionality.

Technologies / Results	Li-ion	NaS	Adv. Pb acid
Equitable weighting	789 (87.65%)	633 (70.36%)	744 (82.71%)
RES integration functionality	765 (85.00%)	615 (68.33%)	755 (83.89%)

Applying the equitable weighting, the Li-ion technology (789 – 88%) is much better than the others with a significant margin, 5% respect to adv. Pb acid (744 – 83%) and 18% respect to NaS technology (633 – 70%). The difference of the adv. Pb acid is due to its low energy density and power to energy ratio values, which are counteracted in part by its low capital cost and high security. Concerning the NaS technology, the main reason of the difference comes from its low security and high maintenance cost.

Applying the weighting defined for the RES integration functionality, the best qualification is also for the Li-ion technology (765 – 85%) but with a lower value than the previous case. This is due to the high capital cost and the BMS cost of the Li-ion that considerably influences the qualification. It must be noticed that the adv. Pb acid technology (755 – 84%) has increased its qualification value, due to its low cost and high security levels. The NaS technology qualification value (615 – 68%) has decreased. Its qualification is even further from the other two technologies because of its low security and high cost which make it more penalized.

These results confirm the choice adopted in the experimental installations of Table 1.4 (Section 1.4.3), where for the RES integration, the most applied technologies are the Li-ion and the adv. Pb acid technologies. Nevertheless, for the present PhD study one of these two technologies must be selected. For that reason, the lithium-ion, which is the best qualified technology, is selected as the storage system technology for the present PhD work. Regarding the current available worldwide energy storage systems, one third of them are based on lithium-ion technology [59] and therefore the selection of lithium-ion is confirmed as a correct selection.

2.2. Case study system description

As a case study of an IPV power plant, a real plant located in Tudela, Navarre, Spain, is considered. This power plant is owned by Acciona Energía [35]. Nevertheless, Ikerlan has participated in a project (ILIS project[14, 129, 130]) to convert this PV power plant in an IPV power plant, installing a BESS. The connection configuration of the BESS to the PV power plant is by means of a centralized storage system connected in AC mode. Thus, the considered system is this real plant, which is detailed in this section.

The considered system is a 1.2 MW PV power plant. The plant covers an area of 70000 square meters and the solar radiation of its location is 1600 kWh/(m^2·year). This power plant was constructed in 2001. Its aerial picture is presented in Figure 2.3.

Figure 2.3: Aerial picture of the PV power plant located in Tudela, Navarre, Spain [14].

2.2.1. Power architecture

The power plant is separated in two areas: a 700 kW / 865.8 kWp centralized generation area and a distributed generation area with 300 kW / 321.11 kWp installed PV power.

The centralized generation area represents 70 % of the PV plant and it is composed of 280 trackers, each one with 36 PV panels in series connection mode. The 10080 PV panels that compose this area are the model BP 585 monocrystalline photovoltaic modules of BP Solar [131]. The 280 trackers generation is connected forming 7 controllable generation units. Each of them, with a peak power of 122.4 kWp, is connected to the internal 380 V_{AC} network by a 100 kW power electronics converter (Voltage source converter, VSC).

The distributed area is composed by 11 types of PV panels of nine manufacturers and five technologies, with a total of 2522 PV panels. This area is considered as a single generation unit without energy management capability and also connected to the internal 380 V_{AC} network.

The PV generation is connected to the medium voltage by a 380 V / 20 kV transformer inside the PV plant and to the transmission system (66 kV) through another transformer located in a substation also owned by Acciona at 2 km from the PV plant.

This configuration was restructured in 2012 in the framework of a European Union supported ILIS project [129, 130], including a storage system and a centralized plant controller to adapt the PV plant to the new interconnection requirements and to experimentally test them as it is explained in [14]. The configuration of this IPV power plant is presented in Figure 2.4. This configuration was only in operation between 2012 and 2013, in the framework of the mentioned European project.

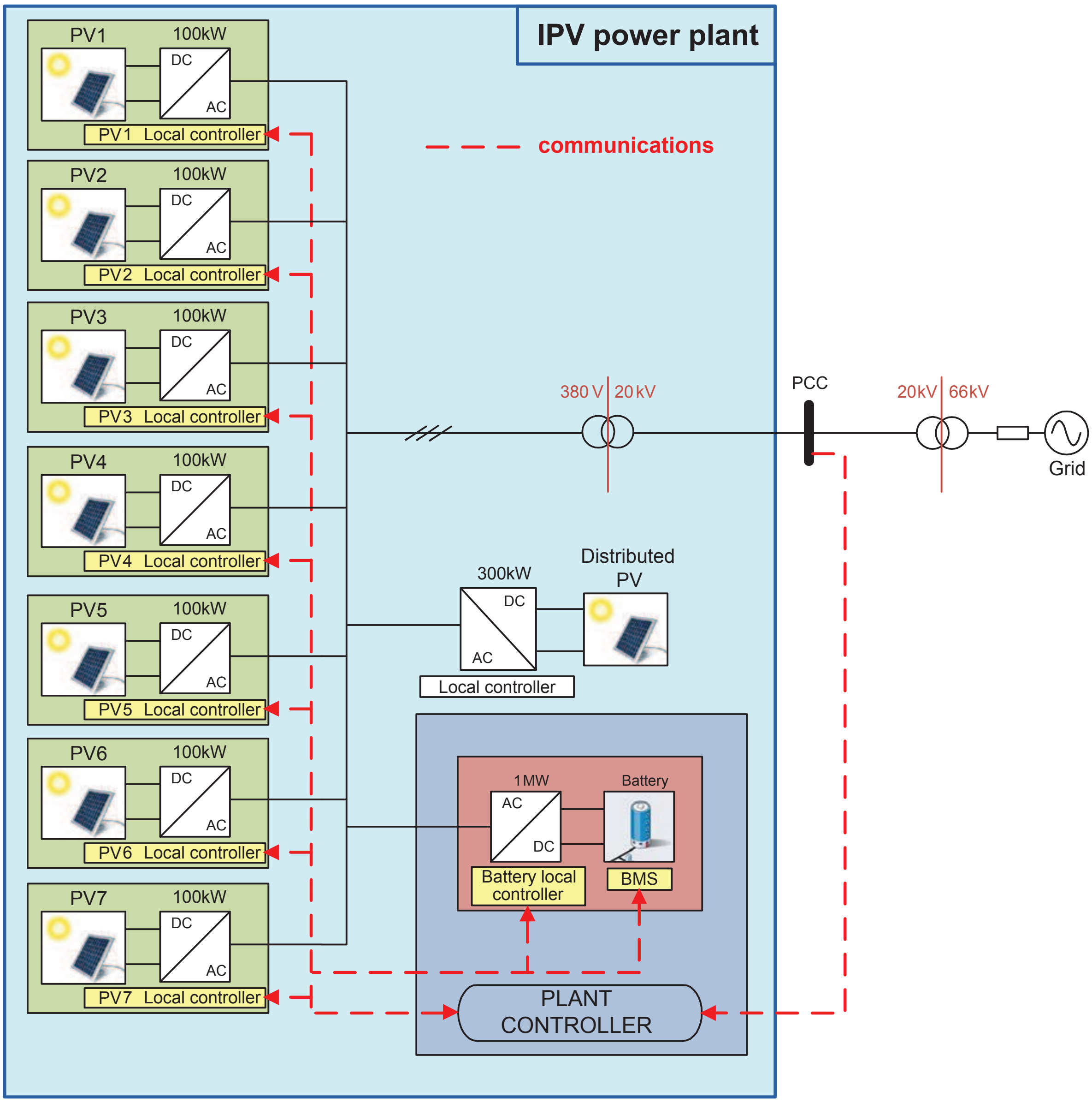

Figure 2.4: Configuration of the IPV power plant (in operation between 2012 and 2013).

The included storage system was a Lithium-ion battery of 1 MW / 560 kWh of SAFT, as it can be shown in Figure 2.5. This storage system was composed by 10 parallel battery strings, each of them built by 29 battery modules. Its nominal voltage was 730 V.

Figure 2.5: Picture of the installed lithium-ion battery of 1 MW / 560 kWh of SAFT [14].

The storage system was connected to the internal network through a 1 MW power electronic converter (VSC). The centralized plant controller carried out the IPV power plant level control and the communications with all lower level controllers of the facility. The existing communications can also be seen by means of the red dashed lines of Figure 2.4.

2.2.2. Control architecture

Related to the control architecture, it is important to mention that the IPV power plant has a hierarchical structure. The higher level controller, which is the plant controller, controls the power injected into the grid measured at the PCC. Based on these measurements, the plant controller sends the needed references to the lower level controllers. These communications are carried out by standard communication protocols. Each of those lower level controllers (which are all of the controllable PV generation units, the converter of the storage system and the storage system itself) have their own local controller, as it can be verified in yellow rectangles in Figure 2.4.

The *PV local controllers* can be controlled in two different ways: in MPPT mode (where the objective is to extract the maximum power from the sun irradiation) and in PQ mode (where the defined active and reactive power set-points of the higher level plant controller are followed). The *battery local controller* was controlled in PQ mode and the *BMS* (Battery Management System) provided information to the plant controller related to the battery, like the state of charge. The *plant controller* carried out the regulation of the active and reactive power injected to the grid at the PCC. For doing so, it had two modules which were the control module and the dispatch module as it can be shown in Figure 2.6.

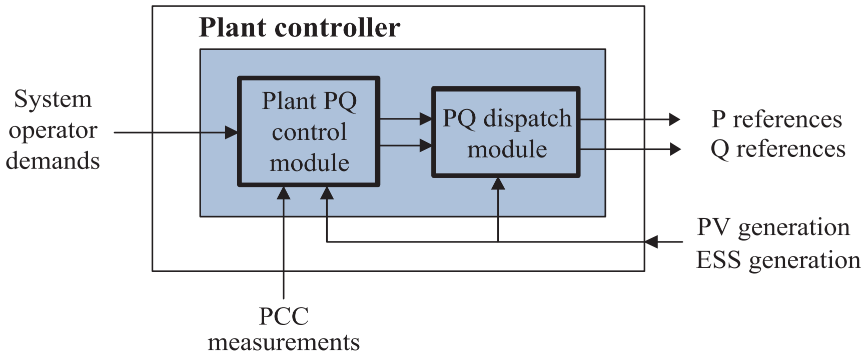

Figure 2.6: Internal control blocks of the plant controller [14].

Plant PQ control module: this module contains the active and the reactive power control loops based on PI controllers. They assure that the global power references received from the system operator are reached at the PCC. These references are calculated taken into account the estimated available PV power and the ESS reserves. Several grid functionalities or services as frequency regulation, voltage regulation, ramp rate control or firming control (constant power production) are implemented in this module.

PQ dispatch module: this module distributes to the controllable PV systems and the storage system the calculated references of the before explained module. It has two different dispatching strategies that are dependent to the PV power availability and the SOC of the storage system. Each strategy is explained in the Table 2.3.

Table 2.3: PQ dispatching strategies.

Mode 1: IPV plant control without ESS		Mode 2: IPV plant control with ESS	
• This mode can be activated when there is no storage system or when it is not available. • Only the PV controllable units participate in the plant control.		• Both PV controllable units and the BESS participate in the plant control. • Depending on the SOC of the storage system, PV controllable units operate in MPPT mode or in PQ mode.	
Mode 1 dispatching equations:		Mode 2 dispatching equations: In MPPT mode:	
$P_{PV_i} = \frac{P_{ref}}{n}$	Eq. 2.2	$P_{PV_i} = MPPT$	Eq. 2.3
$Q_{PV_i} = \frac{Q_{ref}}{n}$	Eq. 2.4	$Q_{PV_i} = \frac{Q_{ref}}{n}$	Eq. 2.5
$P_{ESS} = 0$	Eq. 2.6	$P_{ESS} = P_{ref} - \sum P_{PV_i}$	Eq. 2.7
$Q_{ESS} = 0$	Eq. 2.8	$Q_{ESS} = \frac{Q_{ref}}{n}$	Eq. 2.9
Where: $i = 1, \ldots, 7 \quad and \quad n = 7$		Where: $i = 1, \ldots, 7 \quad and \quad n = 8 = 7(PV) + 1(ESS)$	
		In PQ mode:	
		$P_{PV_i} = P_{ESS} = \frac{P_{ref}}{n}$	Eq. 2.10
		$Q_{PV_i} = Q_{ESS} = \frac{Q_{ref}}{n}$	Eq. 2.11
		Where: $i = 1, \ldots, 7 \quad and \quad n = 8 = 7(PV) + 1(ESS)$	

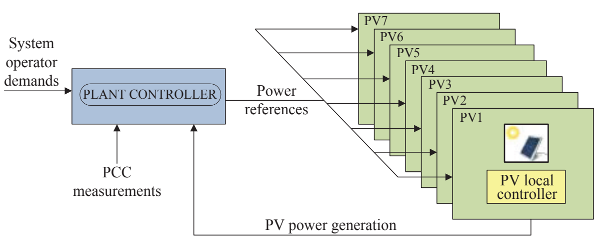

Figure 2.7: Mode 1 dispatching strategy.

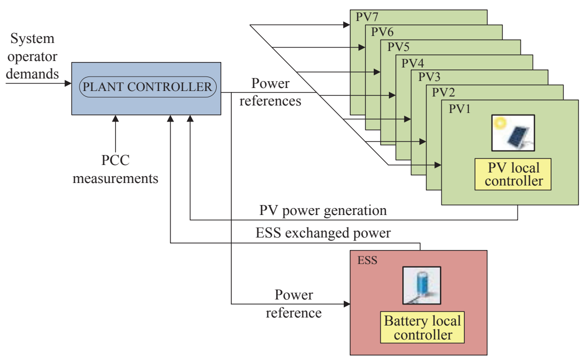

Figure 2.8: Mode 2 dispatching strategy.

The selected dispatching strategy is the Mode 2, which considers the storage system taking advantage of its energy reserves. Among those two operation modes, the MPPT mode is the principal one, because it optimizes the PV generation while controlling the IPV output power by the storage system flexibility. Nevertheless, the PQ mode and the first strategy (without ESS) provide more flexibility to the whole plant for the cases when the SOC of the storage system is near its limits or when there is some kind of problems with the storage system (as communication errors, for example).

As it has been mentioned before, the ESS was in operation between 2012 and 2013, in the framework of the European project, but the centralized plant controller continues today in operation, managing the whole PV power plant with the developed control architecture. Nevertheless, the present PhD work has been developed assuming the scenario where an ESS is connected to the PV power plant, considering then an IPV power plant.

2.3. IPV agents modeling

This section includes all modeling steps of each device or agent of the IPV power plant. As the main objective of the present work is to determine the required energetic capacity of the storage system in order to take advantage of it to participate in the market, the energy storage model is an energetic model, which means taking into account its power and energy values, more than voltage and current values (parameters of an electric model). The economic models of these devices are also considered and explained in this section, as well as the degradation model of the storage system.

2.3.1. PV model

The considered PV models are the electric and the economic ones. They are developed as follows:

2.3.1.1. Electric model

The electric model applied in this study is an energetic one, which means that the output power of a PV subsystem (PV panel + converter) is considered. The PV generation data taken into account is a one yearlong and two minutes sample time generation data [26] (which do not represent real data from Tudela) of the generated kilowatts per installed kilowatt peak value [kW/kWp]. This data is, therefore, the generated power at the converter output in per unit of installed peak power ($PV_{data}\ [kW/kWp]$) and it is presented in Figure 2.9.

From this data, the output power generation of a given PV power plant is easy to obtain, knowing its installed PV peak power. As the experimental validation of the present PhD is done based on a real PV power plant, the model of this plant is considered to determine the output power generation. The mentioned PV power plant has 1.2 MWp installed capacity. Therefore, its output power generation is calculated as in Eq. 2.12.

$$P_{PV} = PV\ installed\ capacity[kWp] \cdot PV_{data}\left[\frac{kW}{kWp}\right] = 1.2\ MWp \cdot PV_{data} \qquad \text{Eq. 2.12}$$

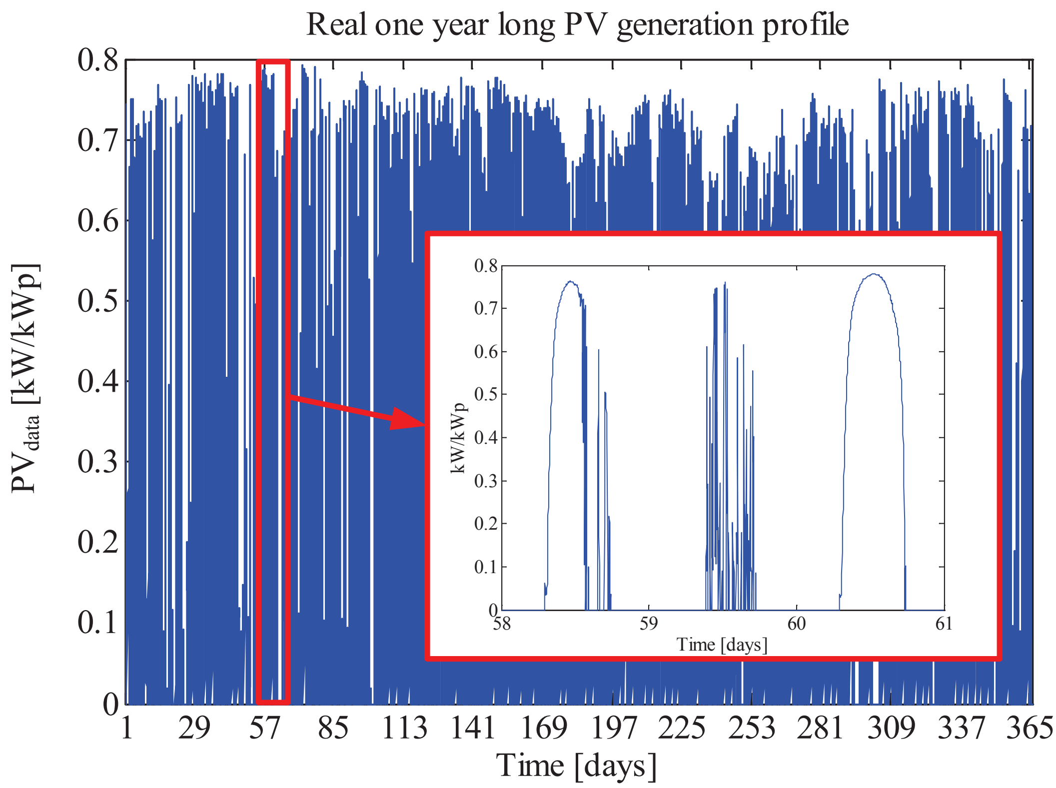

Figure 2.9: Real one year long PV generation profile with a three days detail [26].

2.3.1.2. Economic model

The economic model of the PV system includes the initial investment cost. The initial investment cost is divided in two terms, considering the purely PV installation and its associated power electronics (PE). Therefore, the initial investment cost of the PV system, $c_{ini_{PV}}$, is calculated as in Eq. 2.13.

$$c_{ini_{PV}} = c_{PV_{panels}} + c_{PV_{PE}} \qquad \text{Eq. 2.13}$$

Where $c_{PV_{panels}}$ (€) and $c_{PV_{PE}}$ (€) are the PV panels investment cost and PV related power electronics investment cost. Each of these costs is calculated as in Eq. 2.14 and in Eq. 2.15, respectively.

$$c_{PV_{panels}} = P_{PV_{insta\ lled}} \cdot c_{P_{PV}} \qquad \text{Eq. 2.14}$$

$$c_{PV_{PE}} = P_{PV_{installed}} \cdot c_{P_{PE}} \qquad \text{Eq. 2.15}$$

Where $P_{PV_{installed}}$ (W), is the installed PV power capacity and $c_{P_{PV}}$ (€/W) and $c_{P_{PE}}$ (€/W) are the cost per watt of PV panels and power electronics. The considered costs are 1 €/W and 0.1 €/W, respectively.

2.3.2. Energy storage system model

The energy storage system is detailed in three models which are the energetic model, the degradation model and the economic model. This classification is made to take into account the energetic capacities of the storage system, the degradation that this energetic capacity supports and the cost caused from the degradation that concludes with a replacement of the storage system.

2.3.2.1. Energetic model

The energetic model considered in this study calculates the state of charge (SOC) of the storage system based on Eq. 2.16 [24].

$$SOC(t) = \frac{C(t)}{C_{ref}(t)} \qquad \text{Eq. 2.16}$$

Where $C(t)$ (Wh) is the current energetic capacity and C_{ref} (Wh) is the current maximum capacity. A fresh or new storage system has a nominal capacity value, C_{bat}, and since this moment, the battery is degraded reducing its maximum capacity value. Therefore, the current (t) maximum capacity value is $C_{ref}(t)$.

Although the definition of the SOC can be calculated based on Eq. 2.16, the Coulomb Counting technique is also very extended to calculate the SOC for each moment [132, 133]. This method is also known as Ah-counting and it carries out the integration of the current flowing through the storage system according to Eq. 2.17.

$$SOC(t) = SOC(t_0) - \frac{\eta}{C_n}\int_{t_0}^{t} I(\tau)d\tau \qquad \text{Eq. 2.17}$$

Where η is the efficiency of the charge and discharge processes, which is more than 1 on discharge and less than 1 on charge; C_n (Ah) is the nominal capacity; and $I(\tau)$(A) is the current extracted or injected to the battery over the time. This method, as its name indicates (Ah-counting), calculates the quantity of the Ampere-hours (current during time) flow. Nevertheless, in this study the capacity of the battery (C_{ref}) is considered in watts-hour, instead of ampere-hour, as mentioned in Eq. 2.16. Therefore, the voltage (v) is included as constant value in the integration of the current, to maintain the equation units correspondingly [134]. With this assumption, the Eq. 2.17 is used as Eq. 2.18 in this study.

$$SOC(t) = SOC(t_0) - \frac{\eta}{C_{ref}(t)}\int_{t_0}^{t} I(\tau)\cdot v\, d\tau = SOC(t_0) - \frac{\eta}{C_{ref}(t)}\int_{t_0}^{t} P_{bat}(\tau)\, d\tau \qquad \text{Eq. 2.18}$$

Where P_{bat} (W) is the power exchanged with the battery. The discrete equation of Eq. 2.18 is presented in Eq. 2.19.

$$SOC(k) = SOC(k_0) - \frac{\eta}{C_{ref}(k)} \sum_{m=k_0}^{k} P_{bat}(m) \cdot \Delta t \qquad \text{Eq. 2.19}$$

Where Δt (h) is the sample time counted in hours. As it can be shown in Eq. 2.19, the SOC is a recursive parameter, which means that it is related to its previous values. As in Eq. 2.19, the SOC value of the previous sample time, $SOC(k-1)$, is calculated as in Eq. 2.20.

$$SOC(k-1) = SOC(k_0) - \frac{\eta}{C_{ref}(k-1)} \sum_{m=k_0}^{k-1} P_{bat}(m) \cdot \Delta t \qquad \text{Eq. 2.20}$$

Combining Eq. 2.19 and Eq. 2.20, and assuming that the capacity decay is negligible between two continuous steps ($C_{ref}(k) - C_{ref}(k-1) \approx 0$), a simplified equation of the SOC can be obtained (Eq. 2.21), which calculates the current SOC only with the information of the previous step, which reduces the calculation time. This Eq. 2.21 is the one that is used in the present study.

$$SOC(k) = SOC(k-1) - \frac{\eta}{C_{ref}(k)} \cdot P_{bat}(k) \cdot \Delta t \qquad \text{Eq. 2.21}$$

2.3.2.2. Degradation model

At the present PhD study, a degradation model is also considered to take into account the battery capacity reduction. To do that, the state of health (SOH) of the battery is calculated as in Eq. 2.22.

$$SOH(t) = \frac{C_{ref}(t)}{C_{bat}} \qquad \text{Eq. 2.22}$$

Where $C_{ref}(t)$ (Wh) is the current maximum capacity and C_{bat} (Wh) is the capacity of the battery in its beginning of life (BOL), which means when it is fresh or new battery.

The ageing in storage systems refers to a reduction of the amount of energy that the batteries are able to provide and also to an internal impedance increase. Therefore, when there are degraded, they are able to provide lower amount of energy within lower power values. This degradation is caused by two factors: the cycling ageing and the calendar ageing.

The cycling ageing is modeled as in [24] assuming that the capacity losses are linear according to the discharges of the storage system [135-139]. That means that at each discharge, there is a capacity loss. This fact is modeled in a discrete domain as in Eq. 2.23.

$$C_{ref}(k) = C_{ref}(k-1) - \Delta C_{ref}(k) \quad \textit{at each discharge step} \qquad \text{Eq. 2.23}$$

Where ΔC_{ref} (Wh) is the capacity loss of the step k. This capacity loss is calculated as in Eq. 2.24.

$$\Delta C_{ref}(k) = C_{bat} \cdot Z_{cy} \cdot \big(SOC(k-1) - SOC(k)\big) \qquad \text{Eq. 2.24}$$

Where Z_{cy} is the linear ageing coefficient. This coefficient has different values for different storage systems' technologies [137]. For lithium-ion batteries this coefficient has a $1{,}1 \cdot 10^{-3}$ value [26].

Overwriting the Eq. 2.22 in the discrete domain, the resultant equation is Eq. 2.25 or Eq. 2.26 for different time steps.

$$SOH(k) = \frac{C_{ref}(k)}{C_{bat}} \qquad \text{Eq. 2.25}$$

$$SOH(k-1) = \frac{C_{ref}(k-1)}{C_{bat}} \qquad \text{Eq. 2.26}$$

Replacing Eq. 2.23 in Eq. 2.25 and applying there the Eq. 2.26, Eq. 2.27 is obtained:

$$SOH(k) = \frac{C_{ref}(k)}{C_{bat}} = \frac{C_{ref}(k-1) - \Delta C_{ref}(k)}{C_{bat}} = SOH(k-1) - \frac{\Delta C_{ref}(k)}{C_{bat}} \qquad \text{Eq. 2.27}$$

Finally, replacing Eq. 2.24 in Eq. 2.27, the cycling ageing equation (Eq. 2.28) is obtained:

$$\begin{aligned} SOH(k) &= SOH(k-1) - \frac{C_{bat} \cdot Z_{cy} \cdot \big(SOC(k-1) - SOC(k)\big)}{C_{bat}} \\ &= SOH(k-1) - Z_{cy} \cdot \big(SOC(k-1) - SOC(k)\big) \end{aligned} \qquad \text{Eq. 2.28}$$

As it is aforementioned, this equation models the discharge processes and therefore, by means of the model applied, in the charge processes the capacity and the SOH values are maintained constant [24]. Thus, the SOH equation that models all cases is expressed by Eq. 2.29.

$$SOH(k) = \begin{cases} SOH(k-1) - Z_{cy} \cdot \big(SOC(k-1) - SOC(k)\big), & at\ discharge \\ SOH(k-1), & at\ charge \end{cases} \qquad \text{Eq. 2.29}$$

An example of the real cycling ageing can be shown in Figure 2.10, where 6 same battery cells are tested with different conditions: 25 ºC, 50% middle SOC, 1C (C-rate), and different DOD (depicted in the legend) [140]. The full equivalent cycles (FEC) are counted on each cycling test.

Once the capacity ($C_{ref}(t)$) or the reference $SOH(t)$ value cross the end of life (EOL) threshold (C_{EOL}), it is considered that the storage system is not useful for the current application.

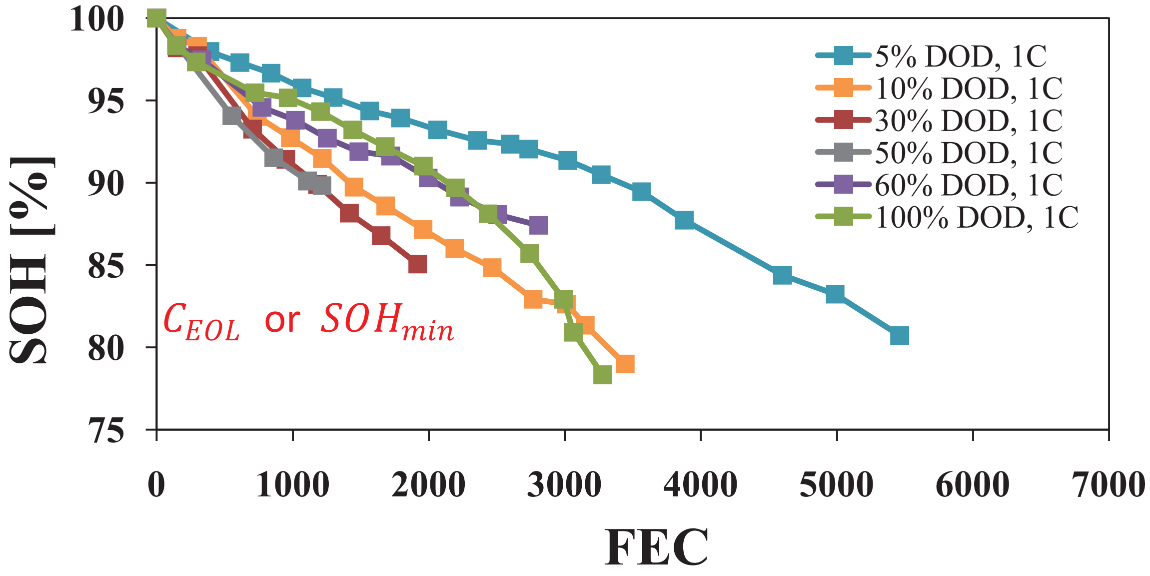

Figure 2.10: Example of cycling ageing for six different DOD [140].

Related to the calendar ageing, it is considered as linear ageing but in this case between the beginning of life (BOL) and the EOL of the batteries. It is known that the calendar ageing is dependent on the temperature, the SOC and the time of storage [141], but the approximation carried out in this work is the linear one.

An example of the real calendar ageing can be shown Figure 2.11, where another 6 same battery cells are stored with different temperature and SOC conditions [141].

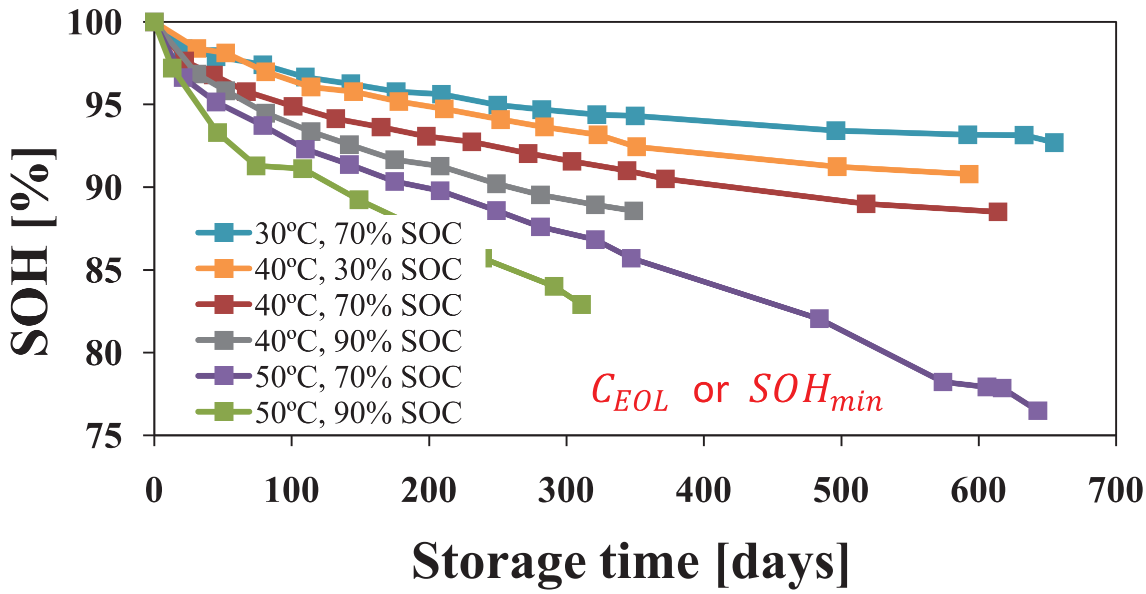

Figure 2.11: Example of calendar ageing for different conditions [141].

Based on a linear equation, the coefficients that model this ageing process can be obtained as in Eq. 2.30.

$$y = m \cdot x + n \leftrightarrow C_{ref}(t) = -\frac{C_{bat}(1 - SOH_{min})}{t_{EOL}} \cdot t + C_{bat} \qquad \text{Eq. 2.30}$$

Considering:

$$C_{EOL} = C_{bat} \cdot SOH_{min} \qquad \text{Eq. 2.31}$$

Where C_{EOL} (Wh) is the end of life capacity value; SOH_{min} is the reference value of C_{EOL} in terms of SOH; and t_{EOL} (years) is the manufacturer data of calendar ageing.

Once the slope of Eq. 2.30 has been defined, the equation to obtain the relation of a given capacity value to each previous one is already determined, as in Eq. 2.32.

$$\begin{aligned} C_{ref}(k) &= C_{ref}(k-1) + m \cdot \Delta t = C_{ref}(k-1) - \frac{C_{bat}(1 - SOH_{min})}{t_{EOL}} \cdot \Delta t \\ &= C_{ref}(k-1) - Z_{cal} \cdot C_{bat} \end{aligned} \qquad \text{Eq. 2.32}$$

Considering:

$$Z_{cal} = \frac{(1 - SOH_{min})}{t_{EOL}} \cdot \Delta t \qquad \text{Eq. 2.33}$$

Where Z_{cal} is the calendar ageing parameter. Combining the Eq. 2.22, with Eq. 2.32 and Eq. 2.33, the resultant equation that models the calendar ageing related to the SOH is the Eq. 2.34.

$$SOH(k) = SOH(k-1) - Z_{cal} = SOH(k-1) - \frac{(1 - SOH_{min})}{t_{EOL}} \cdot \Delta t \qquad \text{Eq. 2.34}$$

As both ageing processes occur at the same time, the addition of both of them must be considered. Therefore, the complete ageing equation is expressed as in Eq. 2.35.

$$SOH(k) = \begin{cases} SOH(k-1) - Z_{cy} \cdot \big(SOC(k-1) - SOC(k)\big) - Z_{cal}, \text{at discharge} \\ SOH(k-1) - Z_{cal}, \text{at charge} \end{cases} \qquad \text{Eq. 2.35}$$

2.3.2.3. Economic model

The economic model of the energy storage system includes the initial investment cost and the replacement cost. The initial investment cost is separated in two terms, considering the battery and the power electronics associated to connect this storage system to the plant. Therefore, the initial investment cost of the ESS, $c_{ini_{ESS}}$, is calculated as in Eq. 2.36.

$$c_{ini_{ESS}} = c_{ESS_{bat}} + c_{ESS_{PE}} \qquad \text{Eq. 2.36}$$

Where $c_{ESS_{bat}}$ (€) and $c_{ESS_{PE}}$ (€) are the battery investment cost and ESS related power electronics investment cost. Each of these costs is calculated as in Eq. 2.37 and in Eq. 2.38, respectively.

$$c_{ESS_{bat}} = C_{bat_{installed}} \cdot c_{C_{bat}} \qquad \text{Eq. 2.37}$$

$$c_{ESS_{PE}} = P_{ESS_{installed}} \cdot c_{P_{PE}} \qquad \text{Eq. 2.38}$$

Where $C_{bat_{installed}}$ (Wh) is the installed battery energetic capacity; $P_{ESS_{installed}}$ (W) is the installed battery power capacity; $c_{C_{bat}}$ (€/Wh) is the cost per watt-hour of batteries; and $c_{P_{PE}}$ (€/W) is the cost per watt of power electronics. The considered battery cost is 0.4 €/Wh and the cost of power electronics is 0.1 €/W.

As the life span of the batteries is not the same as the life span of the whole IPV power plant, the replacement cost of the batteries is considered here. The replacement cost of the batteries is the same as the batteries investment cost, but the difference is that this cost is usually annualized [142]. To annualize it, the Eq. 2.39 is applied:

$$c_{replac} = \sum_{k=1}^{r} (1+i)^{-k \cdot t_{bat}} \cdot c_{ESS_{bat}} \cdot CRF \qquad \text{Eq. 2.39}$$

Where c_{replac} (€/year) is the annualized replacement cost of the batteries; r is the number of needed replacements; i is the interest rate in percentage; t_{bat} is the lifespan of the storage system in years; and CRF is the capital recovery factor, which is a factor that permits to annualize a given cost [142]. It is calculated as in Eq. 2.40.

$$CRF = \frac{i \cdot (1+i)^{t_{sys}}}{(1+i)^{t_{sys}} + 1} \qquad \text{Eq. 2.40}$$

Where t_{sys} is the lifetime of the whole IPV power plant system in years and i is the interest rate in percentage. In this case, the lifetime (t_{sys}) is considered as 25 years and the interest rate (i) is considered as 2.5 %.

To determine the replacements needed (r) and the lifespan of the storage system (t_{bat}), the battery power profile is analyzed. From this profile, the SOC profile is obtained to apply the *Rainflow* cycling counting algorithm [143, 144].

This algorithm counts the charging and discharging cycles analyzing the SOC profile. Its internal process can be summarized in the following three steps [145].

First, the algorithm analyses the discharges cycles beginning from the highest SOC value and counting from top to bottom. It analyzes the discharge curve until finding the lowest SOC value following a continuously decreasing path. The algorithm repeats the previous process starting from the next highest SOC value until finding the next lowest SOC value without overlapping the previous paths. This process is repeated until all the discharges of the SOC profile are analyzed and it is demonstrated by means of an example in Figure 2.12.

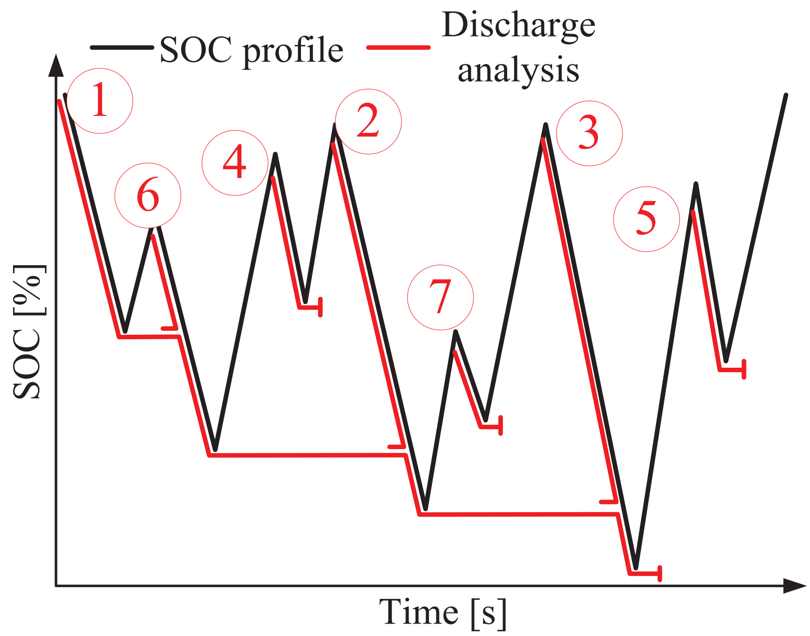

Figure 2.12: First step of *Rainflow* cycling counting algorithm (discharge analysis).

The second step of the algorithm is similar to the previous one but charges and discharges are analyzed in the same way. Thus, beginning from the lowest SOC value and following until the highest SOC value, the first increasing path is determined. This process is repeated from the next lowest SOC value until the next highest SOC value without overlapping previous paths. Figure 2.13 shows this second step on the same example.

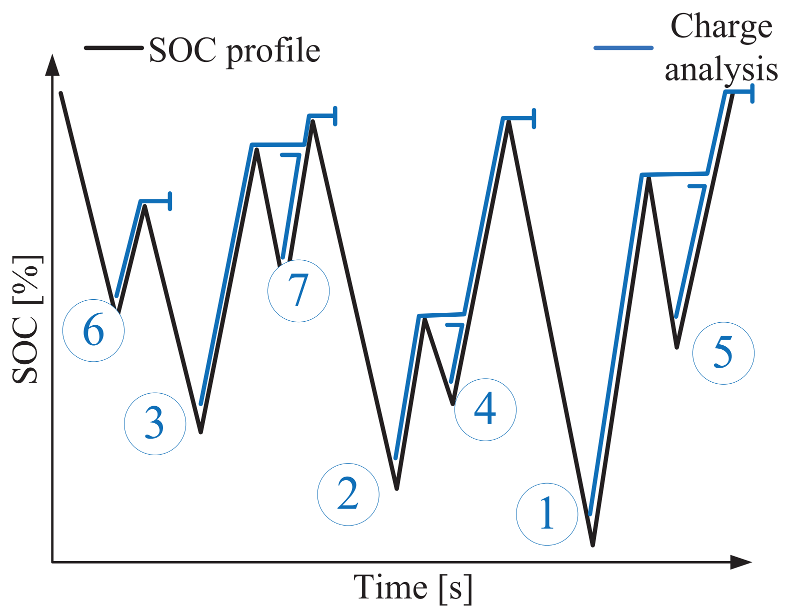

Figure 2.13: Second step of *Rainflow* cycling counting algorithm (charge analysis).

The third and last step matches the discharge and charge semi-cycles completing full cycles of the same depth of discharge (DOD) and from the same upper SOC value and lower SOC value. Figure 2.14 presents this matching process.

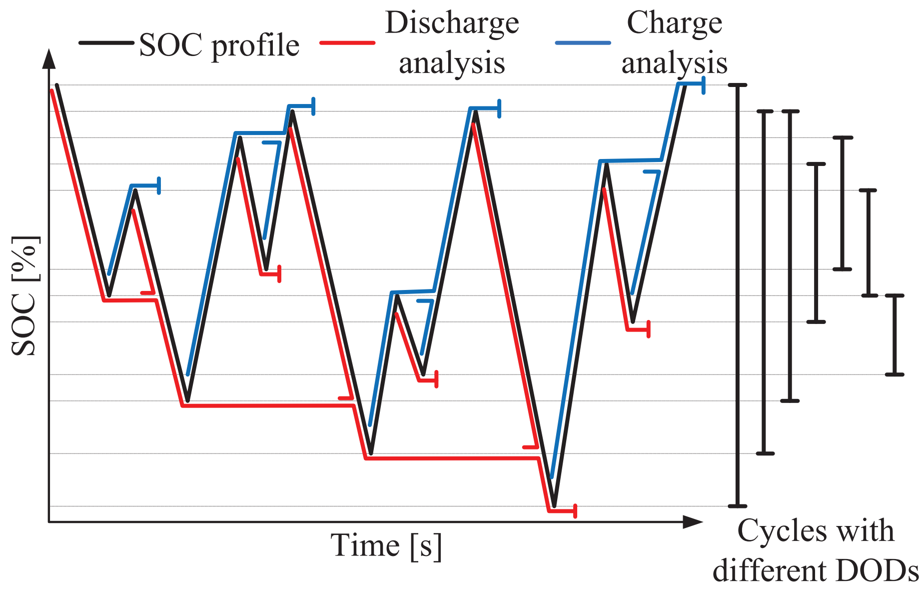

Figure 2.14: Third step of *Rainflow* cycling counting algorithm (matching process).

Once the quantity of cycles has been obtained, these cycles are matched with the lifetime data (specific depth of discharge, DOD, versus the number of cycles) of the datasheet of the battery manufacturer obtaining the lifetime of the storage system [146]. The cycles are grouped ten by ten to a correct match of datasheet data versus the counted cycles. The lifetime is calculated applying Eq. 2.41.

$$t_{bat} = \frac{1}{\sum_{i=1}^{9}\left(\frac{N_{year_i}}{N_{EOL_i}}\right)} \; [years] \qquad \text{Eq. 2.41}$$

Where t_{bat} is the lifetime of the energy storage system [years]; N_{year_i} is the number of cycles counted of i DOD group per year [cycles/year] obtained from the *Rainflow* cycling counting algorithm; and N_{EOL_i} is the number of cycles of i DOD group that causes the EOL of the storage system taken from the datasheet of the manufacturer and also from different cycling tests carried out in the energy storage laboratory of Ikerlan [cycles].

The considered values are the ones depicted on Table 2.4 [146]. These values correspond to a NMC-based 40 Ah battery cell.

Table 2.4: Considered number of cycles per DOD group [146].

DOD_i	DOD interval	N_{EOL_i}
DOD_1	0 – 15 %	70000
DOD_2	15 – 25 %	31000
DOD_3	25 – 35 %	18100
DOD_4	35 – 45 %	11800
DOD_5	45 – 55 %	8100
DOD_6	55 – 65 %	5800
DOD_7	65 – 75 %	4300
DOD_8	75 – 85 %	3300
DOD_9	85 – 100 %	2500

From the obtained lifespan of the storage system (t_{bat}) and the whole IPV power plant lifetime (t_{sys}), the needed replacements (r) are calculated as in Eq. 2.42.

$$r = ceil\left(\frac{t_{sys}}{t_{bat}} - 1\right) \quad \text{Eq. 2.42}$$

Where the $ceil(x)$ mathematical function calculates the following positive integer value of x, in order to have an integer value of replacements.

2.3.3. Electricity market economic model

The electricity market economic model analyzed in the present PhD work includes the revenues and the penalties that an energy producer can generate participating in the electricity markets of the Iberian Peninsula. As it is explained in the chapter 1, the markets where an IPV power plant can participate are the daily market and the six sessions of the intraday market. Therefore, in this section the revenues and penalties obtained from this participation are formulated.

Regarding the revenues, the equation that models them is defined as Eq. 2.43.

$$revenues = \sum_{j=1}^{24} rev_{mkt\_h_j} = rev_{mkt\_h\,1} + rev_{mkt\_h\,2} + \cdots + rev_{mkt\_h\,24} \quad \text{Eq. 2.43}$$

Where $rev_{mkt\_h_j}$ (€) is the revenue of market hour j. Each of this revenue is calculated as in Eq. 2.44:

$$rev_{mkt\_h_j} = c_{cleare\ d_j}^{DM} \cdot E_{cleare\ d_j}^{DM} + \sum_{k=1}^{6} c_{cleare\ d_j}^{IMk} \cdot E_{cleare\ d_j}^{IMk}$$ Eq. 2.44

Where $c_{cleare\ d_j}^{DM}$ (€/Wh) is the cost of the hour j of the daily market (DM); $E_{cleare\ d_j}^{DM}$ (Wh) is the energy cleared in the hour j of the DM; $c_{cleare\ d_j}^{IMk}$ (€/Wh) is the cost of the hour j of the session k of the intraday market (IM); and $E_{cleare\ d_j}^{IMk}$ (Wh) is the energy cleared in the hour j of the session k of the IM.

For almost all of the simulations carried out in this dissertation, the prices are indexed to the year 2014 [147]. From the 365 days of this year, the average value of each hour is calculated. The different days of the year that are included in the simulations have been randomly selected, and for not taking into account specific prices related to multiple factors (seasonality, day of the week, windy days, rainy days), the average values are calculated and taken into account. The daily market prices are shown in Figure 2.15 and the intraday market prices in Figure 2.16.

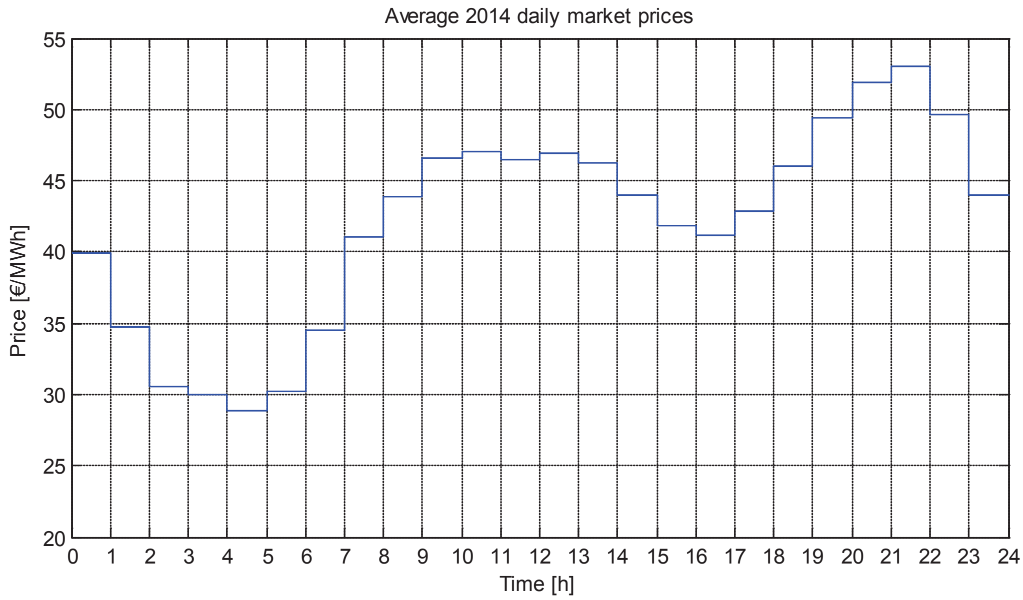

Figure 2.15: Average 2014 daily market prices of the Iberian Peninsula market.

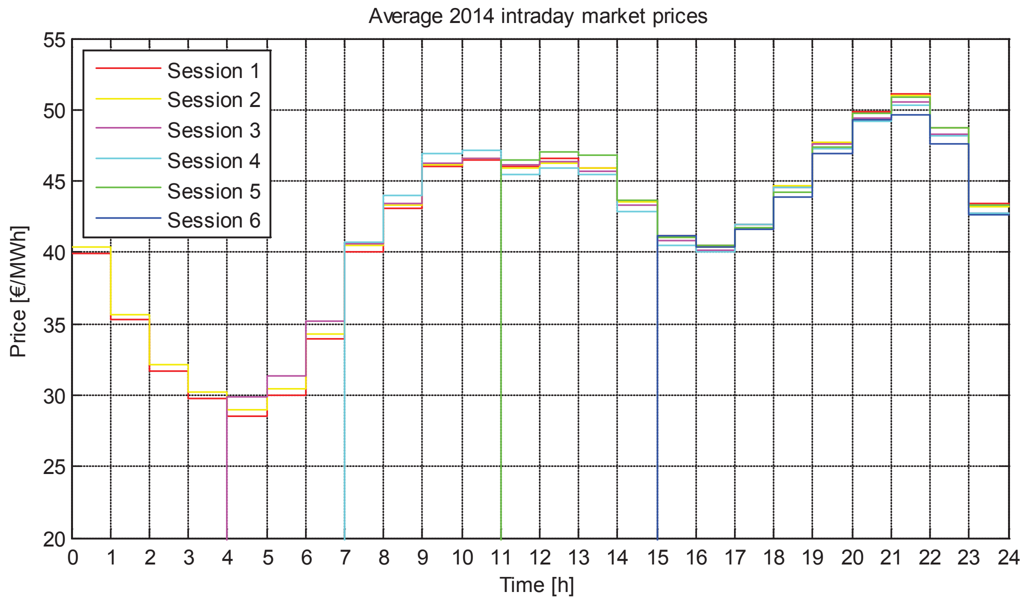

Figure 2.16: Average 2014 intraday market prices of the Iberian Peninsula market.

Regarding the penalties that can be applied to a generation plant, and in this case, from an IPV power plant, the equation that models them (c_{penalt}) is defined as Eq. 2.45. This equation includes the penalties cost caused by the deviation of the supplied grid energy related with the cleared one. The produced deviations are calculated at each market period and can be positive or negative, obtaining a different penalty cost.

$$c_{penalt} = \sum_{j=1}^{24} c_{penalt\ y_j} = c_{penalt\ y_1} + c_{penalt\ y_2} + \cdots + c_{penalt\ y_{24}} \quad \text{Eq. 2.45}$$

Where $c_{penalt\ y_j}$ (€) is the penalty cost of market hour j. An important fact related to the penalties is that at each hour, the generation and the consumption is not completely equal. In this case, if a given generation plant generates more than what it has cleared, and the generation and consumption balance is negative (more consumption than generation), as the given generation plant has collaborated with the balance, this generation plant does not pay for its deviation (because it has unintentionally helped to reduce the consumption and generation difference). For that effect, each of this penalty cost is calculated as in Eq. 2.46:

$$c_{penalt\ y_j} = \begin{cases} c^{+}_{E_{pe\,n_j}} \cdot \left|E_{pe\,n_j}\right|, & E_{pe\,n_j} > 0 \\ 0, & E_{pe\,n_j} = 0 \\ c^{-}_{E_{pe\,n_j}} \cdot \left|E_{pe\,n_j}\right|, & E_{pe\,n_j} < 0 \end{cases} \quad \text{Eq. 2.46}$$

Where $c^{+}_{E_{pe\,n_j}}$ (€/Wh) and $c^{-}_{E_{pe\,n_j}}$ (€/Wh) are the cost per energy of positive and negative penalties of market hour j, respectively; and $E_{pe\,n_j}$ (Wh) is the energy that has caused the penalty of hour j. The penalty costs employed in this study are also the average values of the

2014 whole year and are shown in Figure 2.17. Both the penalty costs and the daily and intraday market prices are available in [147].

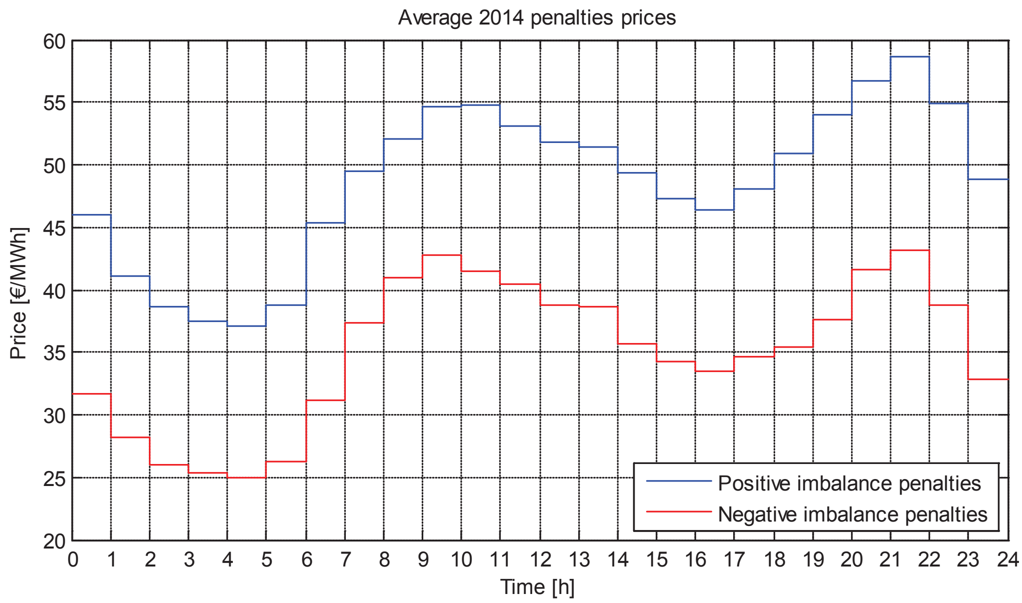

Figure 2.17: Average 2014 penalties costs of the Iberian Peninsula market.

2.3.4. IPV power plant economic model

The economic model of the IPV power plant is based on the economic models of the PV, storage system and the model of the electricity market participation (considering both revenues and penalties). To complete this model the operation and maintenance (O&M) cost of the whole IPV power plant has to be included. $c_{O\&M}$ (€/year) is the annualized operation and maintenance cost, which is calculated as in Eq. 2.47:

$$c_{O\&M} = \sum_{k=1}^{t_{sys}} (1+i)^{-k} \cdot c_{maintenance} \cdot CRF \qquad \text{Eq. 2.47}$$

Where $c_{maintenance}$ (€) is the maintenance cost. This value is considered not dependent on the storage size and could be around 40000 € for a 1 MW PV power plant [148].

The whole economic model equation (f) is represented in Eq. 2.48.

$$f = net\ profit = revenues - costs \qquad \text{Eq. 2.48}$$

Where $revenues$ are the ones calculated in Eq. 2.43 and Eq. 2.44 and $costs$ are defined as in Eq. 2.49.

$$costs = c_{invest} + c_{replac} + c_{O\&M} + c_{penalt} \qquad \text{Eq. 2.49}$$

Where c_{invest} (€/year) is the annualized initial investment cost and is calculated as in Eq. 2.50 and Eq. 2.51; c_{replac} (€/year) is detailed in Eq. 2.39; $c_{O\&M}$ (€/year) is expressed in Eq. 2.47; and c_{penalt} (€/year) is formulated in Eq. 2.45.

$$c_{invest} = c_{ini} \cdot CRF \qquad \text{Eq. 2.50}$$

$$c_{ini} = c_{ini_{PV}} + c_{ini_{ESS}} = c_{PV_{panels}} + c_{PV_{PE}} + c_{ESS_{bat}} + c_{ESS_{PE}} \qquad \text{Eq. 2.51}$$

A summary table with some of the most relevant cost values considered in this study is presented in Table 2.5.

Table 2.5: Summary of the considered cost values detail information.

Symbol	Magnitude	Value
$c_{P_{PV}}$	Cost of PV per installed power	1 €/W
$c_{P_{PE}}$	Cost of PE per installed power	0.1 €/W
$c_{C_{bat}}$	Cost of battery per capacity	0.4 €/Wh
i	Interest rate	2.5 %
t_{sys}	Lifetime of the whole IPV power plant	25 years
$c_{maintenance}$	Maintenance cost	40000 €

2.4. Conclusions

In this second chapter, the bases of the present PhD work have been summarized. A storage technology selection methodology has been proposed, following with the detailed explanation of the case study IPV power plant, and concluding with the modeling of the IPV power plant agents.

First, a methodology to select the most performing storage system technology has been proposed taking into account different criteria, not only technical, but also economic criteria. The proposed storage technology selection methodology has also been applied, obtaining as best qualified technologies the lithium-ion and the advanced lead acid, respectively. That is why the lithium-ion batteries are considered for the present PhD study. Moreover, as the storage system installed in the considered IPV power plant is based on lithium ion technology, the selection of the lithium-ion has been confirmed.

The considered IPV power plant has been detailed, which has several advantages almost necessary for the proposed market participation. As it can be verified, the developed plant controller is able to fix a whole IPV power plant active and reactive power references. It is also able to maintain those references every time that there is sun or there are energy reserves in the storage system. This fact is very important in the present study because it permits to participate in electricity markets providing to the grid constant power during each market period. Moreover, having the PQ control mode in the PV controllable units, if an underestimation of PV production happens and the storage system is fully charged, the PQ control mode can reduce the PV generation, reducing or avoiding therefore, the market penalties.

Finally, the modeling step of the PV, the ESS, the whole IPV power plant and the electricity markets have been presented. First, the detailed economic and electric models of PV have been summarized together with the energetic, degradation and economic models of the energy storage system. The degradation models of the storage system offers and important improvement gap, where both calendar and cycling ageing have been considered. For determining the ESS lifetime, the *Rainflow* cycling counting algorithm has been applied together with battery manufacturer data and some cycling tests data (carried out in energy storage laboratory of Ikerlan). Therefore, the lifetime estimation has been calculated based on real measurements, which provide a realistic approach to estimate the lifetime of different manufacturer batteries. The prices taken into account in the electricity market model are also based on real Iberian electricity market values (from 2014) what provides a realistic approach to the economic analysis that has been presented.

3

Market participation based on rules based control strategies

3. Market participation based on rules based control strategies

This third chapter aims the explanation of the IPV power plant market participation. This market participation is carried out applying the model predictive control (MPC). Firstly, several rules based (RB) control strategies are proposed to provide the firming service. After that, a comparison between different RB strategies is carried out in order to analyze which of the presented strategies is the most performing one for the present application. Finally, the market participation based on MPC and the application of this strategy to the MPC are developed and the obtained results are discussed.

3.1. Standard IPV control strategies

In this section, some standard base control strategies to participate in electricity markets are explained. As it has been mentioned before, one of the requirements to participate in electricity markets is to have the ability to provide constant power during each market programming period, which is an hour. Based on the PV generation and taking advantage of the energy reserves of the storage system, the IPV power plant is able to provide this service, which is called firming service.

The firming service implies, therefore, the maintenance of an amount of power during the whole horizon of a market programming period. The difficulty is to define the value which has to be maintained constant and this is calculated by means of different firming strategies. Some of them can be calculated based on an optimization process, but in this first part, those firming strategies are calculated based on rules.

3.1.1. Description of rules based control strategies

In this section several rules based strategies have been developed to calculate the firming value which is used to provide constant power to the grid. These strategies are applied to the market participation within the IPV power plant management strategy. Each firming control strategy offers to the market a constant power (P_{market}) from the PV generated power (P_{PV}), during each market period. The proposed ones are described as follows.

RB1: Hour initial value. This strategy proposes the power which is expected on the initial point of each hour. During the whole hour, this value is provided to the grid, even if the PV power generation is greater or lower than the hour initial value. In the sunny morning hours, when the PV power generation is continuously increasing (as in Figure 3.1) the storage system absorbs the overproduction, while in the afternoons, when the PV power generation is continuously decreasing the storage system provides the strategy power targets. The equation that models this strategy is calculated in Eq. 3.1.

$$P_{market}(k) = \begin{cases} \hat{P}_{PV}(k), & k = k_{hour}^{i} \\ P_{market}(k-1), & k \neq k_{hour}^{i} \end{cases} \quad \text{Eq. 3.1}$$

Where P_{market} is the market power and strategy output for each k discrete state; $\hat{P}_{PV}$ is the predicted PV power; and k_{hour}^{i} is the discrete state of each hour i on the dot.

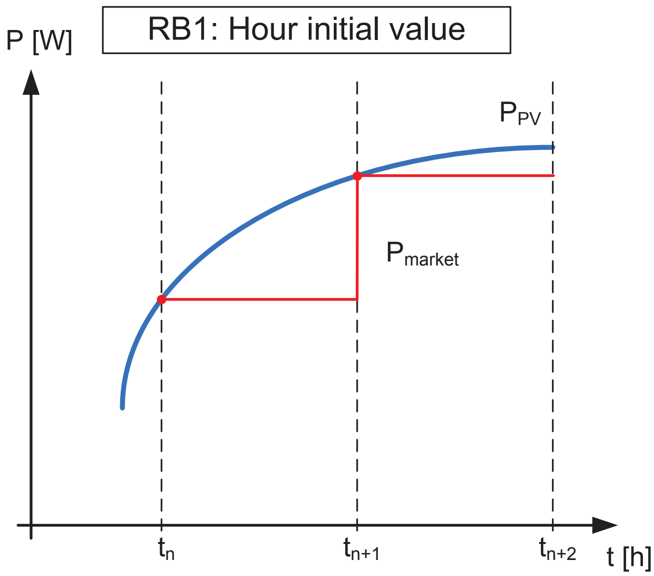

Figure 3.1: RB1: hour initial value strategy example.

RB2: Hour end value. This strategy proposes the power which is expected on the final point of each hour. During the whole hour, the end value is provided to the grid even if the PV power generation is greater or lower than the hour end value. In the sunny morning hours, when the PV power generation is continuously increasing (as in Figure 3.2) the storage system provides the strategy power targets, while in the afternoons, when the PV power generation is continuously decreasing the storage system absorbs the overproduction. The equation that models this strategy is formulated in Eq. 3.2.

$$P_{market}(k) = \begin{cases} \hat{P}_{PV}(k + \Delta k_{hour}), & k = k_{hour}^{i} \\ P_{market}(k-1), & k \neq k_{hour}^{i} \end{cases} \quad \text{Eq. 3.2}$$

Where Δk_{hour} is the difference between each k_{hour}^{i}, which is always one hour.

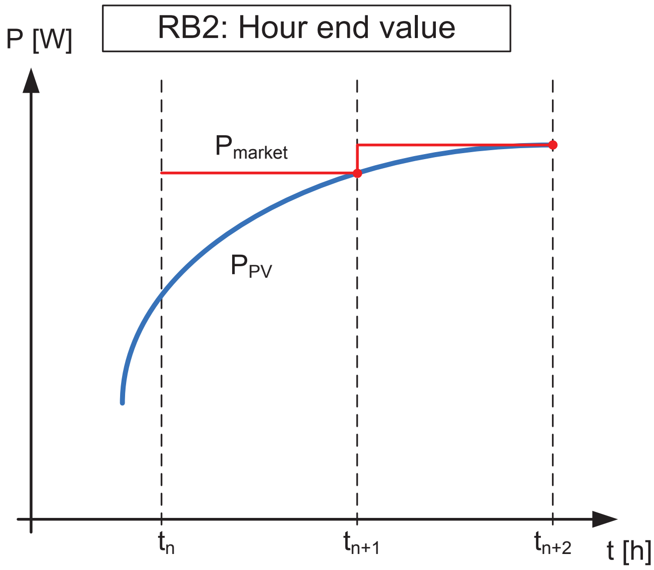

Figure 3.2: RB2: hour end value strategy example.

RB3: Hour middle value. This strategy proposes the power which is expected on the middle point of each hour. It is also similar to the previous strategies, but during the whole day the storage system absorbs and provides energy every hour if the PV power generation is continuously increasing (as in Figure 3.3) or decreasing. The equation that models this strategy is calculated in Eq. 3.3.

$$P_{market}\ (k) = \begin{cases} \hat{P}_{PV}\,(k + \Delta k_{hour}\,/2), & k = k^{i}_{hour} \\ P_{market}\ (k-1), & k \neq k^{i}_{hour} \end{cases} \qquad \text{Eq. 3.3}$$

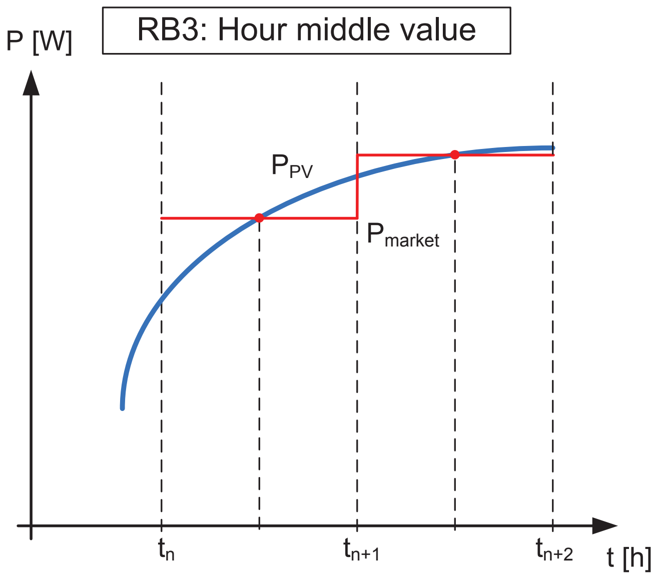

Figure 3.3: RB3: hour middle value strategy example.

RB4: Hour power mean value. This strategy proposes the power which is expected as mean value between the initial and end points of each hour. As the previous strategy, during the whole day the storage system absorbs and provides energy each hour if the PV power generation is continuously increasing (as in Figure 3.4) or decreasing. The previous strategy proposes the time axis middle point for each hour, while this strategy proposes the power axes middle point also for each hour. The equation that models this strategy is determined in Eq. 3.4.

$$P_{market}(k) = \begin{cases} \frac{\hat{P}_{PV}(k) + \hat{P}_{PV}(k + \Delta k_{hour})}{2}, & k = k_{hour}^{i} \\ P_{market}(k-1), & k \neq k_{hour}^{i} \end{cases} \quad \text{Eq. 3.4}$$

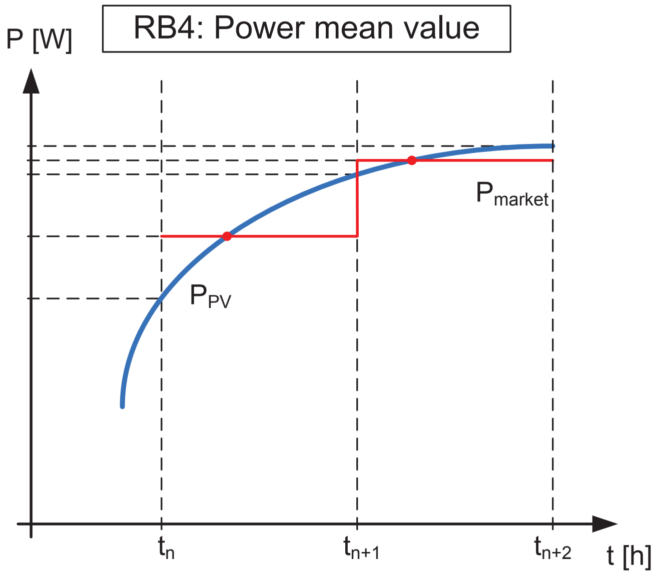

Figure 3.4: RB4: hour power mean value strategy example.

RB5: Hour energy balance value. This strategy proposes the power that obtains an energy balance with the expected power during the whole hour. As the previous strategies (RB3 and RB4), during the whole day the storage system absorbs and provides energy each hour even if the PV power generation is continuously increasing (as in Figure 3.5), decreasing or varying. But in this case, the energy provided and absorbed during each hour is always the same, maintaining the state of charge (SOC) of the storage system in the same point after each hour. The equation that models this strategy is formulated in Eq. 3.5.

$$P_{market}(k) = \begin{cases} \frac{\sum_{k=k_{hour}^{i}}^{k=k_{hour}^{i+1}} \hat{P}_{PV}(k)}{\sum_{k=k_{hour}^{i}}^{k=k_{hour}^{i+1}} 1}, & k = k_{hour}^{i} \\ P_{market}(k-1), & k \neq k_{hour}^{i} \end{cases} \quad \text{Eq. 3.5}$$

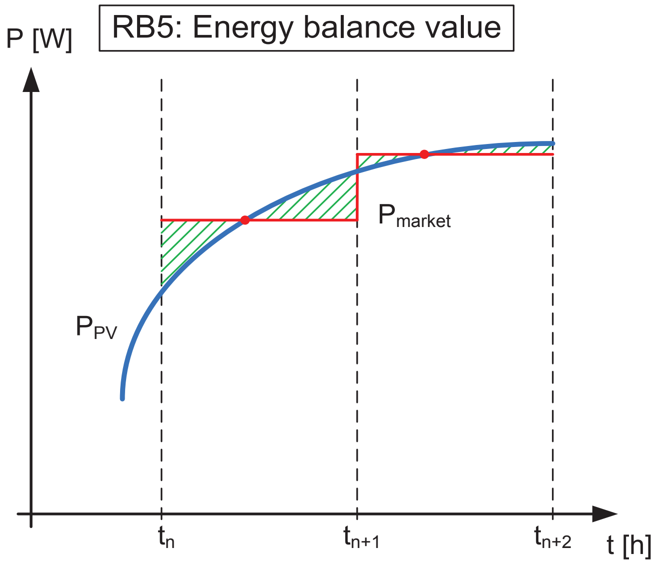

Figure 3.5: RB5: energy balance value strategy example.

3.1.2. Comparison of rules based strategies

To compare the applicability and the results of each proposed firming strategy, a comparison process has been carried out. The objective of this process is to obtain the maximum economic exploitation by means of optimal market participation of the IPV power plant. The market participation is based on the aforementioned firming control strategies. To determine the most appropriate firming control strategy, different criteria are taken into account as the lifetime of the energy storage system and the percentage of time that the IPV power plant provides to the market cleared offer.

Rainflow cycling counting algorithm, the battery manufacturer data and different cycling tests carried out in the energy storage laboratory of Ikerlan have been used to determine the battery lifetime of each strategy. The calculation for obtaining this lifetime of the storage system (t_{bat}) is explained in 2.3.2.3 (Eq. 2.41).

Another crucial parameter to quantify the benefits obtained from the electricity markets is the time in which the market cleared energy has been provided by the IPV power plant ($T_{out_{match}}$) achieving the objective of the correct market participation. If any generator produces more or less than what has been cleared in the market, there are penalties to counteract the overproduction or the not provided production. Therefore, this value must be maximized, trying to obtain the 100%. The time when the IPV plant output power does not match the cleared value produces penalties. These penalties are separated in two other parameters that are the time when the IPV power plant produces more than what has been cleared in the market ($T_{out_{more}}$) and the time when the IPV power plant has not reached what has been cleared in the market ($T_{out_{less}}$). These three values are calculated applying Eq. 3.6, Eq. 3.7, and Eq. 3.8.

$$T_{ou\,t_{matc\ h}} = \frac{t_{matc\ h}}{t_{simulation}} \cdot 100\ [\%]$$ Eq. 3.6

$$T_{ou\,t_{more}} = \frac{t_{more}}{t_{simulation}} \cdot 100\ [\%]$$ Eq. 3.7

$$T_{ou\,t_{less}} = \frac{t_{less}}{t_{simulation}} \cdot 100\ [\%]$$ Eq. 3.8

Where $t_{matc\,h}$ (h) is the time of the simulation in which the market cleared energy is provided; $t_{simulation}$ (h) is the simulation length, which value is the 8760 hours of a whole year; t_{more} (h) is the time of the simulation in which the IPV plant has provided more than what it has cleared; and t_{less} (h) is the time of the simulation in which the IPV plant has provided less than what it has cleared.

The firming control strategies are programmed in Matlab and variable length simulations are carried out using real PV generation data as PV prediction with two minutes time step. For the present work, whole year simulations are performed analyzing the before explained parameters: the lifetime of the storage system and the time percentages in which the market cleared energy is provided by the IPV power plant.

For analyzing the robustness of each control strategy, some PV generation errors are included, from the predicted power generation to the real generation data. The introduced errors are modeled by a normal distribution function with mean parameter $\mu = 0$ and standard deviation parameter $\sigma = 0.01$, which is an additive white Gaussian noise, AWGN. The use of this type of error is very common on this type of studies [149]. Due to the nature of the introduced errors, each simulation obtains different results and for that reason three realizations are carried out introducing the explained errors for each control strategy.

The results with and without error are summarized in Figure 3.6 and Figure 3.7. Figure 3.6 explains the matching time percentages between the market cleared generation and the grid provided energy ($T_{ou\,t_{matc\ h}}$, $T_{ou\,t_{more}}$, and $T_{ou\,t_{less}}$). Figure 3.7 describes the lifetime of the storage system, t_{bat} .

In Figure 3.6 each strategy is depicted with four bars, the first one is calculated without errors between prediction and real data and the next three ones with the previously explained errors. As the value of $T_{ou\,t_{matc\ h}}$ is always above 90%, the presented figure is a zoom over the 90 and 100% of the time in Y axis.

As it could be verified, the most well suited strategy is the RB5, the hour energy balance value. Almost all the time, the market cleared power is provided by the IPV power plant (every time greater than 99.86%), so the economic exploitation is the best one. The next most performed strategies in terms of these parameters are the RB3 and RB4 respectively.

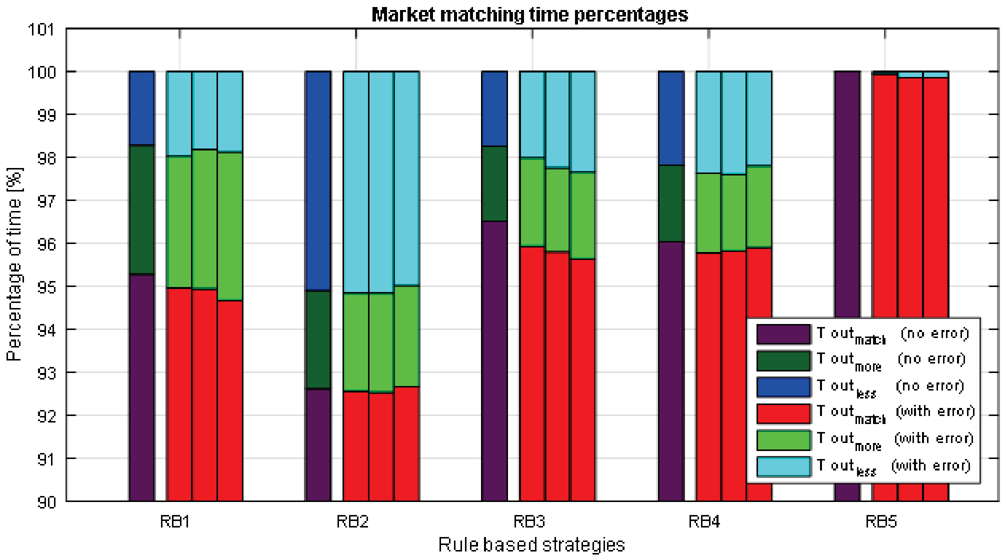

Figure 3.6: Results of market matching time percentages of the whole year simulation with (with error) and without prediction errors (no error).

As in the previous figure, in Figure 3.7, the results are also presented with three realizations of errors and without prediction errors.

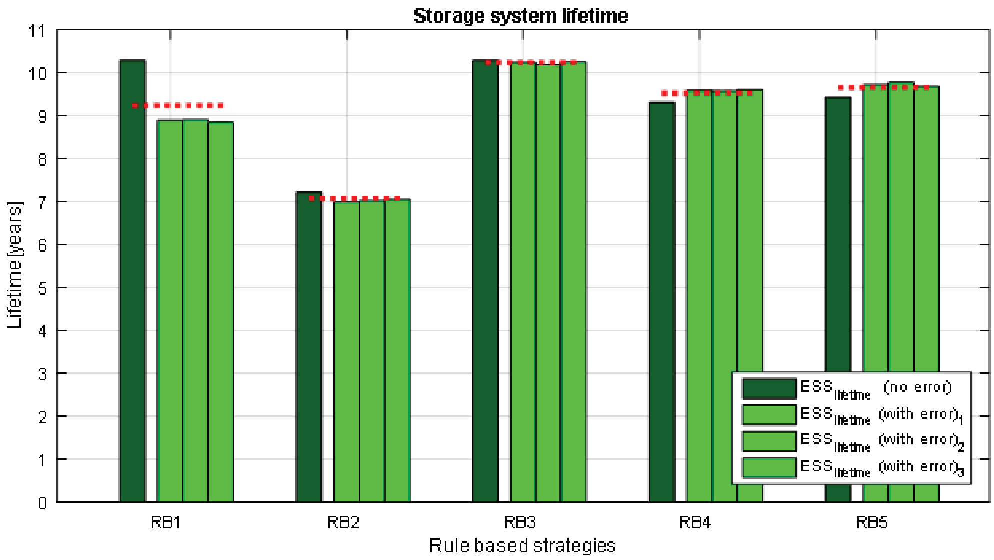

Figure 3.7: Results of storage system lifetime of the whole year simulation with (with error) and without prediction errors (no error).

From the 7 years of the strategy RB2 to the 10.2 years of the other strategies, the difference to be taken into account is important, but analyzing the most interesting control strategies mentioned before, RB5, RB3 and RB4 respectively, all of them obtain similar results, between 9.3 and 10.2 years. Even so, the RB3 obtains the best lifetime results (average 10.2 years), followed by RB5 (average 9.7 years).

The lifetime defined for the present IPV power plant is 25 years, so the storage system demands some replacements apart from the initial investment. Analyzing the storage system lifetime by applying RB3 and RB5, leads to the same amount of replacements (two) calculated as in Eq. 2.42. Therefore, in this case, the RB strategy selection has to be done based on the results related to the matching time percentages.

Thus, it could be stated that the best control strategy among the presented ones is the RB5 (hour energy balance value), which has representative values for the relevant analyzed criteria. For that reason this strategy is being applied in the IPV power plant management strategy for market participation.

3.2. Market participation based on MPC with RB strategy

The market participation is an online operation process to participate in the pool market by the IPV power plant. It is composed by two steps: 1) the *generation planning* of the day d+1, and 2) the *online operation*. This process is carried out on the plant controller of the IPV power plant and it is presented on Figure 3.8.

At the *generation planning* step, the daily market generation offers (an amount of energy for each hour, $E_{offered}^{DM}(k)$, at a given cost, $c_{offered}^{DM}(k)$) based on some control strategies are submitted to the market operator (MO) in order to participate in the daily market. In this case, the control strategy applied to calculate the firming value is the RB5 (hour energy balance value) before explained. These daily market offers are based on the PV generation prediction that will be explained in the following section 3.2.2. In order to make sure that the proposed offer is cleared, the hourly cost offered must be zero or very close to zero. The resolution of the market is composed by the cleared energy ($E_{cleared}^{DM}(k)$) and the marginal prices ($c_{cleared}^{DM}(k)$) for each hour. This planning is transformed into the power references for the IPV power plant, $P_{grid}^{*}(k)$.

After the planning, the *online operation* is developed, using the model predictive control (MPC) to participate in intraday markets. The detailed explanation of this MPC controller will be presented in the next section. This controller has two tasks: the intraday market participation and the control of the battery power to maintain the IPV power plant output power to the targets cleared in the different markets.

Based on the power references of the IPV power plant ($P_{grid}^{*}(k)$), the MPC calculates the intraday markets' (IM) offers (also an amount of energy for each hour, $E_{offered}^{IMj}(k)$, at a given cost, $c_{offered}^{IMj}(k)$) and sends them only in the last sample time before closing each intraday market j session (k_{send}^{IMj}). In this case, the control strategy applied to calculate the firming value is also the RB5 (hour energy balance value), and once again, in order to make sure that the proposed offer is cleared, the hourly cost offered must be zero or very close to zero. The resolution of the market is composed by the intraday market j (IMj) cleared energy ($E_{cleared}^{IMj}(k)$) and the marginal prices ($c_{cleared}^{IMj}(k)$) for each hour. This planning is added to the previous markets' resolutions in order to update the power references for the IPV power plant, $P_{grid}^{*}(k)$.

The whole market participation process is carried out in the plant controller because besides the fact of participating in the market, the plant controller controls the power reference of the storage system, $P_{bat}\,(k)$, as it can be verified in Figure 3.8. That is why this process must be managed in the plant controller. An overview of this market participation process is presented in Figure 3.8, and the flowchart that explains more in detail each step of the market participation sequence is depicted in Figure 3.9.

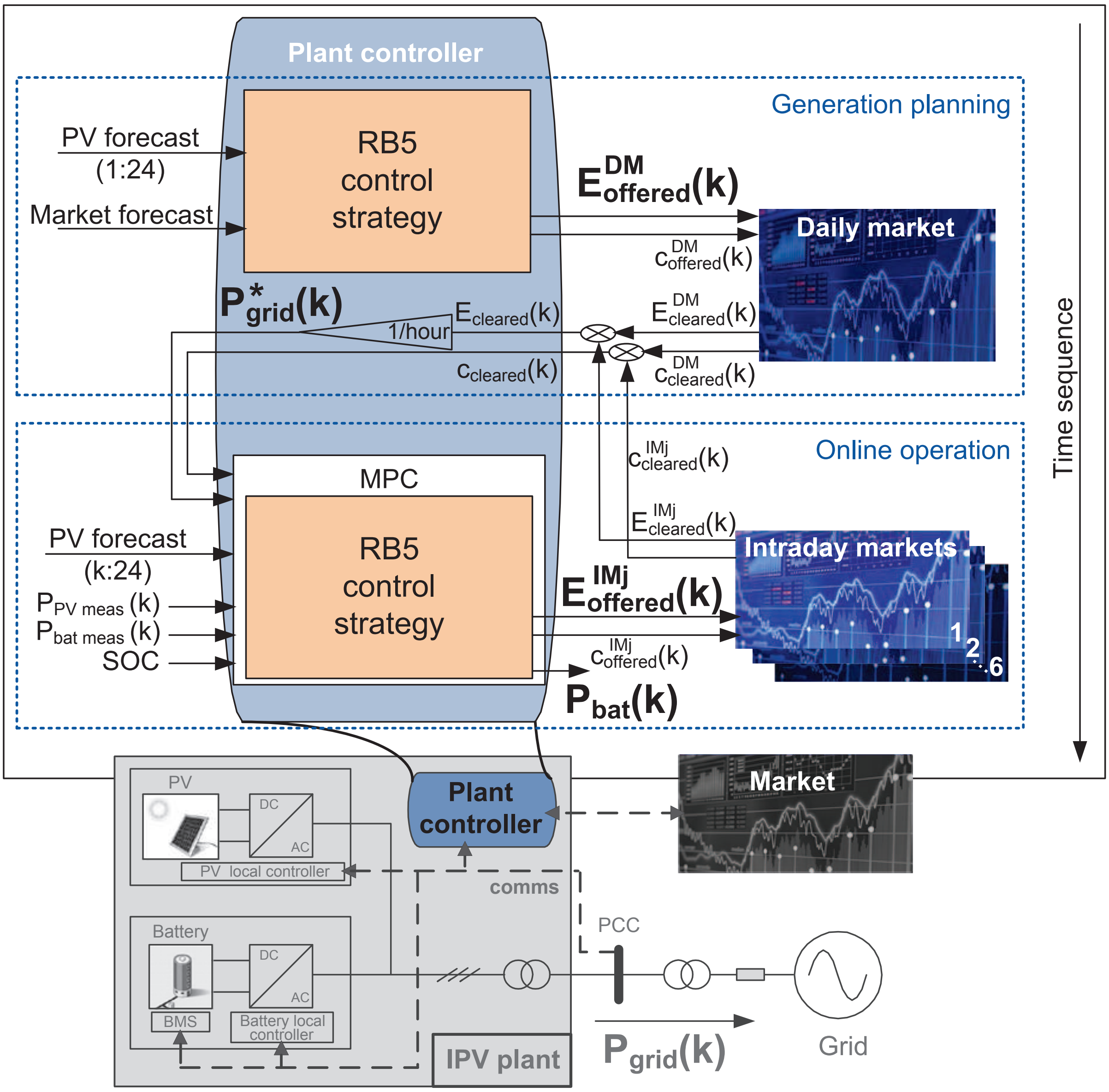

Figure 3.8: Market participation scenario, where the plant controller and different markets' interactions are presented, including the generation planning (to daily market) and the online operation (to intraday markets) steps.

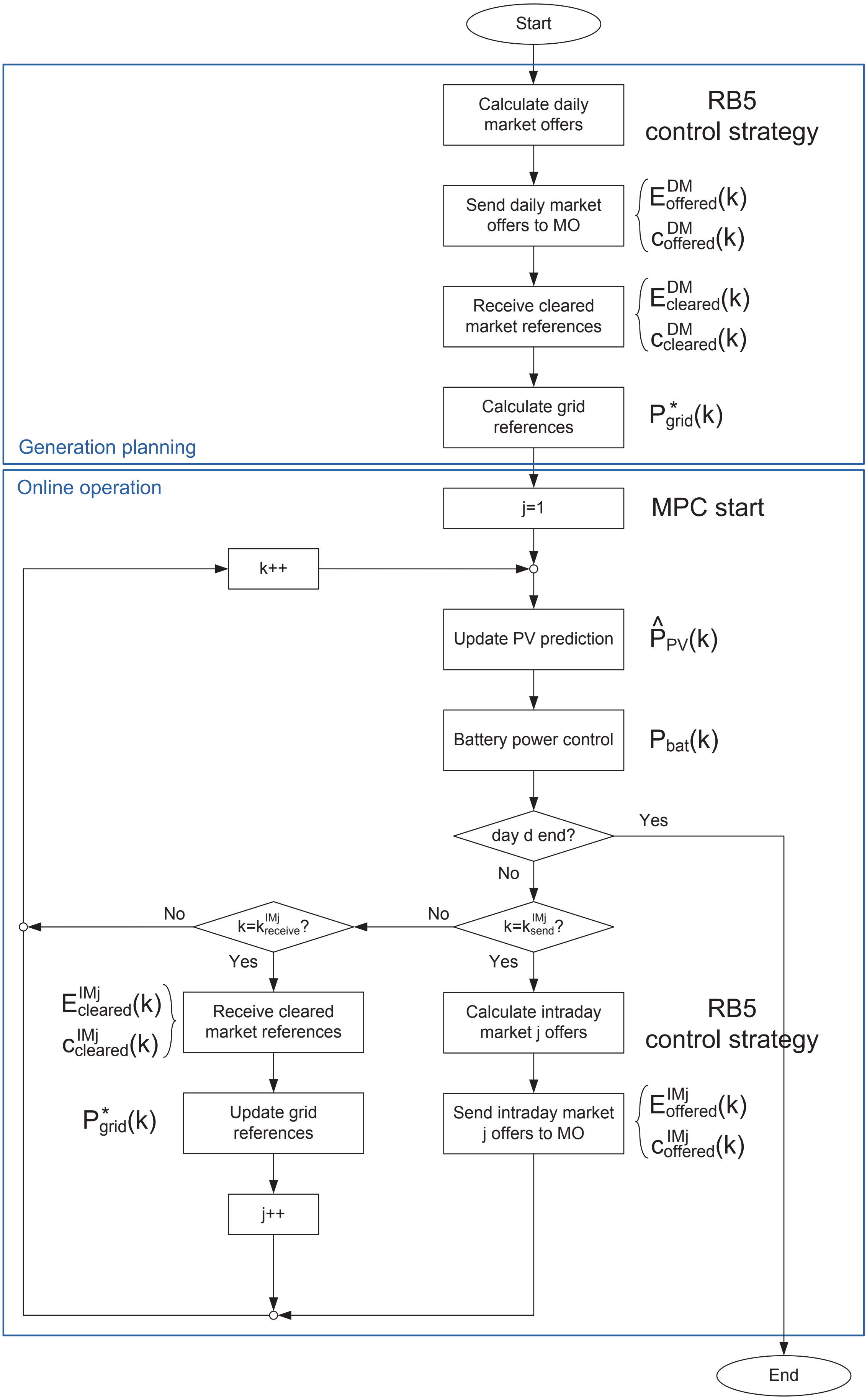

Figure 3.9: Market participation detailed flowchart, with the sequence to manage the whole day participation.

As it can be shown in Figure 3.9, the MPC controls the battery power in each discrete state (k). Moreover, only in some discrete states, when $k = k_{send}^{IMj}$, the MPC manages the intraday market j participation (calculating the offers and sending them). Each intraday market resolution is also always published at some discrete states, when $k = k_{receive}^{IMj}$, and at those moments, the power references for the IPV power plant, $P_{grid}^{*}(k)$, are updated. It is worth to remember that there are 6 intraday markets nowadays in the Iberian Peninsula electricity market.

Once the market participation operation scenario has been detailed by means of different figures, in order to understand the whole system and the internal steps that are carried out in the plant controller, the detailed explanation of the MPC will be developed in the next section.

3.2.1. Detailed MPC explanation

The model predictive control is an advanced control technique, which optimizes a fixed horizon taking into account the preceding inputs and outputs as well as the future predictions [27, 150, 151]. The internal steps that are carried out at every discrete state of the MPC are the next ones, and can be better understood with the diagram of the Figure 3.10.

1) *Horizon definition:* The horizon is shifted from the previous step, maintaining the horizon length fixed. This horizon is called prediction horizon.

2) *Optimal trajectory prediction:* The optimal output trajectory is predicted taking into account the preceding inputs and outputs. The optimal trajectory is, therefore, defined.

3) *Control signals calculation:* The control signals to obtain the predicted optimal trajectory (step 2) are calculated, optimizing a determined criterion. This control signal is the control input $u(k)$ of the Figure 3.10.

4) *First control signal application:* From the control signal sequence ($u(k)$), only the first value is applied to the process, $u_0(k)$.

5) *Process repetition:* The explained process is repeated at every discrete state, shifting the prediction horizon, predicting the new optimal trajectory, calculating the control signal ($u(k+1)$), applying the first value ($u_0(k+1)$) and repeating again the process.

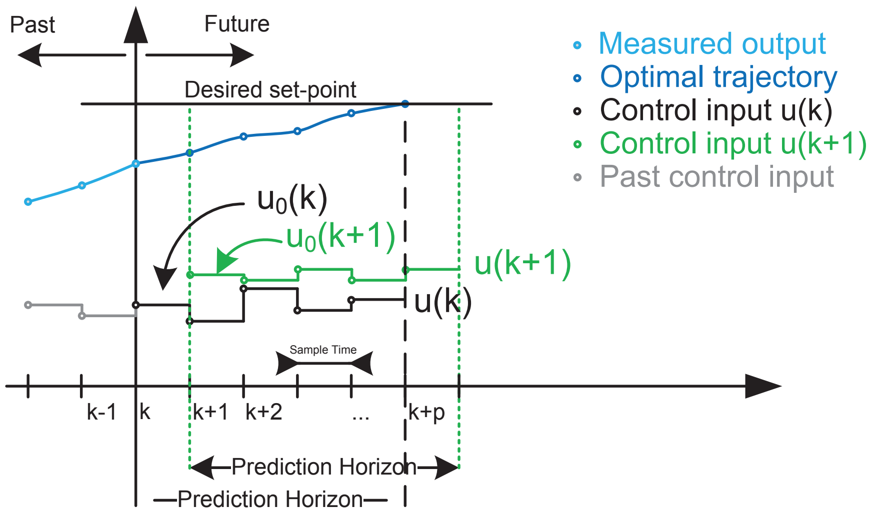

Figure 3.10: MPC operation summary diagram.

Therefore, at every discrete state the MPC calculates the operation of a given window (prediction horizon) based on the predictions and measures of some parameters, in this case the PV generation. At this point, the optimal trajectory applying the RB5 is calculated as well as the control input ($u(k)$) for obtaining this optimal trajectory. From this control input, only the first point ($u_0(k)$) is applied to the system. The control input in this study is composed by two parameters: the battery power, $P_{bat}(k)$, and the intraday markets participation offers (an amount of energy for each hour, $E_{offered}^{IMj}(k)$, at a given cost, $c_{offered}^{IMj}(k)$).

On the one hand, the battery power control is carried out to maintain the IPV power plant output power on the market cleared references. This is calculated subtracting the PV generation to the power references for the IPV power plant, $P_{grid}^{*}(k)$, as in Eq. 3.9.

$$P_{bat}(k) = P_{grid}^{*}(k) - P_{PV}(k) \qquad \text{Eq. 3.9}$$

On the other hand, the MPC calculates the intraday market offers taking into account the last PV predictions. If the PV forecasts of the day $d-1$ are maintained, the MPC do not participate in the intraday market (assuming that the PV generation is already cleared in the daily market). Even so, as there is not an intraday market session every discrete state, the market offers are calculated only in the last discrete state before closing each intraday market j session (k_{send}^{IMj}), as it can be shown in Figure 3.9. This market participation is based on RB5 strategy, whose market offer is calculated as in Eq. 3.5.

3.2.2. PV generation prediction

In this section, the PV prediction ($\hat{P}_{PV}$) calculation is explained. The PV prediction is necessary in order to estimate the PV generation to be able to participate in electricity markets with a given prediction value. The predicted values can be more or less correct, but finally, these are the values the market participation can be carried out with. In this study, the considered different PV predictions are calculated as the following ones, but each PV plant owner can calculate its predictions with different level of detail. Nowadays there are several PV prediction software which are based on meteorological data, historical data, and also based on autoregressive models [152]. In the present work the PV prediction is separated in three different subsections which analyze the year $y-1$ real generation to determine PV prediction for daily market, the preceding days measured generation in order to correct the previous prediction and the own day d generation to correct again the preceding predictions.

1) PV prediction for daily market: In this first step, the PV prediction is calculated as in Eq. 3.10 to determine the daily market offers. In order to include the seasonal effect on PV generation (from a real PV generation data of the year $y-1$), this prediction considers a window of N_{wp} days to estimate the average value. Therefore, for each discrete state of a given day d, the PV prediction is calculated by the average value from the PV generation of the year $y-1$ taking into account the $N_{wp}/2$ preceding days up to the $N_{wp}/2$ following days.

$$\hat{P}_{PV}\left(k_{1_d}:k_{N_d}\right) = \sum_{r=-N_{wp}/2}^{N_{wp}/2} P_{PV}^{real}\left(k_{1_r}:k_{N_r}\right)\Big/N_{wp} \qquad \text{Eq. 3.10}$$

Where k_{1_d} and k_{N_d} are the initial discrete state (midnight of day d) and the last discrete state (discrete state before midnight of day $d+1$) in the day d of the present year y, respectively. k_{1_r} and k_{N_r} are the initial discrete state (midnight of day r) and the last discrete state (discrete state before midnight of day $r+1$) in the day r from the year $y-1$, respectively. P_{PV}^{real} is the real PV generation of the year $y-1$. It is worth mentioning that in Eq. 3.10, the value of each discrete state $\left(k_{1_d}:k_{N_d}\right)$ is the average one by taking into account the values in the same discrete state in each day r.

2) PV prediction in MPC before the day d: once the MPC has started, the PV prediction is separated into two different steps: the one that is calculated before the day under consideration (before midnight), and the one that is calculated during the day under consideration, the day d. The prediction before midnight takes into account the whole horizon of the day d prediction and it is calculated as in Eq. 3.11. It includes the prediction explained in Eq. 3.10 plus the previous N_{wc} days measured generation (P_{PV}^{mes}). These terms are weighed by the factors a and b. Therefore the sum of these two values must be always equal to one. The factor a includes the seasonal effect and the factor b contributes to the current generation (the measured generation of the previous N_{wc} days). After several simulation tests related to the proper weighting values for a and b, it was determined that the factor b is more relevant than factor a due to the fact that the current generation (which is trying to predict it) could follow the trends of the generation of the previous days. In this work, it is assumed the following weighting values: $a = 0{,}2$ and $b = 0{,}8$.

$$\hat{P}_{PV}\left(k_{1_d}\!:k_{N_d}\right) = a \cdot \left(\sum_{r=-\frac{N_{wp}}{2}}^{\frac{N_{wp}}{2}} P_{PV}^{real}\left(k_{1_r}\!:k_{N_r}\right) \Big/ N_{wp} \right) + b \cdot \left(\sum_{i=d-N_{wc}}^{d-1} P_{PV}^{mes}\left(k_{1_i}\!:k_{N_i}\right) \Big/ N_{wc} \right) \quad \text{Eq. 3.11}$$

3) PV prediction in MPC during the day d: The prediction during the day d ($\hat{P}_{PV_{ct}}$) is calculated as in Eq. 3.12, which calculates the PV prediction from the current discrete state (k_{ct_d}) until the final discrete state (k_{N_d}) of the day d. In this case, the considered prediction terms are the ones explained in Eq. 3.12 plus a correction factor (CF) expressed in Eq. 3.13. This term calculates the energetic error generated between the real measured PV generation profile (E_{PV}^{mes}) and the predicted profile ($\hat{E}_{PV}$) until the discrete state of the current time (k_{ct_d}). Considering that this error ($E_{PV}^{mes}\left(k_{ct_d}\right) - \hat{E}_{PV}\left(k_{ct_d}\right)$) will be maintained from the current time ($t(k_{ct_d})$) until the time when the next intraday market starts in operation ($t(k_{os_d}^{IMj})$), the energetic error estimation of this period of time is obtained. The CF is, therefore, calculated by the addition of the energetic error generated and the energetic error estimated divided by the time Δt_{end}. This value is the period of time in hours between the time when the next intraday session j starts its operation and the time of the discrete state of the sunset of the day d, which is $t(\hat{k}_{ss_d})$. This value is estimated based on the sunset of the previous days. Therefore, the CF, which is a power value, is obtained. This CF equation is only applied until the discrete state of the sunset of the day d. The value of the CF discrete states between the sunset and the end of the day d are zero, as it can be verified in Eq. 3.13. The detail of this PV prediction estimation is calculated as in Eq. 3.12, Eq. 3.13, Eq. 3.14, Eq. 3.15 and Eq. 3.16.

$$\hat{P}_{PV_{ct}}\left(k_{ct_d}\!:k_{N_d}\right) = a \cdot \left(\sum_{r=-\frac{N_{wp}}{2}}^{\frac{N_{wp}}{2}} P_{PV}^{real}\left(k_{ct_r}\!:k_{N_r}\right) \Big/ N_{wp} \right) + b \cdot \left(\sum_{i=d-N_{wc}}^{d-1} P_{PV}^{mes}\left(k_{ct_i}\!:k_{N_i}\right) \Big/ N_{wc} \right) + CF\left(k_{ct_d}\!:k_{N_d}\right) \quad \text{Eq. 3.12}$$

$$CF\left(k_{ct_d}:k_{N_d}\right) = \begin{cases} \dfrac{E_{PV}^{mes}\left(k_{ct_d}\right) - \hat{E}_{PV}\left(k_{ct_d}\right) + \dfrac{E_{PV}^{mes}\left(k_{ct_d}\right) - \hat{E}_{PV}\left(k_{ct_d}\right)}{\Delta t_{ct}} \cdot \Delta t_{gap}}{\Delta t_{end}}, & k < \hat{k}_{ss_d} \\ 0, & k \geq \hat{k}_{ss_d} \end{cases} \quad \text{Eq. 3.13}$$

$$\Delta t_{ct} = t(k_{ct_d}) - t(k_{1_d}) \quad \text{Eq. 3.14}$$

$$\Delta t_{gap} = t(k_{os_d}^{IMj}) - t(k_{ct_d}) \quad \text{Eq. 3.15}$$

$$\Delta t_{end} = t\left(\hat{k}_{ss_d}\right) - t(k_{os_d}^{IMj}) \quad \text{Eq. 3.16}$$

Where $E_{PV}\left(k_{ct_d}\right)$ is the energy generated during the day d until the discrete state of the current time. $\hat{E}_{PV}\left(k_{ct_d}\right)$ is the predicted energy generation during the day d until the discrete state of the current time. Δt_{ct} is the period of time in hours between the initial time of the day d and the time of the current discrete state. The initial discrete state of the day is always the midnight, so this variable calculates the time from midnight to the current time in hours. Δt_{gap} is the period of time in hours between the time of the current step and the time when the next intraday session j starts its operation, $t(k_{os_d}^{IMj})$. Δt_{end} is the period of time in hours between the estimated discrete state of the sunset, $t\left(\hat{k}_{ss_d}\right)$, and the time when the next intraday session j starts its operation, $t(k_{os_d}^{IMj})$.

3.2.3. Results of the market participation based on RB5 control strategy

The online IPV power plant market participation is carried out by the plant controller. This market participation includes both daily and intraday market participation, which are the generation planning and the online operation steps, respectively, presented in Figure 3.8 and Figure 3.9. As shown in Figure 3.8, from PV forecast and market forecasts the plant controller calculates the offers for daily market based on the before analyzed firming strategy, RB5, the hour energy balance value. As it has been mentioned before, the IPV power plant generation offers cost is always zero or very close to zero in order to make sure that the proposed offer is cleared.

Assuming that the daily market offers are cleared ($E_{cleared}^{DM}(t) \coloneqq E_{offered}^{DM}(t)$), the plant controller already has every hour generation profile or every hour power reference profile ($P_{grid}^{*}(t)$ in Figure 3.8). These references are obtained the day before the online operation. With these references and the actualization of the PV predictions the online operation can be done. In this case, as explained before, the Model Predictive Control is proposed to calculate these adjustments offering positive or negative offers in intraday different sessions. So, the MPC executes the firming strategy before each intraday session closing, when $k = k_{send}^{IMj}$, providing some references for each hour. If the calculated references are the same as the ones cleared in the daily market, this intraday session offers will be zero.

For clearly explaining the results of the presented IPV power plant market participation, an example of the PV generation with the markets schedule is depicted in Figure 3.11. This example is composed by the time sequence in x axis with a given PV prediction and real generation in the upper section. In the bottom section, daily and intraday markets bidding sessions and operation horizons are presented. This figure is oriented to explain the second day (day d) market participation. For doing so, the market participation must start the first day (day $d-1$) to participate in the daily market (by means of the *generation planning* of Figure 3.8 or Figure 3.9). Therefore, once the daily market offers have been sent (before midday of day $d-1$ shown in the grey rectangle in Figure 3.11), the MPC can start assuming that the sent offers will be cleared due to the proposed cheap cost ($c_{offered}^{DM}(t)$ equals or close to zero). From this point (midday of day $d-1$), for including the 24 hours of operation horizon of the day d, 36 hours of MPC horizon are needed. This horizon is also required due to the fact that the intraday session 1 has 27 hours of length plus the period of time between market closing time and operation starting time (around 30 hours). The MPC prediction horizon is depicted in the red sliding rectangles of Figure 3.11. The operation is finished when the starting point of the MPC prediction horizon crosses the end of the day d. The selected sample time is 10 minutes. This value has been selected as the tradeoff between computational cost of the optimization and the desired simulation detail.

The blue rectangles are the period of time when the intraday markets sessions are opened and the green rectangles are the intraday markets operation horizons (detailed in Table 1.2 of Section 1.4.2.2).

Therefore, at each 10 minutes sample time, the MPC calculates the optimal battery exchanged power ($P_{bat}(t)$), considering the PV generation to maintain the IPV power plant output power ($P_{grid}(t)$ shown in the bottom of Figure 3.8) matching to its reference ($P_{grid}^{*}(t)$), which comes from the market cleared energy. Just before closing the intraday 1 market session (blue rectangle in Figure 3.11 and when $k = k_{send}^{IMj}$ in Figure 3.9), the MPC calculates these market offers, based on the last PV predictions. This process is repeated at each intraday session, knowing that each intraday operation horizon is different. As an example, in Figure 3.11, the PV predictions have changed and the participation on the intraday markets permits to face the prediction changes from the operation starting point of each intraday market.

As it can also be seen in Figure 3.11, between intraday session 5 and 6, the following day (day $d+1$) daily market is resolved, closing the cyclic behavior of the market participation scenario.

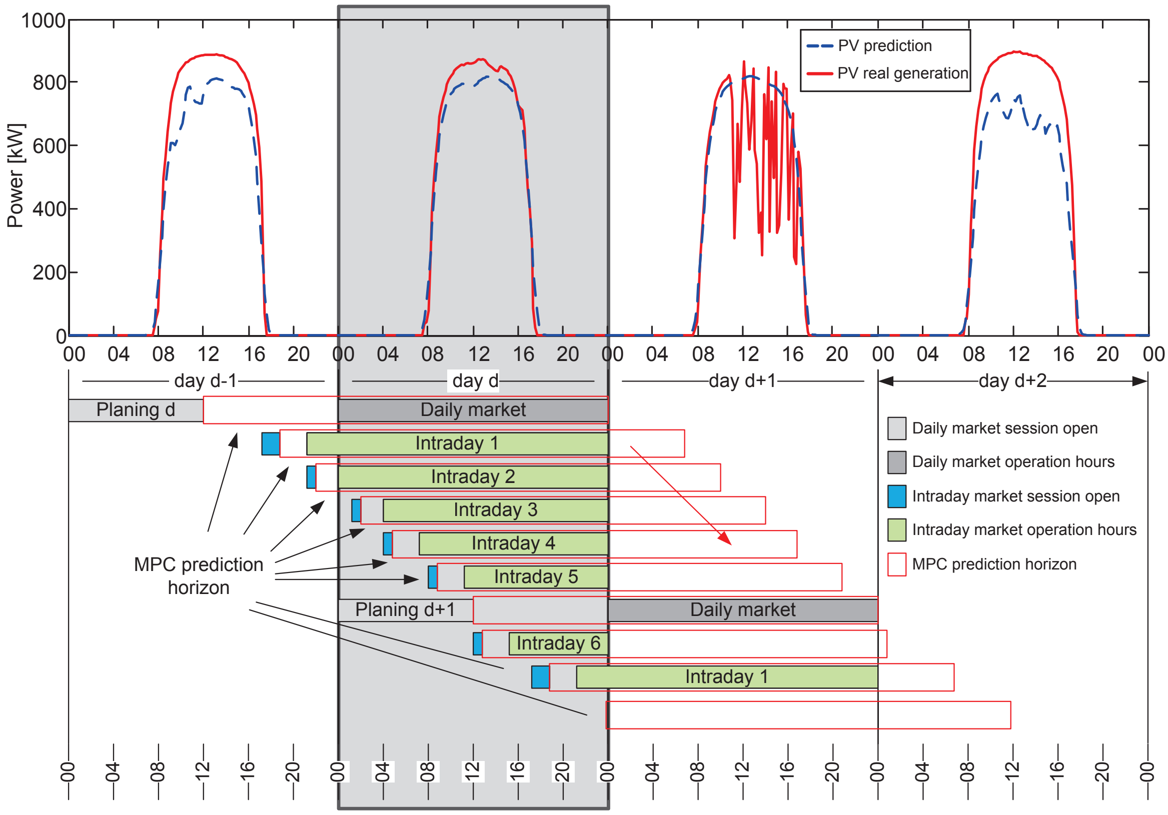

Figure 3.11: Market participation example of the second day (day d) with the different markets operation hours, participation periods and MPC prediction horizon.

Some results of the explained simulation are shown in Figure 3.12, where the simulation of two days market participation is carried out. The first one is detailed in Figure 3.12 a, b and c, and the other one in Figure 3.12 d, e and f. These days are the second (day d) and the third (day $d+1$) days that are presented in Figure 3.11. Therefore, the market participation is executed on a sunny day and on a cloudy day. Figure 3.12 depicts the operation in the last discrete state before closing intraday market 6 session (k_{send}^{IM6}). Figure 3.12 a and d include the PV real generation and the different PV predictions explained in Eq. 3.10, Eq. 3.11 and Eq. 3.12. Figure 3.12 b and e show the market participation (applying the RB5 control strategy) based on the PV generation (measurement and prediction). Figure 3.12 c and f depict the six intraday markets' offers.

As Figure 3.12 a and d are obtained at the discrete state k_{send}^{IM6} (depicted by the pink vertical line), the PV predictions available until this discrete state are: the prediction for the daily market (black profile calculated by Eq. 3.10), the MPC prediction (green profile calculated by Eq. 3.11) and the MPC prediction with the CF (blue profile calculated by Eq. 3.12).

Until the discrete state k_{send}^{IM6}, an energetic error is accumulated between the real generation (red profile on Figure 3.12 a and d) and the predicted generation. This error is positive in the sunny day (Figure 3.12 a) and negative in the cloudy day (Figure 3.12 d). The CF takes into account this error in order to calculate the new prediction, as in Eq. 3.12 and Eq. 3.13, counteracting the PV prediction deviation.

Regarding Figure 3.12 b and e, the included profiles are calculated based on the predictions before explained applying the RB5 control strategy. As the MPC prediction is included once the MPC has started operating, the first intraday market to correct these deviations is the intraday 1 and, therefore, intraday 1 provides important market offers (around 200 kW during several hours of the sunny day as it can be shown in Figure 3.12 c, and more than 200 kW during several hours of the cloudy day as it can be shown in Figure 3.12 f). As it is assumed that this offer is cleared, the offer of the intraday 2 (in both cases, sunny and cloudy day) is a 0 power offer. The grey vertical lines of the Figure 3.12 c and f are the discrete states of the five intraday session's offers sending time (k_{send}^{IM1}, k_{send}^{IM2}, k_{send}^{IM3}, k_{send}^{IM4}, k_{send}^{IM5}) while the pink one is the discrete state of the intraday 6 offer sending time, k_{send}^{IM6}.

From midnight, the PV prediction is corrected through the CF, but in the discrete states when the intraday 3 and 4 are resolved, as there is no PV generation, the CF value is null and therefore, these markets offers are also null (in both cases, sunny and cloudy day). As the offer of the intraday 5 is sent before 8:45 a.m., a little negative energetic error is generated in both cases represented in CF (about some Watts). This error produces a very low intraday 5 market offer, just below zero, that can be appreciated by the light blue profile of Figure 3.12 c and f. Finally, until the period of time when the intraday 6 offer is sent, an important positive energetic error is generated between the prediction and the real generation in the sunny day, and therefore, the CF value is around 100 kW. Consequently, the obtained prediction for calculating the intraday 6 offer takes into account this correction and determines the intraday market 6 offer shown in Figure 3.12 c (red profile). As it can be shown, this offer is sent until the estimated sunset of the day d. On the cloudy day, the inverse effect can be observed. A negative error is generated, computing a negative CF value and, correspondingly, a negative intraday 6 offer is calculated as shown in Figure 3.12 f (also red profile).

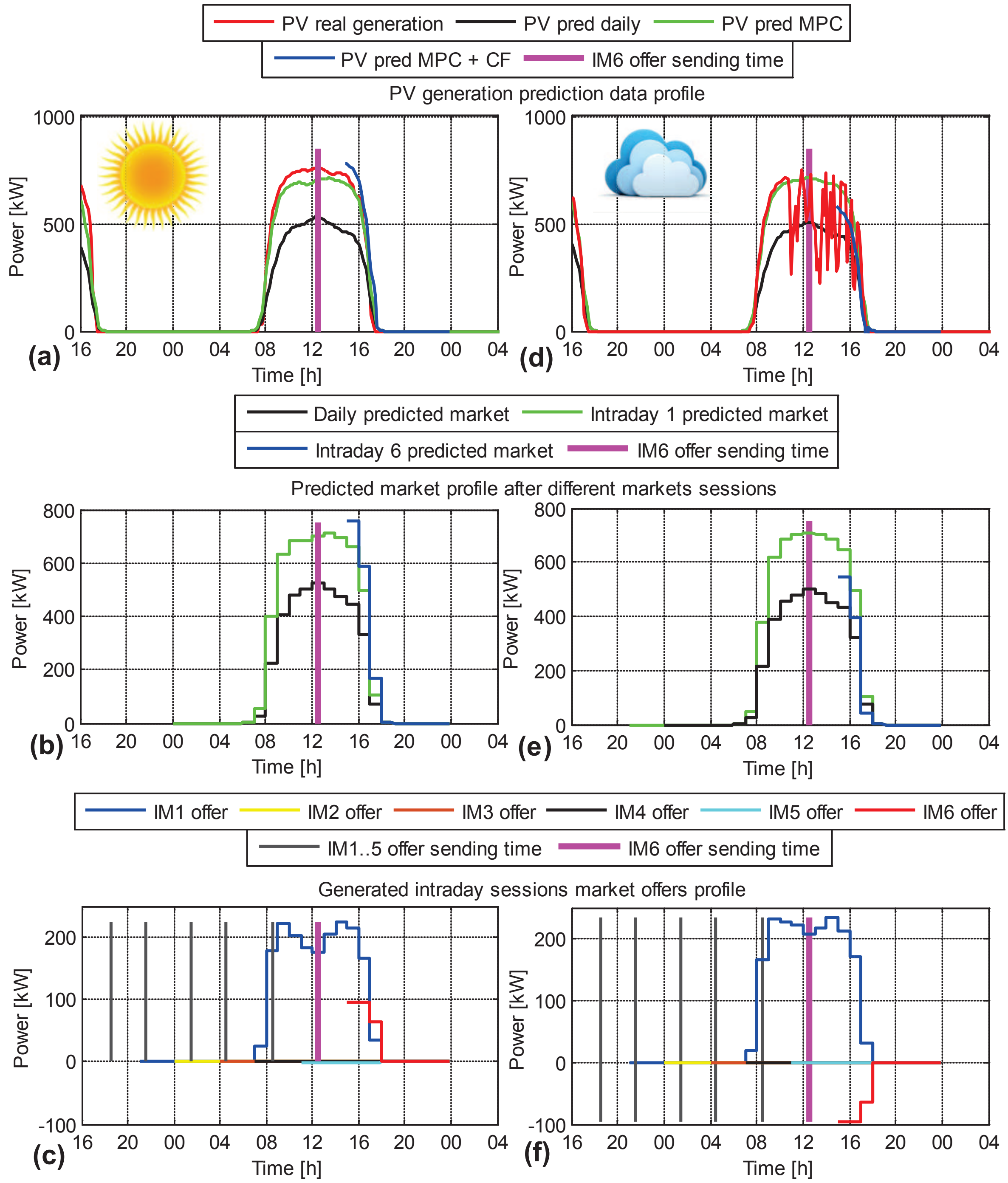

Figure 3.12: Online operation results for a sunny day (a, b and c) and for a cloudy day (d, e and f). a and d: PV generation predictions and real generation; b and e: predicted market profiles; c and f: intraday offers calculated by the MPC.

Thus, as it is verified, the MPC reacts to the predictions changes, improving the *generation planning* (that has participated in daily market) at the *online operation* (that has participated in intraday markets) and reducing penalties caused by the whole IPV power plant.

The economic results related to the MPC application are depicted in Figure 3.13, where it can be seen the economic difference between three cases: a) single day with perfect prediction cleared on daily market (considering the real generation as prediction); b) single day with erroneous prediction (the one calculated as in Eq. 3.10) only using the daily market; and c) single day with erroneous prediction using the daily market and correcting the PV deviations on the intraday markets based on the MPC with the CF. The benefits relation between these three cases is evaluated for the previously presented two days, the sunny day and the cloudy day.

This economic analysis is based on the benefits obtained in electricity markets; therefore, it is based on the energy sold in different markets. This energy comes from the solar resource and also from the energy stored in the battery. All simulations start with the same SOC of the storage system, but they do not finish with the same point of SOC, which indicates that the energy stored in the storage system is different. For that reason, to analyze a more objective scenario, the economic result also takes into account the final SOC difference which indicates a difference in the amount of energy stored for the following days. This SOC or energy difference is economically quantified as the mean daily market price which is 42.12€/MWh in the Iberian Peninsula market of 2014 [147]. Thus, including also this effect, the related benefits depending on predictions and markets participation are presented in Figure 3.13.

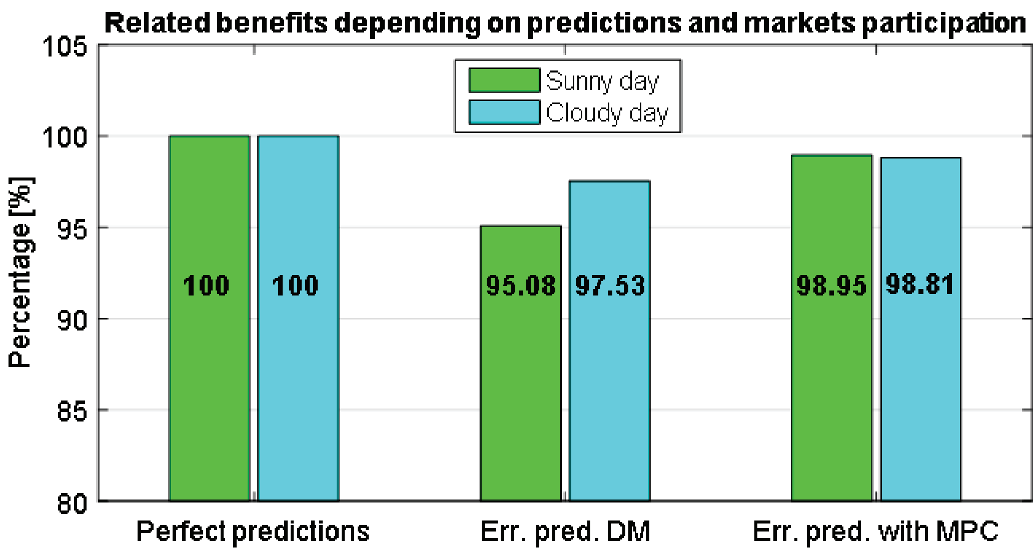

Figure 3.13: Benefits relation between different simulations.

In all cases the economic results are calculated based on the daily market prices and positive and negative deviations prices [147]. These results show the improvement that the use of the MPC includes on the IPV power plant economic exploitation. From the perfect prediction scenario, including prediction errors, without using the MPC and applying only the daily market, the benefits reduction is around 5% in a sunny day and around 2.5% in a cloudy day. Based on these scenarios, including the prediction changes of Eq. 3.11 and Eq. 3.12 during the day, and participating on intraday markets by means of the MPC, the benefits are improved in a 4% and a 1%, respectively, getting more than 98.8% of the perfect scenario benefits in both cases.

As it could be verified, the daily market operation is very important but the MPC for reacting to PV uncertainties in the intraday sessions is as important as daily market participation, due to the fact that it corrects the errors introduced in the daily market caused by erroneous predictions.

3.3. Conclusions

In this third chapter the market participation process has been presented based on the base control strategies, which are some rules based control strategies. Several RB strategies have been presented; a comparison among them has been carried out in order to determine which is the most performing one; and finally, the market participation process has been presented and implemented showing the good results of the market participation process based on the MPC.

Related to the rules based control strategies, it has been demonstrated that the RB5, hour energy balance strategy, is the best firming strategy to introduce the IPV power plant in the electricity spot market. The energy that could be stored in the ESS provides to the IPV power plant the required controllability level to enable the market participation.

In addition to that, the IPV power plant market participation model has been developed, demonstrating the potentiality of renewable generators to participate in electricity markets. The daily market and the intraday different sessions have been explained for the Iberian Peninsula case and a real operation has been simulated. It has been demonstrated that it is possible to participate in electricity markets through the model predictive control. The more accurate PV generation predictions have been considered in the implementation of the MPC which have also updated the firming strategy values, avoiding the important penalties caused by the PV prediction errors. With the proposed strategy, the viability of the renewable generators market participation has been enhanced. This has been obtained thanks to the intraday participation, reducing the penalties caused by the PV prediction errors and achieving almost the 99% of the benefits of the ideal scenario, which is the one with the perfect prediction.

4

IPV storage system sizing and control strategy optimization

4. IPV storage system sizing and control strategy optimization

This fourth chapter explains the optimization process carried out in the present PhD in order to optimize both storage system sizing and control strategy. This optimal control strategy is applied to develop the market participation based on MPC, which is the main contribution of this PhD work.

In the first subsection, the procedure of the sizing and control co-optimization is presented. After that, the sequence to obtain the optimal storage system sizing and the obtained results are summarized, determining the optimal storage system sizing for the given application's conditions. In addition, the market participation sequence to obtain the optimal control strategy is developed. The results of this market participation are presented based on the application of the MPC. Finally, the comparison between the before explained market participation of chapter 3 and the one based on this chapter optimization is carried out, showing the optimality of the presented proposition.

4.1. Sizing and control co-optimization procedure

In this section, the sizing and control strategy co-optimization procedure is described and detailed. All the internal steps included within an optimization process are extensively developed and justified in this section.

4.1.1. Co-optimization procedure

A co-optimization is an optimization procedure that is focused in more than one objective. In this case, the co-optimization term is selected due to the fact that this optimization procedure aims to optimize both storage system sizing and control strategy.

An optimization procedure is composed by several steps. One of the most important steps for the application of an optimization process is the selection of the optimization algorithm. This algorithm is a mathematical tool adapted to the nature of the objective to be optimized, and also to the control variables and procedure states where the optimization problem is applied.

The optimization algorithms search the maximization or the minimization of one or more objectives taking advantage of their own available resources. This process is limited by some constraints which limit the surface of the results, where the final solution is included. To get the optimal introduced objectives, the correct selection and application of the optimization algorithm is needed. Nevertheless, the application of the correct optimization algorithm is only the last step of the whole optimization process. The correct development of all those steps is as important as the selection and application of the optimization algorithm [153].

The steps identified and developed in the present work are summarized in Figure 4.1 and deeply developed in this section.

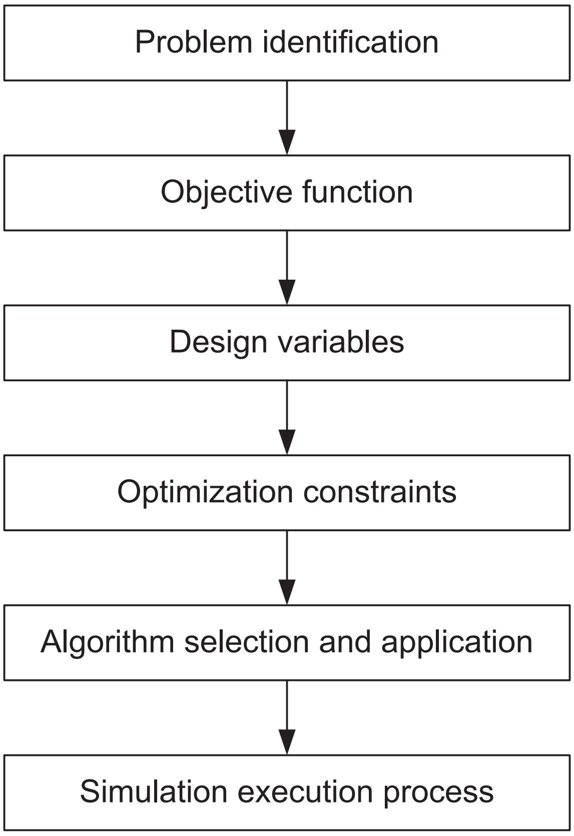

Figure 4.1: Optimization process steps.

4.1.1.1. Problem identification

The first step of this optimization process is the problem identification where the problem to be solved is identified and the optimization objective is grammatically described. In this case, the objectives are both the optimal sizing and the optimal market participation of the IPV power plant in the electricity markets. For that reason a co-optimization process is considered which optimizes the participation taking into account the storage system SOC and its degradation, the PV prediction and the measured real generation and the market prices forecast. Nevertheless, both of the objectives can be achieved by means of **maximizing of the profits of the IPV power plant**, assuming that this maximization will be obtained with the optimal storage capacity able to optimally participate in electricity markets. This problem is the one that will be mathematically introduced in the following objective function step. Therefore, the following objective function will be an economic function.

Another important fact is the identification of the nature of the selected problem. Depending on its nature, the problem can be resolved with a different computational cost, and also with a different speed. As the current optimization process will be applied to control a highly dynamic system, a fast optimization process is needed. For that reason, as the fastest optimization methods are the linear ones, a linear problem is tried to be modeled.

So, considering the objective of a linear problem, the equation that models the linear programming (LP) optimization algorithm is the one formulated in Eq. 4.1.

$$\min_{x} f(x) \text{ such that } \begin{cases} A \cdot x \leq b, \\ A_{eq} \cdot x = b_{eq}, \\ lb \leq x \leq ub. \end{cases} \qquad \text{Eq. 4.1}$$

Where x is the vector composed by the design variables; $f(x)$ is the objective function that has to be a linear equation; A, A_{eq}, b, b_{eq}, lb, and ub are some constraint matrixes and vectors that are explained in the following sections.

4.1.1.2. Objective function

In this case the objective function is an economic one. The economic model of the IPV power plant is the model explained in chapter 2, section 2.3.4. Based on the economic model f, represented in Eq. 2.48, the objective function applied in this optimization process is calculated.

The objective function is, therefore, a cost equation which aims to maximize the net profits. Some terms are not dependent on the optimization design variables (x) and are considered constant (u). Others are the multipliers (c) of the design variables. The optimization process can only optimize the design variables' terms, having as the objective function the function $f'(x)$. For obtaining the maximization of this function, the minimization of its negative function is calculated. These equations are modeled in Eq. 2.1.

$$\begin{aligned} &f(x,u) = c^T \cdot x + k^T \cdot u && \rightarrow economic\ model \\ &f'(x) = c^T \cdot x && \rightarrow objective\ funtion \\ &max\ c^T \cdot x \rightarrow min\ -c^T \cdot x && \end{aligned} \qquad \text{Eq. 4.2}$$

The detailed objective function equation is calculated as in Eq. 4.3.

$$\begin{aligned} min -c^T \cdot x = min \frac{c_{P_{PE}}}{t_{sys} \cdot 365/days} \cdot P_{con\,v_{bat}} + \frac{c_{C_{bat}}}{t_{bat} \cdot 365/days} \cdot C_{bat} \\ - \left(\sum_{k=1}^{n} \Delta t \cdot Price_{marke\ t_k} \right)^T \cdot P_{mkt}(k) \end{aligned} \qquad \text{Eq. 4.3}$$

$$+\left(\sum_{l=1}^{n} \Delta t \cdot Cost^{+}_{E_{pe\,n_l}}\right)^{T} \cdot P^{+}_{penalt}\,(k)$$

$$-\left(\sum_{m=1}^{n} \Delta t \cdot Cost^{-}_{E_{pe\,n_m}}\right)^{T} \cdot P^{-}_{penalt}\,(k)$$

4.1.1.3. Optimization design variables

For determining the optimal storage system sizing, the battery nominal capacity and its nominal power must be determined. The maximum power could be different in charge and in discharge, and for that reason, both cases are considered. Moreover, the selected storage system is connected throughout a given converter, which must be designed for providing the selected maximum power in both directions. Therefore, the sizing related design variables are: $P_{bat_{dch_{max}}}$, maximum battery discharge power (W); $P_{bat_{ch_{max}}}$, maximum battery charge power (W); $P_{conv_{bat}}$, battery converter power (W); and C_{bat} , battery nominal capacity (Wh).

An important improvement introduced in the present optimization process is that the degradation caused in the battery by both the cycling and the calendar effects is taken into consideration. Therefore, the battery instantaneous reference capacity (Wh) is also introduced as design variable, $C_{ref}\,(t)$. This variable provides the information of the state of health (SOH), explained in chapter 2 in the modeling subsection. The other state of the storage system, the state of charge (SOC), is also considered in the present optimization algorithm through the battery instantaneous energy (Wh), $E_{bat}\,(t)$.

Another design variable is the battery instantaneous power (W), $P_{bat}\,(t)$, which must also be controlled for both objectives which are the optimization of the sizing of the storage system and the control strategy of the whole IPV power plant. In the present work, a positive P_{bat} is considered for a charging process and a negative value of P_{bat} is considered for a discharging process.

As the profits of the present application come from the market participation, the market bidding power (W), $P_{mkt}\,(t)$, is another design variable. The optimization of this value makes the difference related to the previously explained market participation of the chapter 3, where the market participation power profile is determined based on some systematic rules.

The last two design variables are the positive and negative penalties, $P^{+}_{penalt}\,(t)$ and $P^{-}_{penalt}\,(t)$, respectively. These penalties can be produced due to the generation deviation that can be generated in the difficult predictable energy sources, that is, in this case, the PV generation.

The summary table with the design variables is presented in Table 4.1.

Table 4.1: Design variables description summary.

Design variable	Description (unit)
$*\ P_{bat_{dch_{max}}}$	Maximum battery discharge power (W)
$*P_{bat_{ch_{max}}}$	Maximum battery charge power (W)
$*P_{conv_{bat}}$	Battery converter power (W)
$*C_{bat}$	Battery nominal capacity (Wh)
$E_{bat}\,(t)$	Battery instantaneous energy (Wh)
$C_{ref}\,(t)$	Battery instantaneous reference capacity (Wh)
$P_{bat}\,(t)$	Battery instantaneous power (W)
$P_{mkt}\,(t)$	Market bidding power (W)
$P^{+}_{penalt}\,(t)$	Positive penalty power (W)
$P^{-}_{penalt}\,(t)$	Negative penalty power (W)

Some of these variables are single values. This is the case of the first four design variables. The last six variables are time dependent, so, each variable has an optimal value for each control strategy step. This means that besides optimizing only the power and capacity values of the storage system, the control strategy is also optimized. x represents the vector that includes all the design variables included in Table 4.1. As the optimization horizon could be different, the design variables parameter, x, will have a different length. Thus, the general overview of the x parameter is shown in Eq. 4.4:

*These variables remain constant during the control strategy stage.

$$x = \begin{pmatrix} P_{bat_{dch_{max}}} \\ P_{bat_{ch_{max}}} \\ P_{conv_{bat}} \\ C_{bat} \\ E_{bat}(t)_{length \times 1} \\ C_{ref}(t)_{length \times 1} \\ P_{bat}(t)_{length \times 1} \\ P_{mkt}(t)_{length \times 1} \\ P^{+}_{penalt}(t)_{length \times 1} \\ P^{-}_{penalt}(t)_{length \times 1} \end{pmatrix}_{(4+6\cdot length) \times 1} \qquad \text{Eq. 4.4}$$

As an example, for the case of a single day optimization with a ten minutes time step, the size of the x parameter length is calculated as follows.

$$length = 24h \cdot \frac{60min}{1h} \cdot \frac{1\ sample}{10\ min} = 144 \rightarrow x[4 + 6 \cdot 144\ \times 1] = x[868\ \times 1] \qquad \text{Eq. 4.5}$$

The lower and upper bounds of the design variables are also included in order to represent a real scenario (the battery capacity can only be a positive value, or the energy stored in the battery must be positive), but giving to the optimization the ability to fix the maximum and minimum values. Therefore, the lower (lb) and upper (ub) bounds of the variables are defined as in Eq. 4.6.

$$lb = \begin{pmatrix} -\infty \\ 0 \\ 0 \\ 0 \\ 0_{length \times 1} \\ 0_{length \times 1} \\ -\infty_{length \times 1} \\ 0_{length \times 1} \\ 0_{length \times 1} \\ -\infty_{length \times 1} \end{pmatrix} \quad and \quad ub = \begin{pmatrix} 0 \\ \infty \\ \infty \\ \infty \\ \infty_{length \times 1} \\ \infty_{length \times 1} \\ \infty_{length \times 1} \\ \infty_{length \times 1} \\ \infty_{length \times 1} \\ 0_{length \times 1} \end{pmatrix} \qquad \text{Eq. 4.6}$$

4.1.1.4. Optimization constraints

The optimization constraints are related to several physical and economic aspects of the whole IPV power plant and are listed below:

- Battery exchange power
- Battery associated converter power
- Update of the state of charge, SOC
- Update of the state of health, SOH
- Battery ageing processes
- Regulatory issues

- Battery operation mode
- Power balance equation of the whole IPV power plant
- Electricity markets operation

Some of these optimization constraints are modeled by inequalities and some other ones by means of equalities.

Inequalities:

The first restriction is the battery power limitation. The battery operation must be maintained within its maximum charging and discharging values. These values do not need to be the same as some batteries are designed to be fast charging, so, their maximum charging value are greater than their maximum discharging value. Therefore, the battery operation needs to respect its bounds expressed as in Eq. 4.7.

$$P_{bat_{dch_{max}}} \leq P_{bat}(t) \leq P_{bat_{ch_{max}}} \quad \text{Eq. 4.7}$$

This limitation is divided in the following two inequalities:

$$P_{bat_{dch_{max}}} \leq P_{bat}(t) \quad \text{Eq. 4.8}$$

$$P_{bat}(t) \leq P_{bat_{ch_{max}}} \quad \text{Eq. 4.9}$$

In order to introduce these inequalities in the optimization algorithm, as both parameters of each inequality (Eq. 4.8 and Eq. 4.9) are considered as design variables, they must be placed on the left side of the inequality. Therefore, the way of introducing them in the algorithm is presented in Eq. 4.10 and Eq. 4.11.

$$P_{bat_{dch_{max}}} - P_{bat}(t) \leq 0 \quad \text{Eq. 4.10}$$

$$P_{bat}(t) - P_{bat_{ch_{max}}} \leq 0 \quad \text{Eq. 4.11}$$

Both Eq. 4.10 and Eq. 4.11 are time dependent. Instead of being a single inequality, there is one inequality for each sampling time of the optimization. That means that the quantity of inequalities is directly dependent on the optimization length. Henceforth, all the time dependent inequalities are composed by a group of inequalities with the length of the optimization samples.

The maximum battery discharge power ($P_{bat_{dch_{max}}}$) and the maximum battery charge power ($P_{bat_{ch_{max}}}$) can be different, but the storage system is electrically connected to a unique bidirectional converter. This bidirectional converter that charges and discharges the storage system must be designed based on a maximum discharge and charge power. These constraints are modeled as Eq. 4.12 and Eq. 4.13, respectively.

$$-P_{bat_{dch_{max}}} \leq P_{conv_{bat}} \quad \text{Eq. 4.12}$$

$$P_{bat_{ch_{max}}} \leq P_{conv_{bat}} \qquad \text{Eq. 4.13}$$

As in the previous case, as both parameters of each inequality (Eq. 4.12 and Eq. 4.13) are design variables, they must be placed on the left side of the inequality. Therefore, the way of introducing them in the algorithm is presented in Eq. 4.14 and Eq. 4.15.

$$-P_{bat_{dch_{max}}} - P_{conv_{bat}} \leq 0 \qquad \text{Eq. 4.14}$$

$$P_{bat_{ch_{max}}} - P_{conv_{bat}} \leq 0 \qquad \text{Eq. 4.15}$$

Those inequalities are not time dependent.

Another group of constraints is related to the energy limitation of the storage system. As in the case of the power limitation, the energy of the storage system must be maintained within its limits as it has been presented in Eq. 4.16. This equation represents the SOC variation, but instead of working with percentage values, it is represented in energy values, Wh.

$$SOC_{min} \cdot C_{ref}(t) \leq E_{bat}(t) \leq SOC_{max} \cdot C_{ref}(t) \qquad \text{Eq. 4.16}$$

Where SOC_{min} and SOC_{max} are the minimum and maximum state of charge of the storage system, both of them in percentage. The other terms are the design variables that have been already explained. This limitation is divided into two inequalities, as follows:

$$SOC_{min} \cdot C_{ref}(t) \leq E_{bat}(t) \qquad \text{Eq. 4.17}$$

$$E_{bat}(t) \leq SOC_{max} \cdot C_{ref}(t) \qquad \text{Eq. 4.18}$$

These inequalities represent the energy limitation downward, when the storage system is fully discharged, and upward, when the storage system is fully charged. The way to introduce them as optimization constraints is presented in Eq. 4.19 and Eq. 4.20.

$$SOC_{min} \cdot C_{ref}(t) - E_{bat}(t) \leq 0 \qquad \text{Eq. 4.19}$$

$$E_{bat}(t) - SOC_{max} \cdot C_{ref}(t) \leq 0 \qquad \text{Eq. 4.20}$$

Another inequality is related to the SOH of the storage system. It considers the capacity losses related to the battery nominal capacity. Therefore, Eq. 4.21 determines the end of life (EOL) of the storage system, analyzing the battery instantaneous reference capacity, $C_{ref}(t)$. This EOL is considered as percentage of the nominal capacity.

$$SOH_{min} \cdot C_{bat} \leq C_{ref}(t) \qquad \text{Eq. 4.21}$$

Where SOH_{min} is the minimum state of health in percentage, the value where the EOL of the storage system is considered. Below this value, the storage system can no longer be used. The way of introducing this inequality in the optimization process is presented in Eq. 4.22.

$$SOH_{min} \cdot C_{bat} \quad - C_{ref}(t) \leq 0 \qquad \text{Eq. 4.22}$$

With reference to the capacity losses and as it has been explained in the modeling section of chapter 2, the ageing approach implemented in the optimization is based on [24], where only the cycling ageing was considered. But in the present work the calendar ageing has also been included. Thus, the applied ageing equation is the same as Eq. 2.35, but instead of being related to the SOH instantaneous value, it is related to the battery instantaneous reference capacity value ($C_{ref}(t)$), as described in Eq. 4.23.

$$C_{ref}(t) - C_{ref}(t - \Delta t) + Z_{cy} \cdot (E_{bat}(t - \Delta t) - (E_{bat}(t)) + Z_{cal} \cdot C_{bat} = 0 \qquad \text{Eq. 4.23}$$

Where Δt is the sample time of the optimization process, and Z_{cy} and Z_{cal} are the linear ageing coefficients of cycling and calendar degradation in percentage, respectively. The ageing caused by the cycling is only considered when the battery is in the discharging process (refer to chapter 2). For that reason, to model this fact, Eq. 4.23 is divided into two different inequalities, one for modeling the charging process, Eq. 4.24, and the other one for the discharging process, Eq. 4.25.

$$C_{ref}(t) - C_{ref}(t - \Delta t) + Z_{cal} \cdot C_{bat} \leq 0 \qquad \text{Eq. 4.24}$$

$$C_{ref}(t) - C_{ref}(t - \Delta t) + Z_{cy} \cdot (E_{bat}(t - \Delta t) - (E_{bat}(t)) + Z_{cal} \cdot C_{bat} \leq 0 \qquad \text{Eq. 4.25}$$

The initial conditions of these groups of inequalities are calculated by Eq. 4.26 and Eq. 4.27 for the charge and discharge cases, respectively.

$$C_{ref}(1) - SOH_{ini} \cdot C_{bat} + Z_{cal} \cdot C_{bat} \leq 0 \qquad \text{Eq. 4.26}$$

$$C_{ref}(1) - SOH_{ini} \cdot C_{bat} + Z_{cy} \cdot \left(SOH_{ini} \cdot SOC_{ini} \cdot C_{bat} - (E_{bat}(1)\right) + Z_{cal} \cdot C_{bat} \leq 0 \qquad \text{Eq. 4.27}$$

Where SOC_{ini} and SOH_{ini} are the initial state of charge and the initial state of health, respectively, both in percentage. To develop a more flexible optimization process, these parameters are implemented as user customizable parameters. Therefore, the initial SOC and SOH storage system states can be selected.

The last group of inequalities comes from the whole IPV power plant grid providing power. This power, which is composed by the PV generation power and the storage system power, must be always positive. Therefore, the charging energy of the storage system must always be charged from the PV generation. This constraint is modeled as in Eq. 4.28.

$$P_{PV}(t) - P_{bat}(t) \geq 0 \qquad \text{Eq. 4.28}$$

Where $P_{PV}(t)$ (W) is the photovoltaic generation power profile. It is worth to remember that a positive battery power is a charge process, and for that reason the battery power profile is included as a negative term to model a battery discharge process, which implies an energy flow from the battery to the grid. In order to introduce this constraint in the optimization process, Eq. 4.28 is transformed into Eq. 4.29. As the $P_{PV}(t)$ is not a design variable, neither a multiplier of some design variables, it must be located in the right side of the inequality.

$$P_{bat}(t) \leq P_{PV}(t) \qquad \text{Eq. 4.29}$$

All the explained inequalities compose the matrix A and vector b of Eq. 4.37 and Eq. 4.38 respectively, which are included in the optimization as follows:

- 1st row: Inequality represented by Eq. 4.14 [1 X (4+6·length)].
- 2nd row: Inequality represented by Eq. 4.15 [1 X (4+6·length)].
- 3rd row: Group of inequalities represented by Eq. 4.10 [length X (4+6·length)].
- 4th row: Group of inequalities represented by Eq. 4.11 [length X (4+6·length)].
- 5th row: Group of inequalities represented by Eq. 4.19 [length X (4+6·length)].
- 6th row: Group of inequalities represented by Eq. 4.20 [length X (4+6·length)].
- 7th row: Group of inequalities represented by Eq. 4.22 [length X (4+6·length)].
- 8th row: Group of inequalities represented by Eq. 4.24 [length X (4+6·length)], with the initial inequality Eq. 4.26.
- 9th row: Group of inequalities represented by Eq. 4.25 [length X (4+6·length)], with the initial inequality Eq. 4.27.
- 10th row: Group of inequalities represented by Eq. 4.29 [length X (4+6·length)].

Equalities:

The first equality represents the battery operation that models its energy flow. This equation is the same as the Eq. 2.21 explained in chapter 2, but considering the energy of the storage system, E_{bat}, instead of the SOC. Moreover, to maintain the objective of modeling a linear problem, the efficiency term (η) is removed due to the fact that it includes a non-linearity. Therefore, the efficiency is not considered in the purely optimization process but it is taken into account in the following step. The equation that models this behavior is shown in Eq. 4.30.

$$E_{bat}(t) = E_{bat}(t - \Delta t) + P_{bat}(t) \cdot \Delta t \qquad \text{Eq. 4.30}$$

Once again, in order to introduce this equation in the optimization process, it is transformed into the form presented in Eq. 4.31.

$$E_{bat}(t) - E_{bat}(t - \Delta t) - P_{bat}(t) \cdot \Delta t = 0 \qquad \text{Eq. 4.31}$$

As this equation is time dependent, there is one equation for each sampling time of the optimization. In this case, the initial condition of this group of equalities is calculated as in Eq. 4.32.

$$E_{bat}(1) - SOH_{ini} \cdot SOC_{ini} \cdot C_{bat} - P_{bat}(1) \cdot \Delta t = 0 \qquad \text{Eq. 4.32}$$

Another constraint to be implemented is the power balance equation of the market participation. Since the penalties have to be also taken into account, the equation is represented as in Eq. 4.33.

$$P_{PV}(t) - P_{bat}(t) = P_{mkt}(t) + P^{+}_{penalt}(t) + P^{-}_{penalt}(t) \qquad \text{Eq. 4.33}$$

Locating each term in the correct form in order to be introduced in the optimization algorithm, the equation is transformed into Eq. 4.34.

$$-P_{bat}(t) - P_{mkt}(t) - P^{+}_{penalt}(t) - P^{-}_{penalt}(t) = -P_{PV}(t) \qquad \text{Eq. 4.34}$$

Since all terms are negative and multiplying each term by the same factor does not vary the result, Eq. 4.34 is changed to Eq. 4.35.

$$P_{bat}(t) + P_{mkt}(t) + P^{+}_{penalt}(t) + P^{-}_{penalt}(t) = P_{PV}(t) \qquad \text{Eq. 4.35}$$

The third and last equality considered is the firming service that has to be provided as market participation mode. The IPV power plant grid provided power must remain constant for an hour. Therefore, once the power for the initial point of each hour, $P_{mkt}(t)$, is calculated, this power must be maintained during the given hour as shown in Figure 4.2.

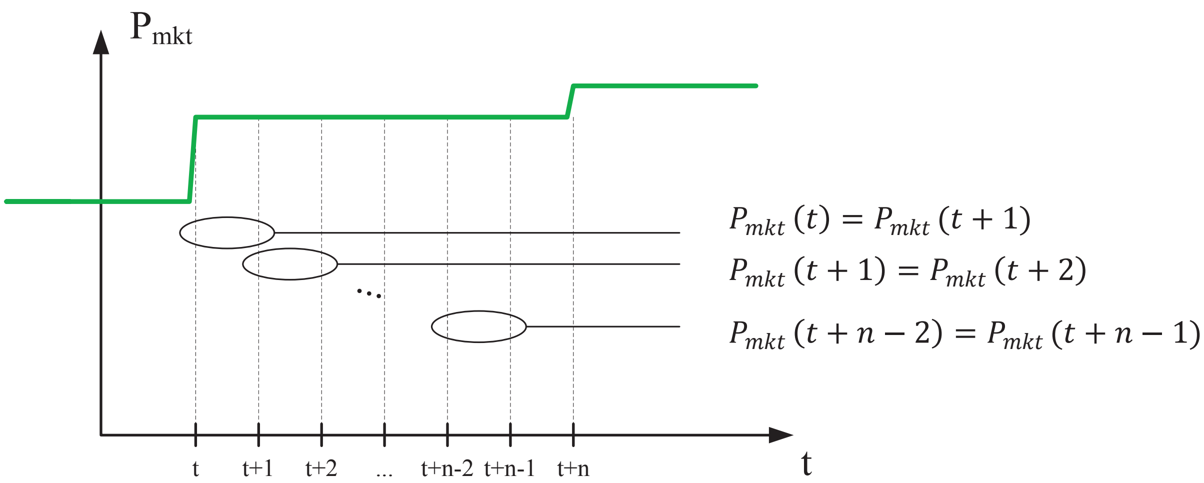

Figure 4.2: Firming service to participate in markets and the corresponding equations to model this operation mode.

Transforming these equations into the optimization algorithm form:

$$\begin{cases} P_{mkt}(t) - P_{mkt}(t+1) = 0 \\ P_{mkt}(t+1) - P_{mkt}(t+2) = 0 \\ \vdots \\ P_{mkt}(t+n-2) - P_{mkt}(t+n-1) = 0 \end{cases} \quad during\ each\ hour \qquad \text{Eq. 4.36}$$

As it can be evaluated from Eq. 4.36, the number of needed equations for each hour is $n-1$, considering n as the number of equations needed for each hour depending on the sample time. This special behavior is modelled by means of the auxiliary matrix T'^{-h}, presented in Eq. 4.43.

All the exposed equalities compose the matrix A_{eq} and vector b_{eq} of Eq. 4.39 and Eq. 4.40 respectively, which are included in the optimization as follows:

- 1st row: Group of equalities represented by Eq. 4.31 [length X (4+6·length)], with the initial equality Eq. 4.32.
- 2nd row: Group of equalities represented by Eq. 4.35 [length X (4+6·length)].
- 3rd row: Group of inequalities represented by Eq. 4.36 [length X (4+6·length)].

$$A = \begin{pmatrix} -1 & 0 & -1 & 0 & 0 & 0 & 0 & 0 & 0 \\ 0 & 1 & -1 & 0 & 0 & 0 & 0 & 0 & 0 \\ U & 0 & 0 & 0 & 0 & 0 & -I & 0 & 0 \\ 0 & -U & 0 & 0 & 0 & 0 & I & 0 & 0 \\ 0 & 0 & 0 & 0 & -I & SOC_{min} \cdot I & 0 & 0 & 0 \\ 0 & 0 & 0 & 0 & I & -SOC_{max} \cdot I & 0 & 0 & 0 \\ 0 & 0 & 0 & SOH_{min} \cdot U & 0 & -I & 0 & 0 & 0 \\ 0 & 0 & 0 & -SOH_{ini} \cdot W + Z_{cal} \cdot U & 0 & T & 0 & 0 & 0 \\ 0 & 0 & 0 & -SOH_{ini}(1 - Z_{cy} \cdot SOC_{ini}) \cdot W + Z_{cal} \cdot U & -Z_{cy} \cdot T & T & 0 & 0 & 0 \\ 0 & 0 & 0 & 0 & 0 & 0 & I & 0 & 0 \end{pmatrix}$$

$$b = \begin{pmatrix} 0_{1 \times 1} \\ 0_{1 \times 1} \\ 0_{length \times 1} \\ 0_{length \times 1} \\ 0_{length \times 1} \\ 0_{length \times 1} \\ 0_{length \times 1} \\ 0_{length \times 1} \\ 0_{length \times 1} \\ P_{PV\,length \times 1} \end{pmatrix}_{2+8\cdot\text{length} \times 1}$$

$$A_{eq} = \begin{pmatrix} 0 & 0 & 0 & -SOH_{ini} \cdot SOC_{ini} \cdot W & T & 0 & -\Delta t \cdot I & 0 & 0 & 0 \\ 0 & 0 & 0 & 0 & 0 & 0 & I & I & I & I \\ 0 & 0 & 0 & 0 & 0 & 0 & 0 & T'^{-h} & 0 & 0 \end{pmatrix}_{(2\cdot\text{length} + (\text{length} - \text{n}_{\text{hours}})) \times (4+6\cdot\text{len}}$$

$$b_{eq} = \begin{pmatrix} 0_{length \times 1} \\ P_{PV\,length \times 1} \\ 0_{length - n \cdot hours \times 1} \end{pmatrix}_{(2\cdot\text{length} + (\text{length} - \text{n}\cdot\text{hours})) \times 1}$$

$$P_{PV} = \begin{pmatrix} P_{PV_1} \\ \vdots \\ P_{PV_n} \end{pmatrix}_{\text{length} \times 1}, U = \begin{pmatrix} 1 \\ \vdots \\ 1 \end{pmatrix}_{\text{length} \times 1}, W = \begin{pmatrix} 1 \\ 0 \\ \vdots \\ 0 \end{pmatrix}_{\text{length} \times 1}, I = \begin{pmatrix} 1 & 0 & 0 \\ 0 & \ddots & 0 \\ 0 & 0 & 1 \end{pmatrix}_{\text{length} \times \text{length}}$$

$$T = \begin{pmatrix} 1 & 0 & \cdots & \cdots & \cdots & 0 \\ -1 & 1 & \ddots & & & \vdots \\ 0 & -1 & \ddots & \ddots & & \vdots \\ \vdots & \ddots & \ddots & \ddots & \ddots & \vdots \\ \vdots & & \ddots & -1 & 1 & 0 \\ 0 & \cdots & \cdots & 0 & -1 & 1 \end{pmatrix}_{\text{length} \times \text{length}}, T^{-h} = \begin{pmatrix} -1 & 1 & 0 & \cdots & \cdots & 0 \\ 0 & -1 & 1 & \ddots & & \vdots \\ \vdots & \ddots & \ddots & \ddots & \ddots & \vdots \\ \vdots & & \ddots & -1 & 1 & 0 \\ 0 & \cdots & \cdots & 0 & -1 & 1 \end{pmatrix}_{\text{length}_{\text{hour}} -1 \times \text{lengt}}$$

$$T'^{-h} = \begin{pmatrix} T^{-h} & 0 & \cdots & 0 \\ 0 & T^{-h} & \ddots & \vdots \\ \vdots & \ddots & \ddots & 0 \\ 0 & \cdots & 0 & T^{-h} \end{pmatrix}_{\text{length} - \text{n}_{\text{hours}} \times \text{length}}$$

The vectors and matrixes presented in Eq. 4.41, Eq. 4.42 and Eq. 4.43 are some sub matrixes or auxili and A_{eq} and vectors b and b_{eq} for an easier visualization:

- The single column matrix P_{PV} includes the PV power generation values for each sample time of t
- The matrix U is a single column auxiliary matrix composed by ones.
- The matrix W is a single column auxiliary matrix composed by one being the first value and all th
- The matrix I is the identity matrix.
- The matrix T is an auxiliary square matrix, which has the main diagonal composed by ones anc minus ones. This matrix is used to represent a subtraction of a given value with its previous one,
- The matrix T^{-h} is an auxiliary matrix composed by the matrix T without its first row. As it is mo the firming service that has to be provided for participating in electricity markets. This matrix mo
- The matrix T'^{-h} is an auxiliary matrix composed by several T^{-h} matrixes in the main diagonal t optimization. For each hour in the developed optimization, a column that includes another T^{-h}

4.1.1.5. Algorithm selection and application

Once the objective function, the design variables and all the constraints have been described, the optimization algorithm selection and application is carried out. As it has been verified, all equations that model the objective function and the constraints are included as linear equations. Thus, the objective of using a linear programming (LP) optimization process is achieved.

The LP optimization algorithm is executed in Matlab by the function $linprog$ (included in the Optimization Toolbox [154]). Therefore, Eq. 4.1 can be rewritten as Eq. 4.44.

$$\min_{x} f(x) = \min_{x} c^T x \ \ such\ that \begin{cases} A \cdot x \leq b, \\ A_{eq} \cdot x = b_{eq}, \\ lb \ \leq x \leq ub. \end{cases} \qquad \text{Eq. 4.44}$$

Where x is the vector composed by the design variables; $f(x)$ is the linear objective function; c^T is the transposed vector composed by the multipliers of x (for that reason is a linear programming problem); A and A_{eq} are the constraints matrixes; b and b_{eq} are the constraints vectors; and lb and ub are the vectors of lower and upper bounds of the design variables.

The LP optimization in Matlab comes with several solvers as the interior-point, the simplex, the dual-simplex, and the active-set [154, 155]. Each of them follows a different iterative process to search the optimal solution. In the present case, the interior-point is used as it is the one recommended for large scale optimization processes.

4.1.1.6. Simulation execution process

With the previous algorithm application the co-optimization process is almost complete but there is an input/output correlation that is solved within the process proposed in the present subsection.

Based on this optimization, the sizing and optimal operation values can be obtained almost simultaneously. Nevertheless, one of the inputs of the objective function is the lifetime of the battery (t_{bat}) which is calculated based on the *Rainflow* cycling counting algorithm and the depth of discharge data of both the battery manufacturer and the different cycling tests carried out in the energy storage laboratory of Ikerlan. Therefore, one of the outputs of the optimization (the battery power profile) has an influence on one of the inputs (the lifetime of the battery). In order to solve this modeling constraint, an iterative execution of the optimization must be carried out, aiming to obtain the optimal values based on the real lifetime of the battery. Thus, the proposed simulation follows the diagram of Figure 4.3.

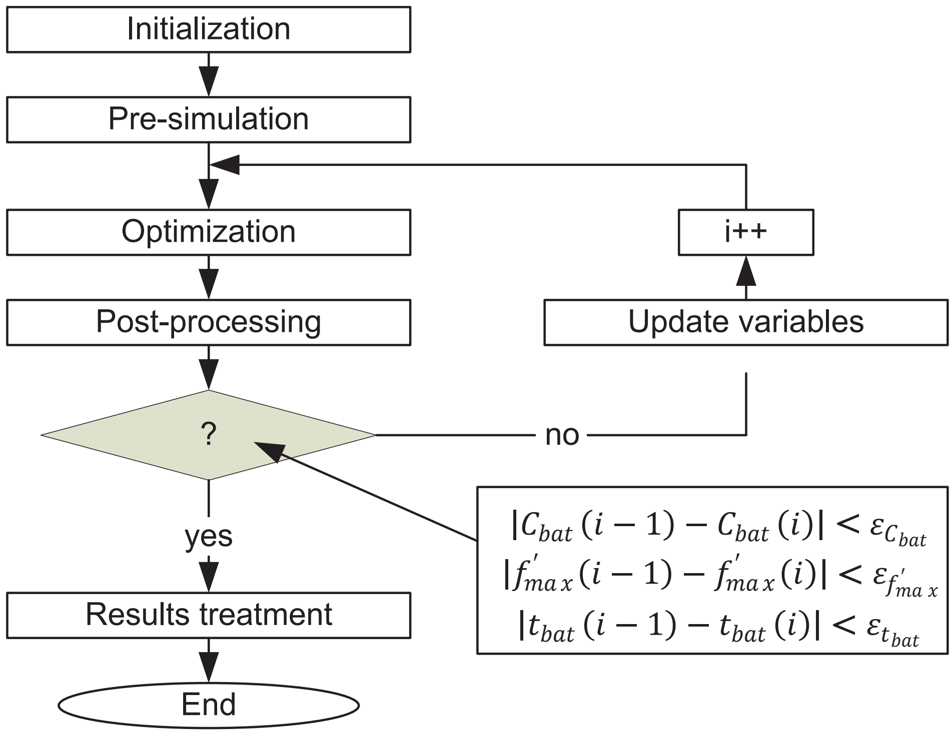

Figure 4.3: Complete simulation execution flowchart.

In the *initialization* step, all the parameters are initialized by means of defining the size of the simulation process. In the *pre-simulation* step, an initial lifetime of the battery is calculated to run the following *optimization* step. The *optimization* step executes the optimization process described in the previous sections. In the *post-processing* step the optimization results are processed in order to verify if the next condition is fulfilled. If the results regarding the battery capacity (C_{bat}), the objective function (f'_{max}) and the lifetime of the battery (t_{bat}) are maintained within their respective error thresholds ($\varepsilon_{C_{bat}}$, $\varepsilon_{f'_{max}}$ and $\varepsilon_{t_{bat}}$, respectively) between the previous optimization iteration ($i-1$) and the last iteration (i), the results are processed (*results treatment*) and the optimization algorithm is finished. If not, the *Rainflow* algorithm is executed in the *update variables* step for running the next optimization iteration. The error thresholds ($\varepsilon_{C_{bat}}$, $\varepsilon_{f'_{max}}$ and $\varepsilon_{t_{bat}}$) have been selected around the 1% of each parameter final result after several trial and error repetitions.

Once the co-optimization process has been explained, the next sections focus on the proposed process to get the optimal sizing and the optimal operation of the IPV power plant. This process is separated into two stages, which are the Design Stage and the Operation Stage. On the first one, the optimal sizing of the storage system is determined and on the second one the optimal control strategy to participate in electricity markets is established. Both stages of this process are detailed hereafter.

4.2. IPV power plant storage system sizing at Design Stage

Once the optimization process has been explained in order to obtain both optimal sizing of storage system and optimal control strategy of the whole IPV power plant, each one of these objectives has been detailed. In this section, the storage system sizing at Design Stage is presented.

4.2.1. Design Stage description

This first stage is developed to be performed before the construction of the IPV power plant. The Design Stage aims to determine the optimal storage system sizing for obtaining the maximum economic revenue of the IPV power plant market participation. To do so, a one year evaluation period is considered to include all seasons' characteristics, related to the irradiance of PV generation and also related to market data [147]. This one year evaluation period is also selected because it is assumed that this pattern is repeated over the time. In addition to the one year evaluation period, the selected time step is 10 minutes. This value has been selected as the tradeoff between the computational cost of the optimization and the desired simulation detail. The diagram of this design stage is presented in Figure 4.4.

As this analysis is carried out to determine the ESS of the IPV power plant, historical PV data and historical market data are introduced as inputs to the optimization process. The other inputs considered are the costs of the PV systems, power electronics, batteries, replacements and operation and maintenance. Within these inputs the optimization carried out in this Design Stage is executed.

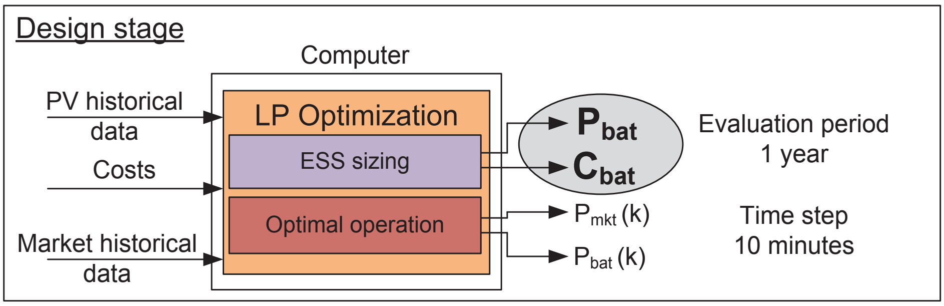

Figure 4.4: Design Stage of the process where the optimal sizing of the ESS is obtained.

The linear programming optimization algorithm computes the optimal ESS sizing (P_{bat} and C_{bat}) where P_{bat} (W) is the maximum charge and discharge power of the storage system and C_{bat} (Wh) is the battery capacity value. Also in this optimization process the optimal market participation profile, $P_{mkt}(k)$ (W), and battery reference power profile, $P_{bat}(k)$ (W), are obtained. The market participation power profile, $P_{mkt}(k)$, is assumed as the whole IPV power reference profile, $P_{grid}(k)$. Both $P_{mkt}(k)$ and $P_{bat}(k)$ are obtained for every discrete state, k, which means that optimal power for each point of the whole profile is obtained from the optimization. From this initial stage, only the optimal values of the ESS sizing (P_{bat} and C_{bat}) are used to design the required storage system, which should be implemented in the IPV power plant.

The other variables included in the before explained design variables parameter (x) are used to verify the correct execution of the optimization and the operation of the storage system.

The evaluation of a whole year requires a large optimization size which cannot be carried out by the solver proposed by the Matlab software. As the selected time step is 10 minutes, the length of the x parameter and of the matrix A of the whole year optimization are calculated as follows:

$$length = 365days \cdot \frac{24h}{1day} \cdot \frac{60min}{1h} \cdot \frac{1\,sample}{10\,min} = 52560$$
$$\rightarrow x[4 + 6 \cdot 52560 \times 1] = x[315364\ \times 1] \qquad \text{Eq. 4.45}$$
$$\rightarrow A[(2 + 8 \cdot \text{length})\ \times\ (4 + 6 \cdot \text{length})] = A[420482\ \times 315364]$$

The class of a standard Matlab variable is double, which means that it is composed by 8 bytes (B) or 64 bits (b). For that reason, the memory allocation of each variable is 8 bytes. Analyzing the 315364 variables of the x parameter, its memory allocation is calculated as:

$$315364\ variables \cdot 8 \frac{bytes}{variable} = 2522912\ bytes \sim 2463kB \sim 2.4MB \qquad \text{Eq. 4.46}$$

The same process is carried out to calculate the memory allocation of the matrix A:

$$(420482 \cdot 315364)\ variables \cdot 8 \frac{bytes}{variable} = 1.061 \cdot 10^{12}\ bytes\ \sim 988\text{G}B \qquad \text{Eq. 4.47}$$

With these sizes (and memory allocations), it is verified that the optimization terms are large enough to be infeasible by the Matlab software in regular conditions. The simulations of this optimal sizing step are implemented on an Intel Core i5 CPU 3.1GHz with 16 GB of RAM. For that reason, it has been decided to reduce the optimization length to a single month. In this way the lengths of the vector and matrix are reduced to the following values (for a 31 day month).

$$length = 31days \cdot \frac{24h}{1day} \cdot \frac{60min}{1h} \cdot \frac{1\,sample}{10\,min} = 4464$$
$$\rightarrow x[4 + 6 \cdot 4464 \times 1] = x[26788\ \times 1] \sim 209kB \qquad \text{Eq. 4.48}$$
$$\rightarrow A[(2 + 8 \cdot \text{length})\ \times\ (4 + 6 \cdot \text{length})] = A[35714\ \times 26788] \sim 7.12GB$$

Although the resulting sizes are still large, the Matlab software and the used computer are able to work with them. Therefore, in order to take into account the whole year, the 12 month optimizations are carried out separately. The flowchart applied to represent this optimization execution is presented in Figure 4.5. It is the same as the one explained in the optimization execution process section (4.1.1.6) with an additional loop that evaluates the 12 months and an additional block to save each month's results.

In the last block named as *Results treatment*, a statistic analysis of the results of this optimization process is applied in order to determine the optimal size for the battery. This process is analyzed in the next results' section.

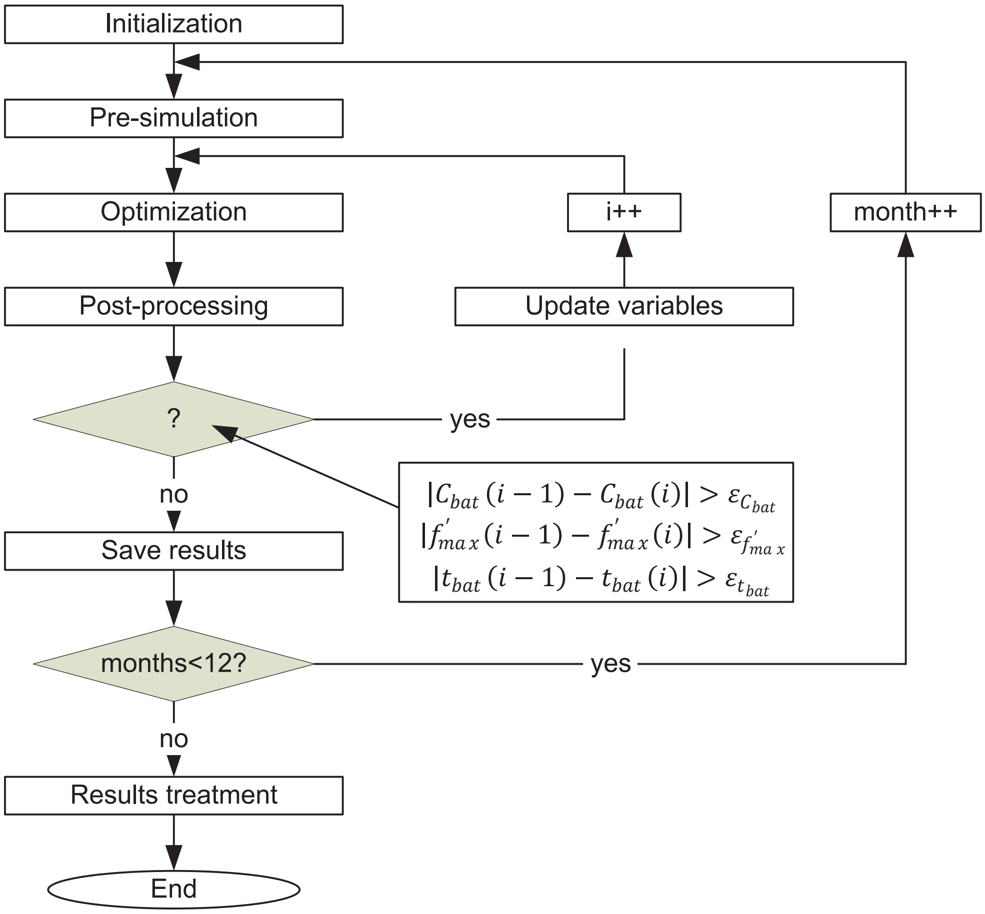

Figure 4.5: Design Stage of the process where the optimal sizing is determined.

4.2.2. Optimal storage system sizing results

In this section the results related to the optimal sizing obtained in the Design Stage are presented. The optimization is applied for the case study presented in chapter 2. In the next table, the main characteristics of this IPV power plant are summarized.

Table 4.2: IPV power plant main characteristics.

Parameter description	Value
Installed PV power	1 MW / 1.2 MWp
Battery inverter maximum power	1 MW
Battery nominal capacity	560 kWh

As it has been mentioned before, a whole year optimization is carried out but based on monthly size optimizations. With a time step of 10 minutes, efficient and computationally *light* monthly length optimizations are carried out obtaining, for each month, the optimal P_{bat} and C_{bat} values. As each month has a different length, the size of each month optimization matrix is different. The size of matrix A is [34562 x 25924] for a 30 days month; [35714 x 26788] for a 31 days month; and [32258 x 24196] for the 28 days of February. The PV predictions taken into account are the real generation data presented in Figure 2.9, in chapter 2, section 2.3.1. Therefore, perfect predictions are considered for this sizing optimization because the objective is to firm the PV generation profile to participate in electricity markets in the optimal operation mode. There will be PV deviations, but in both directions, so it is assumed an error with a null mean value, and thus, the positive deviations are counteracted in a natural way with the negative ones.

The results obtained for each month are summarized in the next figures. In Figure 4.6 each month battery power capacity value (P_{bat}) is presented, with the mean value represented by the red horizontal line. In Figure 4.7, the energetic capacity values are presented (C_{bat}) with the maximum and minimum values highlighted together with the mean and barycenter values. In Figure 4.8, the calculated life span of each optimization is shown also with the average value highlighted. In Figure 4.9, each month benefits of the whole IPV power plant (PV + BESS) are depicted; and finally, in Figure 4.10, the relation between the capacity value and the benefits is shown, together with the calculated barycenter. This value is calculated weighting each month capacity value with the benefits of the own month optimization.

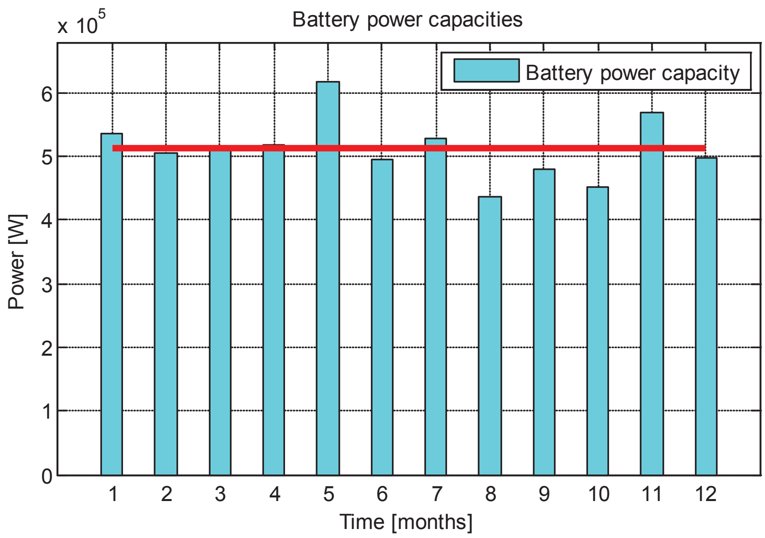

Figure 4.6: Design stage ESS sizing optimization results: battery power capacity values.

The results related to the storage system power needs show a similar optimal value for the whole year. This value, 511kW, is the half of the installed PV power (1 MW), and the half of the installed converter in the case study IPV power plant. This result provides useful information regarding the relation between the PV power and the storage system power needs. The mean value is taken into account as the optimal one, because when the worst case is considered the system is oversized the most part of the time (which is not the objective: indeed, it results in a sub-optimal economic optimization). It means that in that case, the ESS power capabilities will not be able to fully compensate the needed requirement, but from the global (economic) point of view, this is the optimal scenario.

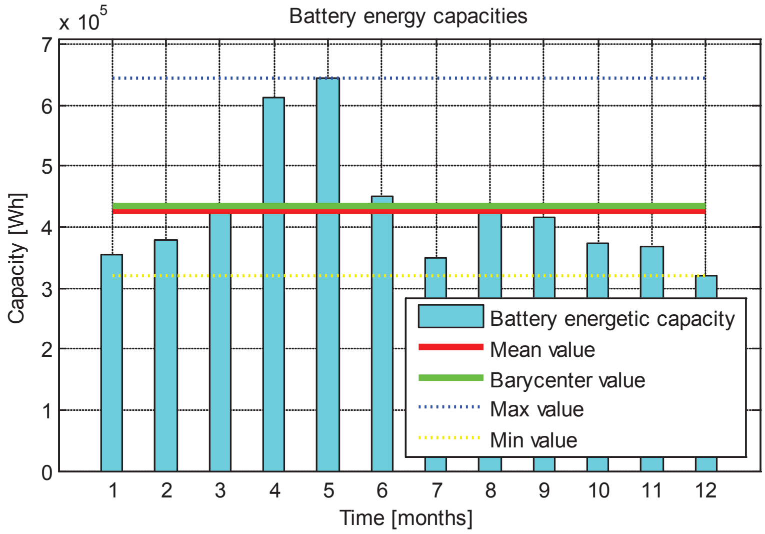

Figure 4.7: Design stage ESS sizing optimization results: battery energy capacity values.

With reference to the capacity value, the difference among the months is much more representative, obtaining almost a factor two between the optimal values of May and April, compared to July and December. Nevertheless, several months' optimal values are similar and are around the average value of 426kWh. In the capacity analysis case, the barycenter is calculated, analyzing each month capacity value related to its benefits. The result of the barycenter is also very similar: 433kWh. As the difference between them is lower than 2%, the optimal value selected is the one obtained using the barycenter (433kWh). This value is more representative because it includes the value of the benefits for each month. This result provides a significant reduction (around 23 %) comparing to the installed storage capacity of the presented case study, which is 560 kWh. As it has been mentioned before, with this capacity the worst case is not fulfilled, but from the global (economic) point of view, it is better than the worst case, which oversizes again the storage system. The objective is not to fulfill all cases but to obtain the optimal storage system.

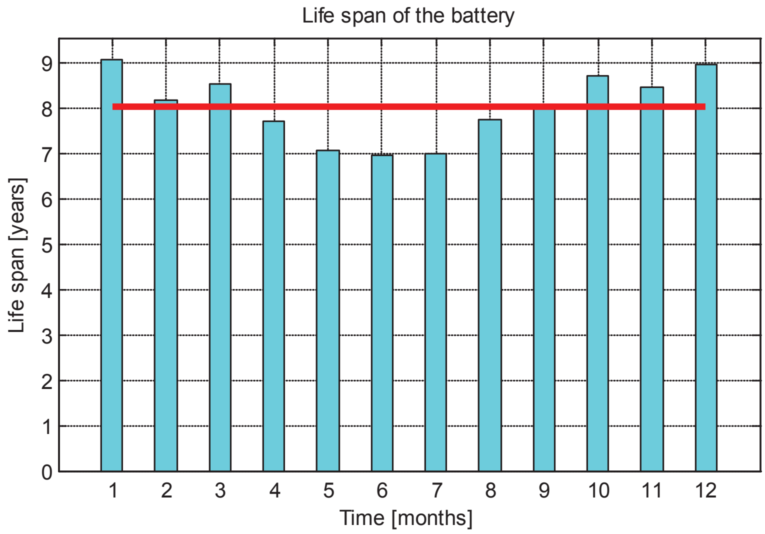

Figure 4.8: Design stage ESS sizing optimization results: battery life span values.

The life span results of the present optimization vary between 7 and 9 years of lifetime. In summer months, the life span is reduced, which could be caused by the greater use of the ESS in this period of time. Nevertheless, the results are close to the average value of 8 years, which enforces the resultant average value.

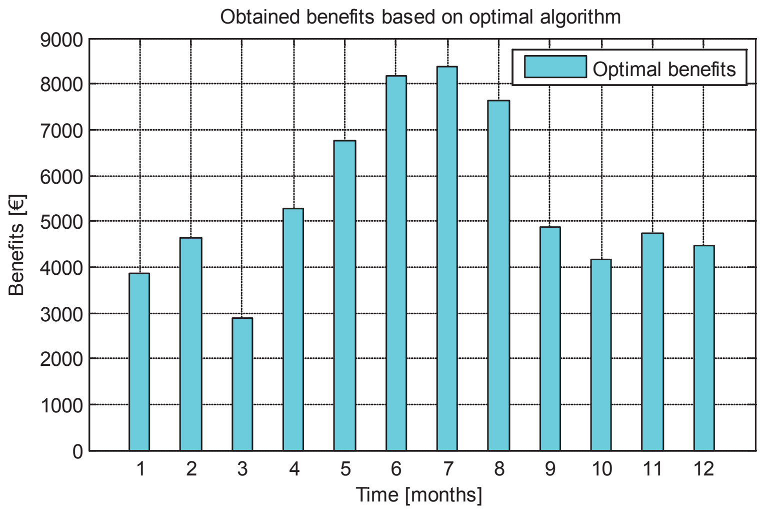

Figure 4.9: Design stage ESS sizing optimization results: obtained benefits values.

The results of the obtained benefits present an inverse effect compared with the previous lifetime results. As in summer there are sunnier days and more hours of sun per day, the obtained benefits increase in the same proportion.

The obtained annual benefit is around 65000€. Although it seems low, the yearly average PV generation in this location is around 1300MWh at an average daily market price of 42 €/MWh. Therefore, the optimization increases the profits from 54600€ to 65000€ (around 20%). Of course, this economic difference justifies the decision of including the energy storage system.

Combining the obtained benefits of the Figure 4.9 with the capacity values of the Figure 4.7, the following figure is generated. Each cross marker includes the data of a different month and indicates the benefits obtained together with the optimal energy storage capacity. The green dot is the calculated barycenter which takes into account every month's benefits and capacity values.

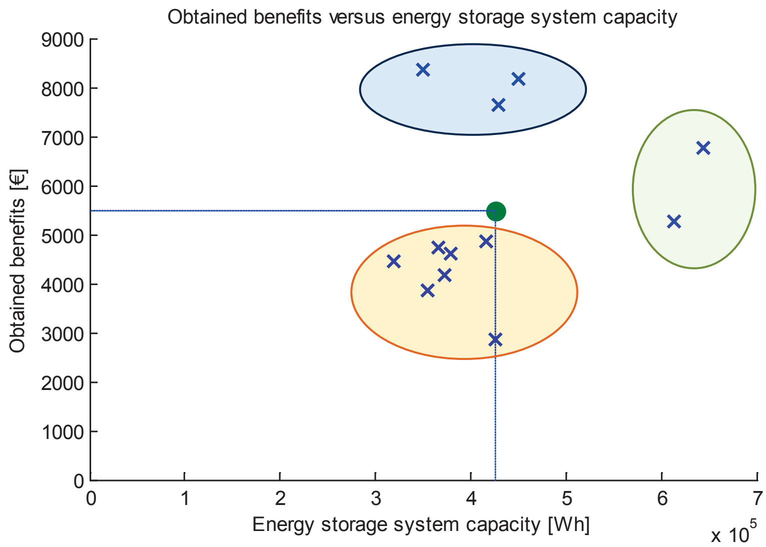

Figure 4.10: Design stage ESS sizing optimization results: obtained benefits versus capacity values.

This figure is very useful to verify how far each month results are compared to the barycenter value, to be able to justify the validity of the barycenter. As there is not any outlier (contributing to a misleading barycenter value), it can be concluded that the barycenter is the optimal point. The characteristics of the data can be separated in three groups which are: 1) the average capacity with greater benefits (summer months highlighted within the blue ellipse); 2) greater capacity values with average benefits (very variable months which demand a greater capacity value, like spring months highlighted within the green ellipse); and 3) slightly lower capacity and slightly lower benefits (the rest of the year highlighted within the orange ellipse). As conclusion, it is quite correct to consider the optimal value based on the global point of view which is the calculated barycenter value (433 kWh).

4.3. IPV power plant control strategy at Operation Stage

Once the optimal storage system has been obtained, in this Operation Stage, the IPV power plant control strategy is optimized, to participate in electricity markets. This section includes the control strategy definition to participate in electricity markets, and the market participation based on MPC with this optimal strategy.

4.3.1. Control strategy definition

The Operation Stage of the proposed process includes two steps related to the two electricity markets that the IPV power plant participates on. The optimization applied in both steps considers a fixed storage system size, which is the output of the previous explained design stage. The first step is the *generation planning* for participating in the daily market of the following day. The second step is the *online operation*, where the PV generation prediction errors are counteracted participating in the intraday markets. This second step is carried out thanks to the MPC in order to be able to participate in the different intraday markets to recover the benefits that the PV prediction errors have been generated. That is why the MPC is implemented and is necessary to be able to have the possibility to participate in the intraday markets in order to improve the economic revenues of the IPV power plant. The operation stage block diagram is presented in Figure 4.11. It is similar to the one explained in chapter 3 but including the optimal control strategy.

Regarding the market participation, instead of the power value calculated by the optimization process, $P_{mkt}(k)$, a detailed market participation offer is composed by an energy offer, $E_{offered}^{mkt}(k)$, at a given cost, $c_{offered}^{mkt}(k)$, for each hour. As in this operation stage the market participation is the core idea, these parameters are used to explain in detail the whole operation.

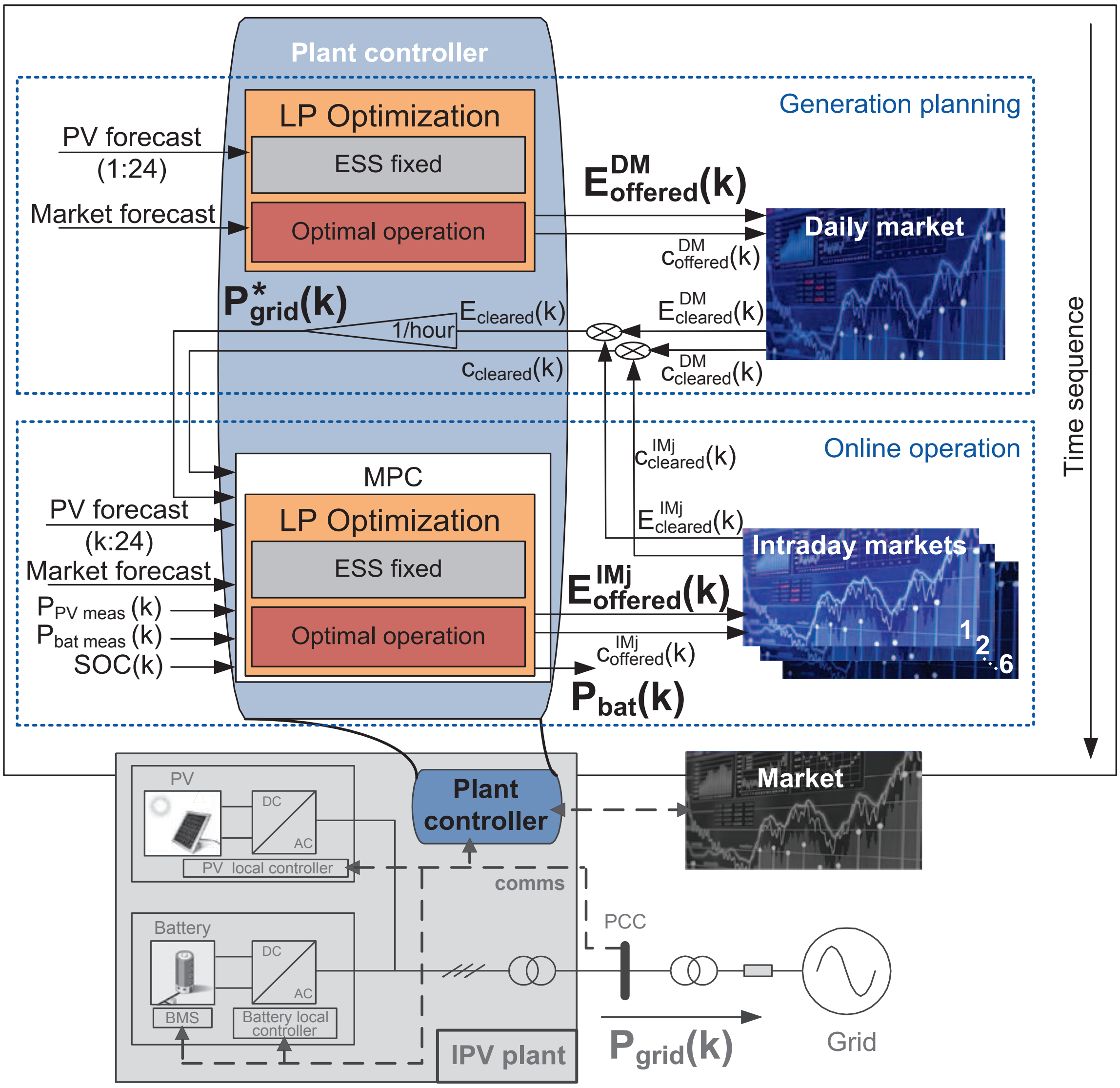

Figure 4.11: Operation Stage block diagram, including the generation planning (to the daily market) and the online operation step (to the intraday market).

The *generation planning* step is similar to the previously explained Design Stage. In this case, the ESS rate is fixed and the relevant output of the applied optimization is the generation planning offers to the daily market (DM) of the following day, $E_{offered}^{DM}\ (k)$, at a given cost, $c_{offered}^{DM}\ (k)$, for each hour. This planning step is carried out the day before the real operation. In order to make sure that the proposed offer is cleared, the offered hourly cost must be zero or close to zero. Therefore, it is assumed that the offers sent to the market operator are always cleared. The resolution of the DM is composed by the cleared energy, $E_{cleared}^{DM}\ (k)$, and the market clearing price, $c_{cleared}^{DM}\ (k)$, for each hour. This information is obtained the day before the online operation and it is transformed into the initial power reference profile, $P_{grid}^{*}\ (k)$ (W), to the *online operation*, which is the second step. This explanation can be followed in the upper dotted blue rectangle of the Figure 4.11. A flowchart to explain more in detail the market participation sequence of Figure 4.11 is presented in Figure 4.12.

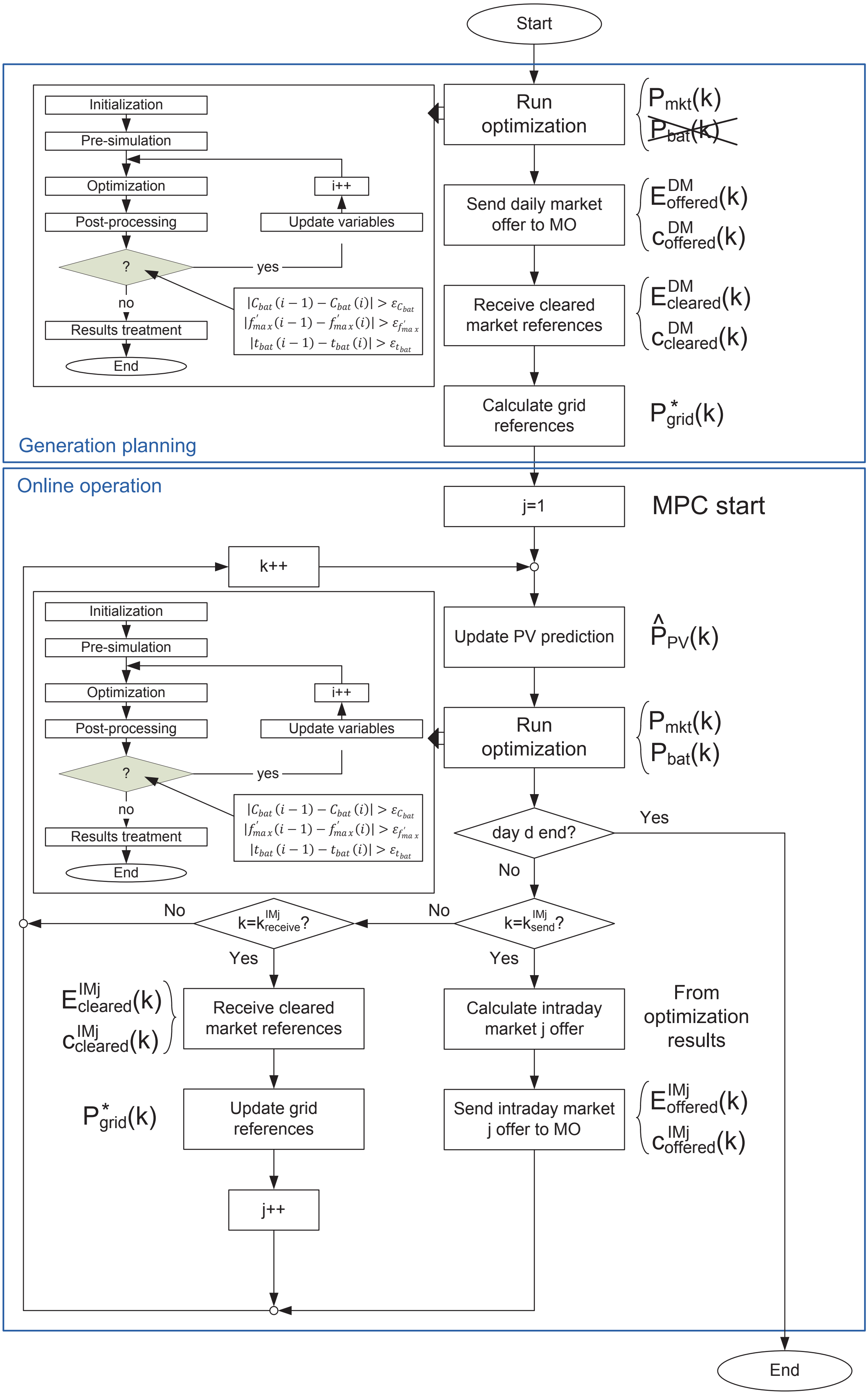

Figure 4.12: Detailed flowchart of the optimal strategy to participate in electricity markets.

The objective of the second step, the *online operation* step, is the operation of the IPV power plant to maximize the economic revenues. This operation is managed using the Model Predictive Control (MPC) [150, 151]. The inputs of this control are: the market cleared power reference, $P^{*}_{grid}(k)$; PV generation forecast, $PV_{forecast}\ (k..24)$ (W); market prices forecast; PV real power generation, $P_{PV\ mea\,s}(k)$ (W); battery power, $P_{bat\ meas}\ (k)$ (W); and the state of charge of the storage system, $SOC(k)$ (%). The control outputs are the intraday market's (IM) offers (also an amount of energy for each hour, $E^{IMj}_{offered}\ (k)$, at a given cost, $c^{IMj}_{offered}\ (k)$) and the storage system reference power, $P_{bat}\ (k)$.

The internal process is detailed in the diagram of Figure 4.12, where it can be shown that in the first step (*generation planning*), the output of the optimization related to the battery profile is not used (and crossed out in the diagram), as the objective is to participate in the daily market but the operation has not started yet. It is worth mentioning that the block called *Run optimization* computes all the before explained process of Figure 4.3.

In the second step (*online operation*), the IPV power plant output power, $P_{grid}\ (k)$, must be controlled every discrete state. Thereby, the optimal storage system reference power, $P_{bat}\ (k)$, is calculated every discrete state to maintain the IPV plant output power matching the market cleared value, as it is stated in Eq. 4.49.

$$P_{grid}\ (k) = P^{*}_{grid}\ (k) = f(P_{bat}\ (k)) \qquad \text{Eq. 4.49}$$

Moreover, the optimal market participation power profile ($P_{mkt}\ (k)$) is calculated every discrete state, in the same optimization where the storage system power reference ($P_{bat}\ (k)$) is calculated. Nevertheless, as there is no intraday market every discrete state, the intraday market j participation offer (an amount of energy for each hour, $E^{IMj}_{offered}\ (k)$, at a given cost, $c^{IMj}_{offered}\ (k)$) is only calculated at the last discrete state before closing each intraday market j session (k^{IMj}_{send}). There is an intraday market every 4 hours. The resolution of the intraday markets is also composed by the intraday market j session (IMj) cleared energy, $E^{IMj}_{cleared}\ (k)$, and the market clearing price, $c^{IMj}_{cleared}\ (k)$ for each hour. This resolution is received at the discrete state $k^{IMj}_{received}$, and added to the previously resolved markets to update the power references for the IPV power plant, $P^{*}_{grid}\ (k)$.

The internal steps of the MPC operation have already been detailed in section 3.2.1 of chapter 3 and therefore are not completely explained in this section. Even so and as a summary, at each discrete state, the MPC optimizes the operation of a given window (prediction horizon) based on the predictions and measures of some parameters, calculating the optimal trajectory and the control input ($u(k)$) for obtaining this optimal trajectory during the whole window. Nevertheless, only the first point of this control input ($u_0(k)$) is applied to the system. At the next discrete state, the operation is repeated, shifting the window but maintaining its length. The optimization executed to calculate the control input is the optimization proposed and explained in the present chapter.

Thus, the MPC runs the optimization every discrete state to obtain the optimal storage system power ($P_{bat}(k)$) and the optimal market participation power profile ($P_{mkt}(k)$). Nevertheless, the market participation offer ($E_{offered}^{IMj}(k)$ and $c_{offered}^{IMj}(k)$) is sent to the market operator (MO) at the last discrete state where each intraday market session is opened, at k_{send}^{IMj}.

These MPC references are applied to the IPV power plant model, where the PV and ESS models are included. As it has been mentioned before, the LP optimization does not take into account the efficiency of the storage system (to be a linear programming optimization). But in the model of the IPV power plant, where the MPC applies its calculated references, this efficiency term (η) is included. The efficiency of the storage system is directly proportional to the charging power and inversely proportional to the discharging power. Therefore, the equations that model this system are Eq. 4.50 and Eq. 4.51, respectively.

$$E_{bat}(t) = E_{bat}(t - \Delta t) + P_{bat}(t) \cdot \eta \cdot \Delta t \quad \text{Eq. 4.50}$$

$$E_{bat}(t) - E_{bat}(t - \Delta t) - \frac{P_{bat}(t)}{\eta} \cdot \Delta t = 0 \quad \text{Eq. 4.51}$$

The introduction of this detailed model of the battery comprises a SOC reduction (or a SOC increase) because when the controller requires a given power value to the storage system (a discharge), in order to provide this amount at the output, a higher value is extracted from the battery. This causes a higher SOC reduction than the expected one by means of the optimization process. For that reason, the SOC is recalculated once the efficiency of the battery is applied, to include the detailed SOC value to the next MPC optimization step, as it can be shown in Figure 4.11.

4.3.2. Market participation based on MPC with optimal strategy

In this section the IPV power plant market participation analysis is presented. This market participation analysis is executed considering the optimal 433 kWh storage system.

The analysis of the results of the market participation is based on a four day simulation, as presented in Figure 4.13. It is the same example as the one used in chapter 3, presented in Figure 3.11. As it can be observed, the presented simulation is oriented to explain the second day (day d) market participation. For doing so, the simulation must start the first day (day $d - 1$) in order to participate in the daily market. Therefore, once the daily market offer has been sent (before midday of day $d - 1$), the MPC starts its operation. From this point, to include the 24 hours of operation horizon of the day d, 36 hours of MPC horizon is needed. This horizon is also required due to the fact that the intraday session S1 has 27 hours of length plus the period of time up to market session closing (more than 29 hours). The MPC prediction horizon is depicted in the sliding red rectangles of Figure 4.13. The selected sample time is 10 minutes. This value has been selected as the tradeoff between computational cost of the optimization and the desired simulation detail.

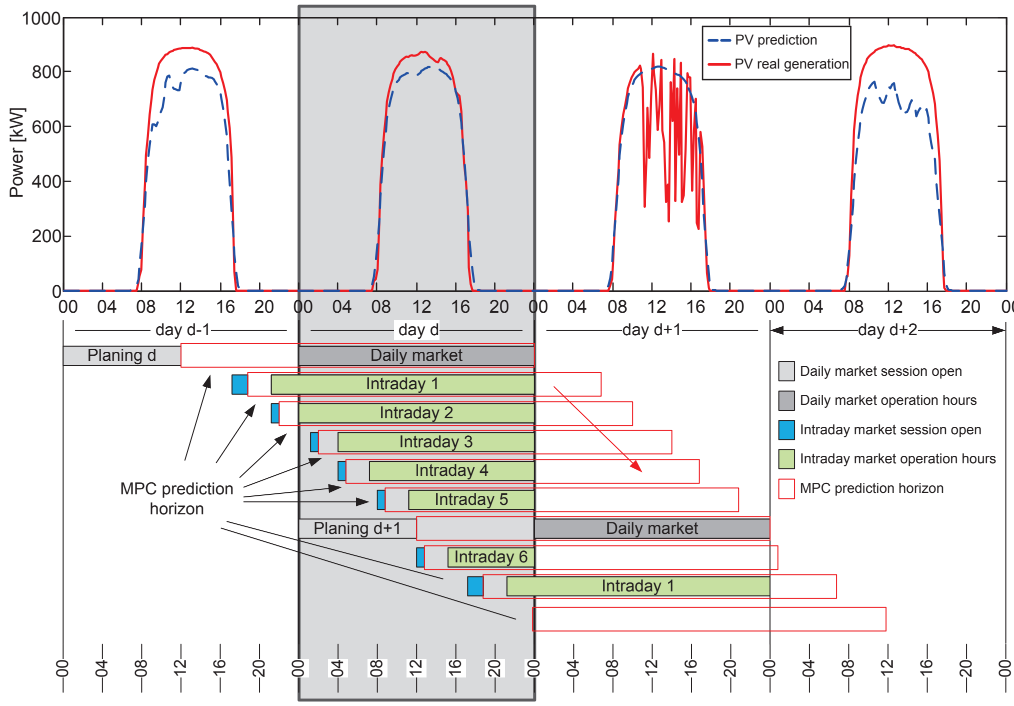

Figure 4.13: Market participation example of the second day (day d) with the different markets operation hours, participation periods and MPC prediction horizon.

At each sample time of 10 minutes, the MPC calculates the optimal battery exchanged power ($P_{bat}(t)$), considering the PV generation to maintain the market cleared power, which is the IPV plant power reference profile ($P^{*}_{grid}(t)$). Just before closing the intraday 1 market session (blue square in Figure 4.13), the MPC calculates this market offer (when $k = k^{IM1}_{send}$), based on the last PV predictions, PV measurements and battery SOC. This process is repeated at each intraday session, knowing that each intraday operation horizon is different. As the intraday markets are solved closer to their operation starting time, the PV prediction could change and the participation on these markets permits to face the prediction changes from their operation starting time. The operation is finished when the starting point of the MPC prediction horizon crosses the end of the day d.

The simulations of this market participation are also implemented in MATLAB. The presented optimization has been performed through the Optimization Toolbox [155]. The whole simulation of a single day market operation is completed in around 15 minutes.

Some results of the explained market participation are presented in Figure 4.14, where the simulation of two days market participation is carried out. The simulated days are identical to the ones explained in chapter 3. The first day is detailed in Figure 4.14 a, b and c, and is the day d presented in Figure 4.13, which represents a sunny day. The second one is detailed in Figure 4.14 d, e and f and is the day $d+1$ presented in Figure 4.13, which is a cloudy day. Figure 4.14 depicts the market participation carried out in all the analyzed markets, which are the daily and the six intraday markets. Figure 4.14 a and d show the PV real generation and the PV predictions calculated by Eq. 3.11 and Eq. 3.12 as explained in Chapter 3. Figure 4.14 b and e include the optimal market participation profile calculated to participate in every market, based on the PV prediction, the measured PV generation and the SOC of the storage system. Figure 4.14 c and f depict the six intraday markets' offers. The vertical grey lines included in Figure 4.14 b, c, e and f are the moments where the different intraday market sessions offers are sent, k_{send}^{IMj} .

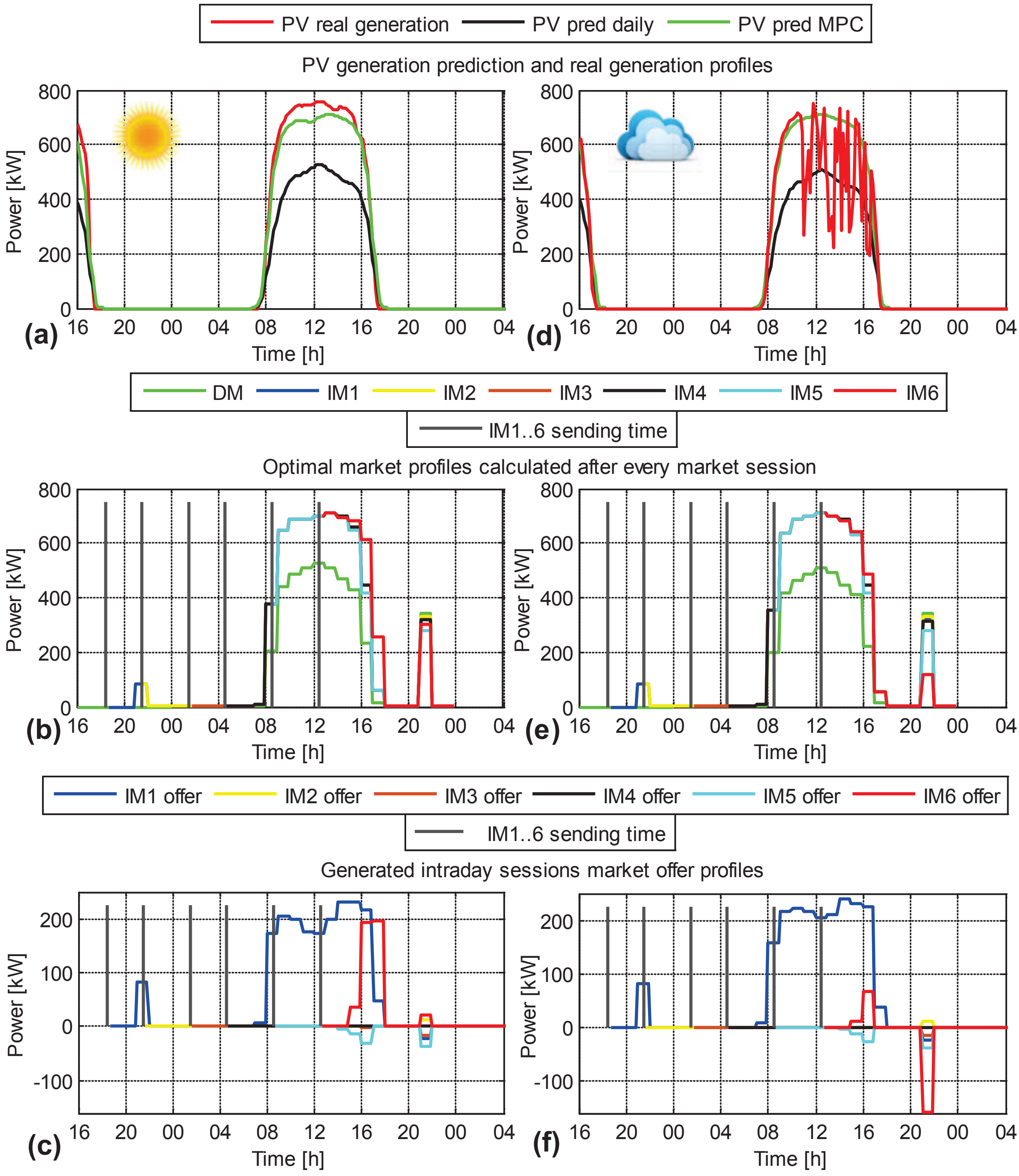

Figure 4.14: Online operation results.

The seasonal effect of the PV prediction (calculated in Eq. 3.11) is presented by the black profile of Figure 4.14 a and Figure 4.14 d. This profile is applied to determine the daily market participation offer. In the MPC operation, where the intraday markets are resolved, the PV prediction is calculated as in Eq. 3.12 and shown in the green profile. This profile is closer to the real PV generation, and with this prediction the intraday markets could improve the daily market cleared generation, maximizing the economic revenues.

Regarding Figure 4.14 b and e, the profiles included are the ones calculated by the optimization of the MPC as optimal market profiles and the daily market offer. As it has been mentioned before, the MPC takes into account the PV prediction, the PV measurement, the SOC and the prices forecast. For that reason, an important power offer appears in all markets in the hour 22 (from 21:00 to 22:00). This is because this hour is the most expensive period in the Iberian Peninsula electricity market. This statement can be verified in Figure 2.15, on the second chapter. Therefore, the MPC decides to sell the overproduction stored in the storage system in this hour.

After the daily market, the intraday S1 is resolved, and as this market can participate in the last 3 hours of the previous day (it can be verified in Figure 4.13), the controller sells the stored energy in the most expensive hour, once again the hour 22 (the first hour of the intraday S1). This event can be shown by the blue profile in Figure 4.14 b and c for the sunny day, and in the Figure 4.14 e and f for the cloudy day. In this intraday market, as it counts with closer and better PV predictions, its market offer is the greatest one of all intraday markets (around 200 kW during the sunny hours of the day).

As the PV prediction has not changed and there is no difference between the generation estimation and the real generation during the night, the S2, S3 and S4 intraday sessions' offers are almost zero, because it has already been cleared in previous markets (daily and intraday session S1).

Until the discrete state where the intraday S5 is sent, there is little PV deviation from the prediction to the real measurement, and for that reason, there is a little program change in some hours (as it can be shown by the light blue profile of Figure 4.14 c and f). Nevertheless, this change is not very representative.

In the intraday S6, there is a different incident in the sunny and in the cloudy day. In the sunny day, the MPC has detected an important PV deviation that has overcharged the storage system. For that reason, it decides to increase some hours' market offer (depicted in red profile of Figure 4.14 c) to counteract this event. Moreover, analyzing that it still has some energy reserves in the storage system, it increases the offer of the most expensive hour, the hour 22, maximizing again the economic revenues.

In the cloudy day, the MPC has detected the inverse effect, which is a reduction in the PV generation. This event has discharged the storage system more than what it was expected. This deviation is counteracted by the intraday S6 market participation (depicted in red profile of Figure 4.14 f). The offer sent is a negative offer due to the fact that the storage system does not have enough energy reserves to provide the before cleared target. This negative offer reduces the potential penalties which are greater than the presented purchase offer (a negative offer can be evaluated as a purchase offer).

As a conclusion and as it is presented in Figure 4.14, the MPC is able to counteract some predictions' corrections, participating in the intraday sessions. As it can be identified in Figure 4.14 c and f, the MPC has decided to participate in intraday session 1 selling some amount of energy in the hour 22 of the day $d-1$. As this is a traditionally expensive hour, the participation on this hour is more beneficial than participating on the first hours of a given day (cheap hours). Due to the same effect, both daily and intraday markets have also calculated a selling offer to the hour 22 of the day under test, day d.

The economic results of the market participation are also analyzed in the present study. The economic benefits obtained on three different cases are summarized in Figure 4.15. The cases taken into account are: a) single day with perfect predictions cleared on daily market (base case); b) single day with erroneous predictions using only the daily market for clearing its erroneous predicted generation; and c) single day with erroneous predictions using the daily market and correcting the PV deviations on the intraday markets applying the MPC based on the optimization developed in the present chapter (simulation detailed in Figure 4.14).

As in the economic analysis carried out in chapter 3 (section 3.2.3), in this case the SOC final value of every simulation is also taken into account to analyze a more objective scenario. This assumption is carried out due to the fact that all simulations have started with the same SOC value, but each one of them has finished with a different SOC value. This difference in a SOC value indicates a difference in the amount of energy stored in the storage system, and for analyzing the economic results in the most realistic way, this SOC difference is included in the analysis. This SOC or energy difference is economically quantified as the mean daily market price which is 42.12€/MWh in the Iberian Peninsula market of 2014 [147]. Therefore, including also this SOC final value effect, the related benefits depending on predictions and markets' participation are presented in Figure 4.15.

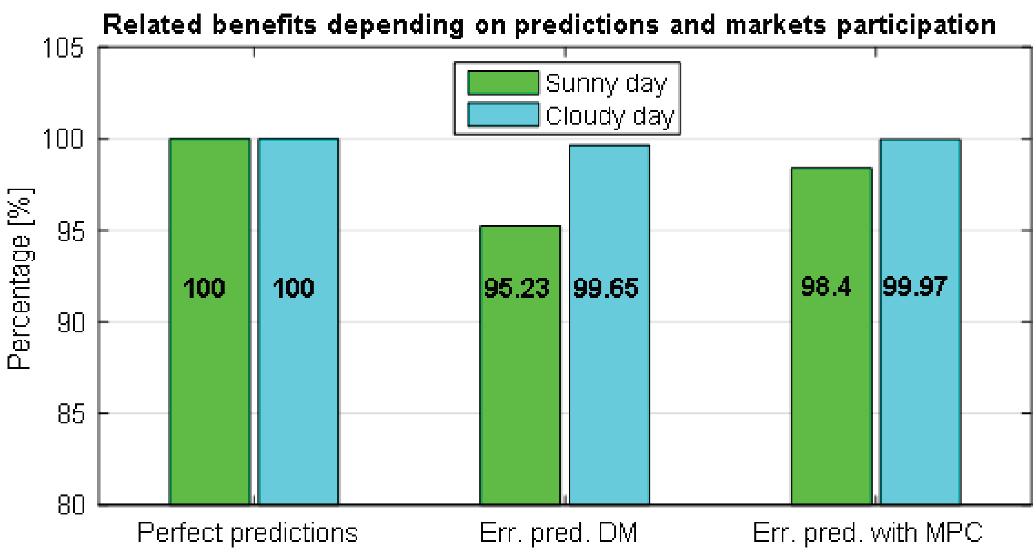

Figure 4.15: Economical results relation between different simulations.

These economic results are calculated based on the daily market, intraday markets and positive and negative deviation penalties' prices of Iberian Peninsula market in 2014 [147]. These values are explained in chapter 2.

The results show how the unique daily market participation considering erroneous prediction can reduce the benefits around 5% in a sunny day and around 1% in a cloudy day, while the MPC based intraday market participation improves these results. Applying the MPC presented in this chapter (which optimizes the participation taking into account the storage system SOC and its degradation, the PV prediction and the measured real generation and the market prices forecast), the economic results are improved by around 3% in a sunny day and maintains them around 99% in a cloudy day, compared to the second scenario. Compared to the base case, both types of days (sunny and cloudy) have obtained around 99% of potential benefits. Assuming that the base case is the ideal scenario, this result (99%) corresponds to a very positive result. This is due to the fact that the MPC has compensated the PV deviation participating in some hours when there is no PV generation but the storage system energy reserves have provided the possibility to sell some energy in other more expensive hours of the day.

Therefore, the intraday market participation carried out by the MPC for reacting to PV uncertainties provides the opportunity to obtain important benefits that justifies the development of the control algorithm.

4.4. Market participation comparison with RB and optimal control strategies

In this section the comparison of the both control strategies presented before, which are related to their market participation, is carried out. The two presented control strategies are the one based on rules (explained in Chapter 3) and the optimal one (explained in the present chapter). The comparison is based on the market participation profile and the economic results.

4.4.1. Market participation comparison

Regarding the market participation comparison, both sunny and cloudy days are compared. In both cases, on the left side of the figures the rules based control strategy results are presented while in the right side the results of the optimal control strategy are presented. It is worth mentioning that each strategy is implemented in a different IPV power plant (with different ESS capacity value), and for that reason, the objective of this comparison is to analyze the philosophy of both strategies, more than the power capabilities, that are influenced by the ESS.

4.4.1.1. Sunny day comparison

The results of the sunny day are compared in this section in the Figure 4.16. In the upper part of the figure, the PV real generation and the used different predictions are presented. In the middle part, the predicted market profiles after different market sessions are presented, while at the bottom of the figure, the intraday sessions' offers are included.

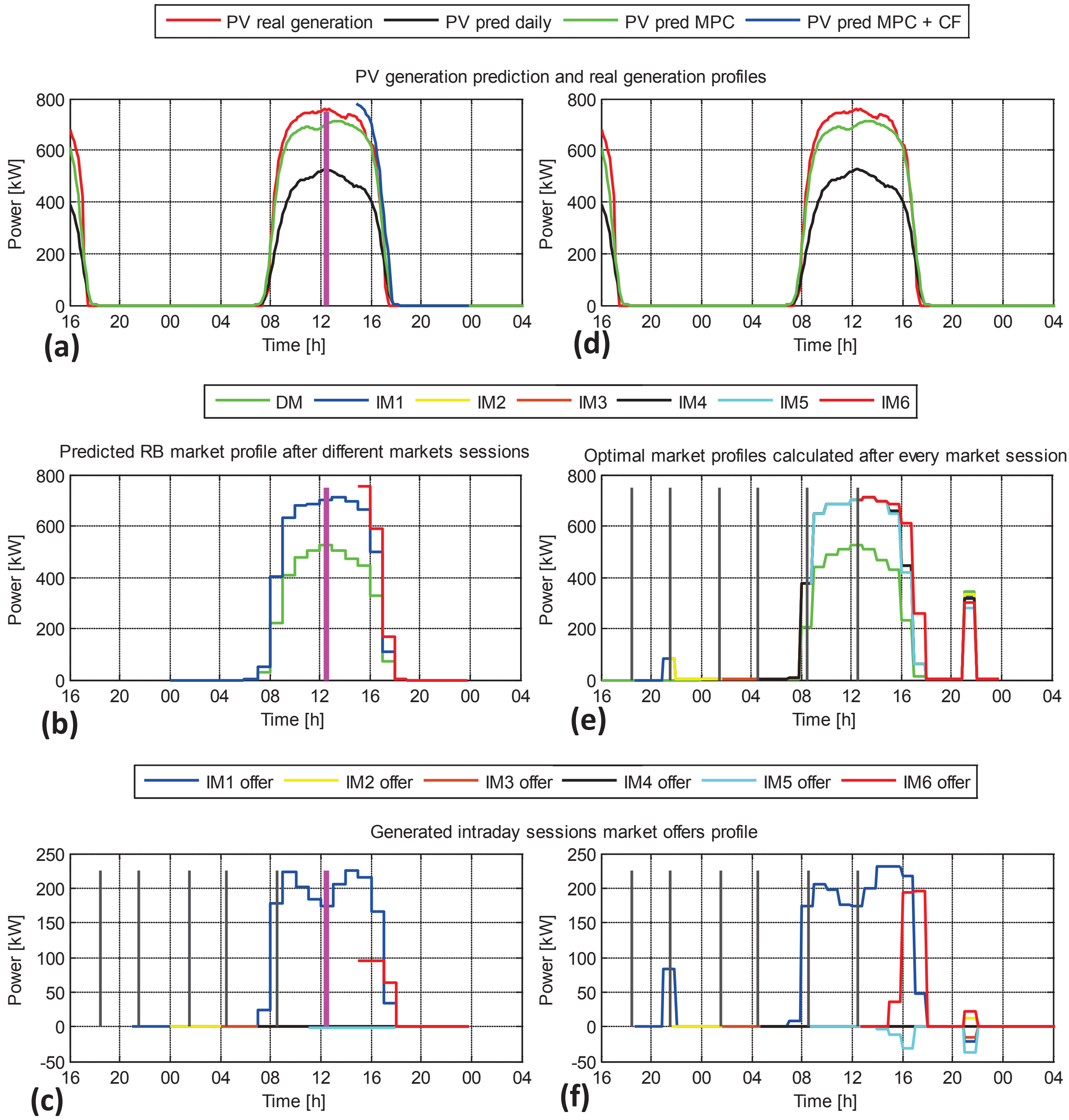

Figure 4.16: Market participation results of the sunny day with both control strategies: rules based and optimal strategy.

The first difference between the RB and the optimal control strategy is that for the RB strategy, the CF is applied to compensate the prediction errors in the online operation and it is not applied on the optimal control strategy. As the RB strategy only takes into account the PV prediction to calculate the market participation profiles in order to participate in the following intraday markets, the CF is needed to compensate the generated errors (between the PV prediction and real measurements). These errors (caused by PV generation deviation) cause a variation of the SOC of the storage system, and as the optimization strategy also takes into account this factor (the SOC), it does not need the CF to be able to compensate the unexpected generated errors. The optimal control strategy, when it measures a lower SOC value, it reduces the following markets' participation in order to recover the SOC reference value and indirectly, to avoid the penalties. This is the main difference regarding the PV predictions for both strategies.

Analyzing the purely market participation operation, there is a relevant difference between one strategy and the other. As it has been mentioned before, as the RB strategy only takes into account the PV generation prediction in order to calculate the market participation profile, it does not optimize the economic revenues; it only obtains the revenues of the hours when there is PV generation. When the PV predictions change, the RB control strategy changes its market participation profile, increasing or decreasing the previously cleared profile. It can be observed that with a change in the PV prediction before participating in the intraday session S1, the RB strategy proposes an incremental production offer. This offer can be observed by the blue profile of Figure 4.16 c and f. The same effect happens in the discrete state when the intraday session S6 is proposed, and it is presented by the red profile of Figure 4.16 c and f.

Moreover, the optimal control strategy, as it takes into account the market prices, the SOC of the storage system, and the produced error between the actual PV generation and the prediction, is able to counteract these events, adapting the intraday sessions offers to each optimal scenario. Also, as it considers the market prices, it decides to participate in the most expensive hour of the day in all intraday sessions. But it is worth mentioning that as the intraday session S1 starts with the most expensive hour of the day, the hour 22, between 9 p.m. and 10 p.m., the optimization of the revenues is still more important than the one obtained with the RB strategy.

As a conclusion just for the control strategy comparison, it can be summarized that the RB strategy is able to react to PV prediction changes but the optimal strategy not only takes into account this information but is also able to react to PV generation changes, market prices changes or SOC variations.

4.4.1.2. Cloudy day comparison

Analyzing the control strategies for the cloudy day, the overall results are similar with some minor changes. The control strategies visual comparison is presented in Figure 4.17.

In this case, the error generated between the PV prediction and the real measurement, results in a negative CF value. This causes a negative intraday session S6 offer based on the RB strategy. The same effect is counteracted in the optimal strategy with a negative market offer in the most expensive hour of the day, during hour 22, reducing the revenues but avoiding more relevant penalties, obtaining the most beneficial scenario with this offer.

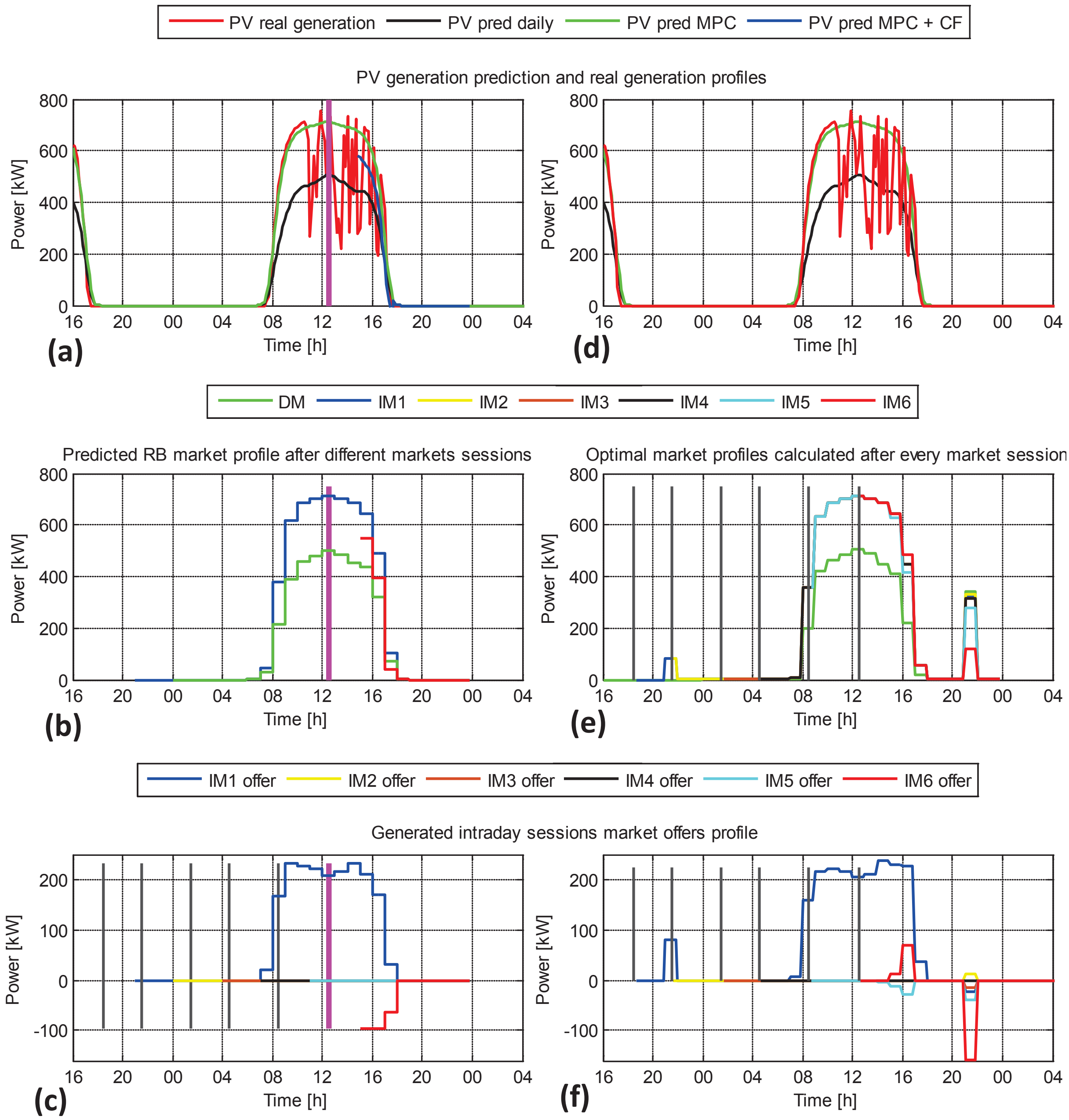

Figure 4.17: Market participation results of the cloudy day with both control strategies: rules based and optimal strategy.

The conclusions are the same as the ones stated for the sunny day, with a little difference of sign for the intraday session S6 offer. This negative offer can be considered as a purchase offer, as it is proposed by a generator. This operation is typical in renewable based generators, in order to reduce their program due to more detailed predictions. Moreover, it is worth mentioning an original effect appearing in the optimal strategy. As the optimal scenario includes a relevant amount of energy offer at the hour 22, this offer serves as a buffer for the predictions' deviation, as it can be observed in the right side (optimal strategy) results of Figure 4.17.

4.4.2. Economic comparison

The economic results of the market participation with both strategies are also analyzed in this section. As it has been mentioned before, the RB control strategy is applied to an IPV power plant with an ESS of 560 kWh, while the optimal control strategy is applied to an IPV power plant with an ESS of 433 kWh, which is the optimal sizing value. As the scenarios are different, the economic comparison is presented in absolute values of obtained benefits, instead of in relative values as presented in the chapter 3 and in the before section of this chapter.

The obtained economic benefits are calculated for the three different cases analyzed in previous comparisons and are presented in Figure 4.18. The cases taken into account are: a) single day with perfect predictions participation only in the daily market (base case); b) single day with erroneous predictions using only the daily market for clearing its erroneous predicted generation; and c) single day with erroneous predictions using the daily market and correcting the PV deviations on the intraday markets applying the MPC. Each of these three cases is simulated for a sunny day and for a cloudy day, and also using RB strategy and optimal control strategy.

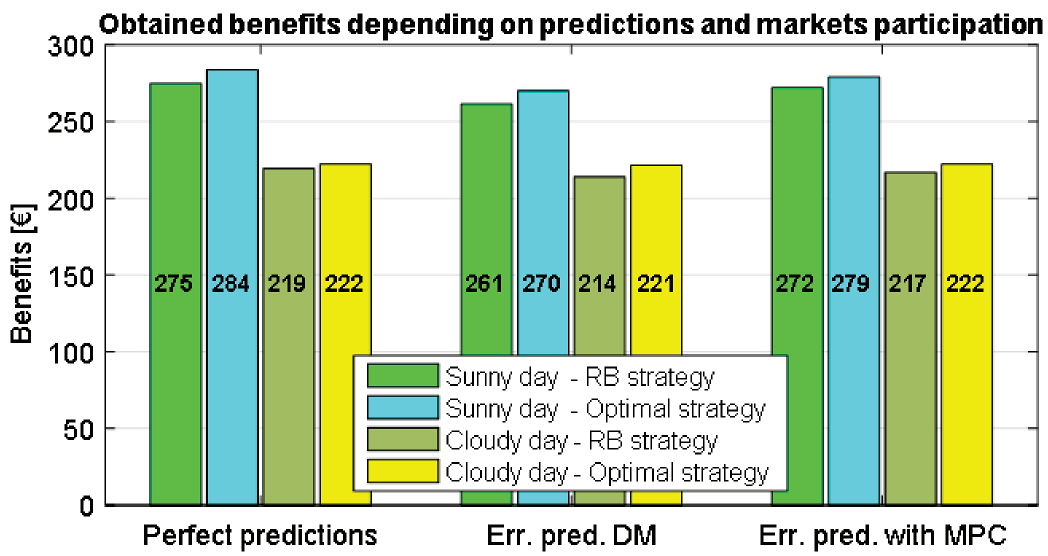

Figure 4.18: Economic results relation between different simulations.

These economic results are calculated based on the daily market, intraday markets and positive and negative deviation penalties prices of Iberian Peninsula market of year 2014 [147], the ones presented in chapter 2.

The results show different conclusions. First of all, as Figure 4.18 is presented in absolute values, it is demonstrated that the economic benefits of the sunny days are greater than the ones of the cloudy days. Moreover, it has to be mentioned that with the erroneous predictions the economic benefits' reduction is not very large (between 1 and 5%) due to the fact that the penalties prices are close to the market prices. This fact can be verified in Figure 2.15 and Figure 2.17 of chapter 2.

Analyzing the purely strategies' results, in all cases the optimal strategy obtains better results than the RB strategy, although the storage system of these scenarios is reduced by 23%, from 560 kWh to 433 kWh. This result demonstrates the advantage of the optimal strategy that considers the whole system (PV predictions, PV measurement, SOC, electricity market prices) compared to a strategy that only considers the PV predictions.

Regarding the use of the MPC, the results are also positives, due to the fact that in all cases, with RB and mainly with optimal strategy, the economic benefits are very close to the ideal scenario, which is the base case of perfect predictions. Moving the benefit closer to the ideal scenario is the most interesting result that can be obtained in this study, and in this case, the benefits have increased up to 99% of the ideal scenario.

Finally, assuming this benefits' increase from erroneous prediction but considering the use of MPC with the optimal strategy, the benefits' increase every year about 3000€, in addition to the ESS reduction.

4.5. Conclusions

This forth chapter contains the main contributions of the present PhD work. The market participation based on the optimal control strategy and the optimal storage system sizing are the objectives that have been presented in the general introduction, and they have been explained and developed in this chapter.

First, the procedure of the optimization has been presented and explained in detail. This procedure includes the details for carrying out both optimal sizing and control of the selected application. The co-optimization process includes the problem identification, the objective function explanation, the design variables selection and lower and upper bound identification, constraints analysis considering inequalities and equalities, algorithm application and simulation execution process explanation. Within these equations the model of the storage system degradation is included (considering both cycling and calendar degradation) together with its operation equation and market operation behavior equation. The objective function includes some terms of the whole economic model presented in chapter 2. The main contribution of the proposed optimization procedure is that both sizing and control strategies variables have been included, having the possibility to run a single optimization which calculates the optimal sizing with the optimal control strategy.

After the model explanation, the sizing and control strategy steps have been presented, considering the two stages that need to be followed, which are the **design stage** of the IPV power plant, defining the size of the storage system; and the **operation stage** where the size of the storage system has been already fixed and the optimal control strategy has been calculated in order to obtain the maximum economic revenues from the market participation of the whole IPV power plant.

Once these stages have been determined, the results of the optimization have been presented, analyzing the results for obtaining the optimal sizing, together with the results of the control strategy. This control strategy has been afterwards included in the market participation based on the MPC, where the operation has been described and the results related to this participation have been also presented. These results are related to each market participation offers (daily market and the six sessions of the intraday market) and also related to the economic benefits. The market participation has been presented for two different days, a sunny and a cloudy day, demonstrating the correct operation of the optimal control strategy in both cases and the relevant improvement gap obtained from the daily market participation case, as presented in Figure 4.15.

Considering that the base case (perfect predictions) is the ideal scenario, reaching 99% of that value represents a very positive result. This is due to the fact that the MPC has compensated the PV deviation participating in some hours when there is no PV generation but the storage system energy reserves have provided the possibility to sell some energy in other more expensive hours of the day. Therefore, the intraday market participation carried out by the MPC for reacting to PV uncertainties has provided the opportunity to obtain important benefits that justifies the development of the control algorithm.

Finally, the results of the presented optimization process and market participation have been compared to the ones presented in chapter 3 where the control strategy has been developed based on the analyzed RB strategy. This comparison shows the good results of the market participation based on rules, and the still better results of the proposed optimization process. The economic results have been improved from the cases where the MPC is not used, and also from the cases where the optimal strategy is not used. Thus, the results applying the MPC with the optimal control strategy have reached also 99% of the ideal scenario results, which is an important benefits increase compared to a case without those algorithms. This case of optimal based MPC has increased the benefits while it has reduced the ESS size of 23%, demonstrating that the optimization based MPC permits to increase the benefits in a considerable way.

5

Real time validation of the rules based and the optimal control strategies

5. Real time validation of the rules based and the optimal control strategies

This fifth chapter presents the real time validation carried out in a Hardware-in-the-Loop (HIL) platform. The objective of this chapter is to demonstrate the possibility of implementation of the control strategies developed and described in chapters 3 and 4 to participate in the electricity market in a commercial real-time IPV controller device.

In the fourth chapter, the optimal sizing of the energy storage system that composes an IPV power plant has been calculated. The obtained results show a lifetime of 8 years (as it is presented in Figure 4.8 of chapter 4), working as the optimization required conditions. These conditions are the ones that calculate the optimal control strategy. This strategy is calculated to extend the lifetime of the storage system and, in the general point of view, it is also calculated to obtain the greatest benefits of the whole system during the complete lifetime of the IPV power plant.

Unfortunately, neither the optimal sizing nor the optimal strategy can be validated in some days, weeks or months, because the optimal strategy is calculated for the whole lifetime of the system, which is of several years. This validation horizon exceeds the time horizon of this PhD work. Therefore, the optimal sizing and the economic optimality of the control strategy cannot be directly validated in the scope of this PhD.

Nevertheless, the real-time operation conditions of the optimal control strategy and the rules based (RB) control strategy can be validated and it is validated in this chapter. Thus, the algorithms of the control strategies are conceptually validated. Moreover, in the case of the optimal control strategy, at every discrete state, an optimization must be carried out, and the possibility to do these optimizations as fast as the selected discrete state is also demonstrated.

Furthermore, from the simulation of a given control strategy to its application in a real system, different steps should be followed. The real time validation is an intermediate step that facilitates the transition from the simulation to the real application.

This validation chapter is composed by the general description of the validation platform, the description of the market participation results with the RB control strategy, and the description of the market participation results with the optimal control strategy.

5.1. General description of the validation platform

In the present real time validation, the used platform is composed with a simulated IPV power plant controlled by a real industrial controller, a PLC (Programmable Logic Controller).

This controller is managing the real PV power plant presented in chapter 2. It is an actual hardware part of the system, programmed and constructed to be able to control a real IPV power plant. Therefore, the validation platform used in this PhD work is very close to the real application, due to the fact that the implemented control strategies can be directly uploaded in the PLC. An overall picture that presents the whole platform is shown in Figure 5.1.

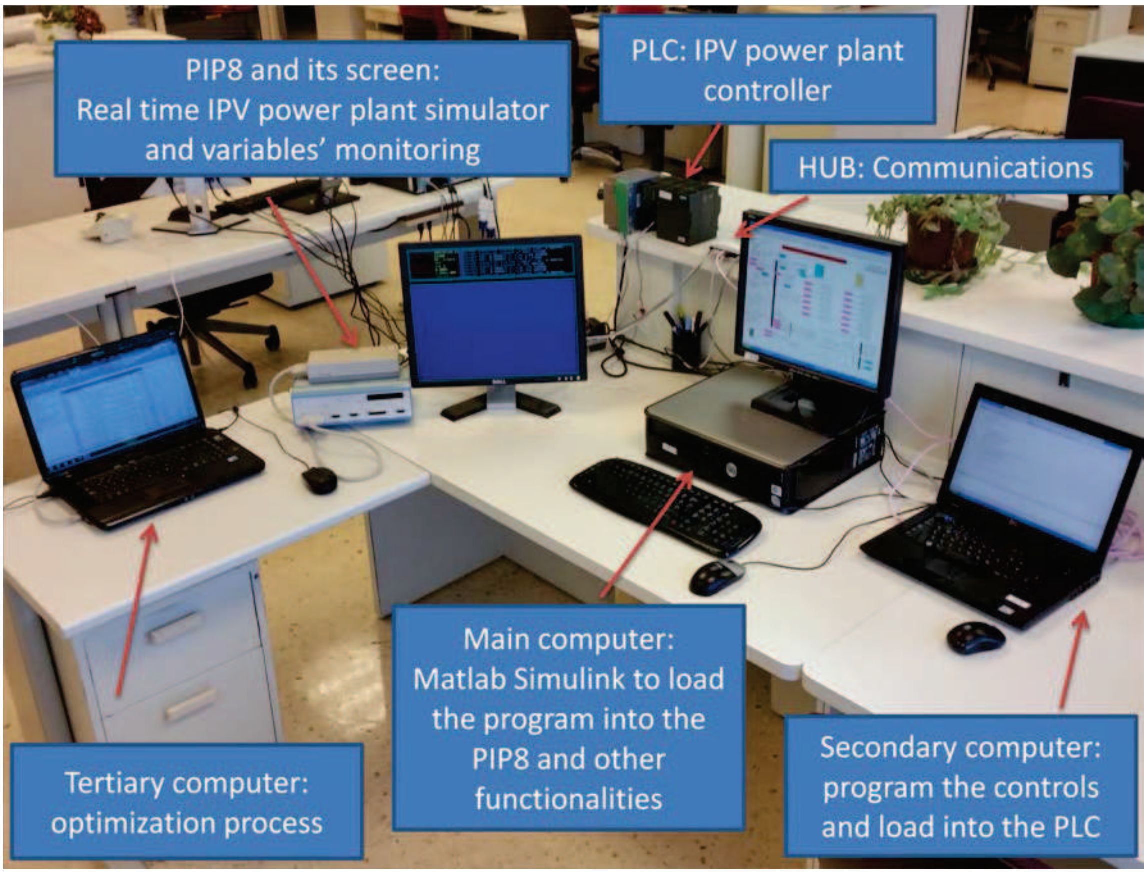

Figure 5.1: Real time validation platform picture.

5.2. Results of the market participation based on RB strategy

In this section, the possibility to run the RB control strategy in the Hardware-in-the-Loop platform is validated. To do so, firstly, the validation platform architecture is described and secondly, the results of a sunny and a cloudy day's real time operation are presented, validating in this way, the possibility to participate in electricity markets with the RB control strategy.

5.2.1. Description of the validation platform architecture

From the complete platform presented in Figure 5.1, not all the devices are used for the validation of the RB control strategy. In this case, the used devices and their main functions are summarized as follows:

- PIP8: IPV power plant and grid electric models real time emulation.
- PLC: IPV power plant control based on market cleared references and IPV power plant measurements.
- Main computer: control references and IPV power plant measurements monitoring, the PV prediction update and the market participation.

Therefore, the diagram to carry out this validation is the one presented in Figure 5.2.

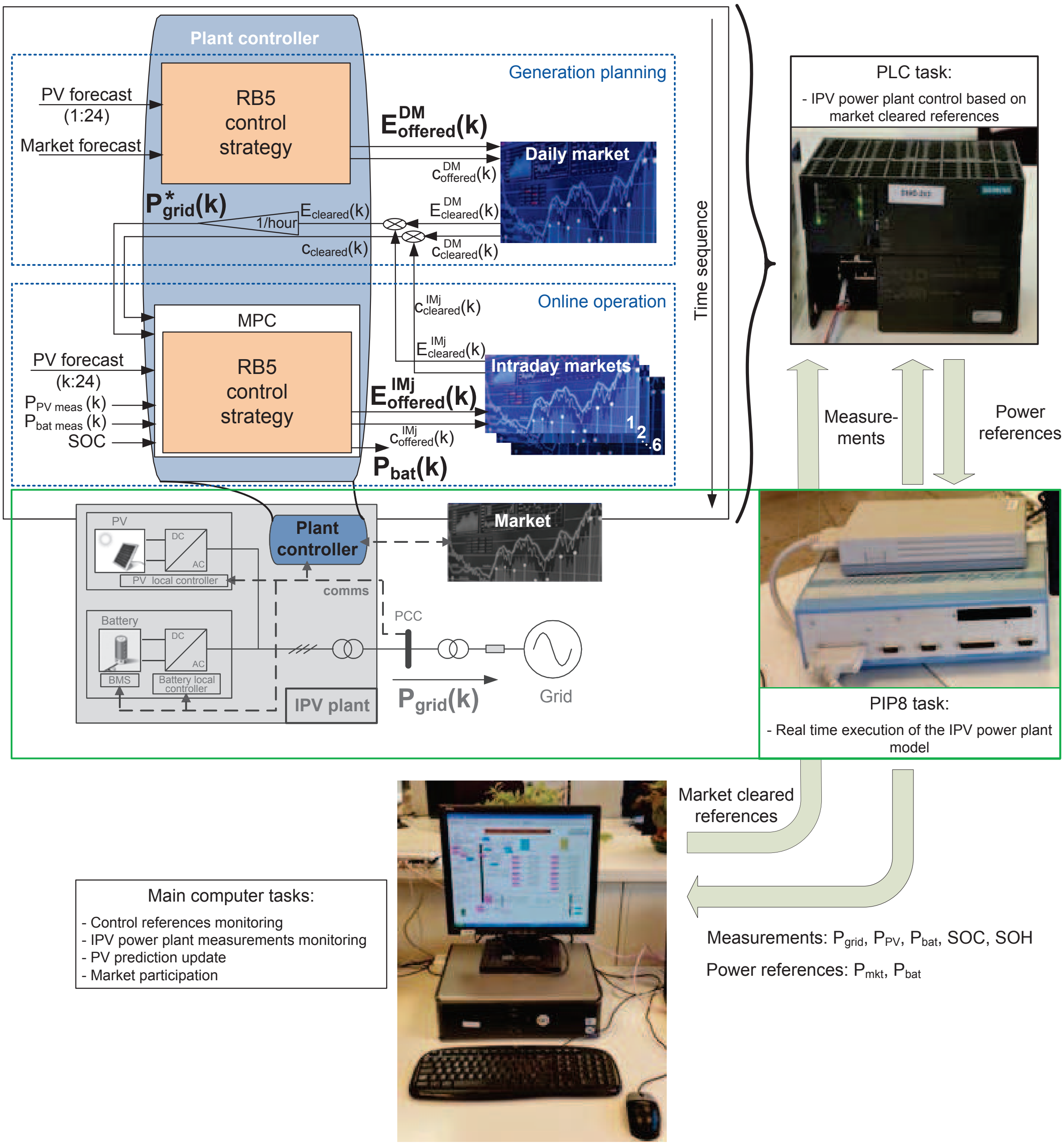

Figure 5.2: Market participation validation scenario based on the RB control strategy.

As it is shown in Figure 5.2, the PLC controls the IPV power plant model (presented in chapter 3) included in the PIP8 and the IPV power plant measurements are sent back to the PLC. The main computer carries out the market participation process and, based on this process, the market cleared references are transferred to the PIP8, in order to control the IPV power plant providing the cleared power references. The main computer also manages the monitoring of all important parameters as the market cleared references, the power references sent from PLC to the PIP8 and the IPV power plant measurements (P_{grid}, P_{PV}, P_{bat}, SOC, SOH, P_{mkt}).

In this validation step, the electrical parameters of the IPV power plant model included in the PIP8 are the ones summarized in Table 5.1.

Table 5.1: Implemented IPV power plant electrical parameters.

Parameter description	Value
Maximum power of PV inverter	1 MW
Maximum power of battery inverter	1 MW
Maximum battery charge power	1 MW
Maximum battery discharge power	1 MW
Battery nominal capacity	560 kWh
Limited maximum SOC	90%
Limited minimum SOC	10%
Initial SOC	50%
Initial SOH	100%

Once the IPV power plant electrical parameters have been defined, the simulation characteristics must be explained. In this case, as the market participation is carried out based on the PV predictions and without taking into account the storage system state of charge of the IPV power plant, the market participation profile is just the same compared with the one calculated in chapter 3. For that reason, and considering that the cleared profile is centered in the 13 hours of the middle of the day (from 6:00 am to 19:00 pm), the real time simulation is carried out considering a time horizon of 15 hours. To maintain the real scope, each real minute is simulated as a second. Therefore, the 15 hours of the real time validation are simulated in 15 minutes. The details of the simulation characteristics are presented in Table 5.2.

Table 5.2: Simulation characteristics of the market participation based on RB strategy.

Parameter description	Value
Ts	0.25ms
Real time simulation length	900s
Real reference time length	15 hours
Starting time	5:00 am

5.2.2. Results of a sunny day market participation process

The results of a sunny day market participation process are presented in this section.

Firstly, the inputs of the process are presented. As the market participation process is calculated based on the PV predictions, the market profile which is the reference for the IPV power plant is calculated as presented in chapter 3. The other input is the real PV generation, which is also presented in chapter 3. Both profiles for a representative sunny day are depicted in Figure 5.3.

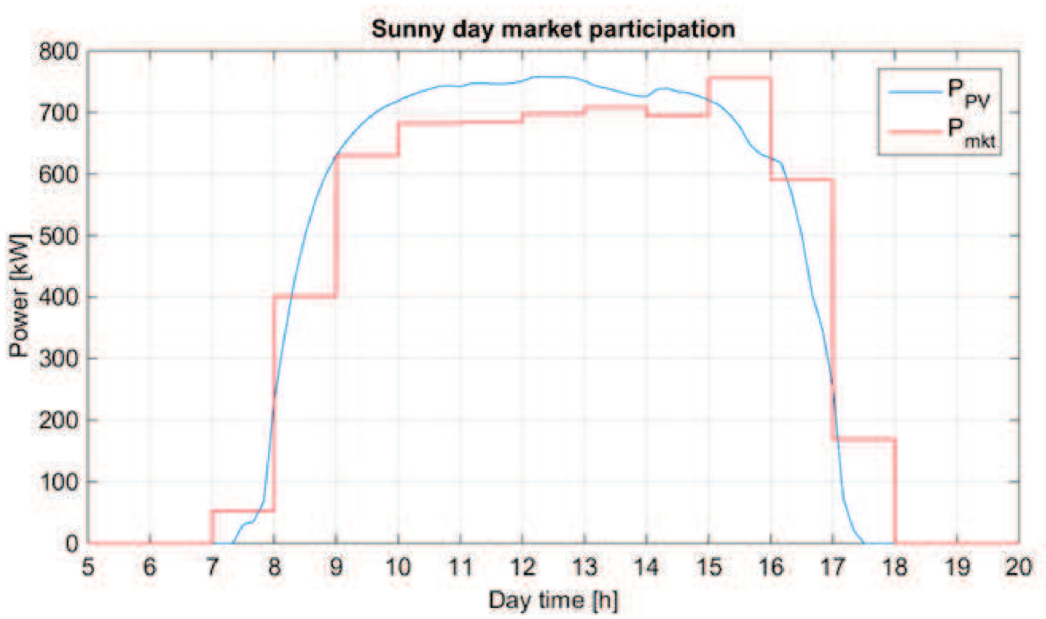

Figure 5.3: Market cleared and the PV generation inputs of the validation for a sunny day.

As it can be shown in Figure 5.3, the market profile is below the PV generation profile during the middle day hours and this difference is counteracted in the final hours of the day, with an increased market profile.

Once the inputs of the model have been introduced, the operation carried out in the validation scenario is presented. The included profiles are the ones included in the last figure

(Figure 5.3, P_{PV} and P_{mkt}) together with the storage system power profile (P_{ESS}) and the generated IPV power plant output power profile or grid provided power profile (P_{grid}). These results are presented in Figure 5.4.

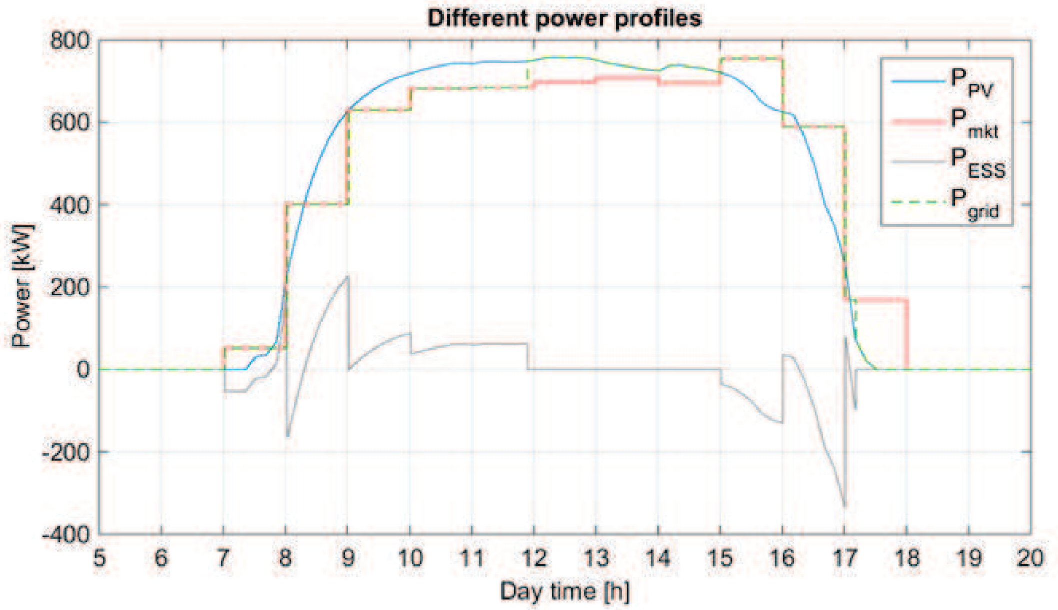

Figure 5.4: Sunny day operation based on RB control strategy.

Figure 5.5 represents the SOC variation of the storage system for providing the power profile shown in Figure 5.4. Both figures must be jointly analyzed to understand the whole day operation.

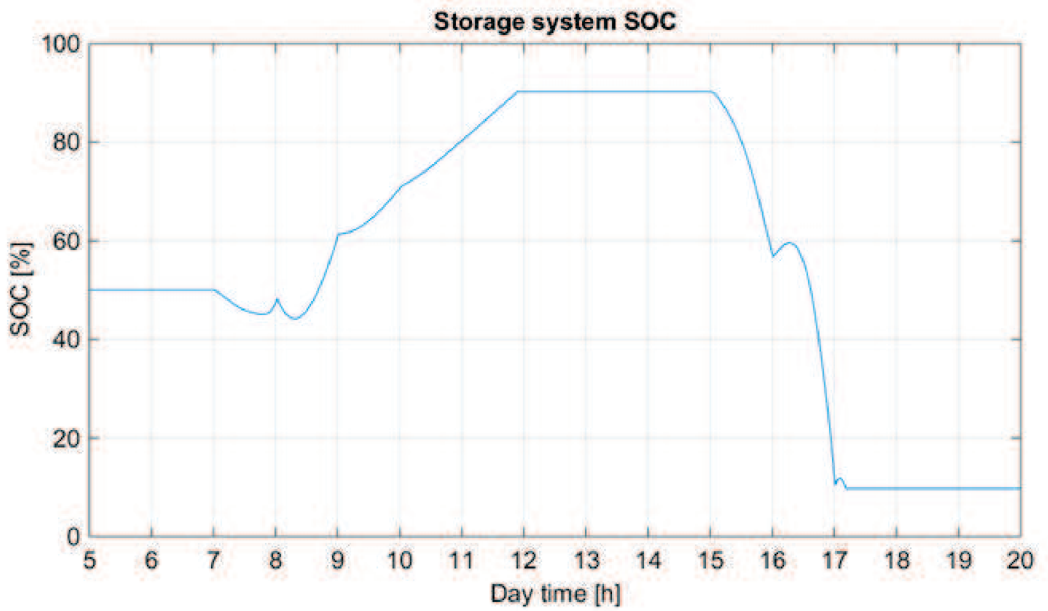

Figure 5.5: Storage system SOC variation corresponding to a sunny day operation based on RB control strategy.

As it can be extracted from Figure 5.4, the IPV power plant perfectly follows the market profile every time the battery is within its operation condition bounds (included in Table 4.1). In the morning hours, as the battery SOC starting point is considered to be 50% of SOC, it follows the market cleared profile, absorbing or providing the necessary energy to maintain the grid power matching with its reference. The following hours overcharge the storage system until its maximum SOC, and from this moment on, the whole IPV power plant provides the PV generation, as the ESS is not able to absorb more energy and the PV generation is above the market cleared reference. After 3 hours, the market cleared reference is greater than the PV generation and from this moment on the storage system starts providing energy to maintain again the reference profile. During this period of time, the storage system is discharging very fast which causes the complete discharge of the storage system and once again the grid output power is only the PV generation, but for the contrary effect. The ESS is fully discharged and the output generation is the remaining PV generation until the sunset.

Therefore, the conclusion of the operation is that the storage system energy collaborates to maintain the market cleared power profile every time it is within its limiting bounds. When this stored energy is not enough, the output power is the PV generation profile. This effect (to not provide the cleared market profile) is the one that causes penalties.

Figure 5.6 shows the market profile and the finally provided grid profile to verify the matching time and to observe the hours that have produced a given penalty due to the saturation of the storage system.

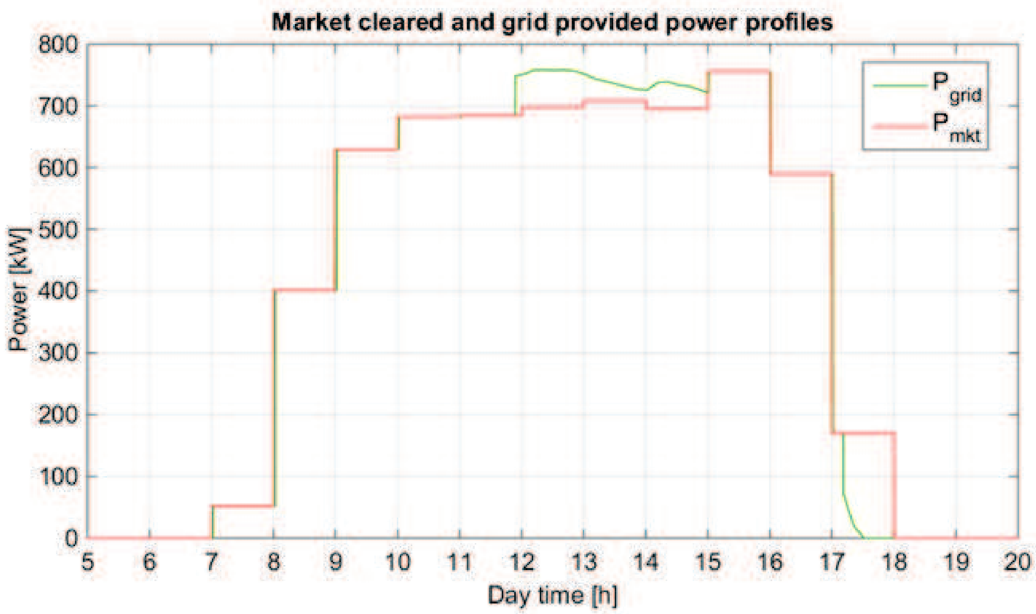

Figure 5.6: Market cleared and grid provided power profiles on a sunny day (RB control strategy).

During this day, there are three hours with positive penalties, which means that the generation is above the cleared profile, and there is one hour with negative penalty, which means that the generation is below the cleared profile.

The economic evaluation of this market participation based on the market prices of the Iberian Peninsula electricity markets is the one presented in chapter 3, in section 3.2.3 and in Figure 3.13 (sunny day).

5.2.3. Results of a cloudy day market participation process

As in the sunny day's market participation process, the results of the cloudy day are also presented in order to analyze the market participation process and the IPV power plant operation.

As in the previous case, the inputs of the market participation based on the RB control strategy are the market cleared profile and the PV generation profile presented in Figure 5.7.

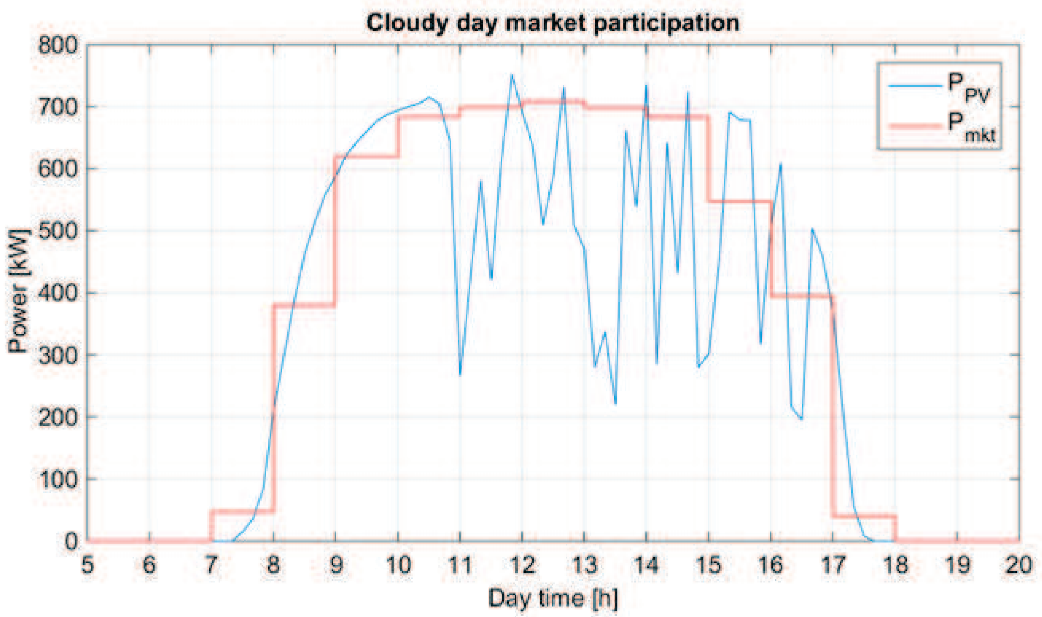

Figure 5.7: Market cleared and the PV generation inputs of the validation for a cloudy day.

In this case, the generation of several hours of the day is below the market cleared reference, with important variability and restrictive peaks that it is supposed that will rapidly discharge the storage system.

The operation of the IPV power plant based on the RB control strategy is presented in Figure 5.8. As in the sunny day case, this figure depicts the PV generation profile, the market cleared profile, the ESS power profile and the IPV power plant output power profile or grid provided profile.

Together with this figure, the following Figure 5.9 shows the storage system SOC variation, which corresponds to the power profile needed and presented in Figure 5.8.

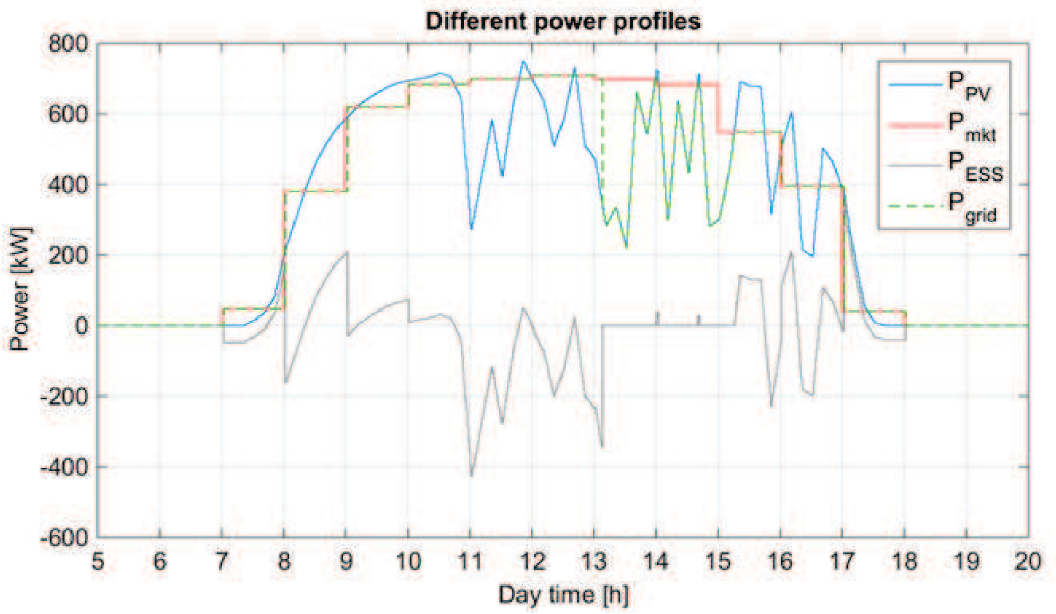

Figure 5.8: Cloudy day operation based on RB control strategy.

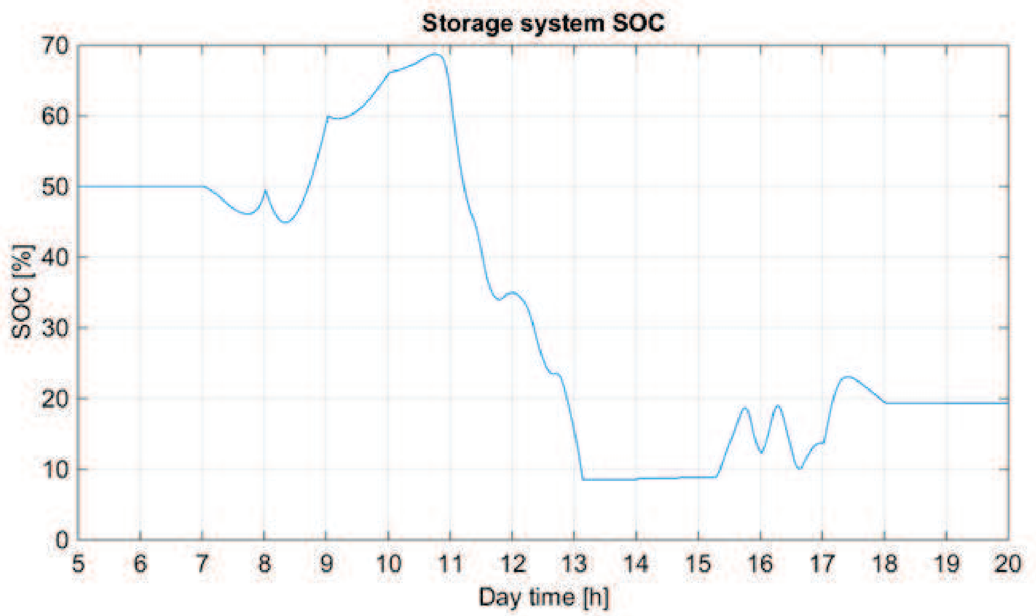

Figure 5.9: Storage system SOC variation corresponding to a cloudy day operation based on RB control strategy.

In this case, as in the previous case, while the battery SOC is within its limits, the grid output power of the whole IPV power plant matches perfectly with the cleared reference power profile. This happens from the dawn until 1 pm. During this period of time, there are several peaks which demand an important power requirement to the storage system (with a maximum peak about 400 kW). The storage system is able to provide this peak and also to vary its operation from providing energy to continuously absorbing energy as it can be verified between 11 am and 1 pm. Around 1 pm, the storage system is completely discharged, and for that reason the output power of the IPV power plant is directly the PV generation. At 2 pm and at 2.45 pm, there are two little peaks of PV generation that overpass the market cleared reference and they are used to charge the ESS. From 3 pm on, the PV generation is still very variable with important peaks (around 400 kW), but above the market cleared power reference, which charges the storage system and matches in this way the output power with the cleared reference until the sunset.

Therefore, the conclusion of the operation is the same as the one of the sunny day operation, which is that the storage system energy collaborates to maintain the market cleared power profile, every time it is within its limiting bounds. When this stored energy is not enough, the output power is the PV generation profile. This effect causes penalties.

Figure 5.10 shows the market profile and the finally provided grid profile in order to verify the matching time and to observe the hours that have produced a given penalty due to the saturation of the storage system.

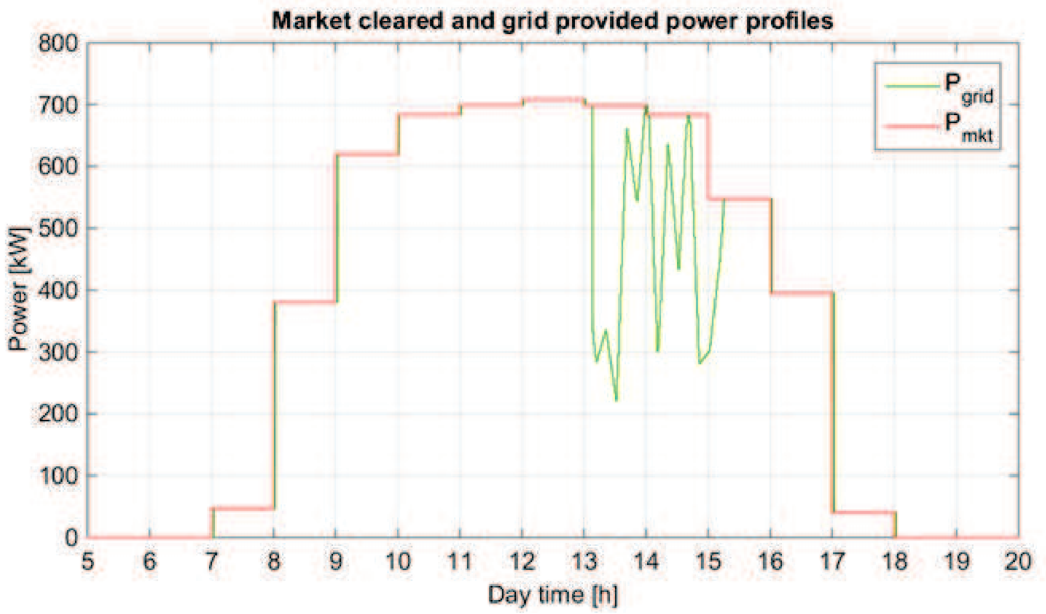

Figure 5.10: Market cleared and grid provided power profiles on the cloudy day.

In this cloudy day, there are three hours that have produced some negative penalties, which means that the generation is below the cleared profile.

The economic evaluation of this market participation based on the market prices of the Iberian Peninsula electricity markets is also the one presented in chapter 3, in section 3.2.3 and in Figure 3.13 (cloudy day).

Therefore, by means of the presented results related to the RB control strategy that has been carried out in the real time validation platform, it has been demonstrated that the developed control strategy is able to be executed in an industrial PLC in order to manage a real IPV power plant, assuming that the PLC that has been used can be installed in a real IPV power plant, which is the case of the IPV power plant described in chapter 2.

5.3. Results of the market participation based on optimal strategy

In this section another configuration of the platform is presented in order to validate the possibility of running the optimal control strategy to participate in electricity markets. To do so, the tertiary computer presented in Figure 5.1 is used to execute the optimization process. Together with the new platform configuration and its description, the market participation process results corresponding to a sunny and a cloudy day are presented.

5.3.1. Description of the validation platform architecture

The necessary devices to carry out the present validation are the ones included in the following list, where their main tasks are also summarized:

- PIP8: IPV power plant and grid electric models real time emulation.
- PLC: IPV power plant control based on market cleared references and IPV power plant measurements.
- Main computer: control references and IPV power plant measurements monitoring, the PV prediction update and the market participation communications (from the tertiary computer to the PLC).
- Tertiary computer: it runs the developed optimization process (chapter 4) to calculate the optimal market participation offers and battery power references.

Figure 5.11 presents a diagram explaining the task of each device and the information sent from one device to the others. Therefore, this scenario presents a real market participation system, which is able to manage a real IPV power plant and is also prepared to participate in electricity markets through the tertiary computer.

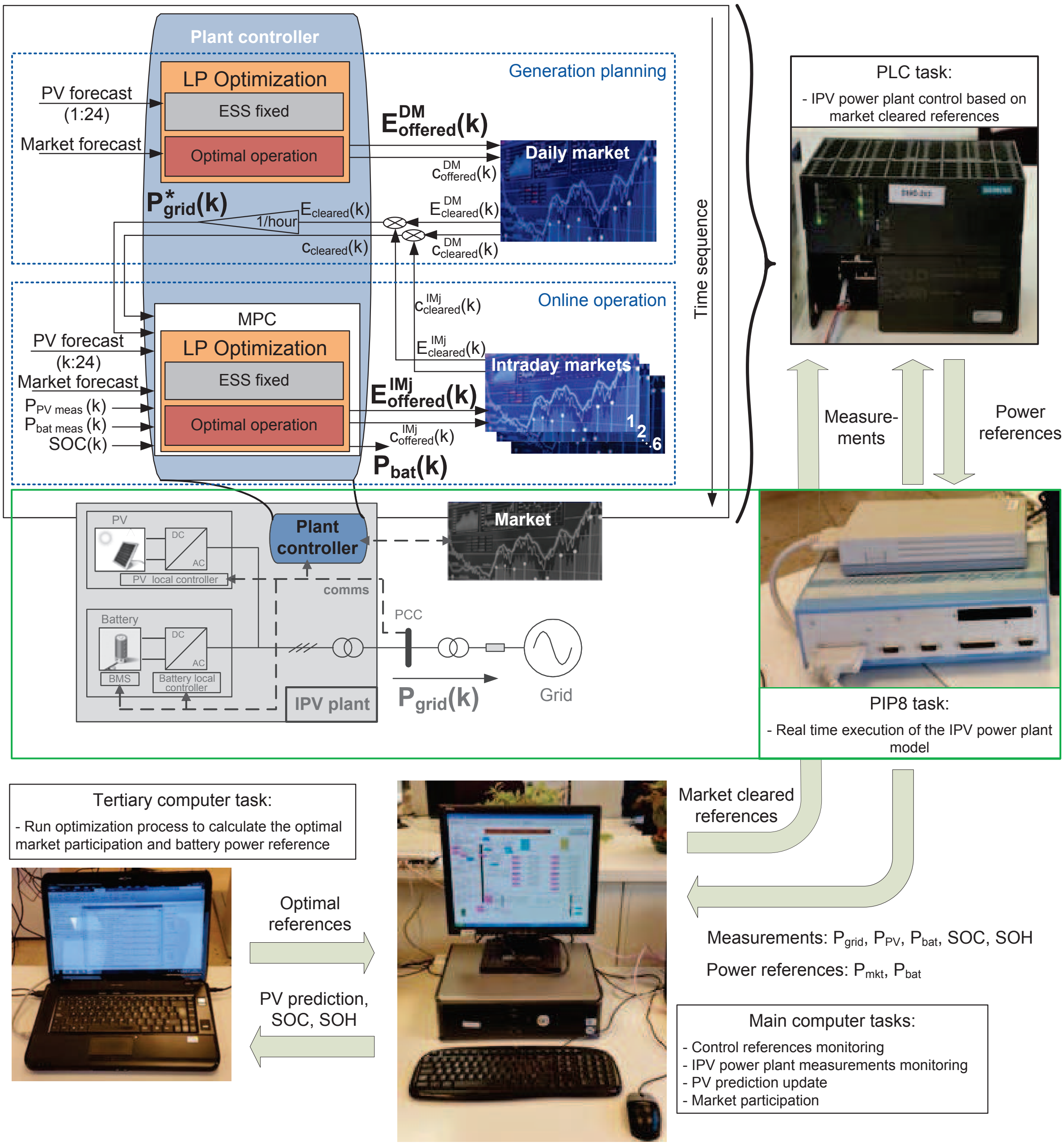

Figure 5.11: Market participation validation scenario based on the optimal control strategy.

As it can be shown in Figure 5.11, the PLC controls the IPV power plant model included in the PIP8 as it has been presented in chapter 4. The measurements of the IPV power plant are sent back to the PLC in order to close the control loop. The main computer sends to the PLC the market cleared references based on the market participation process optimally executed in the tertiary computer. As it has been mentioned before, this optimization based market participation process presented and analyzed in chapter 4 is the main contribution of this PhD work. This market participation is carried out taking into account some internal variables of the IPV power plant as the PV prediction, PV real measurement, and the SOC and the SOH of the storage system. Therefore, based on this optimization based market participation process the market cleared optimal references are transferred from the tertiary computer to the main computer, and from the main computer to the PLC in order to be able to control the PIP8 or the IPV power plant, based on its internal controller. Also in this case, the main computer manages the monitoring of all important parameters like the optimal market cleared references, the power references sent from the PLC to the PIP8 and the IPV power plant measurements (P_{grid}, P_{PV}, P_{bat}, SOC, SOH, P_{mkt}).

In chapter 4, the sizing of the storage that composes the IPV power plant has also been optimized and for that reason, the electrical parameters of the IPV power plant model included in the PIP8 to validate this market participation process are different from the previous validation (the storage system sizing is reduced from 560 kWh to 433 kWh). These characteristics are summarized in Table 5.3.

Table 5.3: Implemented IPV power plant electrical parameters.

Parameter description	Value
Maximum power of PV inverter	1 MW
Maximum power of battery inverter	1 MW
Maximum battery charge power	1 MW
Maximum battery discharge power	1 MW
Battery nominal capacity	433 kWh
Limited maximum SOC	90%
Limited minimum SOC	10%
Initial SOC	50%
Initial SOH	100%

Once the IPV power plant electrical parameters have been defined, the simulation characteristics must be introduced. In this case, as the market participation is composed by the daily market, which is defined before midday of the day $d-1$, the necessary simulation length corresponds to two following days: the first day to participate in some markets (daily and the first two intraday markets) and the second day to operate the IPV power plant and to continue participating in the rest of the intraday markets.

In order to maintain the real scope, each real minute is simulated as a second. Therefore, the 48 hours of the real time validation are simulated in 48 minutes. The details of the simulation characteristics are presented in Table 5.4.

Table 5.4: Simulation characteristics of the market participation based on optimal strategy.

Parameter description	Value
Ts	0.5ms
Real time simulation length	2880s
Real reference time length	48 hours

5.3.2. Results of a sunny day market participation process

Once described the real time validation platform where the market participation based on optimal control strategy is applied, in this section, the results of a sunny day market participation process are presented.

In this case, the inputs of the IPV power plant are the market cleared profiles and the PV generation profile. The market cleared profiles are the ones that have been calculated in the tertiary computer to obtain the optimal market participation process. Although these profiles are presented all together, each one of them is obtained in a different moment with different storage system and PV predictions conditions. The market cleared profiles obtained in the tertiary computer based on the optimal market participation are presented in Figure 5.12.

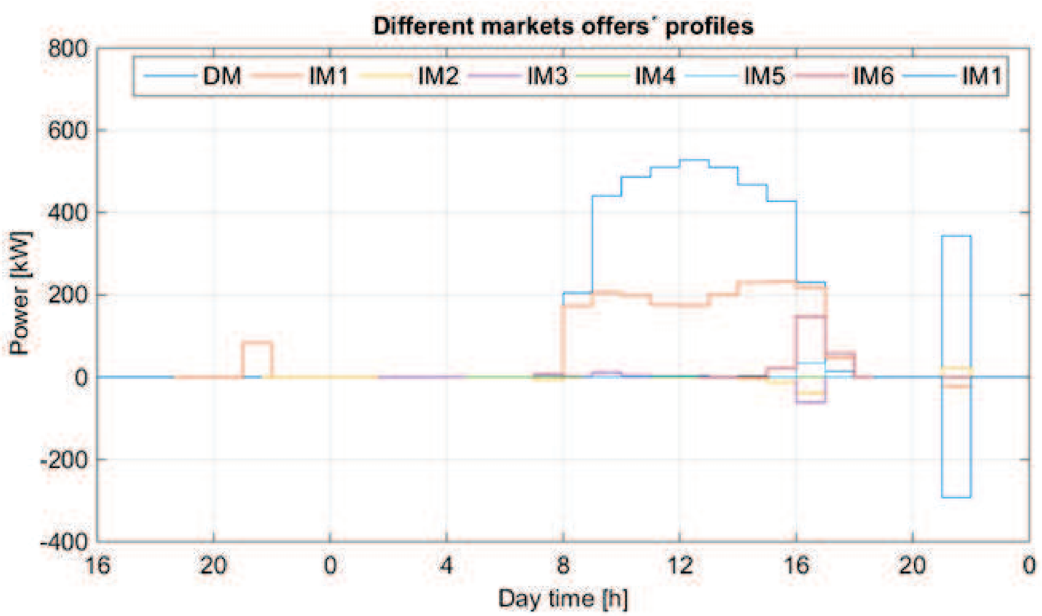

Figure 5.12: Optimal daily and intraday markets participation calculated in the tertiary computer (sunny day).

As it can be concluded from Figure 5.12, the daily market clears a typical PV generation bell (around 500 kW) and the first session of the intraday market clears another important generation area (around 200 kW during the whole part of the day). Moreover, as the intraday 1 is able to participate in the last three hours of the previous day and one of these three hours is the most expensive hour of the day, it calculates an offer from the energy stored in the ESS. Apart from that, all markets reserve an important energy amount for the most expensive hour of the day under consideration (hour 22). That is why all markets make an offer in this hour. The last market that operates in this day is the intraday 1 of the following day, which in this case has reduced the market offer of the hour 22 due to the SOC of the storage system.

Once the market participation profiles have been presented, the operation carried out in the validation scenario is described. Four profiles are included: the addition of the market participation profiles (from Figure 5.12) that compose the market cleared reference profile; the PV power profile; the storage system power profile; and the generated IPV power plant output power profile (or grid provided power profile). These results are presented in Figure 5.13. Figure 5.14 represents the SOC variation of the storage system for providing the power profile shown in Figure 5.13.

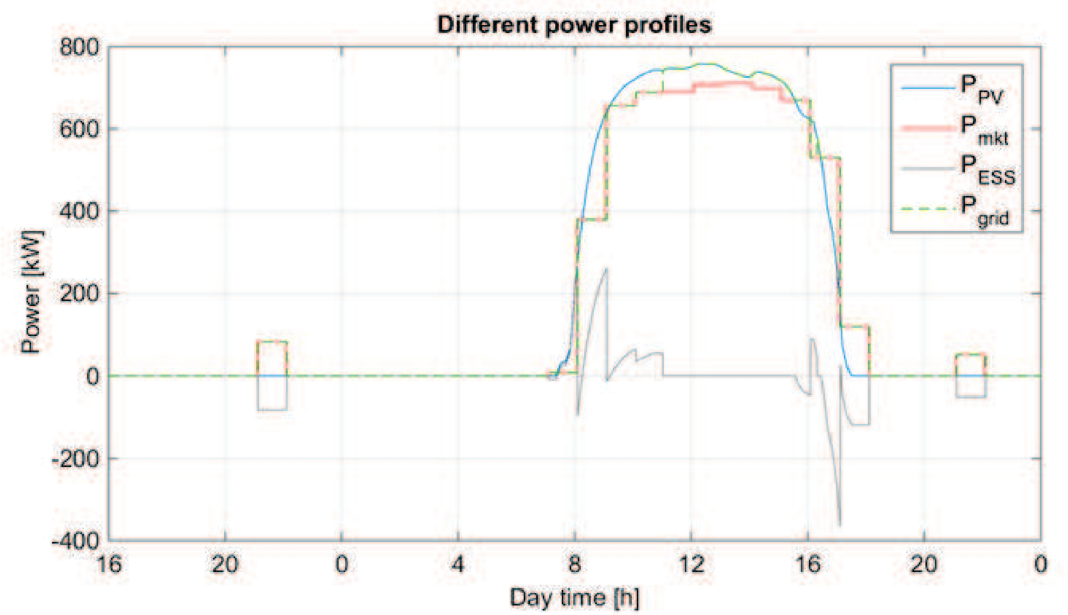

Figure 5.13: Sunny day operation based on the optimal control strategy.

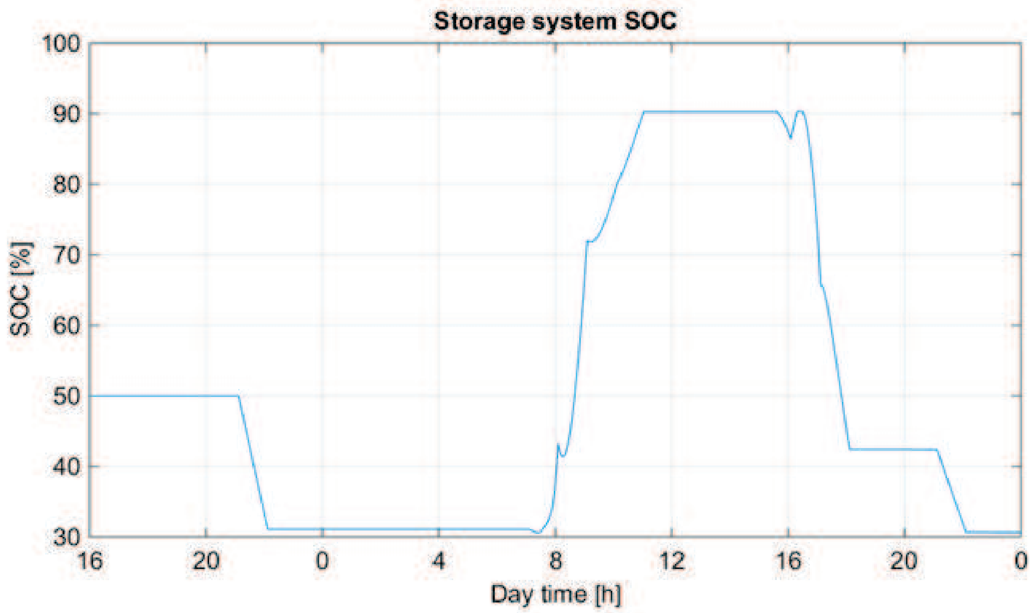

Figure 5.14: Storage system SOC variation corresponding to a sunny day operation based on the optimal control strategy.

Both figures (Figure 5.13 and Figure 5.14) must be jointly analyzed in order to understand the whole day operation. Once again, as in the previous validation, it can be stated that the IPV power plant perfectly follows the market profile while the battery is within its operation condition bounds (included in Table 5.3).

First of all, as the most beneficial hour is the hour 22, the IPV power plant provides some amount of energy discharging in this way the ESS. It is not a complete discharge in order to be able to react in the presence of any unknown effect and for that reason the optimal strategy decides to discharge the storage system until the 30% of SOC.

In the morning hours, the first objective is to recharge the storage system for future events. So, the IPV power plant output power follows the market cleared profile, absorbing or providing the necessary energy to maintain the grid power matching with its reference while it is also charging. From 9 am on, there is an unexpected PV generation that overcharges the storage system until its maximum SOC value. The next intraday market to react to this effect is the intraday 6 that is resolved around midday but that starts in operation at 3 pm. As it can be verified in Figure 5.12, the intraday 6 has an important offer to resolve this fact.

During this period of time, as the PV generation is maintained above the cleared market profile, the storage system is maintained saturated in its upper bound. Moreover, the whole IPV power plant directly provides the PV generation as the ESS is not able to absorb more energy.

At 3pm the last market starts in operation (the intraday 6) and the storage system discharges its energy providing a greater market value than the one of the PV generation while maintaining again the grid provided profile to the cleared one until the sunset. At this point, the energy of the storage system is reserved again to the most expensive hour of the day (hour 22), and at this period of time, it provides an amount of energy to discharge the storage system at the most expensive hour of the day.

Therefore, the conclusion of the operation is that the most expensive hour of the day is selected to discharge an important part of the storage system in order to obtain the highest benefit, which shows how the optimal market participation has been searched.

The last figure to verify the validation of the market participation based on the optimal control strategy is the one presented in Figure 5.15. This figure shows the optimal market profile and the finally provided grid profile to verify the matching time and to observe the hours that have produced a given penalty due to the saturation of the storage system.

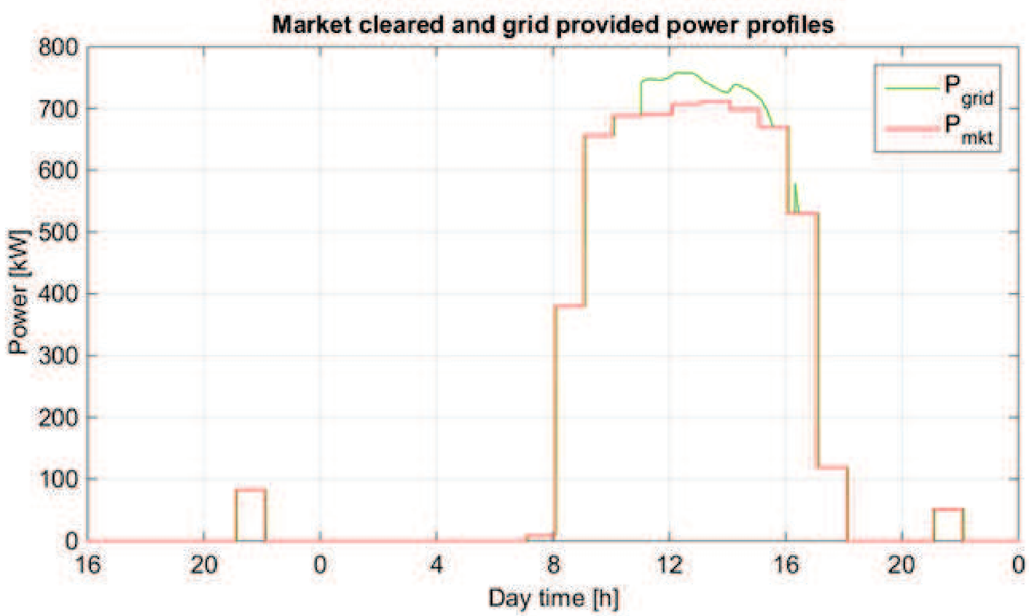

Figure 5.15: Market cleared and grid provided power profiles on a sunny day (optimal control strategy).

In this day, there are several hours that have produced some positive penalties, which means that the generation is above the cleared profile. This is due to an unexpected PV generation excess and it is counteracted in the next intraday market session. Moreover, the market participation has selected the most expensive hour of the day, which maximizes the obtained benefits.

The economic evaluation of this market participation based on the market prices of the Iberian Peninsula electricity markets is the one presented in chapter 4, in section 4.3.2 and in Figure 4.15 (sunny day).

5.3.3. Results of a cloudy day market participation process

As in a sunny day's market participation process, the results of a cloudy day are also presented here, analyzing the same power profiles. They have been analyzed starting from the optimal market participation of all markets (daily and intraday markets) and finishing with the grid provided power profile in order to analyze the economic aspects of the presented optimal market participation.

The optimal market cleared profiles calculated by the tertiary computer are the ones presented in Figure 5.16. As in the sunny day case, there are several important details that demonstrate the optimal market participation. It can be summarized that the daily market clears a typical PV generation bell and the first intraday session also clears an important amount of energy during the whole part of the day in order to increase the market participation due to better and more current prediction. Also in this cloudy day case, the intraday session 1 has participated in the most expensive hour of the previous day, which is the first hour in which it is able to participate. This generation is extracted from the energy stored in the ESS.

In this cloudy day case, all markets profiles also reserve an important amount of energy for the most expensive hour of the day under consideration (hour 22). This can be verified in Figure 5.16. Therefore, as in the previous case, the last market that operates in this period of time is the intraday 1 of the following day, which in this case has reduced the market offer of the hour 22 to reserve some of the stored energy for the following day's operation.

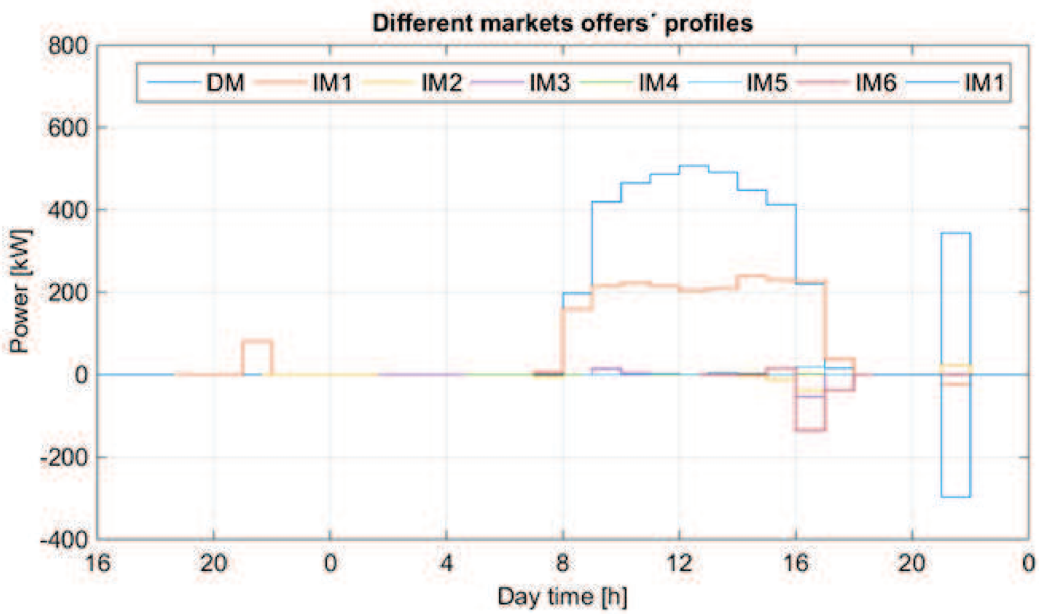

Figure 5.16: Optimal daily and intraday markets participation calculated in the tertiary computer (cloudy day).

Once the market participation profiles have been presented, the operation carried out in the validation scenario is shown. The included profiles are the same four curves as in the sunny day results analysis. These results are presented in Figure 5.17.

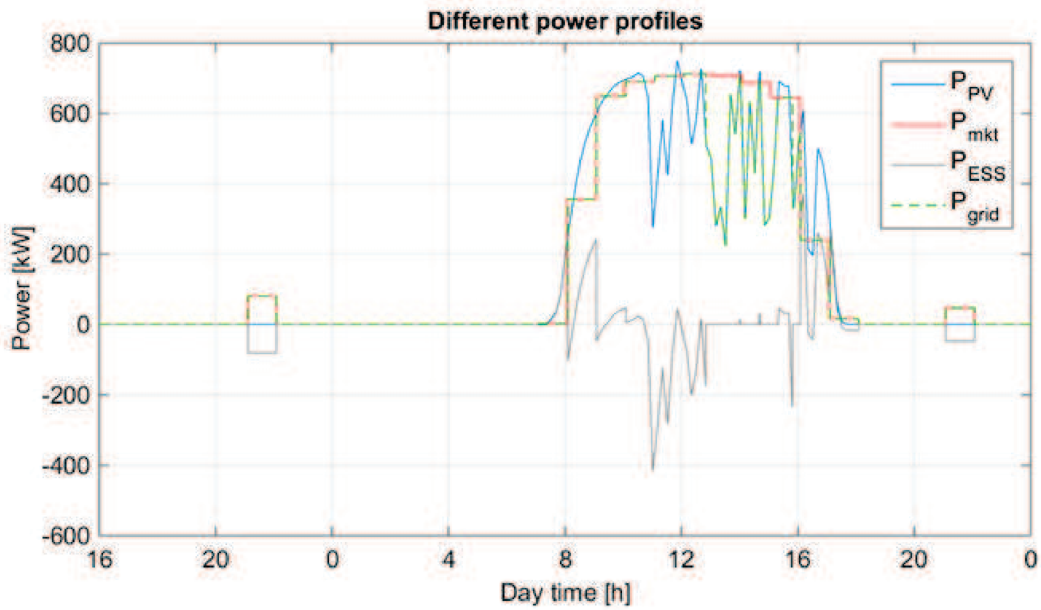

Figure 5.17: Cloudy day operation based on the optimal control strategy.

Figure 5.18 represents the SOC variation of the storage system for providing the power profile shown in Figure 5.17.

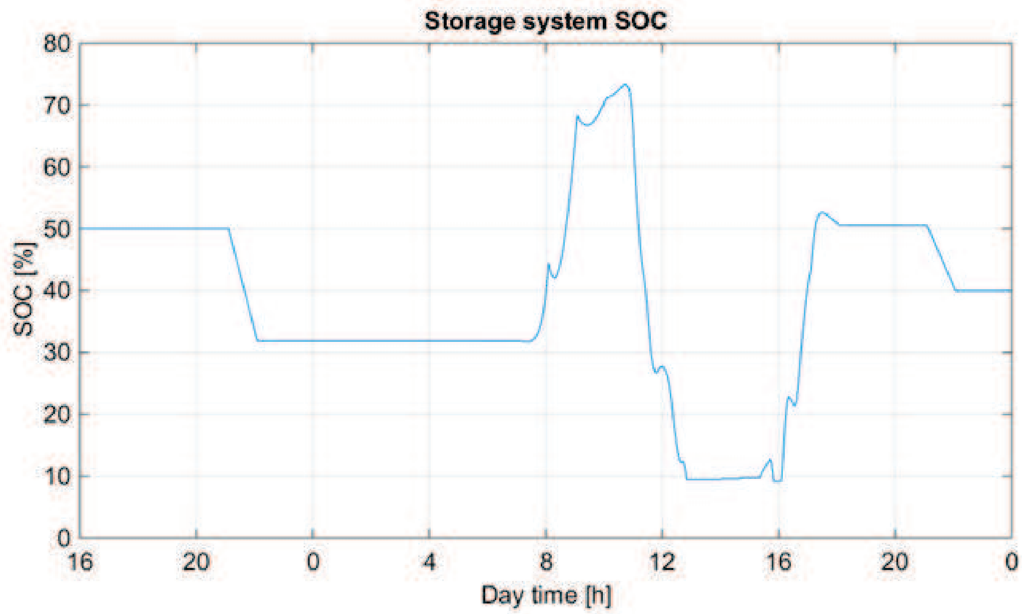

Figure 5.18: Storage system SOC variation corresponding to a cloudy day operation based on the optimal control strategy.

As in the previous case, both figures (Figure 5.17 and Figure 5.18) must be jointly analyzed in order to understand the whole day operation.

First of all, thanks to the intraday session 1, the first hour able to participate is the hour 22 of the previous day. As this hour is the most beneficial hour of the day, the IPV power plant provides some amount of energy discharging in this way the ESS. As in the sunny day case, it is not a complete discharge in order to reserve some energy to be able to react in the presence of an unexpected effect. Nevertheless, this SOC value (around 32%) is calculated by the optimization algorithm, maintaining the SOC within the thresholds of maximum and minimum values included in the Table 5.3.

In the morning hours, also as in the sunny case, the first objective is to recharge the storage system for future events. So, the IPV power plant output power follows the market cleared profile, absorbing or providing the necessary energy to maintain the grid power matching with its reference while it is also charging. Around 11 am, several clouds dramatically reduce the PV generation while the storage system maintains the market cleared profile. Its SOC is rapidly reducing in order to arrive to the lower SOC bound at about 12:30 pm. From this moment on, the IPV power plant output power is directly the PV generation producing cost penalties. In this case, the next intraday market to react to this effect is also the intraday 6 that is resolved at 12:45 pm (Table 1.2) but that starts in operation at 3 pm. As it can be verified in Figure 5.16, the intraday 6 has an important negative offer (around 150 kW during the rest of the day) to resolve this fact.

When this market has started its operation, the SOC has increased until middle values (around 50%) to be prepared for the most expensive hour of this day, once again the hour 22. At this period of time, it provides an amount of energy to discharge the storage system at this expensive hour.

The conclusions of this market participation are the same as the ones obtained in a sunny day. As the market participation is the optimal one, it tries to reduce the penalties and also participates in the most expensive hours of the day in order to obtain the highest benefits.

The last figure to verify the operation of the market participation based on the optimal control strategy is the Figure 5.19. This figure shows the optimal market profile and the finally provided grid profile in order to verify the matching time and to observe the hours that have produced a given penalty due to the saturation of the storage system. The hours that have produced the penalties are the hours when the cloudy effect has undergone and when the stored energy is not sufficient for such a cloudy day.

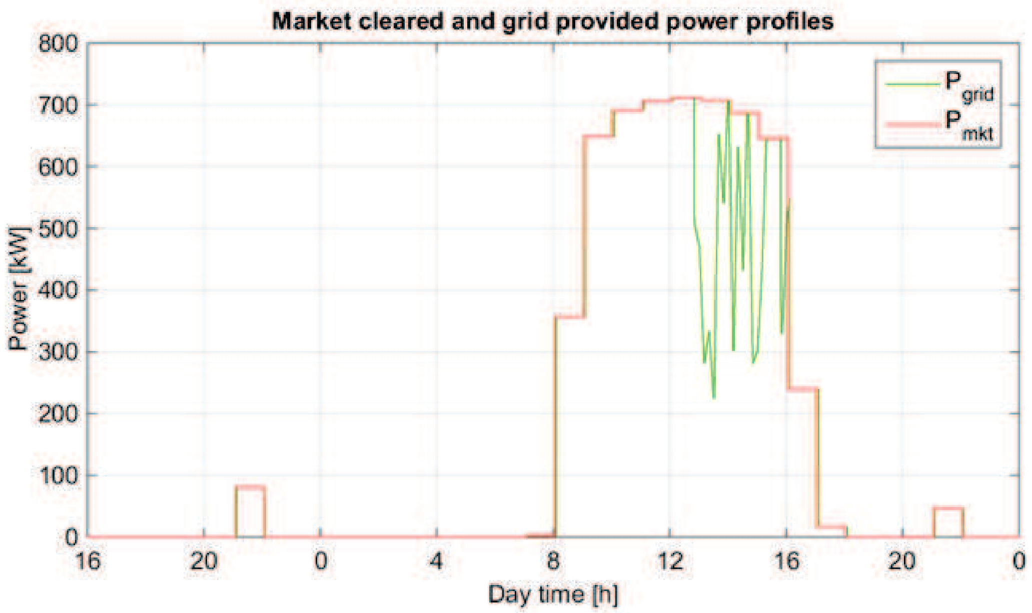

Figure 5.19 Market cleared and grid provided power profiles on a cloudy day (optimal control strategy).

In this day, there are three hours that have produced some negative penalties, which means that the generation is below the cleared profile. This is due to the unexpected PV generation reduction caused by the clouds effect. This fact is counteracted in the next intraday market session. Moreover, the market participation has selected the most expensive hour of the day (hour 22), which maximizes the obtained benefits.

The economic evaluation of this market participation based on the market prices of the Iberian Peninsula electricity markets is the one presented in chapter 4, in section 4.3.2 and in Figure 4.15 (cloudy day).

As a conclusion, by means of the presented results related to the optimal control strategy that has been carried out in the real time platform, it has been demonstrated that the developed optimal control strategy is able to be executed in an industrial PLC in order to manage a real IPV power plant. Moreover, this optimal control strategy, that increases the obtained benefits, is able to increase the viability of the IPV power plants, increasing in this way, the renewable resources rate in energy mixes.

5.4. Conclusions

In this fifth chapter, the real time validation of the proposed market participation process has been presented. The objective of this validation is to demonstrate the possibility of implementation of the developed control strategies to participate in the electricity market in a commercial real-time IPV controller device.

Two different control strategies to manage the market participation process have been validated. The first one is the RB control strategy extensively described in chapter 3 and the second one is the optimal control strategy precisely detailed in chapter 4. Both strategies have been implemented in a real time validation platform.

The strength of the present validation comes from the real PLC that has been used in the platform, which provides the validation of the intermediate step from the simulation based algorithms to the application of those algorithms in real systems. Thus, it can be stated that the validation has been carried out in a scenario very close to the real application, considering an IPV power plant real time conditions.

It has also been stated that the optimal storage system sizing cannot be verified nor validated due to the fact that the validation horizon of this process exceeds the time horizon of this PhD work, but the important fact has been the demonstration of the possibility to participate in electricity markets and the control of the IPV power plant based on the presented participation and control strategies.

Moreover, the simulations carried out in a single computer have been validated in a hardware-in-the-loop system where the obtained results have been the same as the ones obtained in the simulation step. This has been performed for both the RB control strategy and the optimal control strategy, showing that the real time operation does not includes any unexpected effect or delay in the whole IPV power plant.

In addition to that, in the optimal control strategy validation, the time steps of the different markets (the daily one and the six sessions of the intraday market) have been respected sending an offer and assuming a cleared power reference for the different horizon of each market. This fact increases the reality of the current market participation application managed by an IPV power plant.

As a main conclusion, the validation of the proposed market participation has been demonstrated, offering the possibility to participate in electricity markets with the developed process from today on. Moreover, the possibility to implement these strategies in the same PLC that is controlling a real IPV power plant provides the reliability to the proposed control strategies, both RB and optimal control strategies.

And, finally, as the optimal control strategy is also able to be implemented in a real IPV power plant, it is able to increase the economic benefits of the IPV power plants increasing, in this way, the renewable resources' rate in energy mixes.

Conclusions and future research lines

Conclusions and future research lines

In this PhD study the optimal participation of IPV power plants in electricity markets has been developed. To do so, BESS storage capability is used to reduce variability and provide to the entire IPV power plant an increase in controllability. Based on such a system, a PV power plant when associated with an energy storage system may provide different control strategies to participate efficiently in the electricity markets. Moreover, a co-optimization procedure has been developed to optimize both the sizing and the energy management strategy in the same optimization step. The developed control strategies are included in an innovative market participation process through the model predictive control, which provides the possibility to participate in daily and intraday electricity markets.

The system on which the controllability of the whole IPV power plant must be relied, the ESS, has a different operation behavior depending on how it is used. For that reason it is the main and the most complicated system to be determined. That is why its sizing and control has to be optimized to obtain the maximum benefits of the whole IPV power plant.

Therefore, the main contribution of this PhD is the development of a market participation process where the ESS sizing and its control strategy is optimized to maximize revenues based on the participation in the intraday markets by means of the model predictive control, MPC.

Other contributions of this PhD study are summarized as follows:

A **battery energy storage technology selection methodology proposition**. After an analysis about the most often used battery energy storage technologies, a selection methodology has been proposed and applied to obtain that Lithium-ion technology is the most appropriate storage technology to be used for the application considered in the present PhD work.

The **identification of the most beneficial electricity markets to participate in by means of an IPV power plant**. A detailed analysis of the electricity market has been performed to verify and to identify the most beneficial ones. Although some ancillary services markets are excluded for RES, the technical supply of some of those markets is possible, but it is identified and concluded that the most beneficial ones for RES are the spot markets, considering both daily and intraday markets. In addition, the development of **the market participation process of these two markets by means of MPC** has been carried out. Moreover, this market participation process has been applied considering two different control strategies.

One of these two strategies is the most appropriate one among the rules based strategies. Several rules based strategies have been proposed and a selection process to define which is the most beneficial to market matching time and ESS lifetime conditions has been applied. **The "Hourly energy balance value" has been selected as the optimal rules based strategy** and it has been implemented in the MPC based market participation process. The results obtained by the application of this optimal RB strategy have shown that predictions play a crucial role to obtain a significant benefit, though **the MPC that reacts in intraday markets is also as important as the daily market participation**.

As a second strategy, an optimal control strategy of the whole IPV power plant has been carried out within a co-optimization process. This **co-optimization process applied in a design stage has optimized both the ESS sizing and the control strategy** of the whole IPV power plant for optimal participation in the electricity markets. Due to the fact that is able to optimize the sizing of the ESS and also the control strategy this co-optimization is one of the main contributions of this PhD study. Therefore, once the ESS sizing has been optimized, the same co-optimization process may optimally control the whole IPV power plant on an operation stage, leading to a maximization of the economic benefits of the whole system.

The sizing optimization has been carried out considering real PV data and market costs over an entire year. This **optimal sizing value has reduced the ESS size of a considered case study by 23%**. Moreover, the economic benefits obtained with this ESS have improved the results by applying the RB strategy. This multiplies the obtained improvements by two: more benefits and lower ESS size.

As previously mentioned, the co-optimization process has **optimized the control strategy which has been implemented in the market participation process by means of the MPC**. Due to the fact that the MPC has increased the benefits up to the 99% of the ideal benefits both in sunny and cloudy days this optimal market participation process is the other main contribution of this PhD study. Moreover, this has been obtained with the lower ESS size mentioned before. This optimal control strategy has optimized the market participation offers based on PV measurements, battery power measurements, PV predictions, SOC value and also market values. Thus, almost all of the crucial parameters are taken into account to determine the optimal market participation. That is why the complexity of the scenario has required advanced tools to optimize the whole market participation.

Last but not least, the only feasible validation that can be carried out in a reasonable time horizon has been implemented: an **online execution of the proposed control algorithms in a Hardware in the Loop platform**. Both RB and optimal control strategies have been implemented, achieving the same results as obtained through Matlab simulations. Furthermore, this platform has been equipped with a real PLC that currently manages the whole control of a real IPV power plant. This demonstrates the proximity of the validation presented to the real application world. The length of the validations and the sample time selected has provided the possibility to run a two days validation simulation within 48 minutes, participating in each market at its exact time and starting in operation the participation of every market at the appropriate hour.

As main conclusion, the work developed during this PhD contributed developing procedures and strategies to allow optimal IPV power plant participation on electricity markets.

From the work developed in this PhD study, the following future research lines have been identified:

- The analysis of the possibility to participate in other complementary services or functionalities and the evaluation of which of them can be economically profitable. Once an ESS is introduced in a PV power plant, the possibilities of the whole IPV power plant increase. These possibilities include ancillary services supply as the frequency regulation or the voltage regulation. But other services such as the secondary regulation could be evaluated as the Iberian law opens this possibility to renewable based systems since February 2016.
- Sensitivity analysis of the results related to the input parameters. Some of the most important input parameters such as the PV predictions, battery lifetime table and market costs could quantitatively vary the outputs of the market participation process and also the sizing of the storage system. Based on the most relevant parameters, the need of better specifications can be identified, and future research could focus on this.
- Increase the sizing of ESS to a portfolio of RES plants and determine the optimal sizing for the whole portfolio and the optimal location of the ESS. Strategies to analyze the technical and economic viability of including an ESS in a single PV power plant have been developed. Nevertheless, the contribution of an energy storage system in a complete portfolio can increase the controllability level and the complete portfolio revenues. This topic opens a field where the renewable technologies can be matched with conventional generation technologies, or where a storage system can manage a portfolio of renewable generators. Moreover, the size of this ESS can be physically unfeasible from the network point of view, opening again the variety of possibilities to implement more than one ESS and in more than one connection point. Analyzing the sizing and the location of the ESS(s) is identified as a field for investigation together with the definition and the development of the optimal operation management strategy of the global portfolio.

References

References

[1] EPIA, *Global market outlook for photovoltaics 2014-2018*, European Photovoltaic Industry Association, 2014.

[2] IEA, *Energy and climate change, World Energy Outlook Special Report*, International Energy Agency, 2015.

[3] S.P. Europe, *Global Marketl Outlook for Solar Power 2015-2019*, Solar Power Europe, 2014.

[4] S.a.G. Research, *U. S. Solar market insight: 2014 year in review*, Solar Energy Industries Association and GTM Research, 2015.

[5] NEA, *NEA 2014 Report*, National Energy Administration, 2015.

[6] P. Denholm, E. Ela, B. Kirby, M. Milligan, *The Role of Energy Storage with Renewable Electricity Generation*, National Renewable Energy Laboratory (NREL), 2010.

[7] M. Braun, K. Büdenbender, D. Magnor, A. Jossen, *Photovoltaic Self-Consumption in Germany - Using Lithium-Ion Storage to Increase Self-Consumed Photovoltaic Energy*, Hamburg, Germany, 2009, pp. 3121 - 3127.

[8] M. Braun, D. Geibel, *Multifunctional PV battery systems for industrial applications*, Photovoltaics International, (2009) 180-186.

[9] M. Braun, T. Stetz, R. Bründlinger, C. Mayr, K. Ogimoto, H. Hatta, H. Kobayashi, B. Kroposki, B. Mather, M. Coddington, K. Lynn, G. Graditi, A. Woyte, I. MacGill, *Is the distribution grid ready to accept large-scale photovoltaic deployment? State of the art, progress, and future prospects*, Progress in Photovoltaics: Research and Applications, 20 (2012) 681-697.

[10] J. Von Appen, M. Braun, T. Stetz, K. Diwold, D. Geibel, *Time in the sun: The challenge of high PV penetration in the German electric grid*, IEEE Power and Energy Magazine, 11 (2013) 55-64.

[11] a.F. ISEA, Georg and Lunz, Benedikt and Leuthold, Matthias and Sauer, Dirk Uwe, *Technology Overview on Electricity Storage*, ISEA, 2012.

[12] T. Motors, http://www.teslamotors.com/powerwall

[13] ACCIONA, *ACCIONA incorpora almacenamiento a una planta solar fotovoltaica por primera vez en Europa*, (2012), http://www.acciona.es/noticias/acciona-incorpora-almacenamiento-a-una-planta-solar-fotovoltaica-por-primera-vez-en-europa

[14] H. Gaztañaga, J. Landaluze, I. Etxeberria-Otadui, A. Padros, I. Berazaluce, D. Cuesta, *Enhanced experimental PV plant grid-integration with a MW Lithium-Ion energy storage system*, Energy Conversion Congress and Exposition (ECCE), 2013 IEEE, 2013, pp. 1324-1329.

[15] A. Kuwayama, Y. Saito, N. Matsuno, T. Ito, R. Hara, H. Kita, N. Matsuoka, K. Taira, *Grid Connected 5MW PV Plant with Battery Storage System: Results from Four Years Operation of Wakkanai Mega Solar Project*, 25th European Photovoltaic Solar Energy Conference and Exhibition / 5th World Conference on Photovoltaic Energy Conversion, 2010.

[16] M. Niiyama, A. Kuwayama, Y. Saito, H. Kita, Y. Ueda, K. Yamaguchi, *Development of output control technologies for a large-scale PV system with battery storage - Wakkanai mega-solar project*, CIGRE, 2012.

[17] KIUC, *Kaua'i Island Utility Cooperative (KIUC) I*, (2013), http://www.xtremepower.com/advantage/experience#6-kaua'i-island-utility-cooperative-kiuc-i

[18] A. Milo, H. Gaztañaga, I. Etxeberria-Otadui, S. Bacha, P. Rodríguez, *Optimal economic exploitation of hydrogen based grid-friendly zero energy buildings*, Renewable Energy, 36 (2011) 197-205.

[19] REE, *P.O. 12.2 Systems connected to the transmission network and generation systems: design, equipment, operation, service set-up and security minimum requirements*, Red Eléctrica de España, 2009.

[20] REE, *P.O. 12.3 Requisitos de respuesta frente a hucos de tensión de las instalaciones eólicas*, Red Eléctrica de España, 2006.

[21] Eltra, *Specifications for connecting wind farms to the transmission network*, Eltra, 2000.

[22] E.ON, *Grid code high and extra high voltage*, E.ON Netz Gmbh, 2006.

[23] H. Beltran, E. Bilbao, E. Belenguer, I. Etxeberria-Otadui, P. Rodriguez, *Evaluation of storage energy requirements for constant production in PV power plants*, IEEE Transactions on Industrial Electronics, 60 (2013) 1225-1234.

[24] Y. Riffonneau, S. Bacha, F. Barruel, S. Ploix, *Optimal power flow management for grid connected PV systems with batteries*, IEEE Transactions on Sustainable Energy, 2 (2011) 309-320.

[25] C. Gavriluta, I. Candela, J. Rocabert, I. Etxeberria-Otadui, P. Rodriguez, *Storage system requirements for grid supporting PV-power plants*, Energy Conversion Congress and Exposition (ECCE), 2014 IEEE, 2014, pp. 5323-5330.

[26] A. Saez-de-Ibarra, A. Milo, H. Gaztanaga, V.I. Herrera, I. Etxeberria-Otadui, A. Padros, *Intelligent photovoltaic power plants management strategy for market participation*, Energy Conversion Congress and Exposition (ECCE), 2015 IEEE, 2015, pp. 35-42.

[27] E. Perez, H. Beltran, N. Aparicio, P. Rodriguez, *Predictive power control for PV plants with energy storage*, IEEE Transactions on Sustainable Energy, 4 (2013) 482-490.

[28] I. Miranda, N. Silva, H. Leite, A. Carrapatoso, *Distributed energy storage potentiating the participation of PV sources in electricity markets*, 2015.

[29] M.Z. Daud, A. Mohamed, M.A. Hannan, *An improved control method of battery energy storage system for hourly dispatch of photovoltaic power sources*, Energy Conversion and Management, 73 (2013) 256-270.

[30] M. Gitizadeh, H. Fakharzadegan, *Battery capacity determination with respect to optimized energy dispatch schedule in grid-connected photovoltaic (PV) systems*, Energy, 65 (2014) 665-674.

[31] A. Nottrott, J. Kleissl, B. Washom, *Energy dispatch schedule optimization and cost benefit analysis for grid-connected, photovoltaic-battery storage systems*, Renewable Energy, 55 (2013) 230-240.

[32] R. Carbone, *Grid-connected photovoltaic systems with energy storage*, 2009, pp. 760-767.

[33] A. Saez-de-Ibarra, *Analyse des structures de distribution de puissance et contrôle commande pour des parcs photovoltaïques intelligentes avec stockage d'énergie*, ENSE3 - INP Grenoble, 2012.

[34] A. Zanon, *Decentralized Power Generation in PV Plants*, 2013.

[35] ACCIONA, *Planta solar fotovoltaica de 1,2 MW en Tudela*, 2010.

[36] Y.a.K. Ru, J. and Martinez, S., *Storage size determination for grid-connected photovoltaic systems*, IEEE Transactions on Sustainable Energy, 4 (2013) 68-81.

[37] B.J.a. Szymanski, K.c. Kompa, L.b. Roslaniec, A.b. Dmowski, J.d. Szymanski, *Operation of photovoltaic power systems with energy storage*, 2011, pp. 86-91.

[38] P. Arun, R. Banerjee, S. Bandyopadhyay, *Optimum sizing of photovoltaic battery systems incorporating uncertainty through design space approach*, Solar Energy, 83 (2009) 1013-1025.

[39] C.V. Nayar, M. Ashari, W.W.L. Keerthipala, *A grid-interactive photovoltaic uninterruptible power supply system using battery storage and a back up diesel generator*, IEEE Transactions on Energy Conversion, 15 (2000) 348-353.

[40] H. Fakham, D. Lu, B. Francois, *Power control design of a battery charger in a hybrid active PV generator for load-following applications*, IEEE Transactions on Industrial Electronics, 58 (2011) 85-94.

[41] R. Carbone, A. Tomaselli, *Recent advances on AC PV-modules for grid-connected photovoltaic plants*, 2011, pp. 124-129.

[42] L. Rosario, P.C.K. Luk, *Applying management methodology to electric vehicles with multiple energy storage systems*, 2007, pp. 4223-4230.

[43] E. Bilbao, *Energy Management Strategies Based on Dynamic Programming for Applications with Energy Storing Capacity*, École Polytechnique Fédérale de Lausanne, 2013.

[44] REE, *CECOEL Power Control Centre*, Red Eléctrica de España, 2010.

[45] L. Chen, J. Zhong, D. Gan, *Optimal Automatic Generation Control (AGC) Dispatching and Its Control Performance Analysis for the Distribution Systems with DGs*, Power Engineering Society General Meeting, 2007. IEEE, 2007, pp. 1-6.

[46] K.W. Cheung, P. Shamsollahi, D. Sun, J. Milligan, M. Potishnak, *Energy and ancillary service dispatch for the interim ISO New England electricity market*, IEEE Transactions on Power Systems, 15 (2000) 968-974.

[47] X. Xi, R. Sioshansi, V. Marano, *A stochastic dynamic programming model for co-optimization of distributed energy storage*, Energy Systems, (2013) 1-31.

[48] Y. Riffonneau, S. Bacha, F. Barruel, A. Delaille, *Energy flow management in grid connected PV systems with storage - A deterministic approach*, IEEE International Conference on Industrial Technology, ICIT, 2009.

[49] H. Kanchev, D. Lu, F. Colas, V. Lazarov, B. Francois, *Energy management and operational planning of a microgrid with a PV-based active generator for smart grid applications*, IEEE Transactions on Industrial Electronics, 58 (2011) 4583-4592.

[50] T. Zhou, B. Francois, *Energy management and power control of a hybrid active wind generator for distributed power generation and grid integration*, IEEE Transactions on Industrial Electronics, 58 (2011) 95-104.

[51] P. Haessig, B. Multon, H. Ben Ahmed, S. Lascaud, P. Bondon, *Energy storage sizing for wind power: Impact of the autocorrelation of day-ahead forecast errors*, Wind Energy, (2013).

[52] P. Haessig, B. Multon, H. Ben Ahmed, S. Lascaud, L. Jamy, *Aging-aware NaS battery model in a stochastic wind-storage simulation framework*, PowerTech (POWERTECH), 2013 IEEE Grenoble, 2013, pp. 1-6.

[53] H. Beltran, *Energy Storage Systems Integration into PV Power Plants*, UPC, 2011.

[54] A.D. Hansen, P. Sorensen, F. Iov, F. Blaabjerg, *Grid support of a wind farm with active stall wind turbines and AC grid connection*, Wind Energy, 9 (2006) 341-359.

[55] P.C. Kjaer, R. Larke, G.C. Tarnowski, *Ancillary services provided from wind power plant augmented with energy storage*, Power Electronics and Applications (EPE), 2013 15th European Conference on, 2013, pp. 1-7.

[56] Y. Zhu, F. Zhuo, H. Shi, *Power management strategy research for a photovoltaic-hybrid energy storage system*, 2013, pp. 842-848.

[57] M. Akatsuka, R. Hara, H. Kita, T. Ito, Y. Ueda, S. Miwa, N. Matsuno, K. Takitani, M. Saito, *Analysis on fluctuation of PV power plant output with energy storage system*, 24th European Photovoltaic Solar Energy Conference, 21-25 September 2009, Hamburg, Germany, 2009.

[58] I. Serban, C. Marinescu, *Battery energy storage system for frequency support in microgrids and with enhanced control features for uninterruptible supply of local loads*, International Journal of Electrical Power \& Energy Systems, 54 (2014) 432 - 441.

[59] DOE, *Department of Energy*, http://energy.gov/

[60] ESA, *Electricity Storage Association* (2011), http://www.electricitystorage.org/technology/tech_archive/technology_comparisons

[61] H.a.b. Chen, T.N.a. Cong, W.a. Yang, C.b. Tan, Y.a. Li, Y.a. Ding, *Progress in electrical energy storage system: A critical review*, Progress in Natural Science, 19 (2009) 291-312.

[62] M.a. Swierczynski, R.a. Teodorescu, C.N.a. Rasmussen, P.a. Rodriguez, H.b. Vikelgaard, *Overview of the energy storage systems for wind power integration enhancement*, 2010, pp. 3749-3756.

[63] D.L.a. Yao, S.S.a. Choi, K.J.a. Tseng, T.T.b. Lie, *Determination of short-term power dispatch schedule for a wind farm incorporated with dual-battery energy storage scheme*, IEEE Transactions on Sustainable Energy, 3 (2012) 74-84.

[64] G. Xu, L. Xu, D.J. Morrow, *Wind turbines with energy storage for power smoothing and FRT enhancement*, 2011 IEEE PES General Meeting, 2011.

[65] F. Díaz-González, A. Sumper, O. Gomis-Bellmunt, R. Villafáfila-Robles, *A review of energy storage technologies for wind power applications*, Renewable and Sustainable Energy Reviews, 16 (2012) 2154-2171.

[66] A. Saez-de-Ibarra, A. Milo, H. Gaztanaga, I. Etxeberria-Otadui, P. Rodriguez, S. Bacha, V. Debusschere, *Analysis and comparison of battery energy storage technologies for grid applications*, PowerTech (POWERTECH), 2013 IEEE Grenoble, 2013, pp. 1-6.

[67] K.C. Divya, J. Ostergaard, *Battery energy storage technology for power systems-An overview*, Electric Power Systems Research, 79 (2009) 511-520.

[68] G. Fuchs, B. Lunz, M. Leuthold, D.U. Sauer, *Technology Overview on Electricity Storage*, ISEA, 2012.

[69] S.a.B. Mariéthoz, P., *Design methodology of an electric vehicle hybrid energy storage unit for improved energy efficiency*, 2010.

[70] C.W. Tan, T.C. Green, C.A. Hernandez-Aramburo, *A stochastic method for battery sizing with uninterruptible-power and demand shift capabilities in PV (photovoltaic) systems*, Energy, 35 (2010) 5082-5092.

[71] P. Pinson, G. Papaefthymiou, B. Klockl, and J. Verboomen, *Dynamic sizing of energy storage for hedging wind power forecast uncertainty*, 2009 IEEE Power and Energy Society General Meeting, PES '09, 2009.

[72] H. Bludszuweit, and J. A. Domínguez-Navarro, *A probabilistic method for energy storage sizing based on wind power forecast uncertainty*, IEEE Transactions on Power Systems, 26 (2011) 1651-1658.

[73] A. Oudalov, D. Chartouni, C. Ohler, *Optimizing a battery energy storage system for primary frequency control*, IEEE Transactions on Power Systems, 22 (2007) 1259-1266.

[74] R. Bellman, *Bottleneck problems and dynamic programming*, Proceedings of the National Academy of Sciences of the United States of America, 39 (1953) 947-951.

[75] C. Venu, Y. Riffonneau, S. Bacha, Y. Baghzouz, *Battery storage system sizing in distribution feeders with distributed photovoltaic systems*, 2009 IEEE Bucharest PowerTech 2009.

[76] Y. Ru, J. Kleissl, and S. Martinez, *Battery sizing for grid connected PV systems with fixed minimum charging/discharging time*, 2012 American Control Conference, ACC 2012, 2012, pp. 270-275.

[77] Y. Ru, J. Kleissl, and S. Martinez, *Exact sizing of battery capacity for photovoltaic systems*, European Journal of Control, (2013).

[78] Ley, *Ley 54/1997, del Sector Eléctrico*, Gobierno de España, 1997.

[79] RD, *Real Decreto 436/2004, por el que se establece la metodología para la actualización y sistematización del régimen jurídico y económico de la actividad de producción de energía eléctrica en régimen especial*, Gobierno de España, 2004.

[80] RDL, *Real Decreto-ley 14/2010, por el que se establecen medidas urgentes para la corrección del déficit tarifario del sector eléctrico*, Gobierno de España, 2010.

[81] RD, *Real Decreto 1578/2008, de retribución de la actividad de producción de energía eléctrica mediante tecnología solar fotovoltaica para instalaciones posteriores a la fecha límite de mantenimiento de la retribución del RD 661/2007 para dicha tecnología*, Gobierno de España, 2008.

[82] RD, *Real Decreto 661/2007, por el que se regula la actividad de producción de energía eléctrica en régimen especial*, Gobierno de España, 2007.

[83] RDL, *Real Decreto-ley 1/2012, por el que se procede a la suspensión de los procedimientos de preasignación de retribución y a la suspensión de los incentivos económicos para las nuevas instalaciones de producción de energía eléctrica a partir de cogeneración, fuentes de energía renovables y residuos*, Gobierno de España, 2012.

[84] RDL, *Real Decreto-ley 2/2013, de medidas urgentes en el sistema eléctrico y en el sector financiero*, Gobierno de España, 2013.

[85] MIBEL, *Mercado Ibérico de la Electricidad*, http://www.mibel.com/

[86] OMIP, *Operador del Mercado Ibérico – Polo Portugués, The Iberian Energy Derivatives Exchange*, http://www.omip.pt/

[87] OMIE, *Operador del Mercado Ibérico – Polo Español*, http://www.omie.es/inicio

[88] OMIE, *Market Access Guide*, OMIE, 2013.

[89] OMIE, *Daily and intraday electricity market operating rules*, 2013.

[90] REE, *P.O. 9.0 Información intercambiada por el operador del sistema*, Red Eléctrica de España, 2012.

[91] REE, *P.O. 3.2 Resolución de restricciones técnicas*, Red Eléctrica de España, 2013.

[92] REE, *P.O. 3.10 Resolución de restricciones por garantía de suministro*, Red Eléctrica de España, 2010.

[93] REE, *P.O. 3.3 Gestión de desvíos generación-consumo*, Red Eléctrica de España, 2009.

[94] REE, *P.O. 7.4 Servicio complementario de control de tensión de la red de transporte*, Red Eléctrica de España, 2000.

[95] REE, *P.O. 3.9 Contratación y gestión de reserva de potencia adicional a subir*, Red Eléctrica de España, 2013.

[96] REE, *P.O. 7.1 Servicio complementario de regulación primaria*, Red Eléctrica de España, 1998.

[97] REE, *P.O. 7.2 Regulación secundaria*, Red Eléctrica de España, 2009.

[98] REE, *P.O. 7.3 Regulación terciaria*, Red Eléctrica de España, 2009.

[99] REE, *P.O. 4.0 Gestión de las conexiones internacionales*, Red Eléctrica de España, 2011.

[100] REE, *P.O. 4.1 Resolución de congestiones en la interconexión Francia-España*, Red Eléctrica de España, 2009.

[101] P. Rodriguez, *Added values applications in stationary electrical storage systems*, 2013.

[102] PNM, *PNM Prosperity Energy Storage Project*, (2013), http://www.pnm.com/systems/battery.htm

[103] Zhang, *The World's Biggest Battery Energy Storage Solution - China State Grid 6MW/36MWh Project*, 2012.

[104] L. Gaillac, J. Castaneda, A.A. Edris, D. Elizondo, C. Wilkins, C. Vartanian, D. Mendelsohn, *Tehachapi Wind Energy Storage Project: Description of operational uses, system components, and testing plans*, 2012.

[105] L.a. Gaillac, *Tehachapi Wind Energy Storage Project*, 2010.

[106] Kaheawa, *Kaheawa Wind Power II*, (2012), http://www.xtremepower.com/advantage/experience#8-kaheawa-wind-power-ii

[107] Rokkasho, *Rokkasho-Futamata Wind Farm - Case Study*, (2008), http://www.cleanenergyactionproject.com/CleanEnergyActionProject/CS.Rokkasho-Futamata_Wind_Farm___Energy_Storage_Case_Study.html

[108] AES, *AES Laurel Mountain Wind Farm*, (2011), http://www.aesenergystorage.com/projects/laurel-mountain-64-mw-operation.html

[109] PJM, *PJM Manual 11: Energy & ancillary services market operations*, PJM, 2015.

[110] M.E. Hawaiian Electric, Hawai'i Electric Light, *Provision of grid services utilizing demand-side resources*, 2015.

[111] PREPA, *Puerto Rico Electric Power Authority Minimum Technical Requirements for Photovoltaic Generation (PV) Projects*, 2012.

[112] APER, *Minimum technical requirements compliance procedure proposal*, Tech. Rep., 2014.

[113] AEE, *Puerto Rico issues energy storage mandate*, (2014), http://www.powermag.com/puerto-rico-issues-energy-storage-mandate/?hq_e=el&hq_m=2808576&hq_l=4&hq_v=1bebde560c

[114] CDEC-SING, *Tratamiento Dispositivos Tipo BESS Procedimiento DP*, 2008.

[115] Gener, *Observaciones Procedimiento DP: Tratamiento de equipos BESS*, AES Gener, 2009.

[116] R. Française, *Arrêté du 23 avril 2008 relatif aux prescriptions techniques de conception et de fonctionnement pour le raccordement à un réseau public de distribution d'électricité en basse tension ou en moyenne tension d'une installation de production d'énergie électrique*, 2008.

[117] ENTSO-E, *Network Code for Requirements for Grid Connection Applicable to all Generators*, 2013.

[118] CRE, *Reglas generales de interconexión al sistema eléctrico nacional*, 2014.

[119] J. Marcos, O. Storkël, L. Marroyo, M. Garcia, E. Lorenzo, *Storage requirements for PV power ramp-rate control*, Solar Energy, 99 (2014) 28 - 35.

[120] J. Marcos, I. de La Parra, M. GarcÃ-a, L. Marroyo, *Control strategies to smooth short-term power fluctuations in large photovoltaic plants using battery storage systems*, Energies, 7 (2014) 6593-6619.

[121] I. de la Parra, J. Marcos, M. GarcÃ-a, L. Marroyo, *Control strategies to use the minimum energy storage requirement for PV power ramp-rate control*, Solar Energy, 111 (2015) 332-343.

[122] C. Koch-Ciobotaru, A. Saez-de-Ibarra, E. Martinez-Laserna, D.I. Stroe, M. Swierczynski, P. Rodriguez, *Second life battery energy storage system for enhancing renewable energy grid integration*, Energy Conversion Congress and Exposition (ECCE), 2015 IEEE, 2015, pp. 78-84.

[123] M. Conte, P.P. Prosini, S. Passerini, *Overview of energy/hydrogen storage: State-of-the-art of the technologies and prospects for nanomaterials*, Materials Science and Engineering B: Solid-State Materials for Advanced Technology, 108 (2004) 2-8.

[124] D. Rastler, *Electricity Energy Storage Technology Options: A White Paper Primer on Applications, Costs and Benefits*, Electric Power Research Institute, EPRI, 2010.

[125] *Xtreme Power Company Solar Projects*, (2013), http://www.xtremepower.com/projects/solar.php

[126] P. Poonpun, W.T. Jewell, *Analysis of the Cost per Kilowatt Hour to Store Electricity*, IEEE Transactions on Energy Conversion, 23 (2008) 529-534.

[127] A. Nourai, *Installation of the First Distributed Energy Storage System (DESS) at American Electric Power (AEP)*, Sandia National Laboratories, 2007.

[128] JRC, *Technology Map of the European Strategic Energy Technology Plan*, JRC, 2011.

[129] ILIS, *Innovative lithium-ion system management design for MW solar plants*, (2013), http://www.eurogia.com/projects/eurogia-projects/9-ilis.html

[130] ACCIONA, *ACCIONA incorporates energy storage into a grid connected PV solar plant for the first time in Europe*, (2012), http://www.acciona.com/news/acciona-incorporates-energy-storage-into-a-grid-connected-pv-solar-plant-for-the-first-time-in-europe

[131] BP-Solar, *BP 585, 85 Watt high-efficiency monocrystalline photovoltaic module*, (2012), http://www.comel.gr/pdf/bpsolar/BP585.pdf

[132] G. Perez, *Advanced closed loop algorithms for state of charge and state of health estimation in Li-ion batteries at wide operating conditions*, Mondragon Unibertsitatea, 2016.

[133] I.-S. Kim, *The novel state of charge estimation method for lithium battery using sliding mode observer*, Journal of Power Sources, 163 (2006) 584-590.

[134] S. Teleke, M.E. Baran, S. Bhattacharya, A.Q. Huang, *Optimal control of battery energy storage for wind farm dispatching*, IEEE Transactions on Energy Conversion, 25 (2010) 787-794.

[135] A. Delaille, *Development of New State-of-Charge and State-of-Health Criteria for Batteries Used in Photovoltaic Systems*, 2006.

[136] Y. Riffonneau, A. Delaille, F. Barruel, S. Bacha, *System modeling and energy management for grid connected PV systems with storage*, 24th EU Photovoltaic Solar Energy Conference, Valencia, Spain, 2008.

[137] E. Lemaire-Potteau, F. Mattera, A. Delaille, P. Malbranche, *Assessment of storage ageing in different types of PV systems technical and economical aspects*, 24th EU Photovoltaic Solar Energy Conference, Valencia, Spain, 2008.

[138] Y. Guoa, S. Tang, G. Meng, S. Yang, *Failure modes of valve-regulated lead-acid batteries for electric bicycle applications in deep discharge*, Journal of Power Sources, 191 (2009) 127-133.

[139] S. Hua, Q. Zhou, D. Kong, J. Ma, *Application of valve-regulated lead-acid batteries for storage of solar electricity in stand-alone photovoltaic systems in the northwest areas of china*, Journal of Power Sources, 158 (2006) 1178-1185.

[140] E. Sarasketa-Zabala, I. Gandiaga, E. Martinez-Laserna, L.M. Rodriguez-Martinez, I. Villarreal, *Cycle ageing analysis of a LiFePO4/graphite cell with dynamic model validations: Towards realistic lifetime predictions*, Journal of Power Sources, 275 (2015) 573-587.

[141] E. Sarasketa-Zabala, I. Gandiaga, L.M. Rodriguez-Martinez, I. Villarreal, *Calendar ageing analysis of a LiFePO4/graphite cell with dynamic model validations: Towards realistic lifetime predictions*, Journal of Power Sources, 272 (2014) 45-57.

[142] B. Zakeri, S. Syri, *Electrical energy storage systems: A comparative life cycle cost analysis*, Renewable and Sustainable Energy Reviews, 42 (2015) 569-596.

[143] C. Amzallag, J.P. Gerey, J.L. Robert, J. Bahuaud, *Standardization of the rainflow counting method for fatigue analysis*, International Journal of Fatigue, 16 (1994) 287-293.

[144] R. Dufo, *Dimensionado y control optimos de sistemas hibridos aplicando sistemas evolutivos*, Universidad de Zaragoza, 2007.

[145] V. I. Herrera, H. Gaztañaga, A. Milo, A. Saez-de-Ibarra, I. Etxeberria-Otadui, T. Nieva, *Optimal energy management of a battery-supercapacitor based light rail vehicle using genetic algorithm*, 2015 IEEE Energy Conversion Congress & Expo. (ECCE), Montreal, Canada, 2015, pp. 1359-1366.

[146] V. I. Herrera, A. Saez-de-Ibarra, A. Milo, H. Gaztañaga, H. Camblong, *Optimal energy management of a hybrid electric bus with a battery-supercapacitor storage system using genetic algorithm*, 2015 International Conference on Electrical Systems for Aircraft, Railway, Ship Propulsion and Road Vehicles (ESARS), Aachen, Germany, 2015, pp. 1-6.

[147] REE, *Sistema de Información del Operador del Sistema Eléctrico Español* Red Eléctrica de España, (2014), http://www.esios.ree.es

[148] H. Ossenbrink, T. Huld, A. Jäger Waldau, N. Taylor, *Photovoltaic Electricity Cost Maps*, Report JRC 83366, European Commission, Joint Research Centre - Institute for Energy and Transport, 2013.

[149] N. Lu, R. Diao, R. P. Hafen, N. Samaan, Y. V. Makarov, *A comparison of forecast error generators for modeling wind and load uncertainty*, 2013 IEEE Power and Energy Society General Meeting (PES), Vancouver, Canada, 2013, pp. 1-5.

[150] E. F. Camacho, C. Bordons, *Model Predictive Control, Second Edition*, Springer, London, 2007.

[151] D. Q. Mayne, J. B. Rawlings, C. V. Rao, P. O. M. Scokaert, *Constrained model predictive control: stability and optimality*, Automatica, 36 (2000) 789-814.

[152] P. Haessig, *Dimensionnement & gestion d'un stockage d'énergie pour l'aténuation des incertitudes de production éolienne*, École Normale Supérieure de Cachan, 2014.

[153] A. Milo, *Metodología de aplicación de la optimización para el aumento de la eficiencia energética en las redes de distribución de baja tensión*, Mondragon Unibertsitatea, 2011.

[154] Mathworks, *Matlab Optimization Toolbox 3*, 2007.

[155] Mathworks, *Optimization Toolbox User's Guide*, (2015), http://uk.mathworks.com/help/pdf_doc/optim/optim_tb.pdf

Nomenclature

Abbreviations

AC	Alternative Current
Adv. Pb acid	Advanced lead acid batteries
ACU	Automatic Control Unit
AGC	Automatic Generation Control
AOFC2	Adaptative Optimized Five-step Charge Controller
APAC	Asia Pacific
AWGN	Additive White Gaussian Noise
BES	Battery Energy Storage
BESS	Battery energy storage System
BMS	Battery Management System
BOL	Beginning of Life
CAES	Compressed Air Energy Storage
CRE	French Electricity Regulation Commission (in French, *Commission de Régulation de l'Énergie*)
DC	Direct Current
DM	Daily Market
DOD	Depth of Discharge
DP	Dynamic Programming
EMS	Energy Management Strategy
EOL	End of Life
ESA	Electricity Storage Association
ESS	Energy Storage System

FBES	Flow Battery Energy Storage
FCF	Fluctuation Center Following
FEC	Full Equivalent Cycles
FES	Flywheel Energy Storage
GA	Genetic Algorithm
HCPS	Hourly Constant Power Step
HIL	Hardware in the Loop
HT-TES	High Temperature Thermoelectric Energy Storage
HY	Hybrid method
ILIS	Innovative Lithium-Ion System management design for MW solar plants
IM	Intraday Market
IPV	Intelligent Photovoltaic power plant
IWP	Intelligent Wind Power plant
Li-ion	Lithium-ion battery
LP	Linear Programming
LT-TES	Low Temperature Thermoelectric Energy Storage
MA	Moving Average
MAD	Mean Absolute Deviation criterion
MIBEL	Iberian electricity market (in Spanish, *Mercado Ibérico de la electricidad*)
MO	Market Operator
MPC	Model Predictive Control
MPEMS	Modular Power and Energy Management Structure
MPPT	Maximum Power Point Tracking
NaS	Sodium Sulphur battery

NiCd	Nickel Cadmium battery
NiMH	Nickel Metal Hydride battery
NMC	Lithium Nickel Manganese Cobalt Oxide battery
O&M	Operation & Maintenance
OMIE	Spanish section of the Iberian Market Operator (in Spanish, *Operador del mercado Ibérico – Polo Español*)
OMIP	Portuguese section of the Iberian Market Operator (in Spanish, *Operador del mercado Ibérico – Polo Portugués*)
PCC	Point of Common Coupling
PE	Power Electronics
PHF	Hourly Final Program (in Spanish, *Programa Horario Final*)
PHS	Pumped Hydroelectric Storage
PLC	Programmable Logic Controller
PQ	Active power (P) and reactive power (Q) control mode
PV	Photovoltaic
RB	Rules Based
REE	Red Eléctrica de España
RES	Renewable Energy Source
RPC	Reactive Power Control
RT-Lab	Real Time Laboratory
SCPS	Single Constant Power Step
SMES	Superconducting Magnetic Energy Storage
SO	System Operator
SOC	State of Charge
SOH	State of Health

T&D	Transport and Distribution
VSC	Voltage Source Converter
ZEB	Zero Energy Building

Symbols

a	Weighting factor for PV prediction (seasonal effect)
$a_i(f)$	Weigh up value of the f functionality for the i criterion
A and A_{eq}	Inequalities and equalities constraints' matrixes
b	Weighting factor for PV prediction (current effect)
b and b_{eq}	Inequalities and equalities constraints' vectors
c	Multipliers of design variables (x)
$c_{C_{bat}}$	Cost per watt-hour of batteries
$c_{cleared}^{DM}(k)$	Daily market cleared energy's cost profile
$c_{cleared}^{IMj}(k)$	Intraday market j cleared energy's cost profile
$c_{cleared_j}^{IMk}$	Cost of the hour j of the session k of the intraday market (IM)
$c_{ESS_{bat}}$	ESS batteries investment cost
$c_{ESS_{PE}}$	ESS related power electronics investment cost
$c_{E_{pen_j}}^{+}$	Cost per energy of positive penalties of market hour j
$c_{E_{pen_j}}^{-}$	Cost per energy of negative penalties of market hour j
c_{ini}	Initial investment cost
$c_{ini_{ESS}}$	Initial investment cost of the ESS
$c_{ini_{PV}}$	Initial investment cost of the PV system
$c_{invest.}$	Annualized initial investment cost
$c_{maintenance}$	Maintenance cost
$c_{offered}^{DM}(k)$	Daily market energy offer's cost profile
$c_{offered}^{IMj}(k)$	Intraday market j energy offer's cost profile
$c_{offered}^{mkt}(k)$	Cost of detailed market participation energy offer for each hour

$c_{O\&M}$	Annualized operation and maintenance cost
$c_{penalt.}$	All penalties cost
$c_{penalty_j}$	Cost of penalties of market hour j
$c_{P_{PE}}$	Cost of power electronics per installed power
$c_{P_{PV}}$	Cost of PV per installed power
$c_{PV_{panels}}$	PV panels investment cost
$c_{PV_{PE}}$	PV related power electronics investment cost
$c_{replac.}$	Annualized replacement cost
C_{bat}	Battery initial capacity value
$C_{bat_{installed}}$	Installed battery capacity
C_{EOL}	End of life capacity value
C_n	Nominal capacity
$C_{ref}(k)$	Current (t) maximum capacity value, or reference capacity value
$Cost^{+}_{E_{pen.j}}$	Cost per energy of positive penalty of market hour j
$Cost^{-}_{E_{pen.j}}$	Cost per energy of negative penalty of market hour j
CF	Correction Factor
CRF	Capital recovery factor
ΔC_{ref}	Capacity loss of the step k
d	Given day to participate and operate in electricity market
$days$	Number of days for optimization process
$\varepsilon_{C_{bat}}$	Battery capacity error threshold
$\varepsilon_{f'_{max}}$	Objective function error threshold
$\varepsilon_{t_{bat}}$	Battery lifetime error threshold
$E_{bat}(k)$	Battery instantaneous energy

$E^{DM}_{cleared}\ (k)$	Daily market cleared energy profile
$E^{DM}_{cleare\ d_j}$	Energy cleared in the hour j of the DM
$E^{IMj}_{cleared}\ (k)$	Intraday market cleared energy profile
$E^{IMk}_{cleare\ d_j}$	Energy cleared in the hour j of the session k of the IM
$E^{DM}_{offered}\ (k)$	Daily market energy offer profile
$E^{IMj}_{offered}\ (k)$	Intraday market j energy offer profile
$E^{mkt}_{offered}\ (k)$	Energy offer detailed market participation
$E_{pen\ \cdot j}$	Energy penalty of market hour j
$\hat{E}_{PV}$	Predicted PV energy profile
E^{mes}_{PV}	Real measured PV generations' energy profile
$E_{PV}\left(k_{ct_d}\right)$	Energy generated during the day d until the discrete state of the current time (ct)
$E_{supplie\ d_j}$	Energy supplied during hour j
η	Efficiency of the charge and discharge processes
$f(x,u)$	Economic model cost function
$f'(x)$	Optimization objective function (cost function)
i	Interest rate
$I(\tau)$	Current extracted or injected to the battery over the time
k	Each discrete state
k_{1_r}	Initial discrete state (midnight of day r)
k_{1_x}	First discrete state of day x
k_{ct_d}	Current discrete state
k^{i}_{hour}	Discrete state of each hour i on the dot

k_{N_r}	Last discrete state (discrete state before midnight of day $r+1$) in the day r
k_{N_x}	Last discrete state of day x
$k_{received}^{IMj}$	Discrete state where IMj resolution is received
k_{send}^{IMj}	Discrete state where IMj offer is sent
$K_{Criterion}$	Value of each criterion for each technology
Δk_{hour}	Difference between each k_{hour}^{i}
lb, ub	Lower bound and upper bound of x
n	Number of equations needed for each hour depending on the sample time
N_{EOL_i}	Number of cycles of i DOD group that causes the EOL of the storage system
N_{wp}	Previous year (past) prediction window size
N_{wc}	Previous days (current) measured window size
N_{year_i}	Number of cycles counted of i DOD group per year [cycles/year]
$P_{bat}(k)$	Battery power reference profile
$P_{bat_{chmax}}$	Maximum battery charge power (W)
$P_{bat_{dchmax}}$	Maximum battery discharge power (W)
$P_{bat\ meas}(k)$	Measured battery power profile
$P_{conv_{bat}}$	Battery converter power (W)
$P_{ESS_{installed}}$	Installed ESS power
$P_{grid}(k)$	IPV power plant grid provided profile
$P_{grid}^{*}(k)$	IPV power plant reference profile
$P_{mkt}(k)$	Market participation power profile
$P_{penalt}^{+}(k)$	Positive penalty power profile

$P_{penalt}^{-}(k)$	Negative penalty power profile
$\hat{P}_{PV}(k)$	PV predicted power profile
$P_{PV\ meas}(k)$	Measured PV power generation profile
$P_{PV_{installed}}$	Installed PV power
P_{PV}^{real}	Real PV generation of the year $y-1$
$Price_{marke\ t_j}$	Market clearing price of hour j
PV_{data}	Real PV generation data of the year $y-1$, in $[kW/kWp]$
$PV_{forecast}$	PV generation forecast
r	Batteries replacements needed during t_{sys}
$rev_{mk\ t\_h_j}$	Revenues of market hour j
$SOC(k)$	State of charge profile
SOC_{ini}	Initial state of charge, SOC, of the batteries
SOC_{max}	Maximum SOC of the batteries
SOC_{min}	Minimum SOC of the batteries
SOH_{ini}	Initial state of health, SOH, of the batteries
SOH_{min}	Minimum SOH of the batteries
t	Current time of the optimization process
t_{bat}	Lifespan of the storage system in years
t_{EOL}	Manufacturer data of calendar ageing in years.
t_{less}	Time of the simulation in which the IPV plant has provided less than what it has cleared
$t_{matc\ h}$	Time of the simulation in which the market cleared energy is provided
t_{more}	Time of the simulation in which the IPV plant has provided more than what it has cleared
$t_{simulation}$	Simulation length

t_{sys}	Lifetime of the whole IPV power plant
$t(k_{os_d}^{IMj})$	Time when the next intraday market j starts in operation
$t(\hat{k}_{ss_d})$	Time of the discrete state of the sunset of the day d
$T_{out_{less}}$	Time when the IPV power plant has not reached what has been cleared in the market
$T_{out_{match}}$	Time in which the market cleared energy has been provided by the IPV power plant
$T_{out_{more}}$	Time when the IPV power plant produces more than what has been cleared in the market
T'^{-h}	Auxiliary matrix.
Δt	Sample time of the optimization process
Δt_{ct}	Period of time in hours between the initial time of the day d and the time of the current discrete state
Δt_{end}	Period of time in hours between the estimated discrete state of the sunset and the time when the next intraday session j starts its operation
Δt_{gap}	Period of time in hours between the time of the current step and the time when the next intraday session j starts its operation
u	Constant factors of economic model
$u(k)$	Control input
x	Optimization design variables
Z_{cal}	Calendar ageing coefficient
Z_{cy}	Cycling ageing coefficient

List of figures

List of tables

Publications

Journals

A. Saez-de-Ibarra, A. Milo, H. Gaztañaga, V. Debusschere, S. Bacha, "Co-Optimization of Storage System Sizing and Control Strategy for Intelligent Photovoltaic Power Plants Market Integration", in *IEEE Transactions on Sustainable Energy*, vol. 7, no. 4, pp. 1749-1761, 2016.
doi: 10.1109/TSTE.2016.2555704

A. Saez-de-Ibarra, V. I. Herrera, A. Milo, H. Gaztañaga, I. Etxeberria-Otadui, S. Bacha, A. Padrós, "Management Strategy for Market Participation of Photovoltaic Power Plants including Storage Systems", in *IEEE Transactions on Industry Applications*, vol. 52, no. 5, pp. 4292-4303, 2016.
doi: 10.1109/TIA.2016.2585090

A. Saez-de-Ibarra, E. Martinez-Laserna, D. Stroe, M. Swierczynski, P. Rodriguez, "Sizing Study of Second Life Li-ion Batteries for Enhancing Renewable Energy Grid Integration", in *IEEE Transactions on Industry Applications*, vol. 52, no. 6, 2016.
doi: 10.1109/TIA.2016.2593425

V. I. Herrera, H. Gaztañaga, A. Milo, **A. Saez-de-Ibarra**, I. Etxeberria-Otadui and T. Nieva, "Optimal Energy Management and Sizing of a Battery-Supercapacitor-Based Light Rail Vehicle With a Multiobjective Approach", in *IEEE Transactions on Industry Applications*, vol. 52, no. 4, pp. 3367-3377, July-Aug. 2016.
doi: 10.1109/TIA.2016.2555790

Conferences

Andoni Saez-de-Ibarra, Aitor Milo, Haizea Gaztañaga, Ion Etxeberria-Otadui, Pedro Rodríguez, Seddik Bacha, and Vincent Debusschere, "Analysis and comparison of battery energy storage technologies for grid applications", *2013 IEEE Grenoble PowerTech (POWERTECH)*, Grenoble, 2013, pp. 1-6.
doi: 10.1109/PTC.2013.6652509

V. I. Herrera, **A. Saez-de-Ibarra**, A. Milo, H. Gaztañaga and H. Camblong, "Optimal energy management of a hybrid electric bus with a battery-supercapacitor storage system using genetic algorithm", *2015 International Conference on Electrical Systems for Aircraft, Railway, Ship Propulsion and Road Vehicles (ESARS)*, Aachen, 2015, pp. 1-6.
doi: 10.1109/ESARS.2015.7101452

A. Saez-de-Ibarra, E. Martinez-Laserna, C. Koch-Ciobotaru, P. Rodriguez, D. I. Stroe and M. Swierczynski, "Second life battery energy storage system for residential demand response service", *2015 IEEE International Conference on Industrial Technology (ICIT),* Seville, 2015, pp. 2941-2948.
doi: 10.1109/ICIT.2015.7125532

A. Saez-de-Ibarra, A. Milo, H. Gaztañaga, V. I. Herrera, I. Etxeberria-Otadui and A. Padrós, "Intelligent photovoltaic power plants management strategy for market participation", *2015 IEEE Energy Conversion Congress and Exposition (ECCE)*, Montreal, QC, 2015, pp. 35-42.
doi: 10.1109/ECCE.2015.7309666

V. I. Herrera, H. Gaztañaga, A. Milo, **A. Saez-de-Ibarra**, I. Etxeberria-Otadui and T. Nieva, "Optimal energy management of a battery-supercapacitor based light rail vehicle using genetic algorithms", *2015 IEEE Energy Conversion Congress and Exposition (ECCE)*, Montreal, QC, 2015, pp. 1359-1366.
doi: 10.1109/ECCE.2015.7309851

C. Koch-Ciobotaru, **A. Saez-de-Ibarra**, E. Martinez-Laserna, D. I. Stroe, M. Swierczynski and P. Rodriguez, "Second life battery energy storage system for enhancing renewable energy grid integration", *2015 IEEE Energy Conversion Congress and Exposition (ECCE)*, Montreal, QC, 2015, pp. 78-84.
doi: 10.1109/ECCE.2015.7309672

Yo me siento mucho mejor siendo un loco

Milesker   Muchas gracias   Merci beaucoup   Thank you   Moltes gràcies